PAVEMENT SUBGRADE PERFORMANCE STUDY

Volume 2

Results from accelerated pavement testing of an A-2-4 subgrade soil at higher-than-optimum moisture content

by

Vincent Janoo [(1)]
Edel Cortez [(1)]
Robert Eaton [(1)]
Michael Ferrick [(1)]

[1.] U.S. Army Cold Regions Research and Engineering Laboratory, 72 Lyme Road, Hanover, New Hampshire 03755, United States

EXECUTIVE SUMMARY

This is the third in a series of reports on the subgrade failure criteria research study conducted in the Frost Effects Research Facility (FERF) at the Corp of Engineers, Engineering Resources Development Center, Cold Regions Research & Engineering Laboratory in Hanover, New Hampshire. The hypothesis for the study is that the failure criterion depends on the subgrade type and the in-situ moisture content. Many of the current mechanistic design procedures incorporate the results from AASHO Road Tests conducted in the late fifties. The criterion is based on one soil type (A-6), and, most of all, it was difficult to discern the effect of load and environment on the failure criterion. Our assertion is that the criterion is not applicable to other subgrades and possibly to areas other than where it was developed. Also, the criterion was inferred from surface distresses rather than from actual in-situ stress and/or strain measurements.

As part of the research program, four subgrade soils were selected for testing in the FERF. The test program includes testing each subgrade soil at three moisture contents. One of the subgrade moisture conditions was designed to be at or near optimum density and moisture content. A second moisture condition was designed to be at higher than optimum moisture content. A third moisture condition was designed to be lower than optimum moisture content. A test section was built or will be built to represent each soil at each of the three moisture conditions.

The test sections, consisting of 85 mm of asphalt concrete and 203 mm of crushed base over the test subgrade soil, were instrumented with stress, strain, moisture, and temperature sensors. The test sections were then subjected to accelerated loading under controlled environmental conditions.

This report presents the results from the accelerated pavement for one of the test subgrade soil. The subgrade, based on AASHTO soil classification system, was an A-2-4. It was constructed at wet of optimum density and moisture content of 1825 kg/m3 and 16.5 % by weight, respectively. During construction, layer density, moisture content, and CBR were recorded. Accelerated traffic load testing was applied to each of six test windows in this test section coded 703. Each test window, coded c1 to c6, was approximately 6.0 m long and 1 m wide. Traffic loads were applied unidirectionally at an average speed of 13 km/hr. The test section, barring any breakdowns, was subjected to about 700 load repetitions per hour. Testing was conducted for 22 hours per day. The remaining 2 hours were used for maintenance. At three of the six test windows, the load was kept constant at 58.5 kN. At one test windows, the load was kept at 71.2 kN. At other test window, the load was kept constant at 80 kN. At another test window, the load was varied from 20, 40, 53.4, and 66.7 kN for various sets of traffic passes. The load was applied through dual truck tires, with the tire pressures averaging around 710 kPa.

Stress, strain, and surface rut measurements were taken periodically. Stress measurements were available in three of the four windows. All stress measurements were taken in the subgrade at approximately 212 mm from the top of the subgrade. In one of the test windows, stress measurements were also taken at 322 mm from the top of the subgrade. Dynamic and permanent strains in the base and subgrade were measured in all four windows.

This report presents the measured response of this test section to accelerated loading. It was found that even with a 100% crushed base course, approximately 44% of the total deformation occurred in the base. It was also found that the vertical permanent strains were significantly larger than their corresponding longitudinal and transverse strains. In the vertical direction the majority of the deformation occurred in the base and within the top 300 mm of subgrade.

INTRODUCTION

As a result of the work by Dormon and Metcalf (1965) using data from the AASHO Road Tests, the current design criteria for pavements stipulates that the failure of the subgrade can be minimized, by limiting the level of vertical compressive strain on top of the subgrade. However, it must be remembered that this limiting subgrade strain criteria was based exclusively on the A-6 soil at the AASHO Road Test. This failure criterion may not be applicable for other material types (gravel, sand, silt or clay), nor for other moisture condition. For example, practical experience of pavement and geotechnical engineers indicate that a silt subgrade rut more easily than gravel, and that moisture conditions near saturation are more critical than when the subgrade is at or near optimum.

As part of an international study on pavement subgrade performance, several full-scale test sections were constructed in the Frost Effects Research Facility (FERF) at the U.S. Army Cold Regions Research & Engineering Laboratory (CRREL) in Hanover, New Hampshire. The test sections were constructed from different subgrade soils at different moisture contents. A detailed overview of the project can be found in Janoo et al (1999).

This is Volume 3 in a series of reports each containing details and results from Test Section 703..Test section 703 (TS703) is a continuation of a previous test section (TS701). Details and results from TS701 can be found in Janoo et al (2000). TS701 was built with a test subgrade, which classified as an A-2-4, using the AASHTO soil classification system, and was constructed at near optimum density and moisture content of 1934 kg/m^3 and 10% respectively. To study the effect of moisture content on the failure criteria for an A-2-4 subgrade soil, TS703 was constructed using the same subgrade soil but at a higher moisture content (15%), Janoo et al (1999). The base and asphalt wearing courses were replicates of TS701, i.e., 76mm of AC over 250mm crushed aggregate base.

The test section was again divided into six test windows and each window was subjected to accelerated loading using the Heavy Vehicle Simulator (HVS).

Surface rut depth measurements were taken periodically during the accelerated load tests. Failure was assumed to occur when the surface rut depth equaled or exceeded 12.5mm. The test windows were instrumented with stress and deformation sensors. In addition, temperature and moisture sensors were installed at various depths in the test section. Subsurface stress and strain measurements were recorded periodically, whereas subsurface moisture and temperatures were recorded hourly.

The locations of the test windows that were closer to the south wall were moved to allow more distance from the wall in order to reduce boundary effects.

MATERIAL PROPERTIES

A brief description of the subgrade and base course materials is presented here. Additional details can be found in Janoo et al, 1999, 2000. The subgrade soil was a blend of an A-1 soil obtained from a local quarry and an A-4 soil to produce the A-2-4 (AASHTO Classification) soil or SM (ASTM), Figure 1. Routine classification tests conducted on the test soil included optimum moisture, maximum density, gradation and hydrometer analyses, specific gravity, and liquid and plastic limits. Standard AASHTO test procedures were used. The A-2-4 subgrade soil has approximately 30% passing the

0.074mm sieve. The average liquid limit (LL) and plasticity index (PI) of the soil was 30% and 2.1 respectively. The average specific gravity was 2.72. The average optimum density and moisture content (AASHTO T 99-90) was 1934 kg/cm^3 and 10% respectively. The results from the classification tests are summarized in Table 1. The base course was crushed gravel classified as No 304 under NH State DOT base course specification, equivalent to an AASHTO A-1-a or ASTM GP-GM, Figure 1. The gradation of the base course is shown in Figure 2. The asphalt material of the wearing course conformed to the standard NH AC 20 for surface course mix.

Table 1. 703 subgrade soil properties.

Soil Type	AASHTO A-2-4
Spec. Gravity	2.72
LL	30
PI	2.1
Pass. #10	71.8 %
Pass. #200	29.9 %
Optimum Moisture Content	10 %
As Built Moisture Content	15 %
Optimum Density	1934 kg/m^3
As Built Average Density	1851 kg/m^3

DESCRIPTION OF TEST SECTION

TS703 was constructed in the Frost Effects Research Facility (FERF) at the Engineering Research Development Center, Cold Regions Research & Engineering laboratory (ERDC/CRREL) in Hanover, New Hampshire. A detail description of the FERF can be found in Janoo et al (1999). The test section was built in the northeast section of the FERF, Figure 2. The plan and elevation views of TS703 are shown in

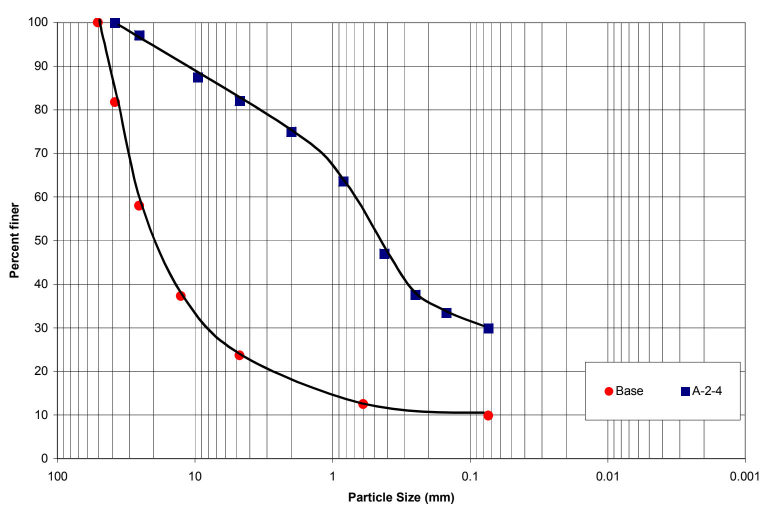

Fig. 1: Grain size distribution of the subgrade and base materials.

Figure 3. The available area for the test section was 42 m long by 6.4 m wide and 3.7 m deep. The actual length used for testing was approximately 23 m long, Figure 3. As shown in Figure 3, are the 6 test windows within the test area for conducting accelerated load tests. Each test window was 7.8 m long of which the beginning and the end 0.9m were used as acceleration and de-acceleration areas for the wheel. The area in between the ends (6m long by 0.9m) was the area where the constant velocity tests were conducted. The center-to-center distance between the test windows was 1.2 m. Based on observations of lower densities in TS701 near the south wall, the test windows were moved an additional 1.5m from the south wall.

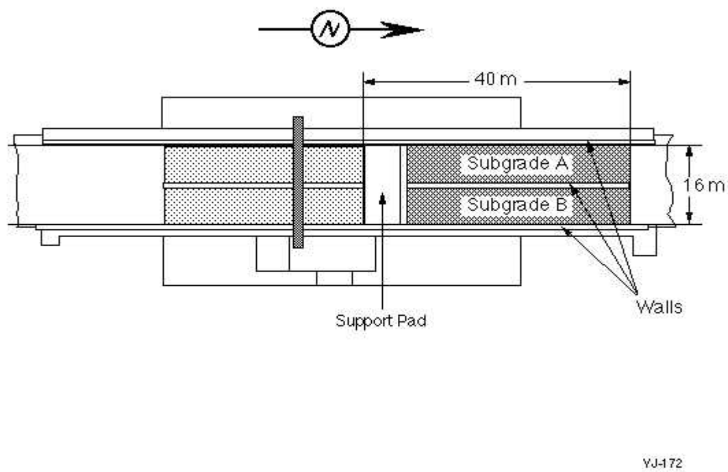

Figure 2. Location of test section (TS703) in the FERF.

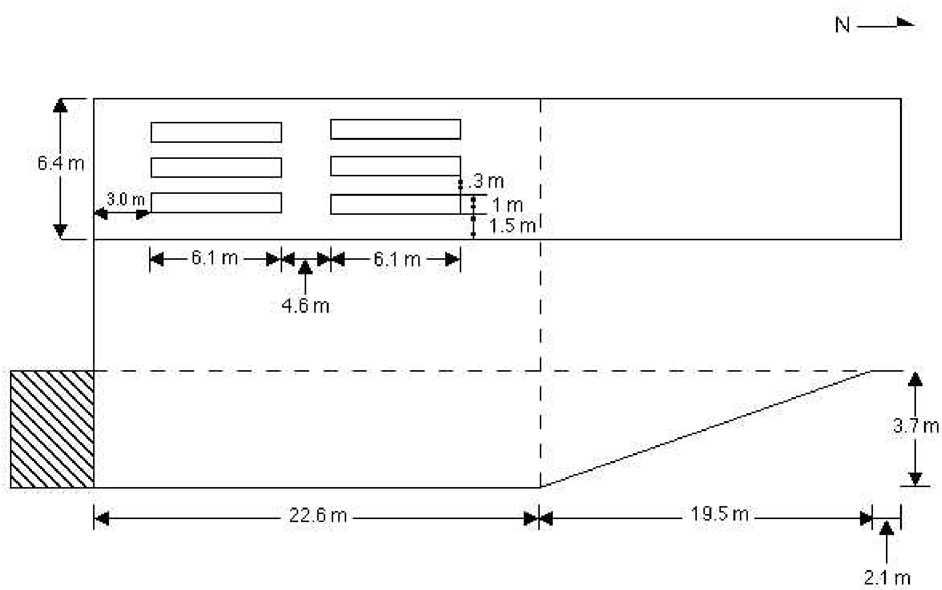

Figure 3. Plan and cross sectional views of Test Section 703.

CONSTRUCTION OF TEST SECTION

The cross section of TS 703 is shown in Figure 4. As seen in the Figure, the test section consisted of nominal 76 mm of asphalt concrete over nominal 250mm crushed base course over the test subgrade. In TS703, the subgrade consisted of two parts. The specifications required that the upper subgrade be constructed from the same soil stockpile used for TS701. In addition, as before, the specifications required that the subgrade be constructed in lifts of 150mm thickness and that each lift be compacted at moisture contents within ± 2% of the optimum and to a density between 95 and 100% of the maximum dry density obtained from the Standard AASHTO T99 test procedure. The A-2-4 subgrade soil was preconditioned for a target moisture content of 15% ± 2%. The optimum moisture content for this soil was 10%.

Figure 4. Cross section of Test Section 703.

An analysis by Hilderbrand and Irwin (1994) indicated that, below 1.5m from the pavement surface, the effect of the wheel load was minimal. In addition, results from TS701 indicated that the stresses at this depth was insignificant. In addition, the vertical strain measured at this depth was around 400 µstrains and the horizontal and transverse strains were insignificant(< 50 µstrains). For comparison purposes, the vertical strain at the top of the subgrade was in the range of 1200 µstrains. This finding supported our decision to retain the bottom 2 m of subgrade soil from TS701.

After the testing of TS701 was completed, the asphalt wearing course, the base course and the upper 1.52 m of the subgrade were removed. Then, a new upper subgrade was built in similar fashion as for Test Section 701, except that now the upper subgrade soil had higher moisture content. The soil was placed at in-situ moisture content and wetted. During the wetting process, the soil was roto-tilled for uniform moisture content. Periodically, moisture contents were taken and the soil re-wetted and roto-tilled if the target moisture content was not reached. Although during construction, the subgrade soil was soft at the target moisture content of 15 %, Figure 5, it was found that if the layer was left uncovered for a period of several days, the moisture content in the layer dropped significantly to near its optimum value. If construction had to be halted, a small head of water was placed on the surface so as to minimize the drying of the soil.

The asphalt wearing course had a nominal thickness of 76 mm, The base course was nominally 229 mm thick. The upper 1.52 m of the subgrade was built in layers each approximately 150mm thick. As in TS701, in TS703 stones larger than 50mm were manually removed from the subgrade material during construction. For each subgrade layer, once the grade was reached, the layer was compacted using a 9000kg steel wheel roller. Compaction started at one end of the longitudinal wall and moved approximately in 0.3m increments towards the other longitudinal wall. The compaction was done in the non-vibratory mode so as not to disturb any instrumentation in the layers below. The area approximately 1.5m long from the south supporting pad was compacted using a hand compactor since the steel wheel compactor could not reach this area due to the wall.

CONSTRUCTION CONTROL

During the construction of the subgrade, a series of tests were conducted on the compacted layers. These measurements were conducted on every 300-mm lift unless otherwise noted. Measurements included layer thickness, which were taken with a survey level and in-place TROXLER™ nuclear moisture/density measurements. No Clegg hammer or dynamic cone penetrometer (DCP) tests were taken. The subgrade was extremely soft and the Clegg hammer left a significant dent and the DCP cone penetrated into the soft soil with a single drop.

For density and moisture contents, approximately 30 measurements were taken on each lift using the direct method for a total of 180 measurements in the subgrade layer. The location for each moisture/density was carefully planed to avoid interference with other embedded sensors. Figure 6 shows the location of the measurements with reference to the location of the test windows. Elevation measurements were taken at locations on each 300-mm lifts as shown in Figure 7. Forty-eight measurements were taken on each lift

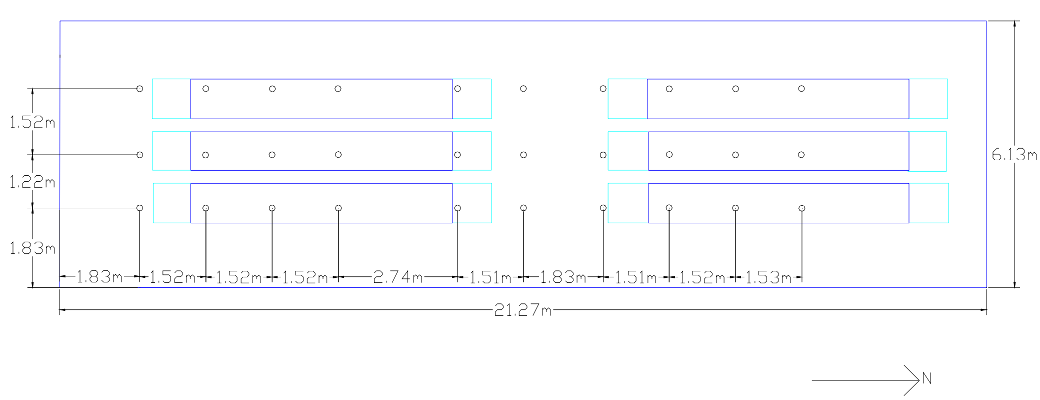

Figure 6. Locations for moisture and density measurements in TS703.

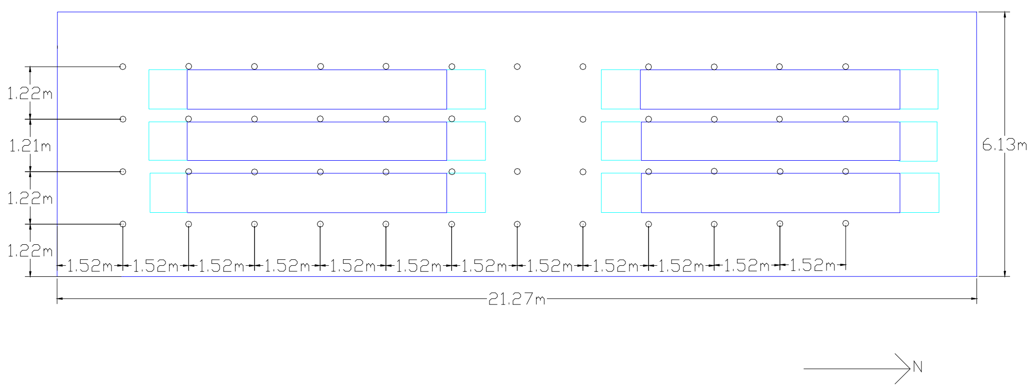

Figure 7. Location for elevation measurement in TS703.

Densities

The mean dry density of the upper 1.52 m of subgrade was 1853 kg/m^3 with a COV of 2.5 %. The mean density of the base layer was 2137 kg/m^3 with a COV of 6.3%. The results of the measurements are tabulated in Table A-1, Appendix A. Figure 7 presents a histogram and cumulative frequency plot of the relative compaction of the upper 1.52m of subgrade.. The relative compaction is based on the laboratory optimum density of 1860 kg/m^3 measured at the water content of 15%. Based on the laboratory results, the subgrade was compacted at a degree of saturation of around 90%. Approximately 88 % of the density measurements equaled or exceeded the specified relative compaction of 95%.

Moisture Contents

Moisture measurements were taken simultaneously at the same locations and depths as densities using the TROXLER nuclear gage, Figure 6. The mean moisture content of the test subgrade soil was 15.4 % with a COV of 1.13%. The distribution of the moisture contents in the subgrade is shown in Figure 9 and tabulated in Table A-2, Appendix A. Approximately 70% of the data was within the ± 2% specification. The relative difference in moisture content with the target moisture content is shown in Figure 10. The mean difference is about ± 0.36% with a COV of 49%.

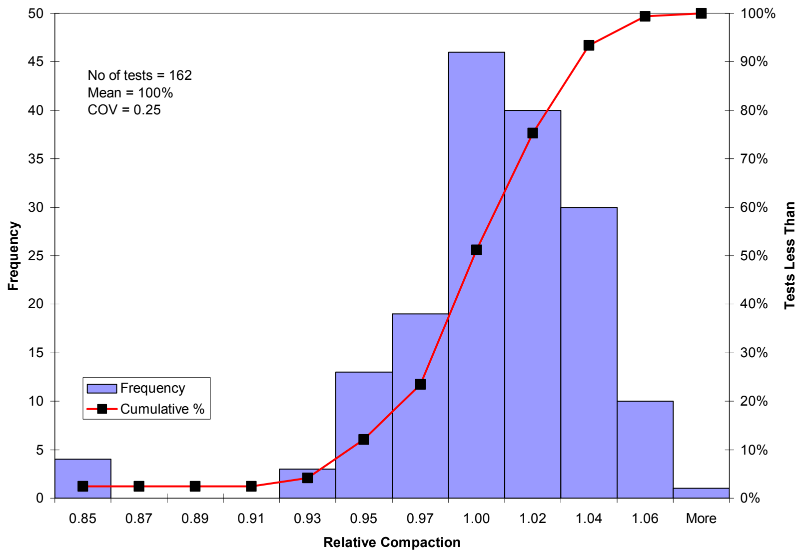

Figure 8 . Constructed relative densities of the top 1.52 m of subgrade.

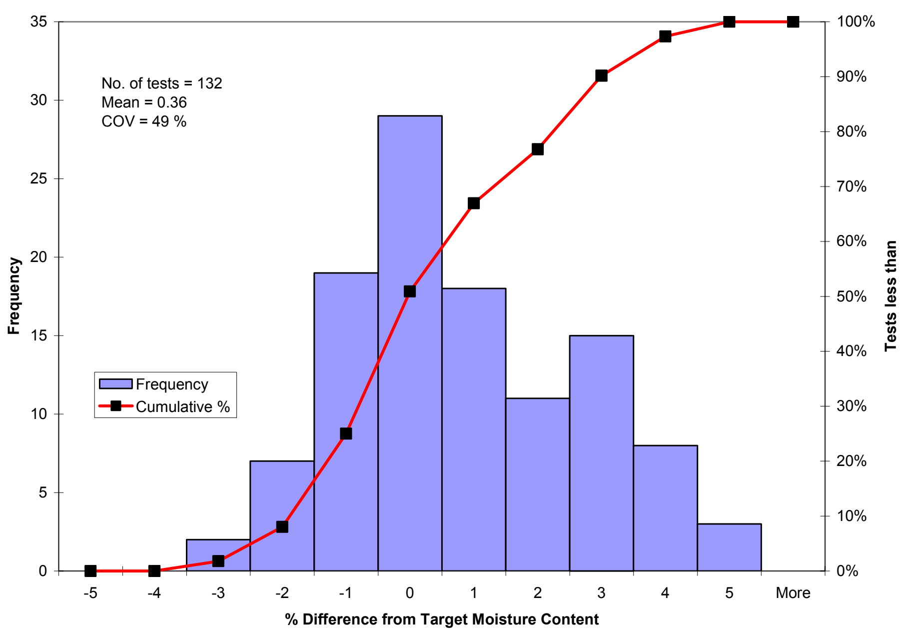

Figure 9. Distribution of moisture content in upper 1.52 m subgrade.

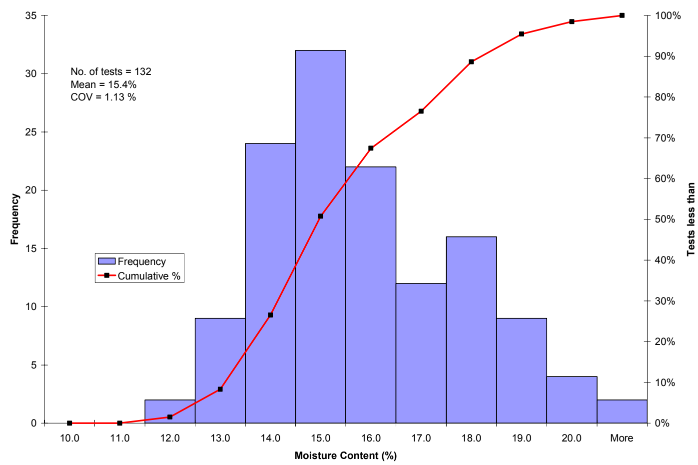

Figure 10. Percent difference in subgrade measured and target moisture content.

When wet, the soil was quite plastic as shown by the indentations of the TROXLER test equipment I Figure 10a. However, we also found that with this soil, if the surface was allowed to sit in the open for over a couple of days, the surface tended to dry to near its optimum value. This can be seen in Table A-2, where the final layer (measurements taken after several days of placement) moisture content was close to the optimum value. We tried to keep to the target moisture content by continuously keeping the uppermost layer wet prior to placement of the next layer or base course. The mean moisture content of the base course was 3.7 % with a COV of 2%.

Figure 10a. Degree of softness of subgrade soil at 15% moisture content.

<u>Elevation Measurements</u>

Lift thickness measurements were taken after 300mm of subgrade soil had been placed and compacted using a rod and level. The results are presented in Table A-3, Appendix A. The distribution of layer thickness during the construction of the subgrade is shown in Figure 11. The mean layer thickness of the subgrade was 284mm with a COV of 21%. The mean lift thickness of the base layer was 250 mm with a COV of 5.7%. *The mean thickness of the asphalt concrete layer was 84mm with a COV of 14%.(Check this out)*

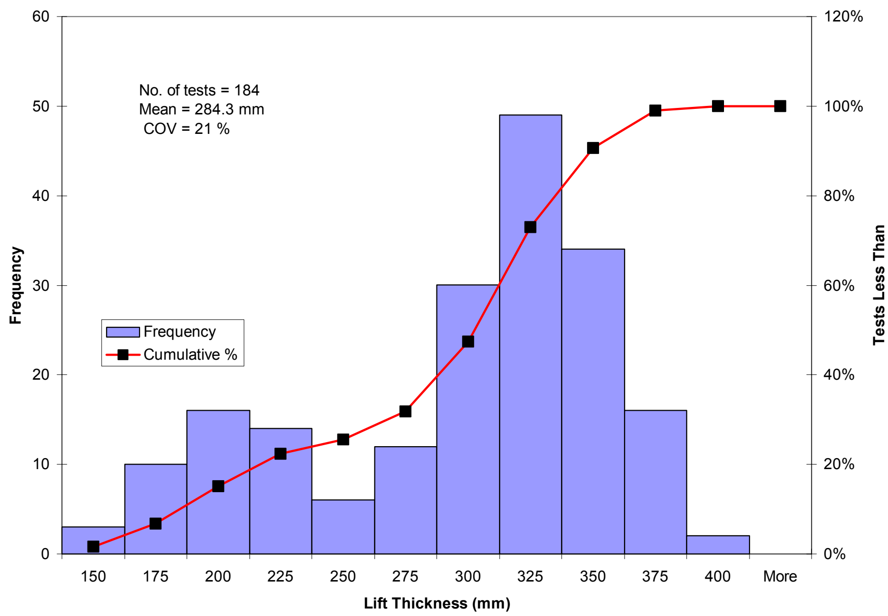

Figure 11. Distribution of layer thickness during subgrade construction.

<u>INSTRUMENTATION</u>

Instrumentation for measuring stress, strain, temperature and moisture content were installed in the pavement structure during construction of the test section. The locations of the gages are shown in Figures 12. In Figure 12a, a plan view of the location of all the gages are presented. In Figures 12 b,c and d, the location of the moisture, stress cells and strain and temperature gages as a function of depth are presented respectively. A brief description of the gages is presented here. Detail descriptions of the gages can be found in Janoo et al, (1999).

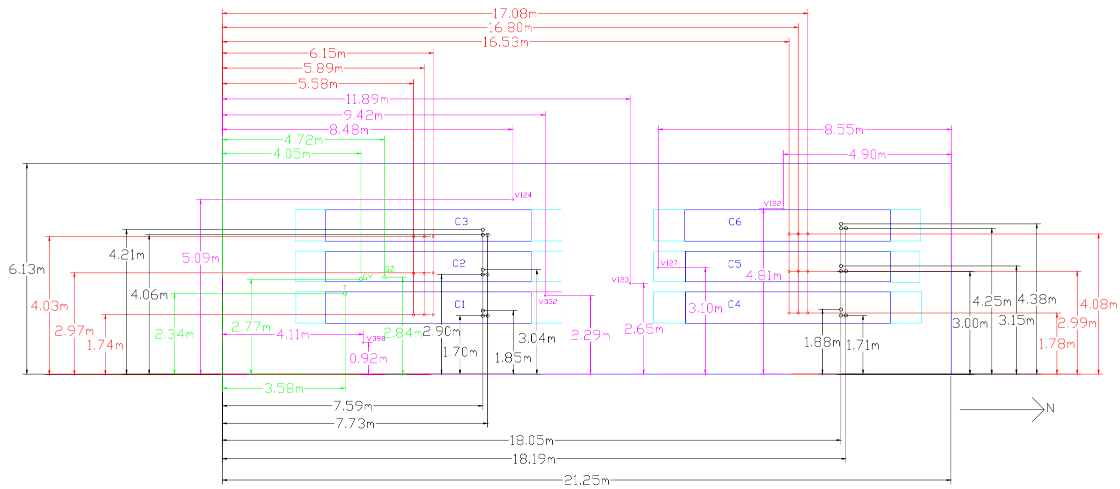

Figure 12a. Plan view showing the location of instrumentation in TS703.

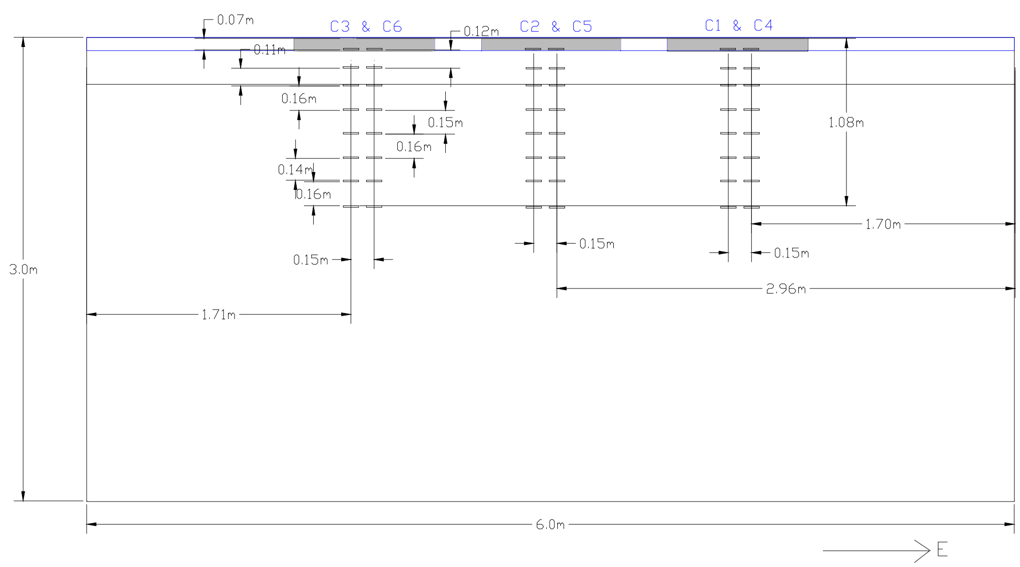

Figure 12b. Location of εmu coil gages in test section.

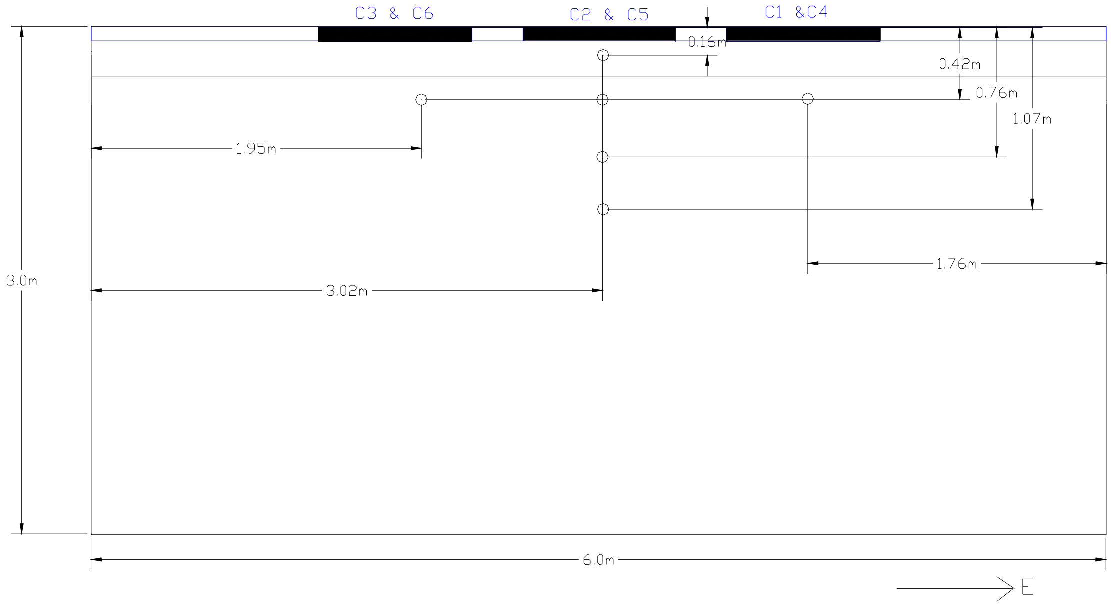

Figure 12c. Location of stress gages in test section subgrade.

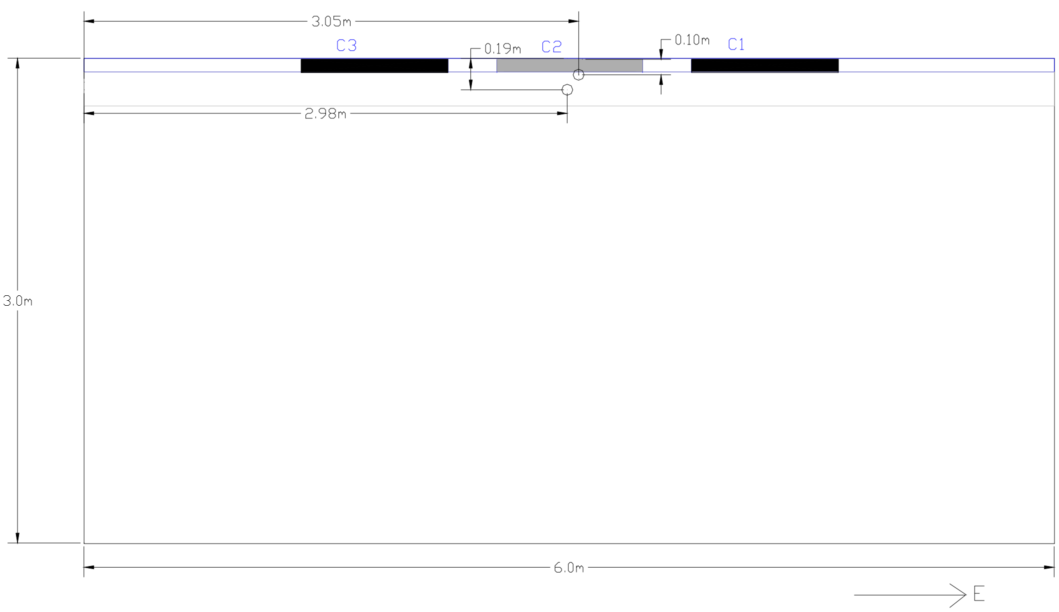

Figure 12d. Location of stress gages in test section base course.

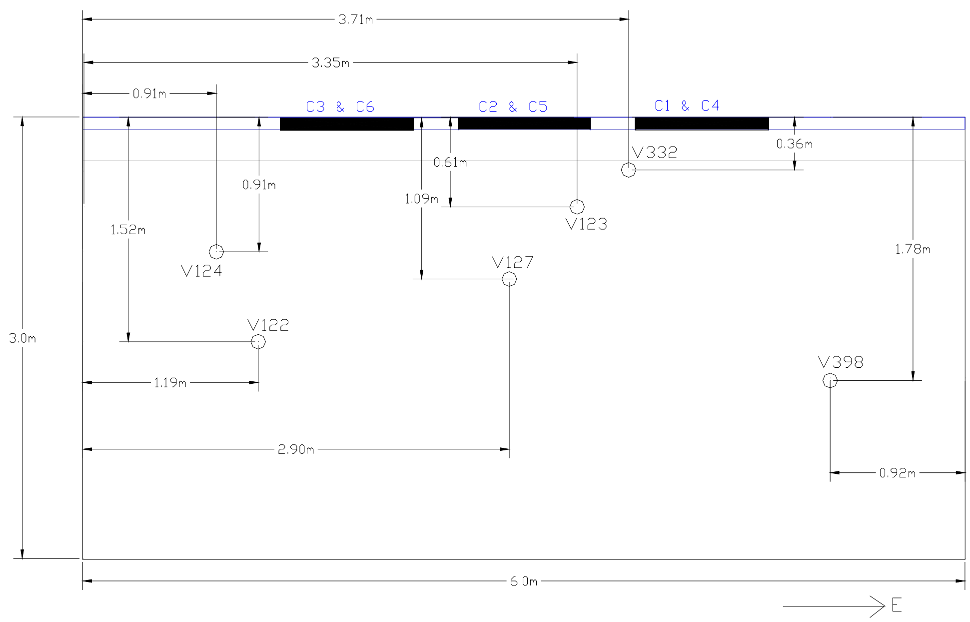

Figure 12e. Location of moisture gages in test section.

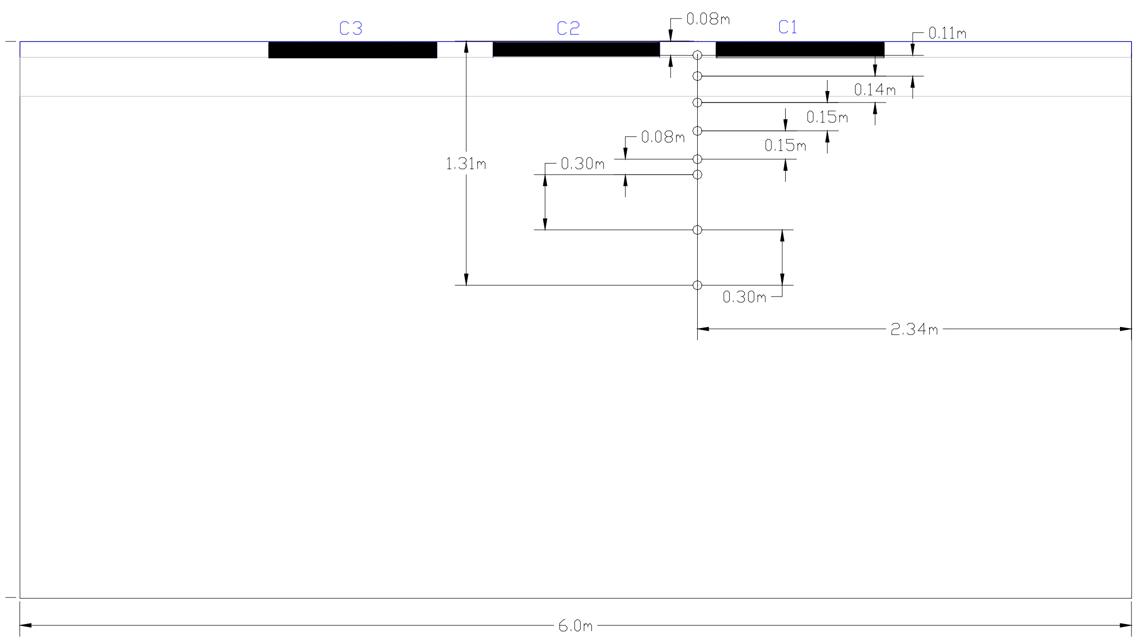

Figure 12f. Location of temperature sensors in test section.

Strain measurements

Triaxial strain measurements were made with the εmu system. The system consisted of one sending coil and three receiving coils (longitudinal (x), transverse (y), and vertical (z)), the εmu signal conditioner, and a computer data acquisition system. Details of the system can be found in the users manual by Dawson (*1994*), Janoo et al., (1999, 2000). In principle, the system works when an alternating current is passed through a coil of wire, an alternating magnetic field is generated. Another coil placed within this field will have an alternating current induced in it. The magnitude of the induced current is proportional to the distance between the coils. A photo of the coils is shown in Figure 13.

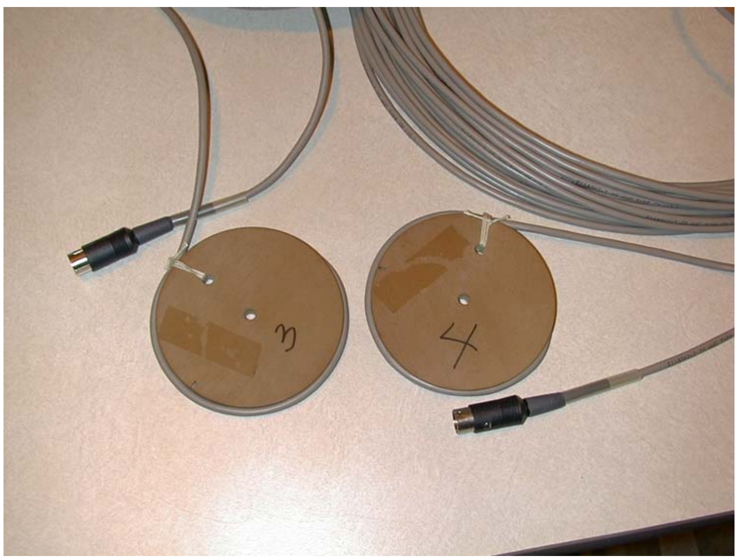

Figure 13. εmu coils for measuring strain

Sets of 100-mm-diameter coil sensors were installed in each test window in the base course and subgrade, Figure 12b. They measure the displacements in the vertical direction (designated as the z-direction) and in two perpendicular horizontal directions (x- and y-directions). The z-direction coils are coaxial, while the x- and y-direction coils are coplanar. The x-direction is parallel to the wheel travel, and the y-direction is perpendicular to it. Note that the coil gages were installed 7.6-m from the south wall in windows C1, C2 and C3. In windows C4, C5 and C6, the distance was 18-m from the south wall. This was based on observations in TS701 where the compaction around the south wall was lower than in other areas of the test section.

The coils were installed at eight depths in columnar stacks, starting below the pavement surface and extending to 1.2 m at a nominal center-to-center spacing of 150 mm in the subgrade, Figure 12b. In TS703 an additional pair of coil gages were added in the base course at a nominal thickness of 114mm apart. A loose coil was used on the asphalt surface to measure the permanent deformation of asphalt layer. The ID and location of the coils in each window are presented in Tables B-1, Appendix B. The horizontal locations are based from a datum located 0.3 m in the y direction from the northeast corner of the test section (see Figure 12a). The column identified as layer in Table B-1 represents the material between the vertical coil pairs. For example layers 1 and 2 represent the material in the base course. Layers 3 and above represent the materials in the subgrade.

The coil gages were calibrated in the co-axial and co-planar directions. In TS703, based on experience with coil gage failures in the vertical direction , the X and Y pairs in the vertical stack were also calibrated for their co-axial calibration constants. To relate the output voltage to the coil spacing in engineering units (millimeters), the following power equation gave a good fit:

$$V = a\,D^{n}$$

where D = static distance between the transmit and receive coils,
V = demodulated (d.c.) "static" voltage from the coils, and
a and n= regression constants for a pair of coils.
Details on the calibration process can be found in Janoo, 1999a, 1999b. The power coefficients for each coil pair are presented in Table B-2.

The placement of the instrumentation was modified from TS701and TS702 because of the low strength of the subgrade soil. In previous installations, coil gages were installed once 150mm lift of subgrade soil had been prepared. In TS703, coil gages were installed after a lift of 300mm of subgrade soil had been achieved. A hole approximately 300mm in diameter was dug to the bottom of the lift (300mm). Three coil gages were installed in the triaxial configuration at the bottom of the hole. Then 150mm of test soil was added to the hole and the next set of coil gages were installed on the surface of the fill. Once completed, the remaining 150mm of subgrade soil was added to the hole and the surface re-compacted. To assure that the coil was aligned coaxially with the coil immediately below, the next lower coil was excited and the static response from the upper coil was measured. The coils were aligned when a maximum output from the coil pair was achieved. The coil was pressed down on the surface, checked with a carpenter's level, and shimmed with soil, if necessary, to assure that it was level. The thickness of the underlying compacted lift of soil was then measured. A thickness of approximately 150 mm was desired.

In the base course, once a height of 114 mm was achieved, the coil gages were installed on the surface. The remaining base course material was added and at final grade the next set of coil gages were installed. This process is similar to that used in TS701 and TS702.

Stress measurements

Vertical, longitudinal and transverse stress measurements in the bas and subgrade were made with the DYNATEST and GEOKON soil pressure cells. They were used to measure the dynamic stresses generated in the base and subgrade from a moving wheel load on the surface of the test windows. The locations of the stress cells in the test section are shown in Figure 12 c & d. The longitudinal (x) and transverse distances in Table B-4 are based from a datum located 0.3m in the y direction from the north east corner of the test section The depths presented in Table B-4 are from the surface of pavement surface Details of the stress cells and calibration procedure can be found in Janoo et al, 1999.

Usually unless otherwise noted, DYNATEST stress cells with a range of 10-200 kPa were used to measure the horizontal stresses, while stress cells with a range of 100-800 kPa were used to measure the vertical stresses, Figure 14. The longitudinal direction stress cell had its sensing elements facing the direction of wheel travel, while the transverse direction stress cell had its sensing element facing the transverse direction of wheel travel. All windows had one triaxial set of stress cells located at about 150mm from the top of the subgrade. In test windows, C2 and C5, additional triaxial distribution of stress cells were located at 300mm from the top of the subgrade. Also in C2 and C5, vertical stress measurements were made at a depth of 750mm from the top of the subgrade. Finally, a set of DYNATEST stress cells were installed in the base course at a depth of 160mm from the AC surface. We also installed a pair of GEOKON pressure cells in the base course. The pressure cells were 229mm in diameter and one was placed at a depth of 193mm to measure the vertical stress. The second gage was used for measuring the transverse stress in the base course. The location of transverse stress cell shown in Table B-4 is from the top of the cell. The additional stress cells in C2 and C5 were used to determine the stress distribution with depth. We were unable to instrument the other windows as extensively as C2 and C5, because of limited number of available stress cells for the test program.

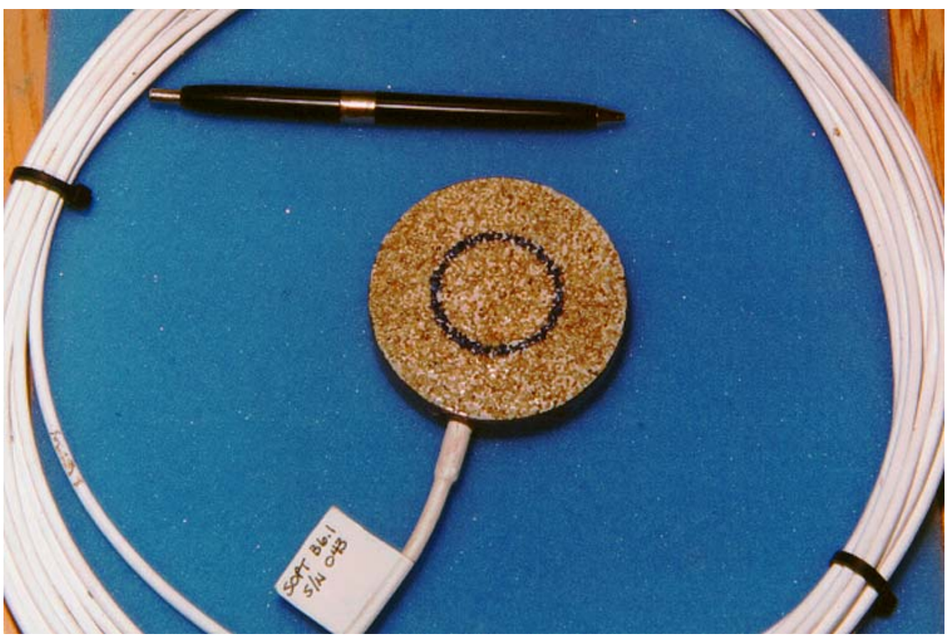

Fig. 14a: DYNATEST soil pressure cell.

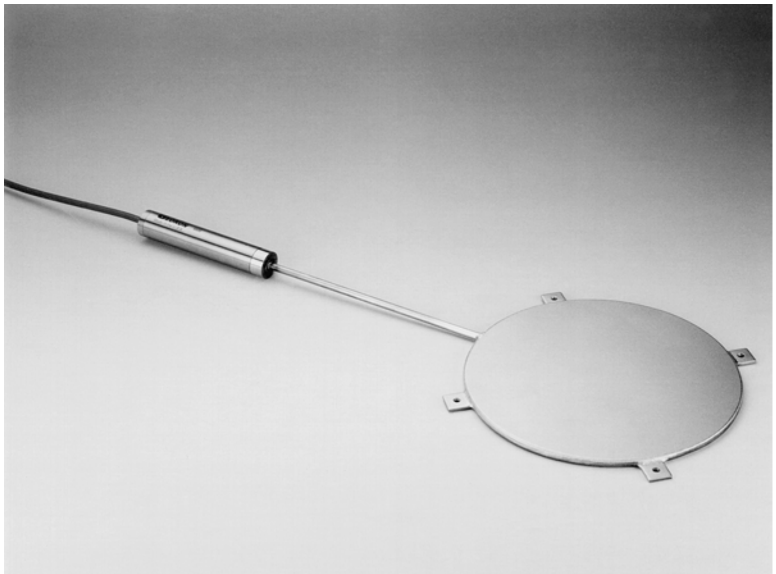

Figure 14b. GEOKON soil pressure cell.

For the DYNATEST soil pressure cells, the calibration between stress and voltage is given below;

$$\sigma(kPa) = \frac{(1000 \times V)}{(V_{ex} \times Gain \times GF \times 10^{-5})}$$

where

σ = measured stress,
V = measured voltage,
V_{ex} = excitation voltage = 10 volts,
GF = gain factor (see table 10),
Gain = 500 x A/D Card Gain.
A/D card gain = 8

For the GEOKON pressure cells, the stress conversion from voltage is as follows:

$$\sigma\ (kPa) = \left(\frac{(1000 \times V)}{(0.5 \times Gain)} \right) \times 6.895$$

where

σ = measured stress,
V = measured voltage (Volt
Gain = A/D Card Gain = 8

Moisture measurements

Soil moisture was measured with 'Hydra' soil moisture probes (Figure 15) manufactured by VITEL, Inc. Details on the probe can be found in Janoo et al. (1999). The probe was used to measure in-situ soil moisture and temperature at various depths as shown in Figure 12e. Basically, the Hydra probe performs high frequency (50 MHz) electrical measurements of the capacitive and conductive properties of soil. The capacitive component is then used to determine the dielectric constant (permissivity) of the soil which is a function of moisture content. The dielectric constant of a typical dry soil is of order of 4.5 at room temperature and for bulk water at 20 C is 80.2 as reported by Lide (1999). The accuracy of the volumetric moisture content is ± 2% using the calibration equations provided by the manufacturer. The accuracy is further increased to ±0.5% if calibrations are conducted with the test soil. The reproducibility of the measurements is ± 0.3%. The reliability of the data deteriorates below – 10 °C.

The Hydra probe also has a built-in thermistor that provides the temperature information needed for the computation of volumetric soil moisture content. The temperature from the thermistor was used as a backup to the thermocouple temperature measurements. The accuracy of thermistor temperatures is ± 0.1 C.

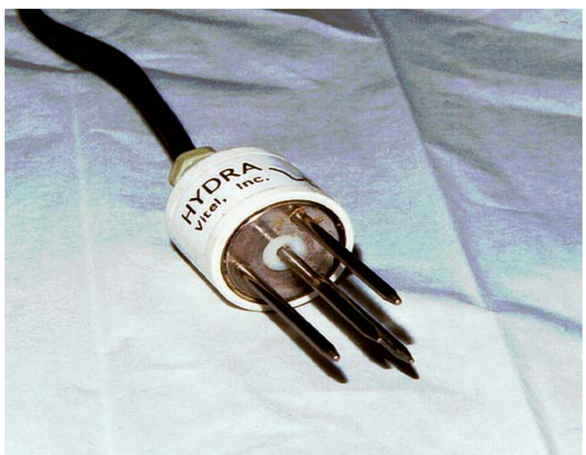

Figure 15. VITEL Hydra Moisture Probe

The Vitel Hydra moisture probes were calibrated for the test subgrade soil, Figure 16. The sand calibration equation in the Vitel software was used to convert the dielectric constant to volumetric moisture content. Details on the calibration of the probes can be found in Janoo et al., 1999. The volumetric moisture content from the VITEL gages were then corrected with the laboratory calibration shown below.

$$\omega_{vol} = 0.8173 * (\text{VITEL}) + 0.067 \qquad R^2 = 0.91$$

where ω_{vol} = calibrated volumetric moisture content

VITEL = volumetric moisture content measured from Vitel Hydra probe.

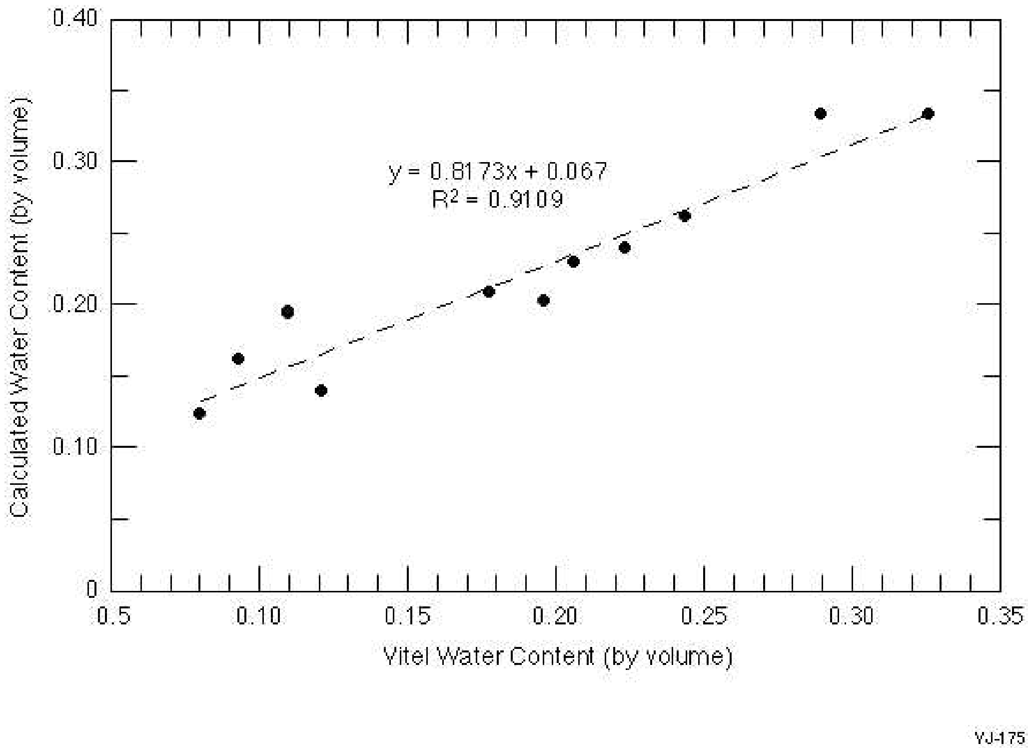

Figure 16. Calibration results for the A-2-4 soil.

These same equation was used fot TS701. Finally, the volumetric water content was converted to gravimetric water content by means of the following equation:

$$\omega_{grav} = [(\omega_{vol})/((100\text{-}\omega_{vol})\text{*}SG] * 100$$

where ω_{grav} = percent gravimetric moisture content

ω_{vol} = percent calibrated volumetric moisture content

SG = specific gravity of the soil (From laboratory tests, the specific gravity of the A-2-4 soil was 2.72.)

Five sensors were installed in the reconstructed subgrade in TS703, Figure 12e. A sixth sensor was left in the old TS701 subgrade. These sensors were mostly located outside the test windows. The locations of the moisture gages are presented in Table B-4. The longitudinal (x) and transverse distances in Table B-4, are based from a datum located 0.3m in the y direction from the north east corner of the test section (see Figure 12a). The depth is from the surface of the asphalt pavement. Details of the installation procedure can be found in Janoo et al, 1999. Moisture measurements were taken on an hourly basis from the end of construction to the end of all the testing of test section 703.

Temperature measurements

Air, surface and subsurface temperatures were taken using thermocouple sensors. These thermocouples have an accuracy of ± 0.5 °C. A thermocouple string was installed in the reconstructed subgrade as shown in Figure 12a & f and tabulated in Table B-5. One set of thermocouples were installed only in top 1.2m of subgrade and in the base. Single thermocouples were also used for measuring the air and asphalt concrete surface temperatures.

TESTING PROGRAM

Accelerated pavement testing were conducted on 703C2, 703C3, 703C5 AND 703C6. Prior to the accelerated load tests, FWD measurements were taken on top of the base and on the surface of the AC layer at locations shown in Figure 17. Initial transverse profiles were measured using the 3-m length laser profilometer (Figure 18). The laser located 45cm from the ground surface measures the surface profile at approximately 9mm intervals. In addition to the profilometer measurements, level surveys were made during every test to determine whether the profilometer reference points moved. The results from the level surveys indicated that the points were stationary throughout the test.

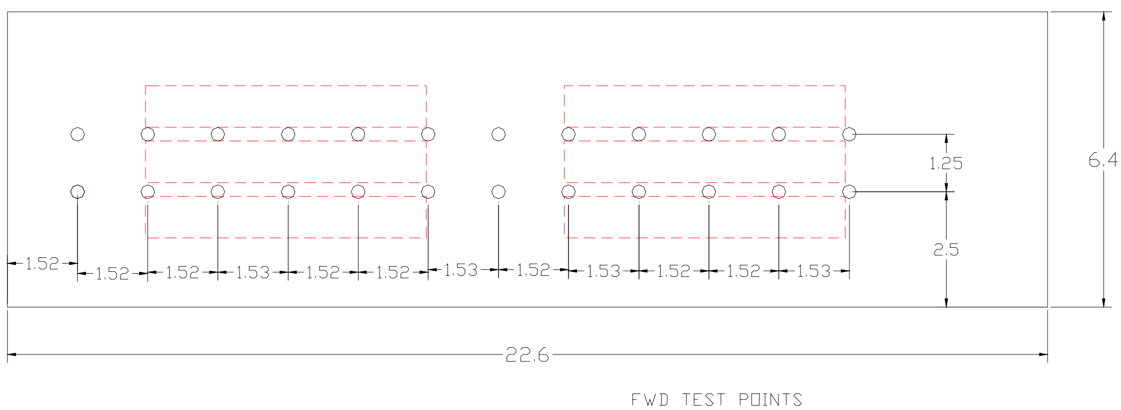

Figure 17. Location of FWD test points in TS703.

Fig18: The Laser profilometer.

Twenty-four transverse cross-section measurements spaced 0.3m apart were made in each window, Figure 19.

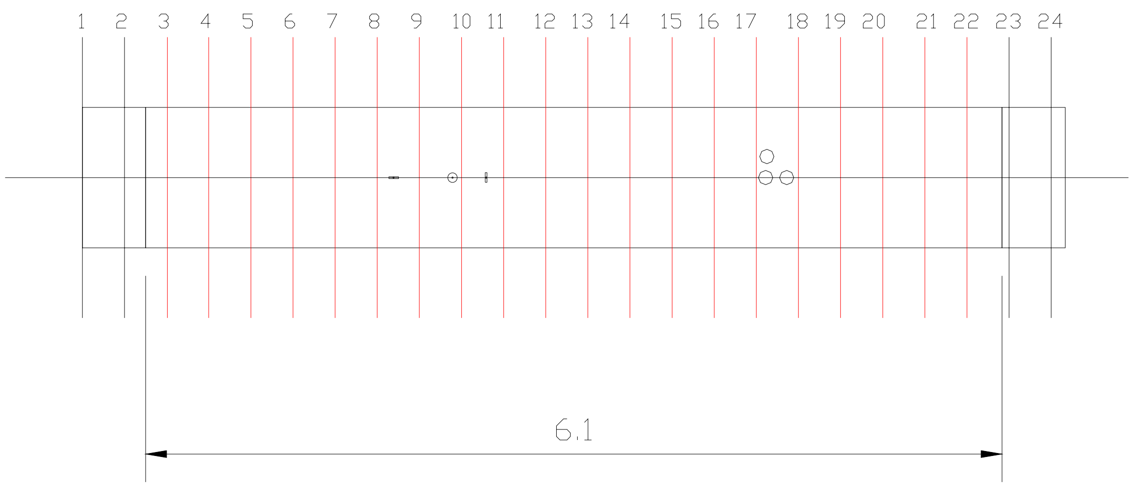

Figure 19. Locations for profile measurements in test section 701.

Surface profile measurements were made at or near at 500, 1,000, 2,500, 5,000, 10,000, 25,000, 50,000, 100,000, 200,000, 500,000, 1,000,000, etc. load repetitions.. Testing was terminated when a surface rut depth of 12.5 mm was reached or exceeded.

Subsurface stresses, strains, and permanent displacements were also measured in the vertical and in two perpendicular horizontal directions at or near at 0, 500, 1,000, 2,500, 5,000, 10,000, 25,000, 50,000, 100,000, 200,000, 500,000, 1,000,000, etc. load repetitions. Dynamic stress and strain measurements in the test windows were taken when the wheel was at 3 positions on the test section. The test positions are shown in Figure 20. Measurements were taken at these 3 locations because one of the tires was either on top or very close to the sensors as the wheel traversed the test section. At the end of the dynamic stress strain measurements, permanent deformation measurements were taken using the εmu coils. A loose coil gage on the surface was used to measure the permanent deformation between the surface and the first coil in the base course. The locations in Figures 20a, b and c were identified as Position 1, Position 2 and Position 3 respectively.

Accelerated Loading of the Test Sections

The test windows were loaded using the Mark IV Heavy Vehicle Simulator (HVS), accelerated loading system, Figure 21. The tire pressure was set to 690 kPa and the tests were conducted in the uni-directional mode at 13 km/hour. At 13 km/hour, the average number of load repetitions was 700 per hour. The tests were conducted for approximately 22 hours per day, seven days a week. The load was wandered over the test window in 50mm increments. Additional details on the HVS can be found in Janoo et al, 1999, 2000.

Figure 20a. Location of test wheels over coil and stress cells for Position 1 measurements.

Figure 20b. Location of test wheels over coil and stress cells for Position 2 measurements.

Figure 20c. Location of test wheels over coil and stress cells for Position 3 measurements.

Fig. 21. The Heavy Vehicle Simulator (HVS), Mark IV, used for accelerated testing of the pavement.

RESULTS

TEMPERATURE & MOISTURE

Temperature

The mean daily temperatures of the test sections and the air above during the test period are presented in Figure 22. Only small temperature gradients were registered in the test section. The air temperature fluctuated somewhat more as expected. For the purpose of these experiments, the temperature variations recorded at large are expected to play an insignificant role. These temperatures were measured with thermocouples.

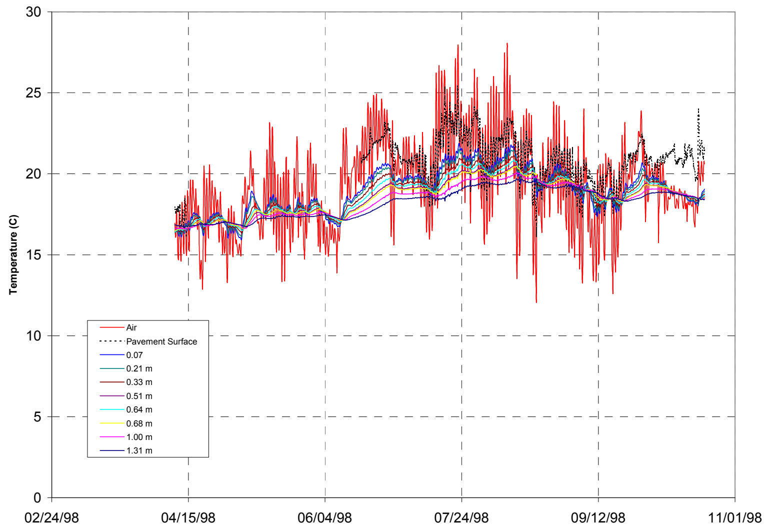

Figure 22. Mean daily temperatures during the test period.

The mean subsurface temperature was 18.6 °C with a COV of 0.02% during the test period, Figure 23.

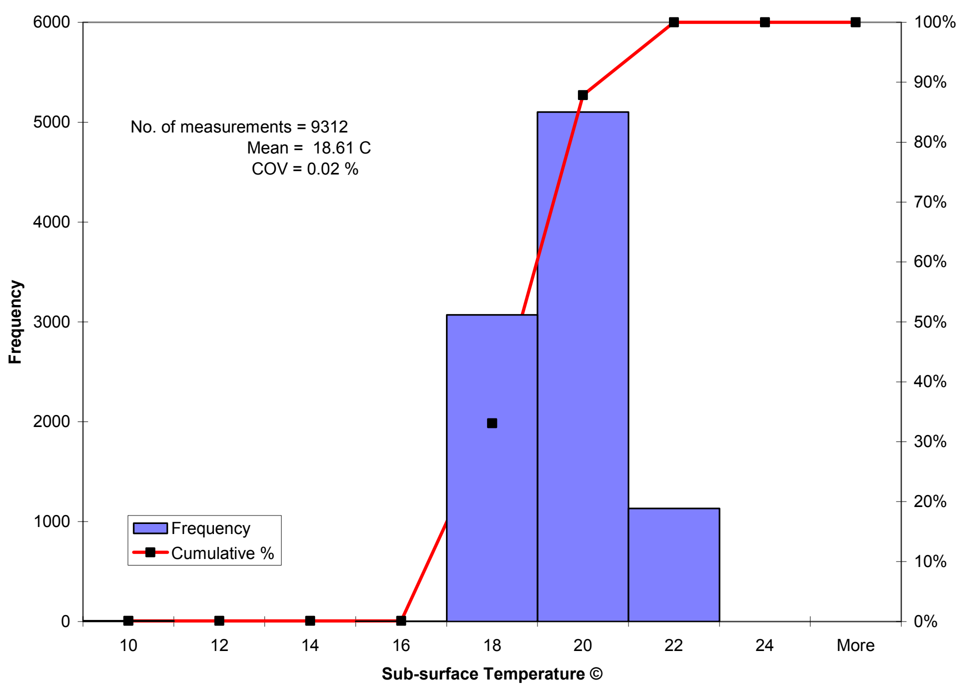

Figure 23. Variation of sub-surface temperature during test period.

Moisture Measurements

The variation of moisture content is presented under the discussion of results from each section.

703C2

Testing of window 703C2 began on May 4, 1998 and ended on May 8, 1998. Based on load measurements from the HVS and tire pressure monitoring during the tests, Figure 24, the mean test load was 62.3-kN with a COV of 2.2 % and the tire pressure was 721-kPa with a COV of 7.3%.

In addition to test loads and tire pressure, moisture content and temperature measurements were monitored in the test section during the test, Figure 25. The average sub-surface temperature in the test section was 17 °C with a COV of 3.5%. The average moisture content was 13.6 % with a COV of 5.1%. The target moisture content during construction was 15 ± 2%. We did observe during construction that water left standing on the surface tended to drain within a couple of days, leaving the surface where it was once was unable to bear construction equipment able to do so. This drainage of the surface water was assumed to be due to vertical drainage into the subgrade. However, this does not explain the reduction of the moisture content near the boundary of the old 701 and the new 703 subgrade, Figure 25b. The bottom measurement at a depth of 1524mm was in the old test section and it appears that it has dried to an average of 6.2%. The moisture content as a function of depth and time are presented in Table 2.

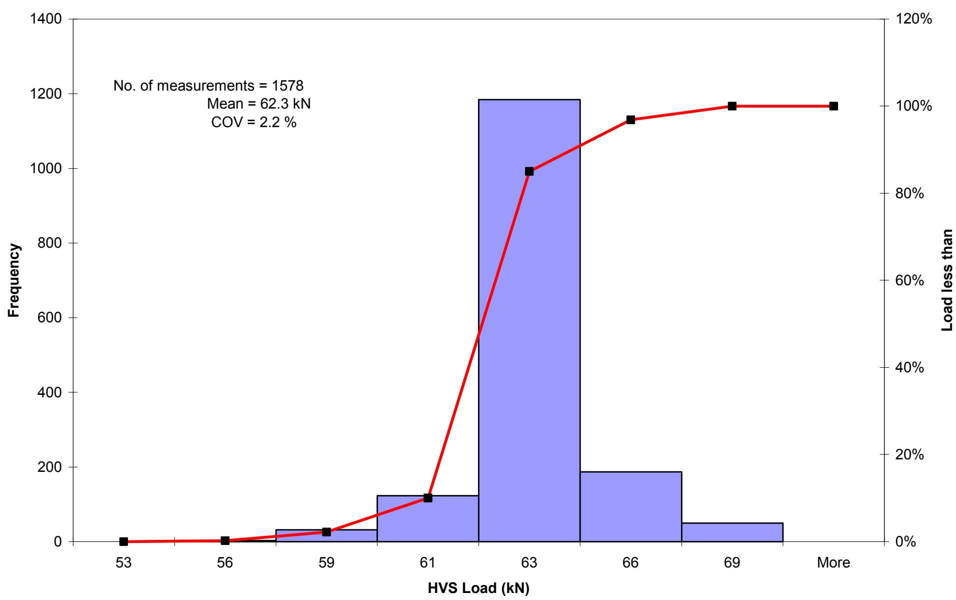

FIgure 24a. Statistical presentation of test load on 703C2.

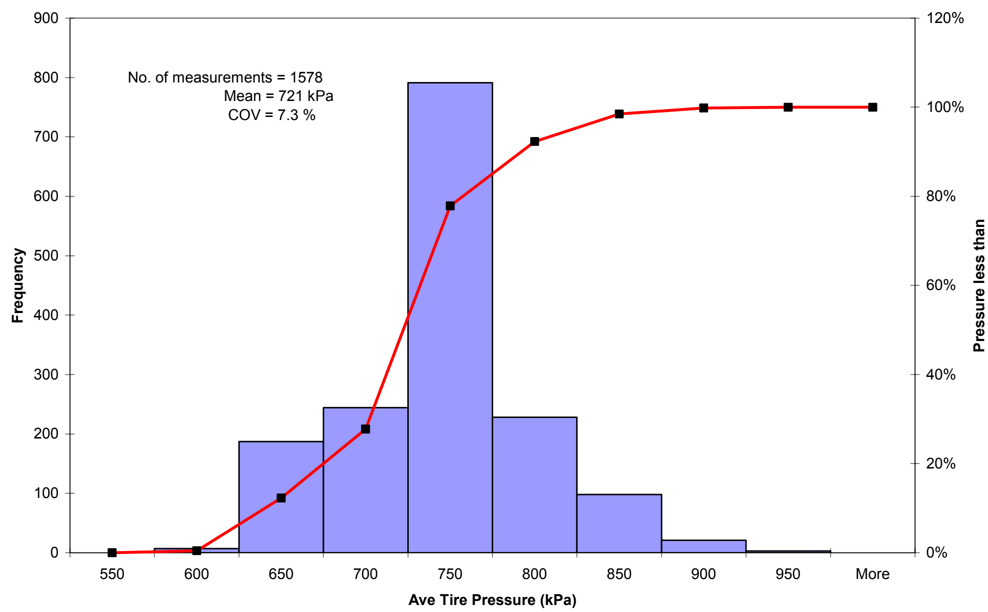

Figure 24b. Statistical representation of tire pressure on 703C2.

Table 1. Average moisture content in TS703 during APT on 703C2

Depth (mm)	5/4/1998	5/5/1998	5/6/1998	5/7/1998	5/8/1998
356	13.15	13.38	12.92	12.93	12.92
610	13.35	14.00	12.54	12.51	12.53
914	14.22	14.24	14.24		
1092	14.26	14.53	14.06	14.04	14.03
1524	6.16	6.24	6.10	6.14	6.14

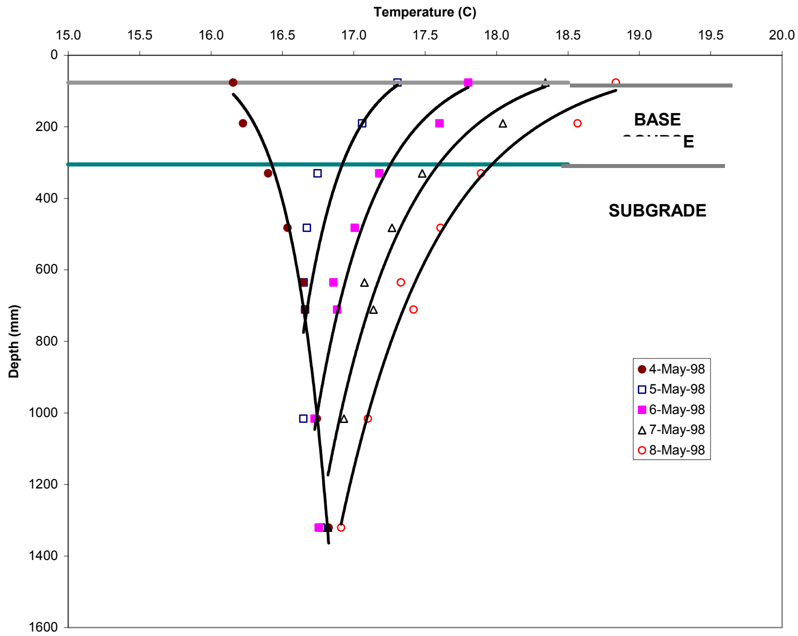

Figure 25a. Temperature variation in test section when accelerated testing was conducted on 703C2.

Dynamic Stress

Stress measurements were made in the base course and at a several depths in the subgrade, Figure 12c & d. In this window, GEOKON pressure cells were installed at mid-depth of the base course to measure the vertical and transverse dynamic stresses. Three DYNATEST pressure cells were also installed in the base course to measure the vertical, longitudinal and transverse dynamic stresses. These cells were installed at a depth of 160mm from the surface. In the subgrade, similar pattern of three DYNATEST pressure cells were installed at depths of 420mm and 760mm. A single DYNATEST pressure cell to measure the vertical dynamic stress was installed at 1076mm from the AC surface.

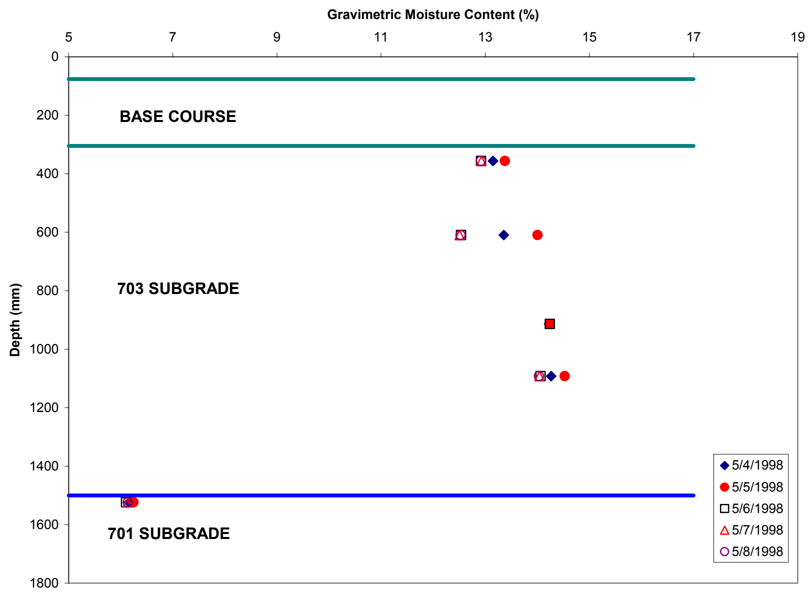

Figure 25b. Moisture variation in test section when accelerated testing was conducted on 703C2.

Typical stress responses near the beginning and at the end of testing are shown in Figures 26 and 27. Negative values indicate compressive stress. The maximum stresses occur when the sensors are directly under both the wheels, i.e., at position 2. With respect to the vertical stress near the top of the subgrade (z = 453 mm), there was a 25% increase in the stress (91-kPa to 113.5-kPa) from the beginning to the end of testing. There was a rapid increase of stress to 2500 load repetitions, after which the change was more gradual. At z = 762 mm, the increase reduced to about 9%. (42-kPa to 46-kPa). There was a similar rapid increase in stress to 10000 load repetitions, after which the change was more gradual. At z = 1067 mm, there was a 57% decrease in the stress from the beginning to the end of the test, Figure 28. The decrease in stress was rapid near the beginning and the rate of decrease did not level out with increasing load repetitions, it was continuously increasing. We also observed that the maximum compressive stress was decreasing (22-kPa to 10-kPa), there was a slight increase (3-kPa to 8-kPa) in the extension stress as the wheel approached and departed the stress gage (z = 1067 mm). We did not observe similar behaviors with the stress response at the upper heights. The change in the vertical stress with depth is shown in Figure 28.

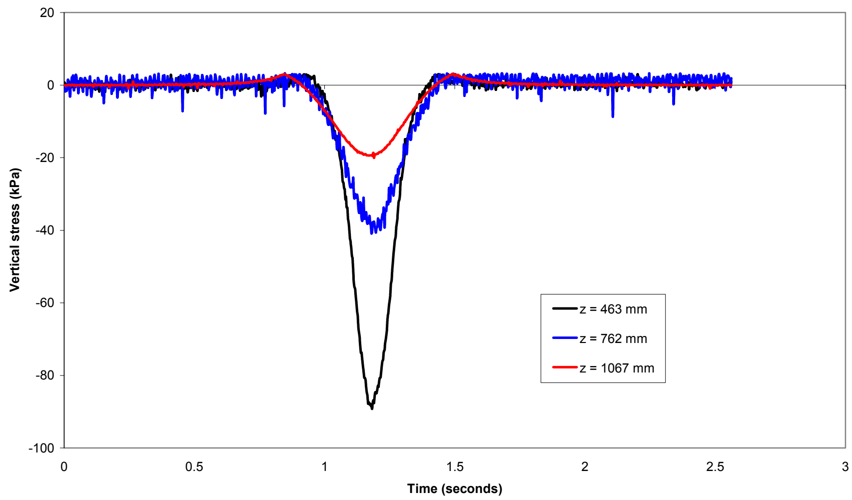

Figure 26a. Vertical stress response in the subgrade after 500 load repetitions, (62.3kN load, 721kPa tire pressure).

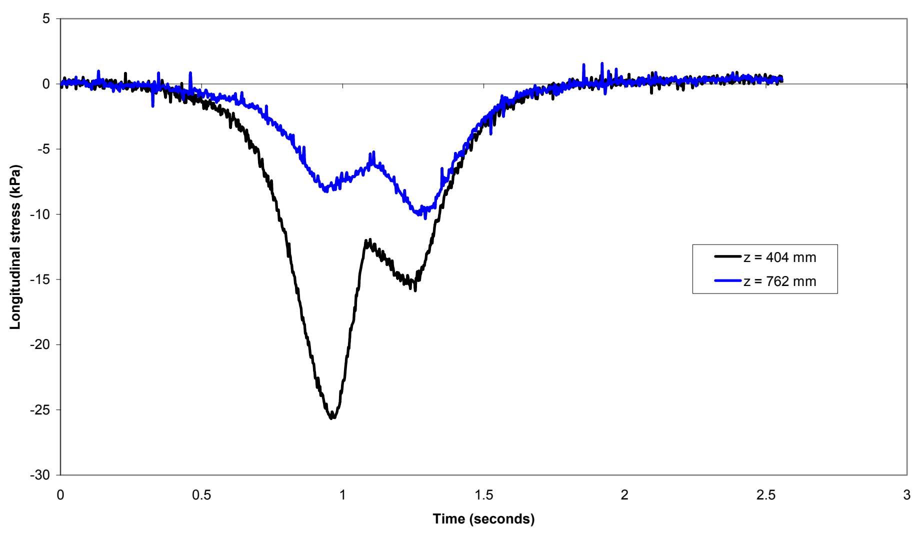

Figure 26b. Longitudinal stress response in the subgrade after 500 load repetitions, (62.3kN load, 721kPa tire pressure).

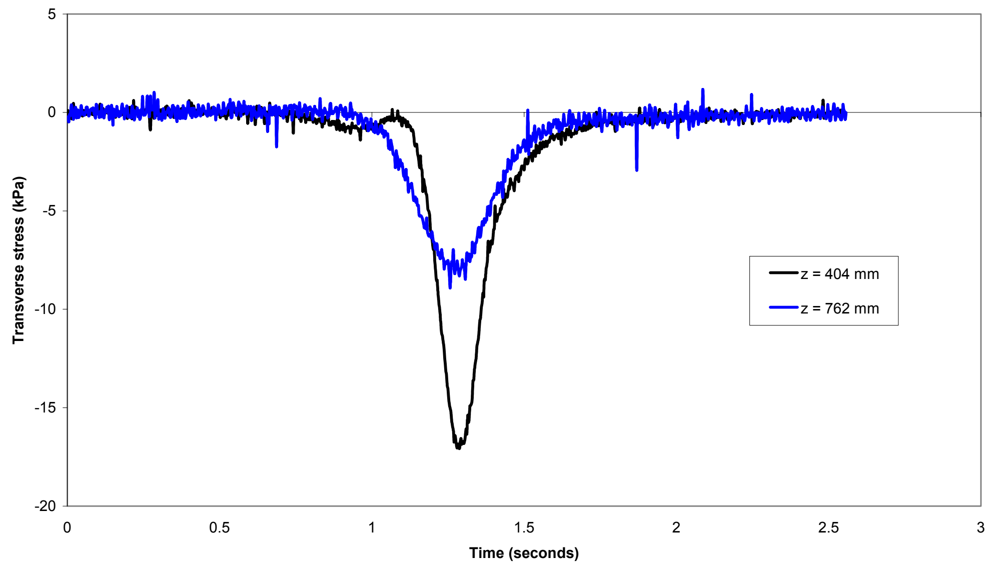

Figure 26c. Transverse stress response in the subgrade after 500 load repetitions, (62.3kN load, 721kPa tire pressure).

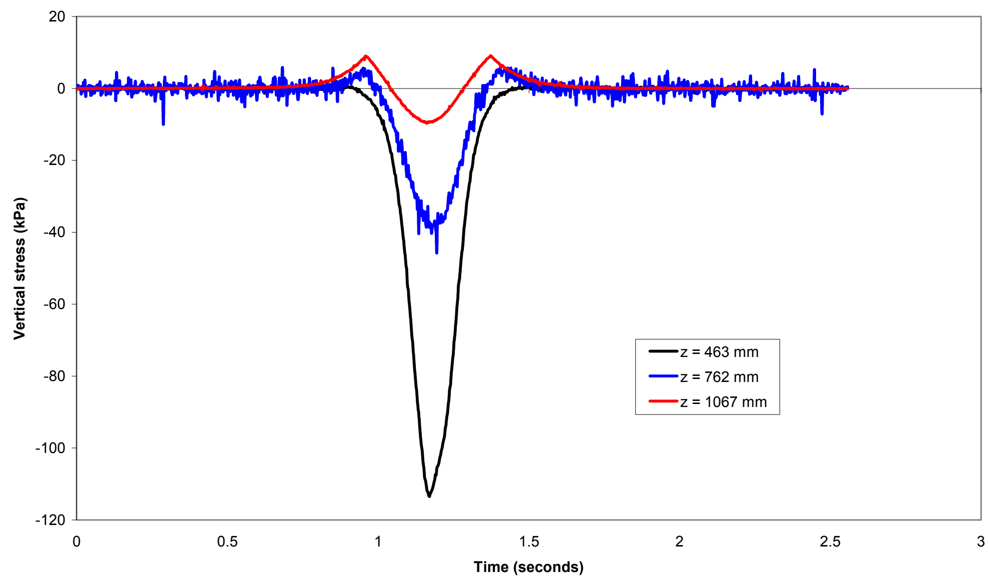

Figure 27a. Vertical stress response in the subgrade after 50000 load repetitions, (62.3kN load, 721kPa tire pressure).

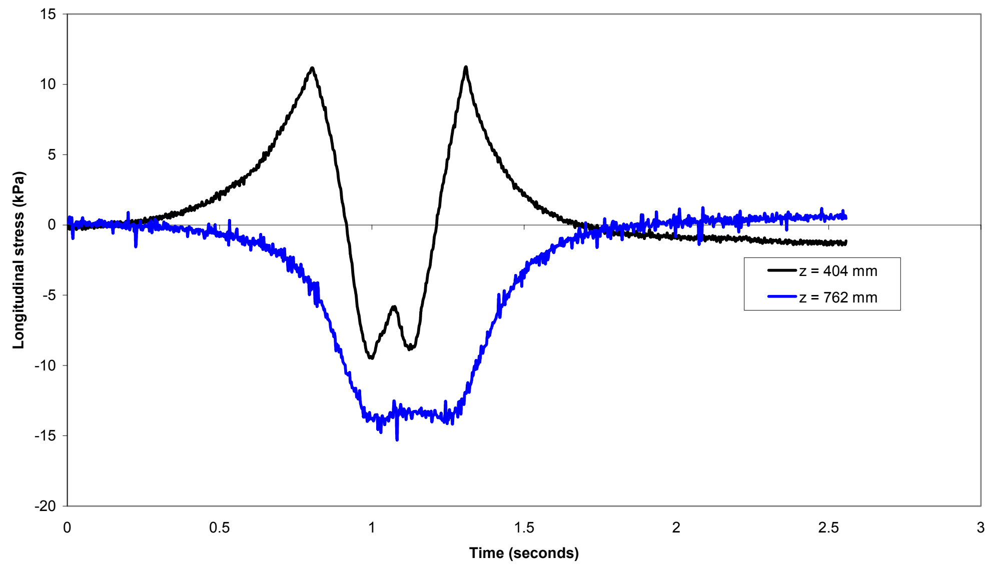

Figure 27b. Longitudinal stress response in the subgrade after 50000 load repetitions, (62.3kN load, 721kPa tire pressure).

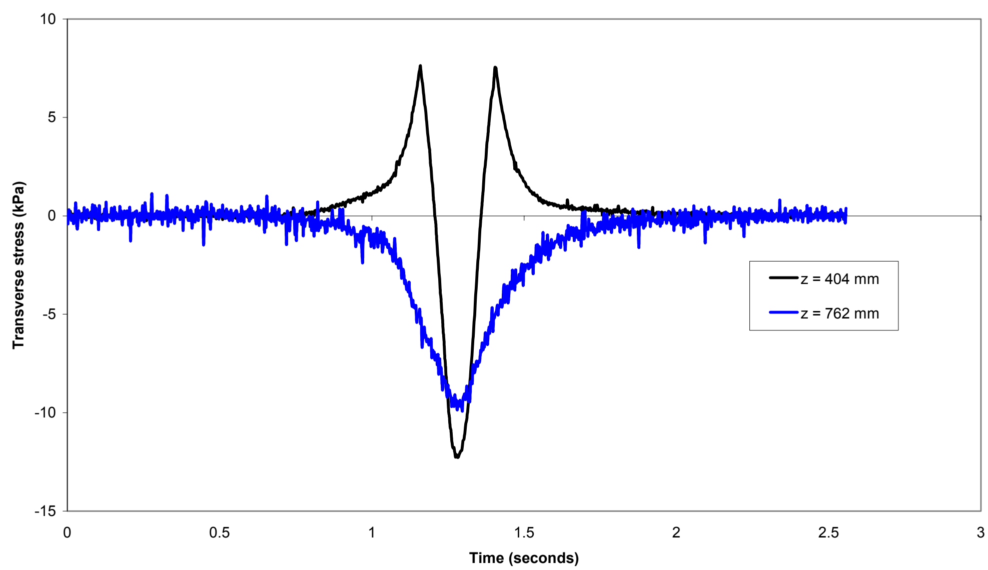

Figure 27c. Typical transverse stress response in the subgrade after 50000 load repetitions, (62.3kN load, 721kPa tire pressure).

With respect to the longitudinal stresses, measurements were taken at z = 404mm (near the top of the subgrade) and at z = 762mm. The shape of the stress response near the top of the subgrade was W-shaped, similar to what was observed in Test Section 701. We hypothesized that the W-shaped was due to the effect of the stress gage thickness. As the load passed over the stress gage, there was a drop in stress due to the thickness of the gage. At this height, the first peak stress is the maximum stress in the longitudinal direction. Typical responses are shown in Figures 26b & 27b. The stresses were compressive, but with increasing load repetitions, we found that there was an increase in the extensional stress as the wheel approached and departed the stress gage.

At z = 404 mm, the peak longitudinal compressive stress remained around 29-kPa for about 5000 load repetitions. After 5000 load repetitions, the peak compressive stress decreased non-linearly to 10-kPa, Figure 29. While the peak compressive stress decreased with load repetitions, we found that the extensional stress was increasing to about 10-kPa at the end of the test. The development of the extensional stresses with increasing load repetitions, suggest a development of an over-consolidated state in the longitudinal direction creating 'locked-in' stresses. Since we did not see these formations in the vertical & transverse directions, the repeated loading is creating an anisotropic stress state. Overall there was about 68% reduction in the peak compressive longitudinal stress at the end of the test.

At z = 762 mm, the stresses were compressive. The peak compressive stress appears to remain for a longer period of time (i.e. the curve is more flattened) with increasing load repetitions. Figure 25b & 26b. The longitudinal stress stayed around 10 until after 10,000 passes. After which the stress increased to 15-kPa, which was an increase of increase of approximately 30%, Figure 29. There were no developments of extensional stresses with increasing load repetitions as seen at the top of the subgrade.

Transverse stress measurements were taken at the same depths as the longitudinal stresses. The transverse stresses in the subgrade were compressive, Figures 25c & 26c. As with the longitudinal stresses we found that the transverse stresses at z = 404 mm, we again found that there was an increase in the extensional stress as the wheel approached and departed the stress gage with increasing load repetitions. We did not see any extensional stresses at z = 762 mm.

At z = 404 mm, the transverse stresses increased from an initial value of 18-kPa to 25-kPa at 10000 load repetitions. After 10000 load repetitions, the stresses started to decrease non-linearly to 12-kPa, Figure 30. At z = 762 mm, the transverse stress remained fairly constant at around 9kPa. An observation was made on the value of the transverse stresses at this depth being nearly the same as the longitudinal stresses, suggesting an isotropic condition in the horizontal plane.

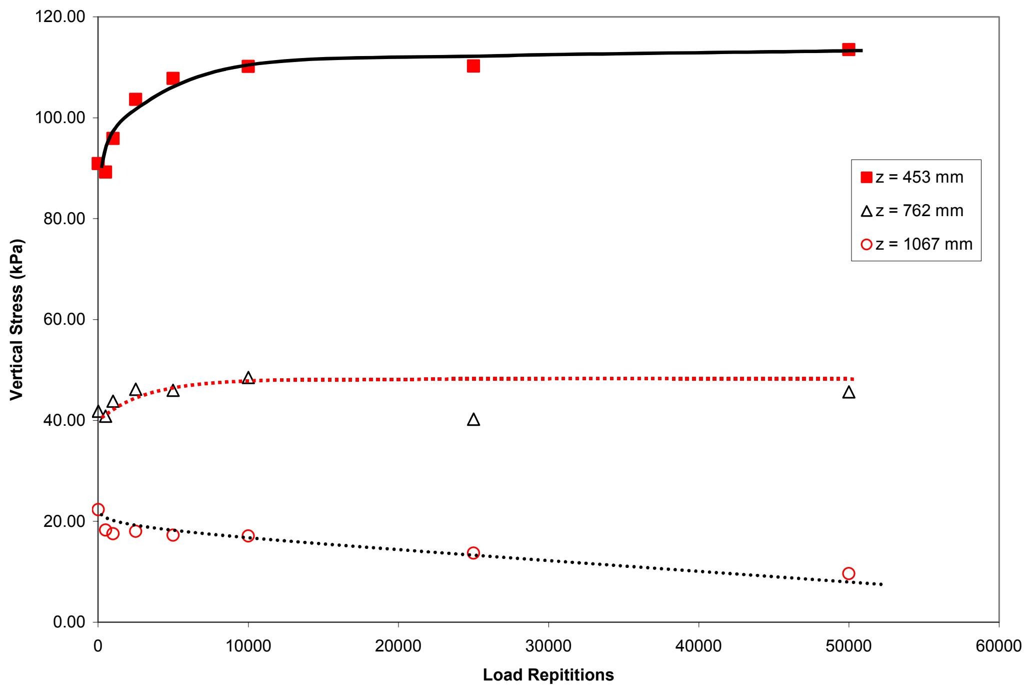

Figure 28. Development of vertical stress as a function of load repetitions and depth.

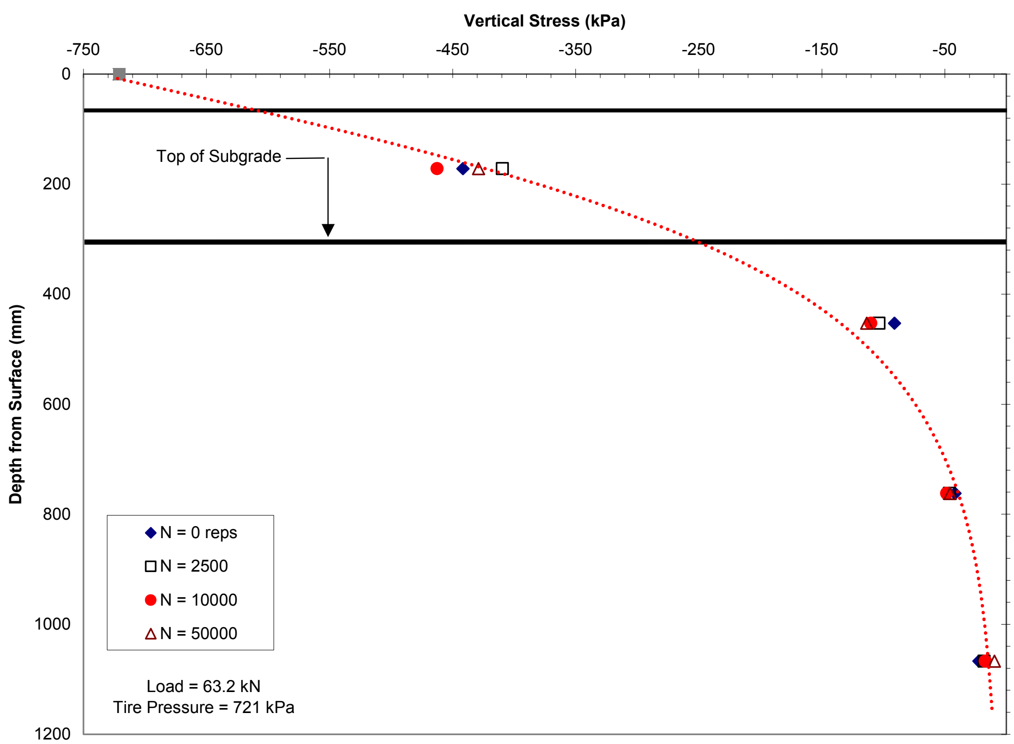

Figure 29. Distribution of stress as a function of depth & load repetitions.

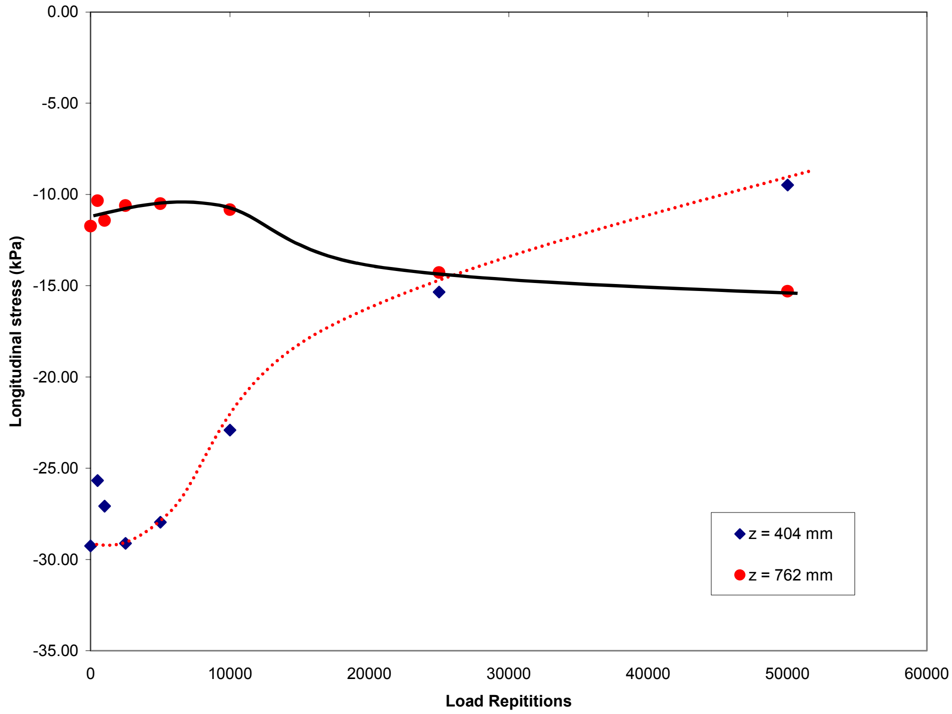

Figure 30. Development of longitudinal stresses as a function of load repetitions and depth.

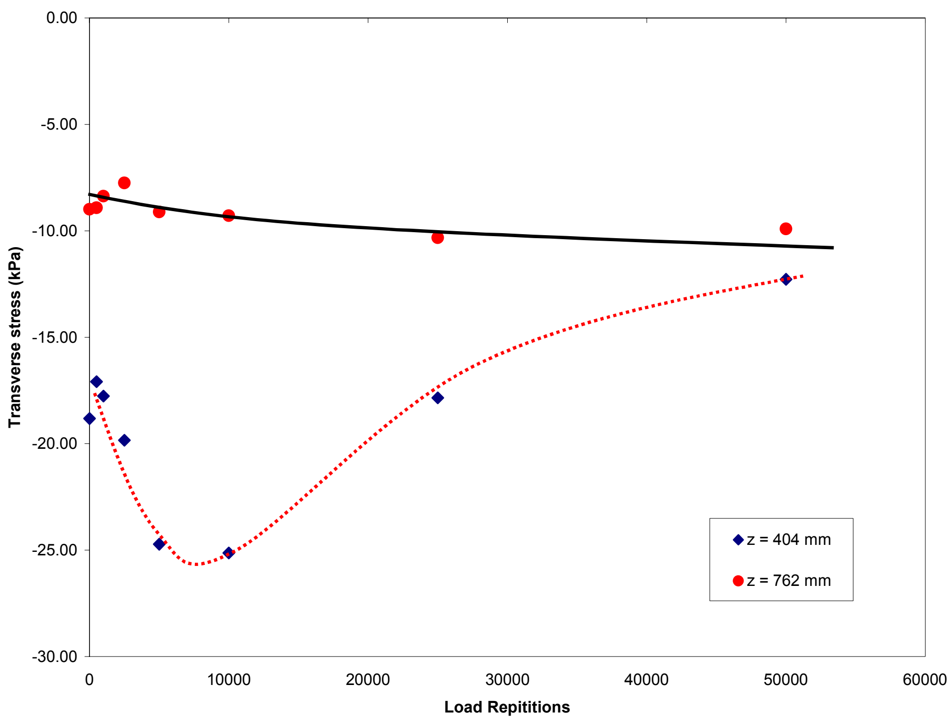

Figure 31. Development of transverse stresses as a function of load repetitions and depth.

Dynamic Strains

Vertical, longitudinal and transverse dynamic strains were measured as a function of load repetitions at the 3 wheel locations. Generally, the vertical strains were compressive, while the longitudinal and transverse strains were expansive. It was also found that in general the maximum displacements occurred when the wheel was in position 2.

The maximum displacements and strains in Table D-1 to D-10 were obtained after the data was smoothed using a 10 points averaging scheme. Displacement data are presented in the Appendix, based on comments from the report on 701(Janoo et. Al, 2000). It was suggested by some that displacements instead of strain may be the parameter of choice when developing the subgrade failure criteria. However, to be consistent with the report on 701, the discussion here will be with respect to strain. The vertical displacements were measured at physical locations of the coils, whereas the vertical strains were at the midpoints of the coil pairs. In the longitudinal and transverse directions the displacements and strains, were measured at the actual location of the coil gages. The difference between the vertical and horizontal strain measurements is about 75mm. As with TS701, three sets of measurements are reported for the longitudinal strain, initial compressive strain, maximum expansive strain and the compression strain during unloading (see Figure D-2).

Typical vertical strains in the subgrade at a given load repetition are presented in Figures 32. As expected we found the strains to decrease with depth, Figure 32 & 33.

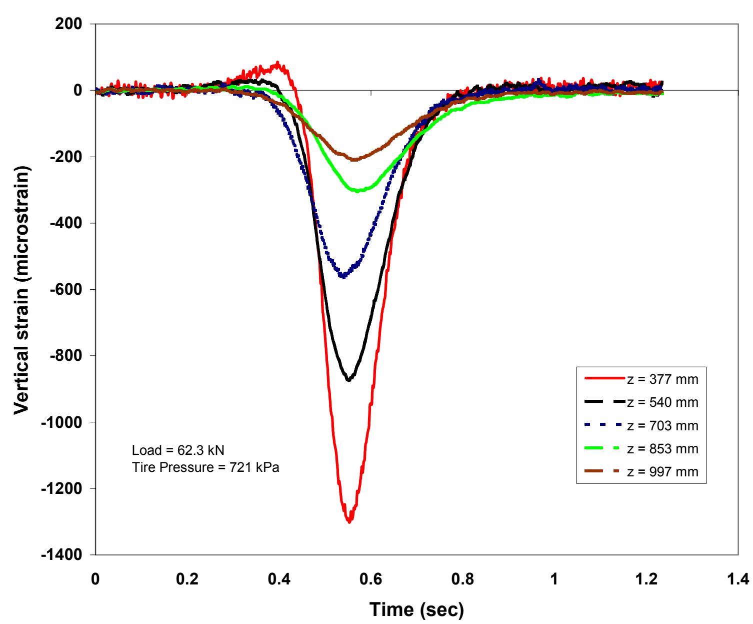

Figure 32. Typical dynamic vertical strains as a function of depth (N = 5000 reps).

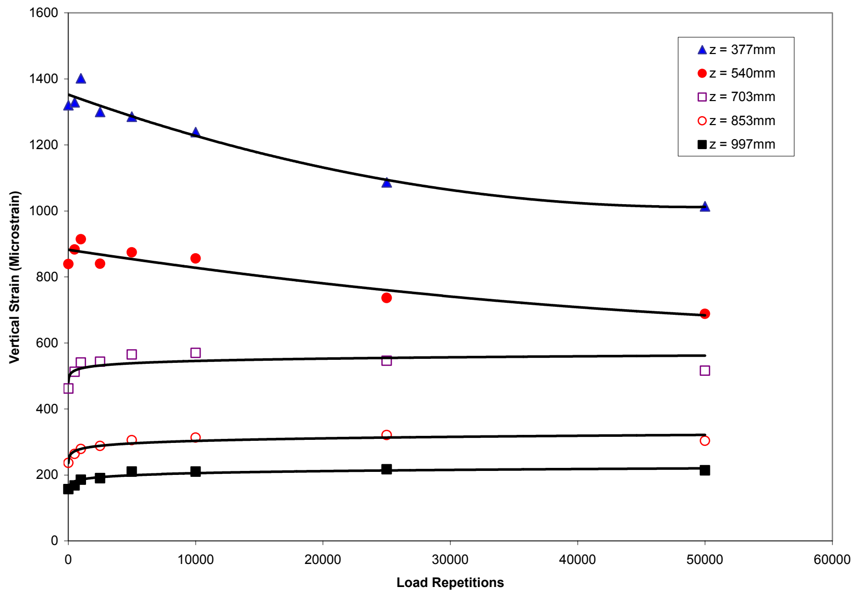

Figure 33. Vertical strains as a function of depth and load repetitions.

It was found that the displacements ranged between –0.2 mm near the top of the subgrade to about –0.02mm at a depth of 925 mm from the AC surface, (Table D-1). These displacements translated to average strains of –1400 and -170 µstrains respectively, Table D-1 and D-2. It was also found a third order polynomial fitted the change of strain with depth (Figure 33) much better than a power curve.
The development of the vertical displacements in the subgrade as a function of load repetitions on an arithmetic scale is presented in Figure 34. From Figure 34, it can be seen that the at the top of the subgrade, (approx. top 300 mm), there is a decrease in the vertical strain with increasing load repetitions. At depths below, we saw strains increasing with load repetitions, which is what we normally expect. A careful review of the displacement and strain data for the upper 300mm indicate a slight increase in the displacement (strains) up to 1000 load repetitions. After 1000 repetitions, we started to see a decrease in the strain (displacement) with increasing load repetitions. A possible reason for this subgrade stiffening may be due to movement of water under the load, leading to a localized stronger subgrade.

The data was re-plotted on a log-log scale and power curves fitted to them, Figure 35. We found that for the upper 300mm, a second order polynomial gave a better fit then a power relationship. Both relationships are presented in Table 2

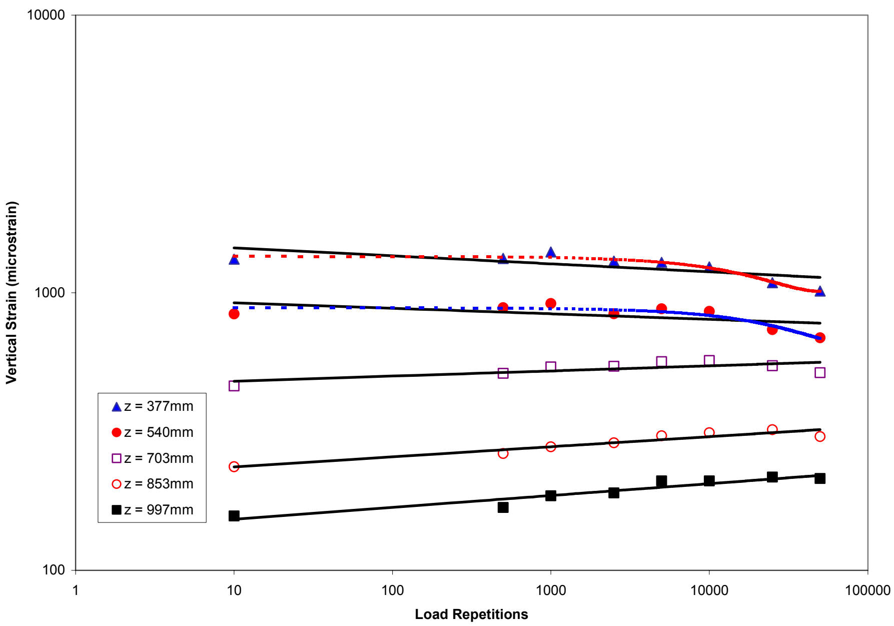

Figure 34. Change in vertical strains as a function of load repetitions in the subgrade (703C2).

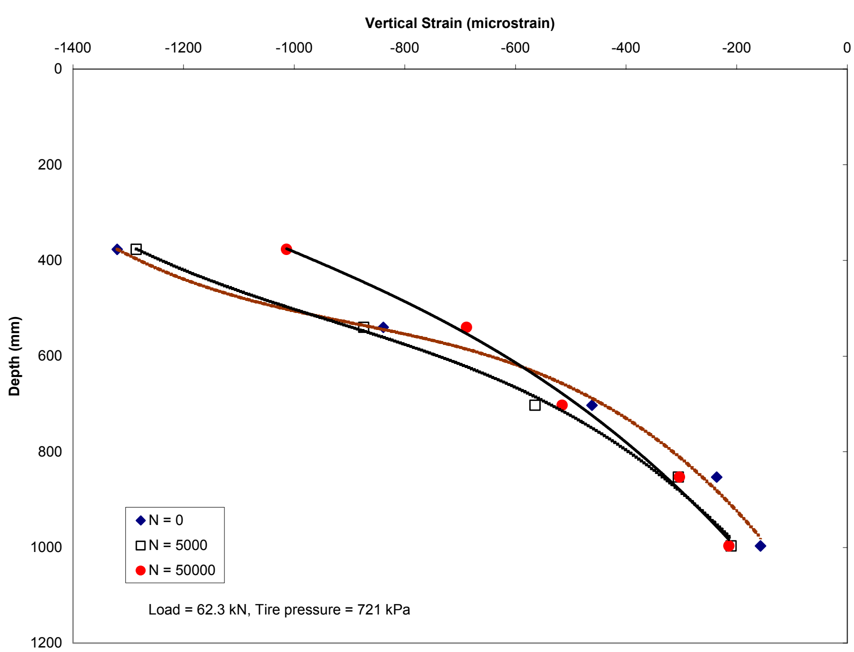

Figure 35. Change in vertical strains as a function of load repetitions (log-log scale) in the subgrade (703C2).

Table 2. Coefficients for power law curves for dynamic vertical strains

	Depth (mm)	A	n	R^2
Subgrade	377	1550	- 0.0288	0.49
	540	963	- 0.0199	0.30
	703	460	0.0184	0.53
	853	217	0.0363	0.91
	997	139	0.0426	0.90

The following second order polynomial relationships were established for the subgrade at:

Z = 377mm, $1E-07x^2-0.0139x+1352$ $R^2 = 0.95$

Z = 540mm, $4E-08x^2-0.0058x+882$ $R^2 = 0.86$

In the longitudinal direction, we found that the strains were expansive. In the subgrade, there were no compression strains as the wheel approached or left the sensor as we found in TS701. We also found that the longitudinal displacement on top of the subgrade was in the range of 8mm, Table D-3, which was significantly larger than in the other layers where the range was somewhere around 0.02 to 0.05 mm. The corresponding strains are presented in Table D-4. The changes in the longitudinal strains as a function of load repetitions are presented in Figure 36. There is an initial increase in strain with load repetition, but after 2500 load repetitions, the strains generally start to decrease with increasing load repetitions. This was similar to the vertical strain response at top of the subgrade, Figure 34. The change in the longitudinal strains at other depths are presented in Figure 37.

We observed that the longitudinal strain at z = 454mm, decreased with increasing load repetitions. This response was similar to the vertical strain response at about the same depth, Figure 34. We found a third order polynomial fitted the data quite well, Table 3. At the other depths, again similar to the vertical strain responses at about the same depths, the strain increased with increasing load repetitions. We found a power curve fitted the data reasonably well, Table 3, Figure 38.

In the transverse direction, the strains were all expansive. In the base and upper subgrade (z = 300mm), the maximum strain occurred when the load was in position 3, see Figure 20f. We were unable to measure the transverse strain at z = 454mm because of failure of the gage. Below this depth, we found that the strain was the highest when the load was in position 2. A typical set of transverse strain measurements in the subgrade is shown in Figures 39 and 40. The maximum transverse displacements and corresponding strains are presented in Table D-5 and D-6, Appendix D.

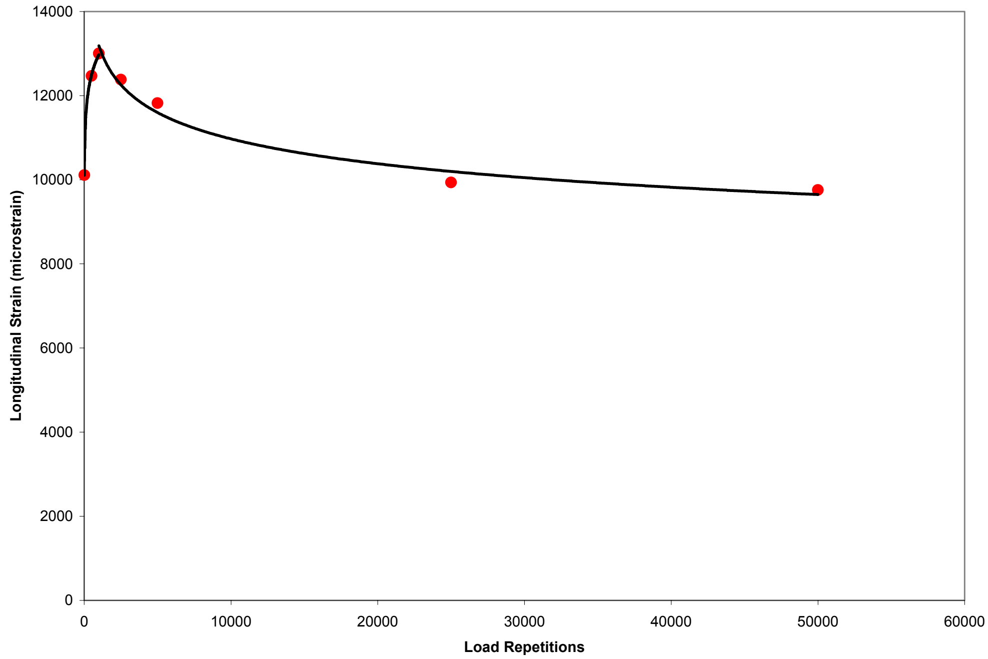

Figure 36. Change in longitudinal strain as a function of load repetitions near the top of the subgrade (z = 300mm), (703C2).

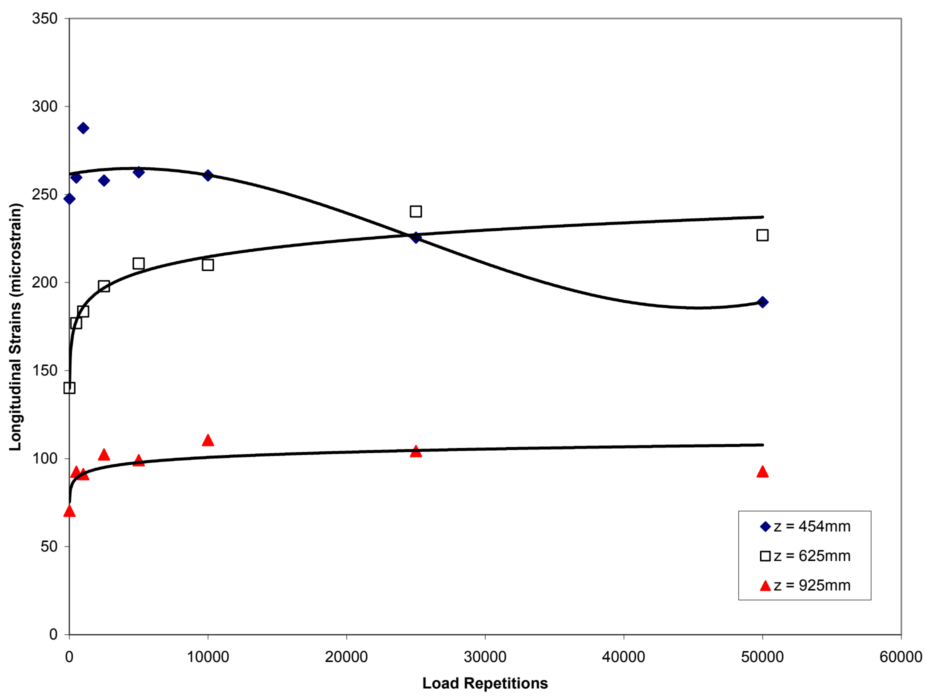

Figure 37. Change in longitudinal strain as a function of load repetitions in the subgrade (703C2).

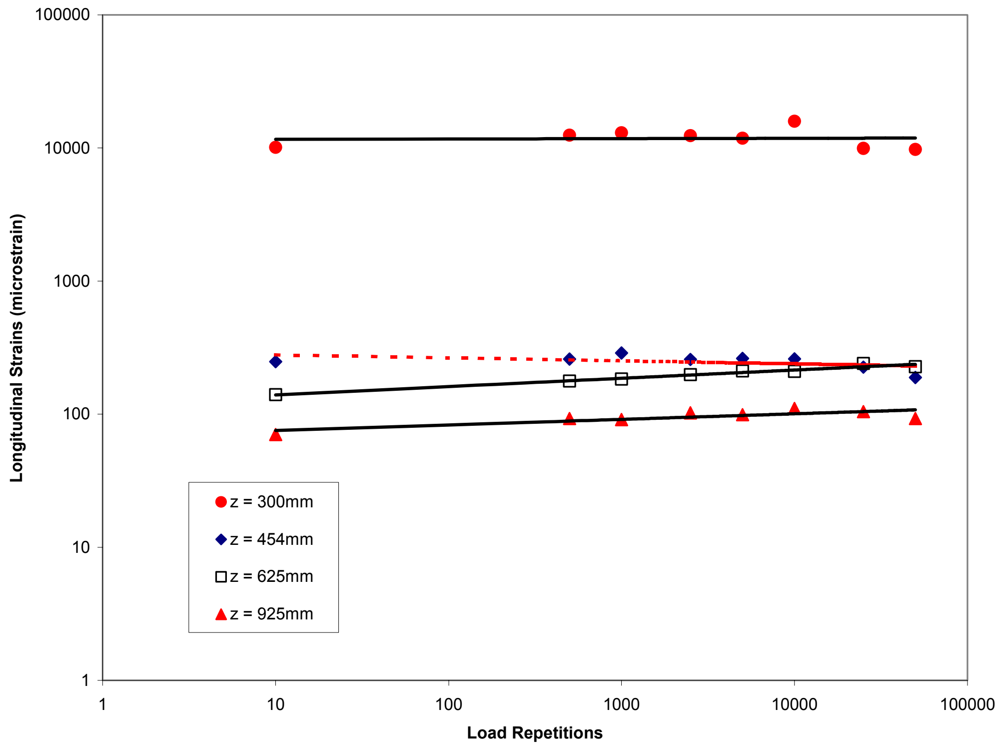

Figure 38. Change in longitudinal strains as a function of load repetitions (log-log scale) in the subgrade (703C2).

Table 3. Coefficients for power law curves for dynamic longitudinal strains.

	Depth (mm)	A	n	R^2
Subgrade	300, $N \leq 2500$	8918	.0543	0.99
	300, $N > 2500$	22904	.0799	0.98
	454	3rd Order Polynomial		
	625	121	0.0620	0.97
	781			
	925	68	0.0420	0.67

For z = 454 mm, the following polynomial equation can be used to estimate the strains;
y = 2E-12x3 - 2E-07x2 + 0.0015x + 261.55

where,
y = longitudinal strain (µstrain)
x = load repetitions

The maximum transverse strains ranged between 140 and 180 μstrains near the top of the subgrade and dropped to between 75 and 100 μstrains at z = 925 mm from the surface. The data shows that in the top 325mm of subgrade, the transverse strain remains fairly constant. The change in the transverse strains as a function of load repetitions and depth are presented in Figures 41 and 42. The change of the transverse strain with depth and load repetitions are shown in Figure43. Power curves were used to fit the strain versus load repetition data (Figure 42) and the coefficients for the power curves are presented in Table 4.

Table 4. Coefficients for power law curves for dynamic transverse strains.

	Depth (mm)	A	n	R^2
Subgrade	300	123.7	0.0377	0.85
	454			
	625	123.7	0.0377	0.85
	781	101.9	0.0390	0.79
	925	69.75	0.0282	0.55

Permanent Strains

The permanent deformations and strains were obtained from static measurements of the εmu coils. The measurements are presented in Tables D-7 & 8, Appendix D. The vertical deformations at the end of the test ranged between –0.3 to- 4mm in the various layers. The total vertical deformation of the layers at the end of the test exceeded -13mm as no measurements were available in the subgrade at a depth of 540mm from the surface, Table D-7. The variation of the vertical permanent deformation with depth as a function of load repetitions is shown in Figure 44. As seen in the figure, a significant amount of deformation occurred in the base. Approximately, 40% of the deformation occurred in the base course. We also found that approximately 20% of the deformation occurred in the asphalt concrete layer.

The development of vertical strains as a function of load repetitions are presented in Figure 45 and on a log-log scale in Figure 46. Power curves were fitted to the data in Figure 46, and the coefficients are presented in Table 5. For plotting purposes, the vertical strains were converted to positive values. The strain in the surface layer and the top base layer were quite similar, Figure 45. The strain in the lower part of the base was smaller than the top subgrade layer.

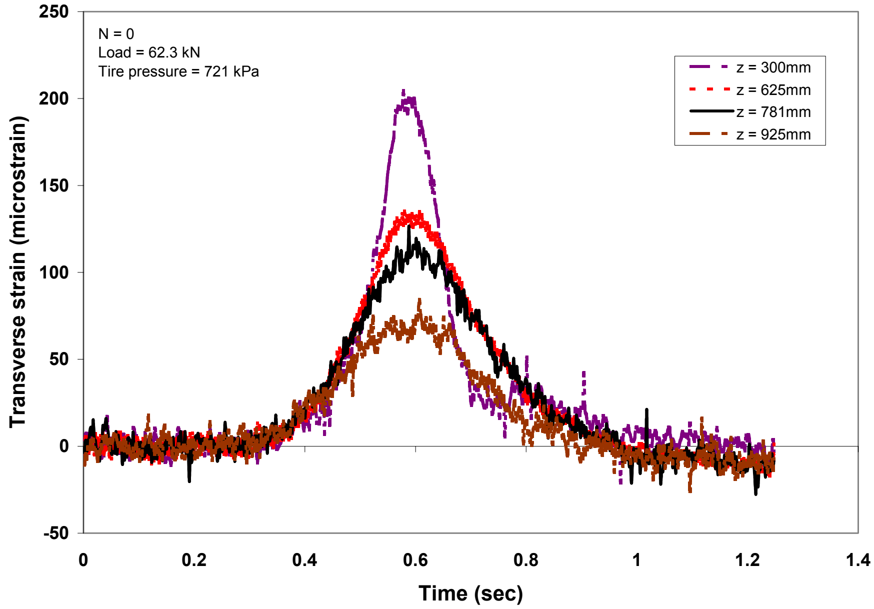

Figure 39. Typical dynamic vertical strains as a function of depth (N = 0 reps).

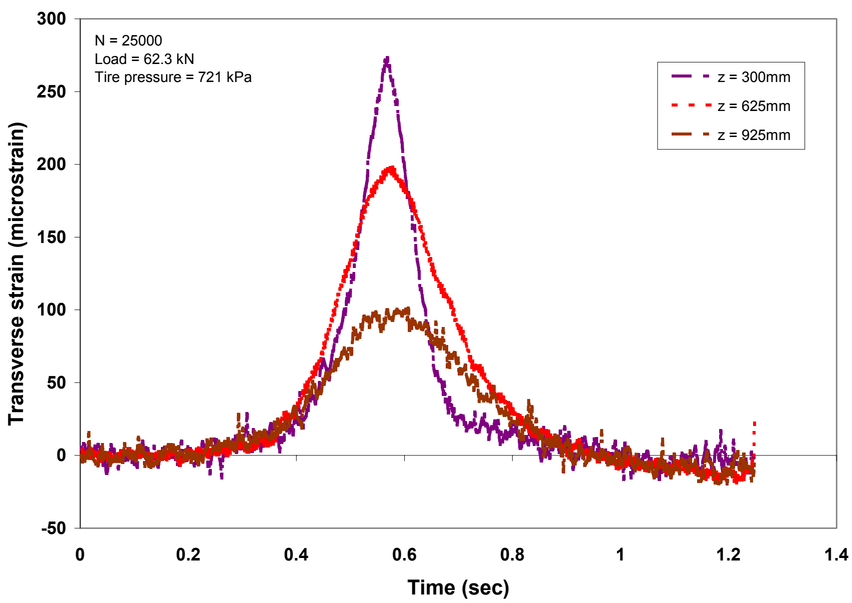

Figure 40. Typical dynamic vertical strains as a function of depth (N = 25000 reps).

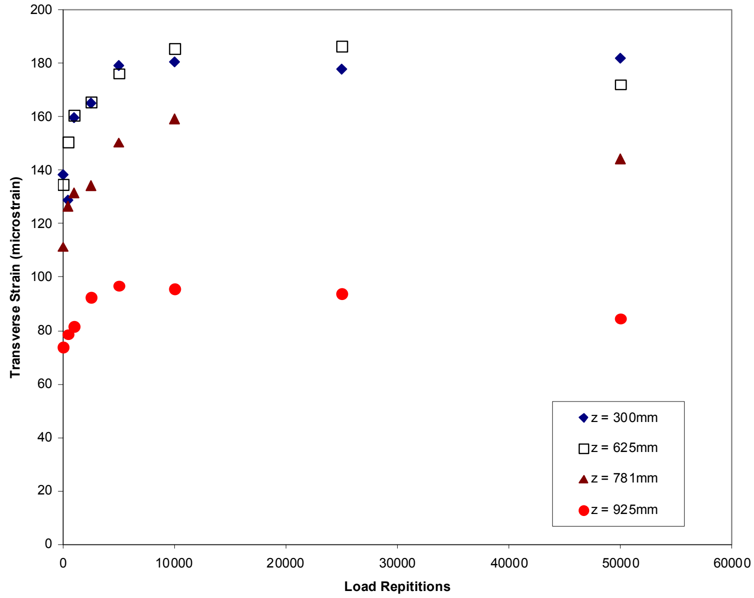

Figure 41. Change in transverse strain as a function of load repetitions in the subgrade (70cC2).

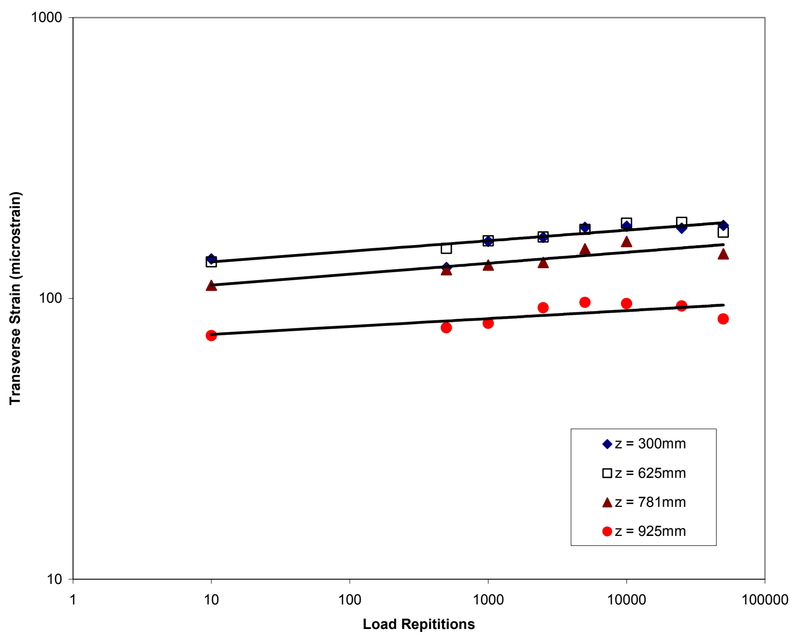

Figure 42. Change in transverse strains as a function of load repetitions (log-log scale) in the subgrade (703C2).

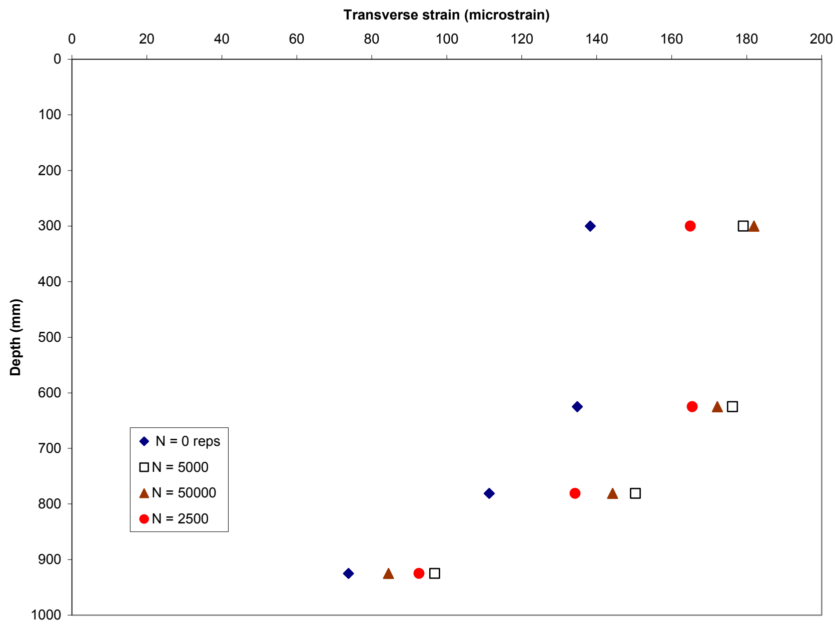

Figure 43. Transverse strains in the subgrade as a function of depth and load repetitions.

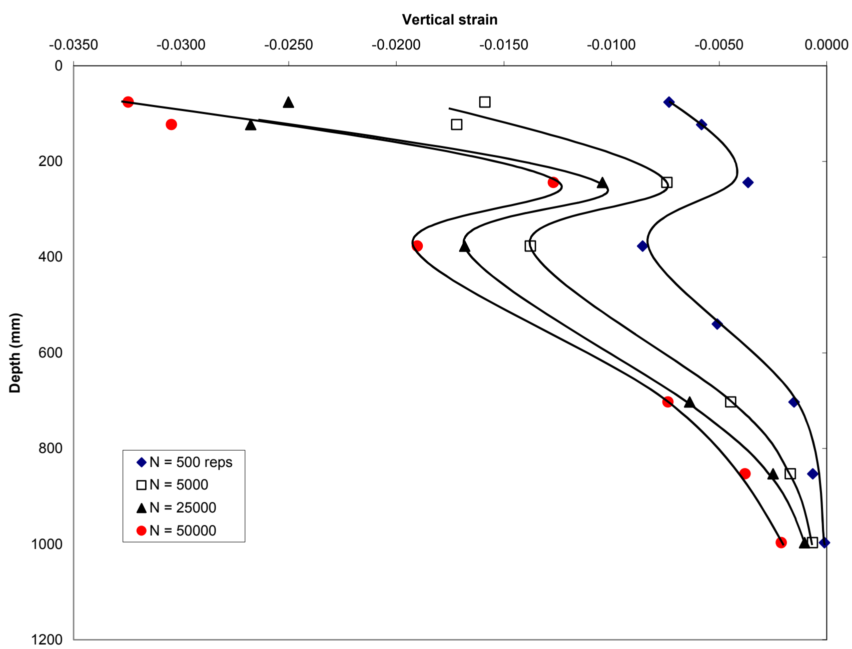

Figure 44. Vertical strain as a function of depth and load repetitions.

Table 4. Coefficients for power law curves for permanent vertical strains.

Layer	A	n	R^2
Surface	0.0009	0.3280	0.99
Base (z = 123mm)	0.0008	0.3436	0.96
Base (z = 244mm)	0.0008	0.2619	0.99
Subgrade (z = 377mm)	0.0033	0.1635	0.97
z = 540mm			
z = 703mm	0.0003	0.2926	0.88
z = 853mm	8.00E-05	0.3576	0.95
z = 997mm	3.00E-06	0.5932	0.86

In the longitudinal direction, we were measuring extremely high deformations (in the range of 1000 to 1200 mm) at the top of the subgrade. This was outside the calibration range and the data was not reported. We also found similar deformations in the subgrade at z = 781mm. High deformations were also noted at the bottom of the base at 2500 and higher load repetitions. With the remaining data, we did not see any significant increase in strain in the subgrade with increasing load repetitions, Figure 47. In the transverse direction, we also found that the transverse strains remained fairly constant with increasing load repetition in the subgrade, Figure 48. The exception was in the bottom measurement in the subgrade where it was extremely small.

Surface Profile Measurements

The variation in rut depth in the longitudinal direction started around 27% at the beginning of the test and was in the vicinity of 14% at the end of the test. As seen in Figure 50, most of the variation at the locations 7 to 9.

A comparison of the total rut depth measured from the profilometer and strain coil gages is shown in Figure 51. The maximum difference between the 2 sets of data is approximately 3mm. Note that vertical permanent deformation data from z = 454mm in the subgrade was unavailable and has contributed to this difference.

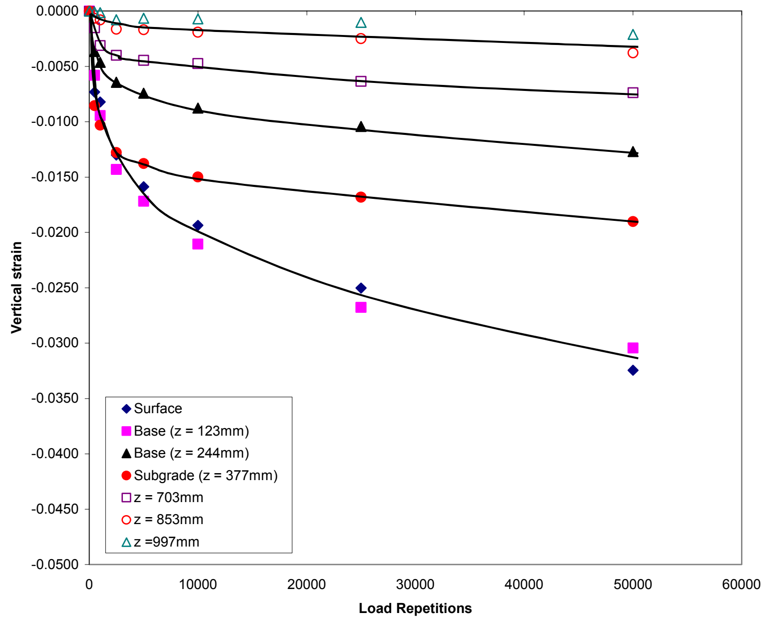

Figure 45. Change in vertical permanent strains as a function of load repetitions in the base & subgrade (703C2).

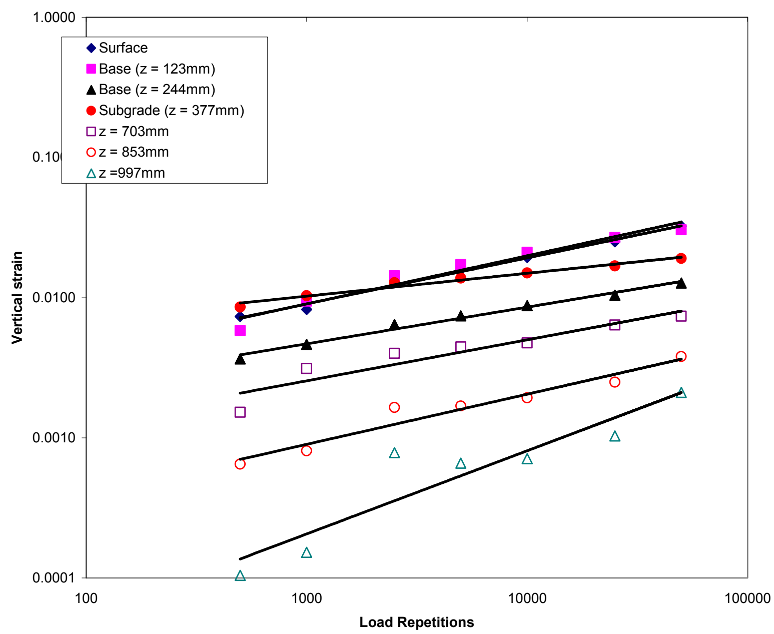

Figure 46. Change in vertical permanent strains as a function of load repetitions (log-log scale) in the base & subgrade (703C2).

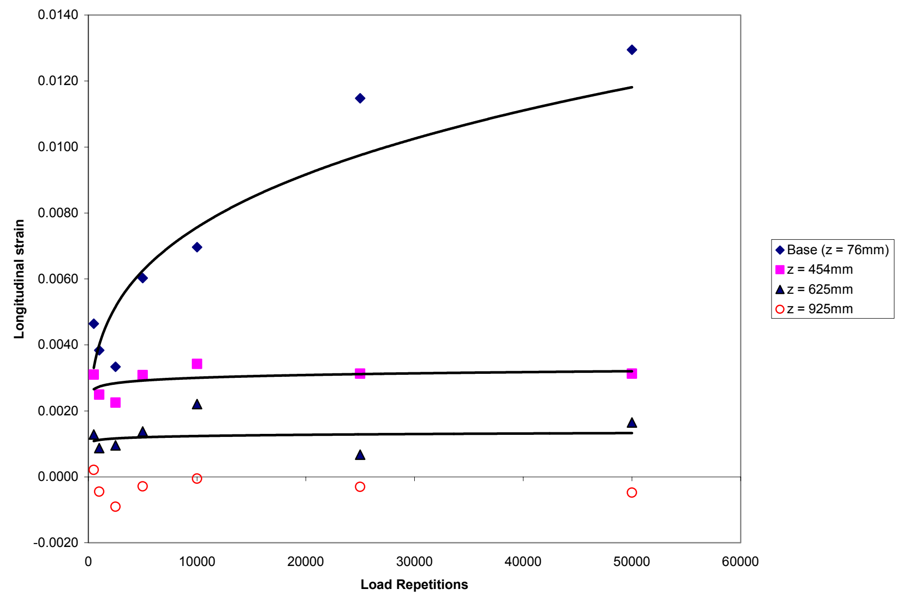

Figure 47. Change in longitudinal permanent strains as a function of load repetitions in the base & subgrade (703C2).

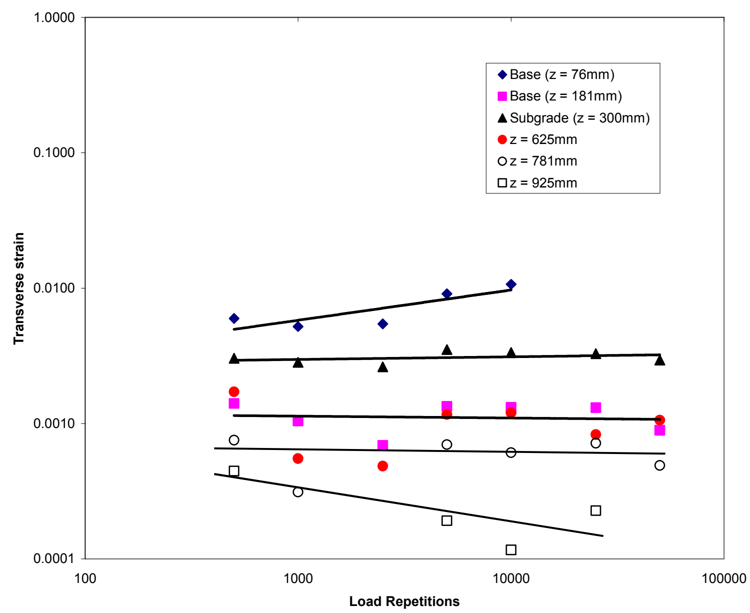

Figure 48. Change in transverse permanent strains as a function of load repetitions in the base & subgrade (703C2).

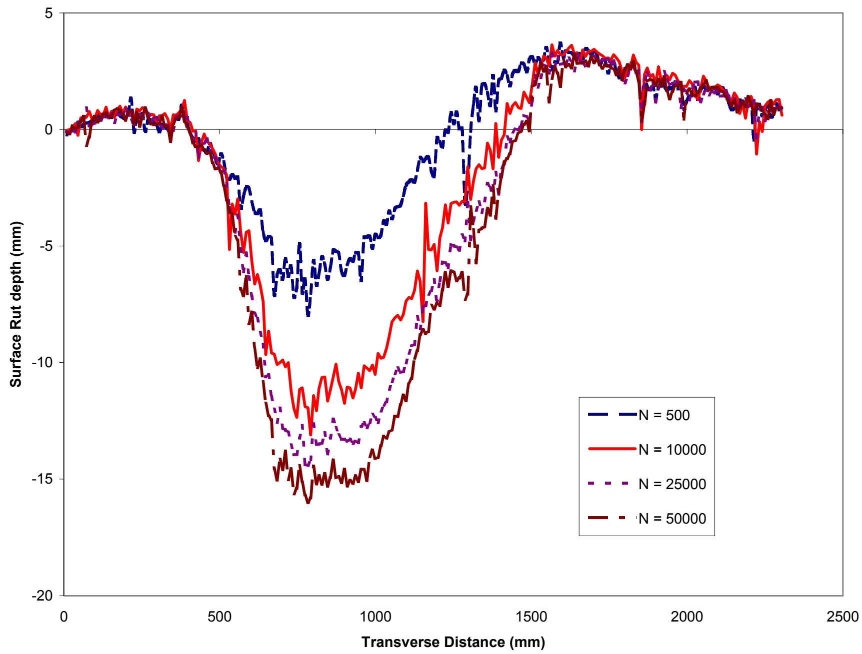

Figure 49. Typical rut depth response as a function of load passes.

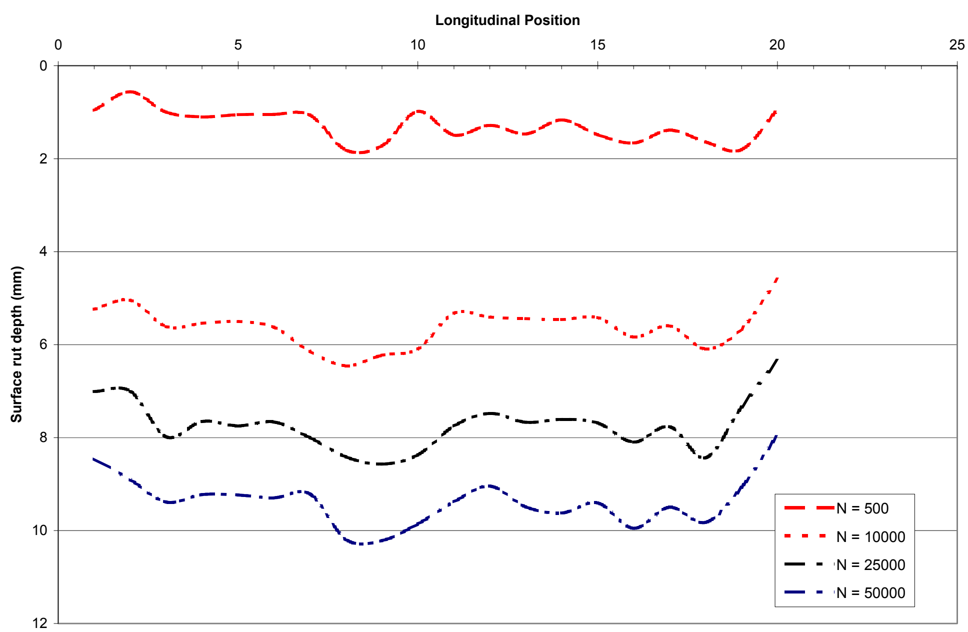

Figure 50. Longitudinal surface rutting as a function of load repetitions.

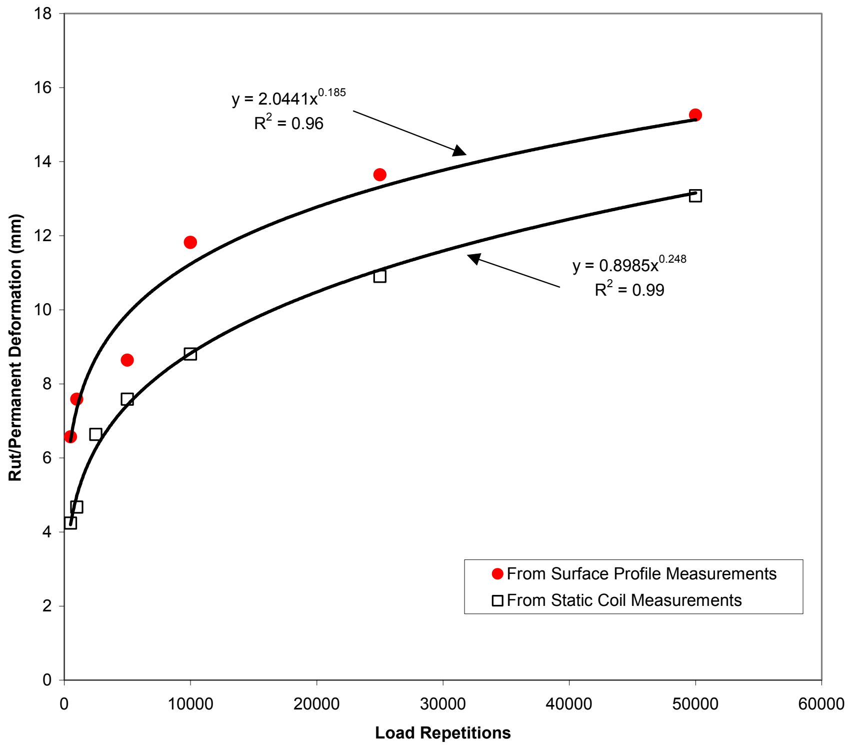

Figure 51. Comparison of total pavement deformation between profilometer and coil gage systems.

703C3

Testing of window 703C3 began on October 15, 1998 and ended on November 16, 1998. Based on load measurements from the HVS and tire pressure monitoring during the tests, Figure 52, the mean test load was 62.2-kN with a COV of 0.9 %. No tire pressure measurements were taken due to failure of the tire pressure sensors. However, tire pressures were checked periodically and was set at 690-kPa.

The average sub-surface temperature in the test section was 17.8 °C with a COV of 3.1%. The average moisture content in the test section during the test was 13.7 % with a COV of 5.1%, Figure 53. The target moisture content during construction was 15 ± 2%. The nearest VITEL gage to the test window is located at a depth of 910mm from the surface. Unfortunately, due to measurement errors, data was not collected from this gage until day 12. Based on the other gages, we expect a similar trend. Note that the sudden increase in moisture content is about 0.5% with the exception at z = 610 mm, where the increase is about 2%. We believe the increase is not from the loading as the gage at z = 610mm is located near window C4. Window C4 (see Figure 12a).

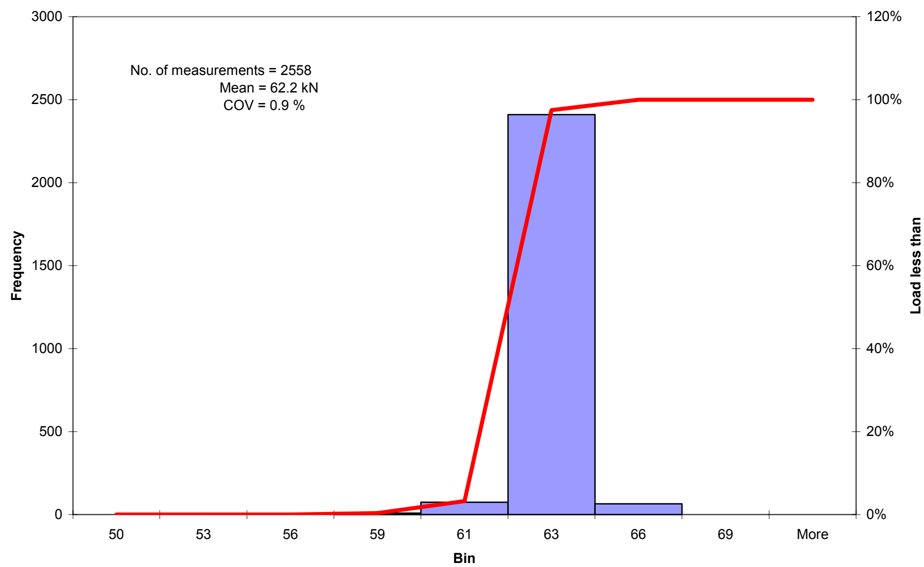

Figure 52. Statistical presentation of test loads on 703C3.

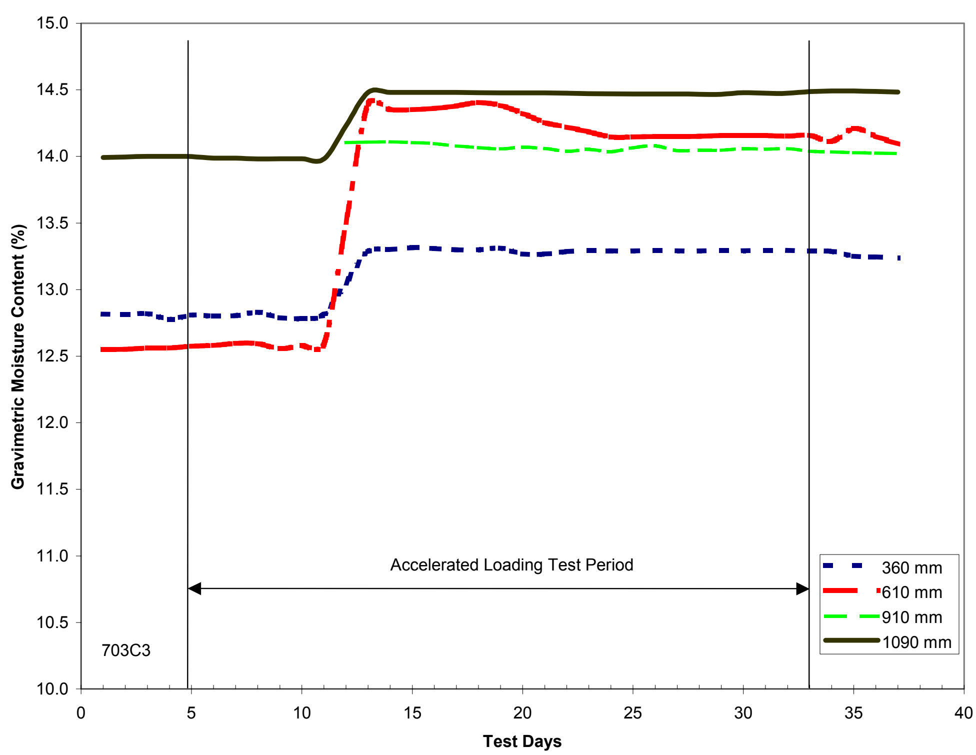

Figure 53. Distribution of moisture content in test section during testing of 703C3.

Dynamic Stress

Stress measurements were made at the top of the subgrade, Figures 12c & d. Three DYNATEST pressure cells were also installed to measure the vertical, longitudinal and transverse dynamic stresses. These cells were installed at a depth of 160mm from the surface. There were problems with the transverse stress measurements and during the early part of the longitudinal stress measurements. The shape of the vertical and longitudinal stress response curves were similar to those in 703C2, Figure 26. Maximum stresses from the test are presented in Table 5. Negative values indicate compressive stress. With respect to the vertical stress near the top of the subgrade (z = 453 mm), after an initial decrease, the stresses stayed fairly constant until after 100000 passes, where it increased to slightly higher then its initial value, Figure 54.

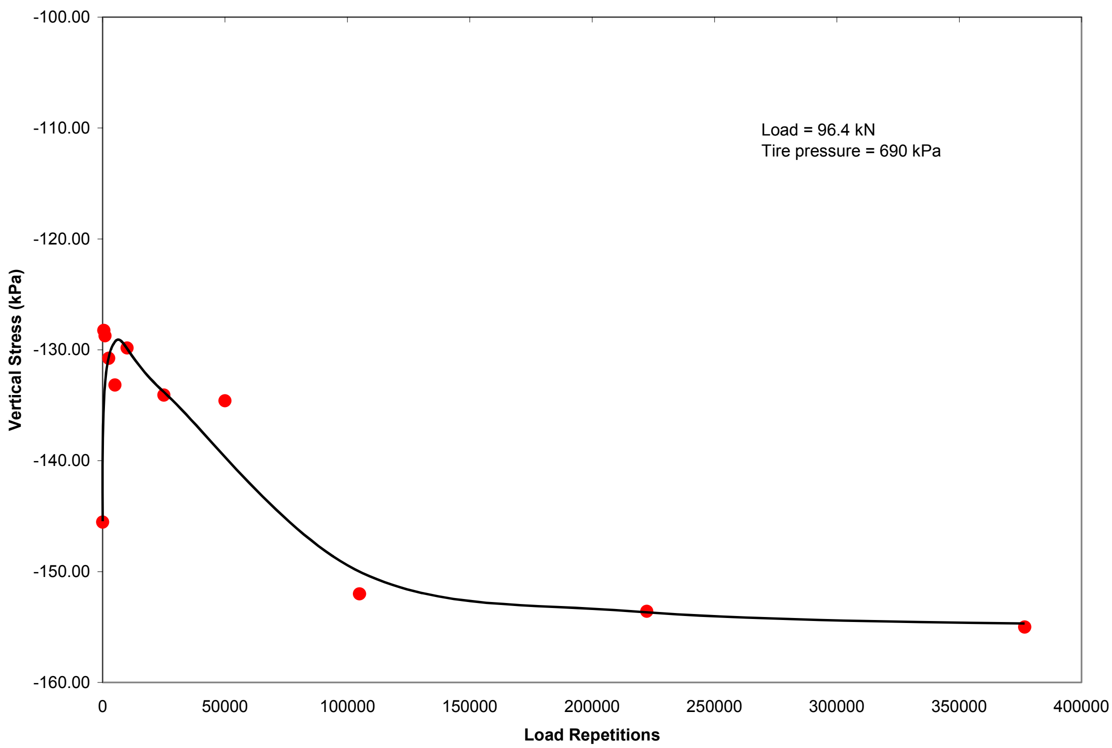

Figure 54. Stress development at the top of the subgrade as a function of load repetitions (703C3).

With respect to the longitudinal stresses, measurements were taken at z = 404mm (near the top of the subgrade). The stresses were compressive and we did not find any significant extensional stresses as the wheel approached and departed the stress gage with increasing load repetitions. The peak longitudinal compressive stress initially decreased with increasing load repetition. After 50000 passes, the stresses started to increase and remained fairly constant after about 200000 passes at 18-kPa. This is close to the initial longitudinal stress.

Table 5. Maximum stress at the top of the subgrade in the vertical & longitudinal directions as a function of load repetitions.

Load Repetitions	Vertical			Longitudinal		
	Position 1	Position 2	Position 3	Position 1	Position 2	Position 3
0	-87.50	-145.54	-144.76			
500	-72.28	-128.24	-128.40			
1000	-74.19	-128.75	-127.96			
2500	-74.99	-130.76	-130.81			
5000	-77.34	-133.17	-129.09	-13.30	-18.88	-19.03
10000	-73.67	-129.83	-128.67	-12.68	-18.29	-18.63
25000	-78.84	-134.08	-130.78	-12.28	-17.55	-17.78
50000	-78.93	-134.59	-132.38	-7.47	-11.63	-11.84
105000	-92.77	-152.01	-148.09	-7.23	-11.14	-13.11
222340	-95.96	-153.59	-149.11	-11.12	-15.53	-17.00
376750	-97.81	-155.00	-153.30	-11.87	-16.14	-17.64

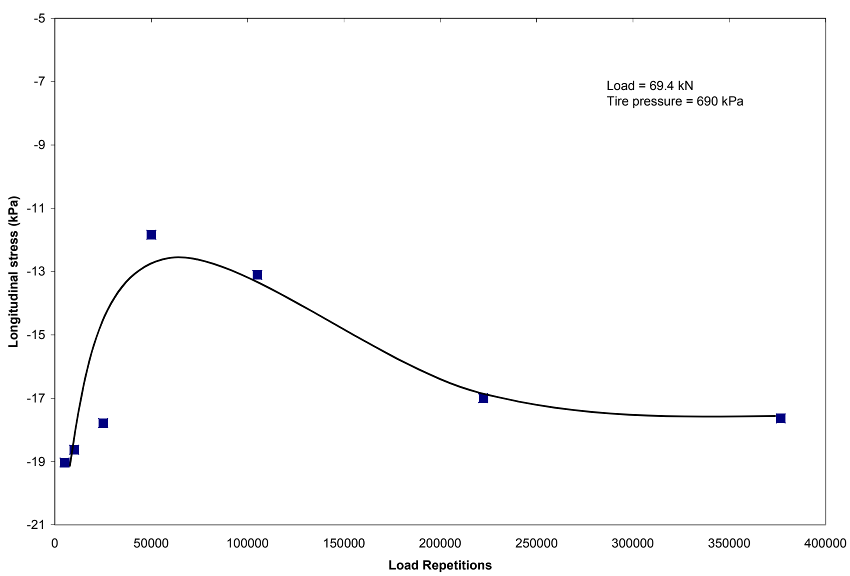

Figure 55. Longitudinal stress at top of the subgrade as a function of load repetition (703C3).

Dynamic Strains

As before, vertical, longitudinal and transverse dynamic strains were measured as a function of load repetitions at the 3 wheel locations. Generally, the vertical strains were compressive, while the longitudinal and transverse strains were expansive. It was also found that in general the maximum displacements (strains) occurred when the wheel was in position 2.

The maximum displacements and strains in Table E-1 to E-10 were obtained after the data was smoothed using a 10 points averaging scheme. As with other windows and test sections, in the longitudinal and transverse directions the displacements (strains), were measured at the actual location of the coil gages. The difference between the vertical and horizontal strain measurements is about 75mm below the horizontal strain. As with TS701, three sets of measurements are reported for the longitudinal strain, initial compressive strain, maximum expansive strain and the compression strain during unloading (see Figure D-2).

With respect to the vertical displacements and strains, the measurement system failed (faulty wiring) and the problem was not caught until after 10,000 passes. Other problems also occurred with the HVS system during the no-load measurements. These measurements were necessary for converting the voltages from the εmu coils to displacements. Additional details can be found in Janoo et. Al., 1999. At 25,000 passes and after, the vertical displacement measurements were taken through the εmu amplifiers dedicated for the transverse measurements. The displacements and strains are presented in Appendix E, Tables E-1 and E- 2. Again, as before, the maximum displacements (strains) occurred when the wheel was in position 2.

Based on the limited data, it was found that the displacements ranged between –0.1 mm near the top of the subgrade to about –0.03mm at a depth of 909 mm from the AC surface, (Table E-1). These displacements translated to average strains of –800 and -200 µstrains respectively, Table E-2.

The development of the vertical strains in the subgrade as a function of load repetitions on an arithmetic scale is presented in Figure 56. Note that in Figure 56, trends were drawn based on experience from other test sections and windows. Based on these trends, estimates were made for the strains at 500, 1000, 2500, 5000 and 10000 passes. The estimated data from Figure 56 and the initial strain prior to testing are shown in Table 6. The estimated values are italicized. The initial strain were estimated based on previous tests. We found that on the average the initial strain was between 80 to 86% of the strains measured at 500 load repetitions.

Using the data in table 6, the data was re-plotted on a log-log scale and power curves fitted to them, Figure 57. The open data points in Figure 57 are the estimated data. The coefficients for the power curves are presented in Table 7.

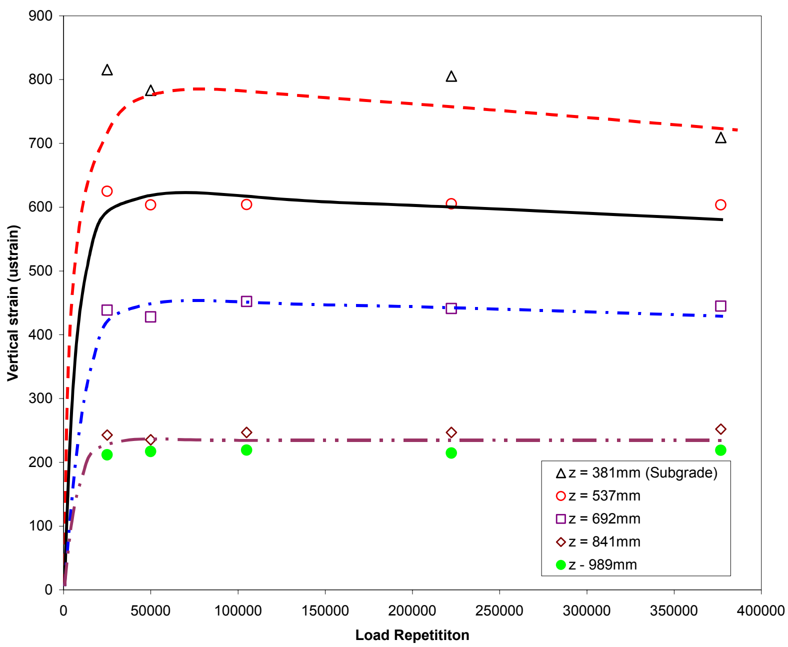

Figure 56. Change in vertical strains as a function of load repetitions in the base & subgrade (703C3).

Table 6 Maximum subgrade vertical strain data from TS703C3.

Repetitions	z = 381 mm	z = 537 mm	z = 692 mm	z = 841 mm	z = 989 mm
0	*-623*	*-432*	*-353*	*-202*	
500	*-700*	*-540*	*-420*	*-230*	
1000	*-775*	*-620*	*-450*	*-240*	
2500	*-780*	*-620*	*-455*	*-239*	
5000	*-760*	*-625*	*-440*	*-240*	
10000					
25000	-816	-625	-439	-243	-212
50000	-783	-604	-428	-235	-217
105000		-604	-452	-247	-219
222340	-805	-605	-441	-247	-215
376750	-709	-603	-445	-252	-219

Table 7. Coefficients for power law curves for dynamic vertical strains

	Depth (mm)	A	n	R^2
Subgrade	381	645	0.017	0.43
	537	464	0.026	0.54
	692	372	0.017	0.52
	841	204	0.017	0.78
	989	204	0.017	0.78

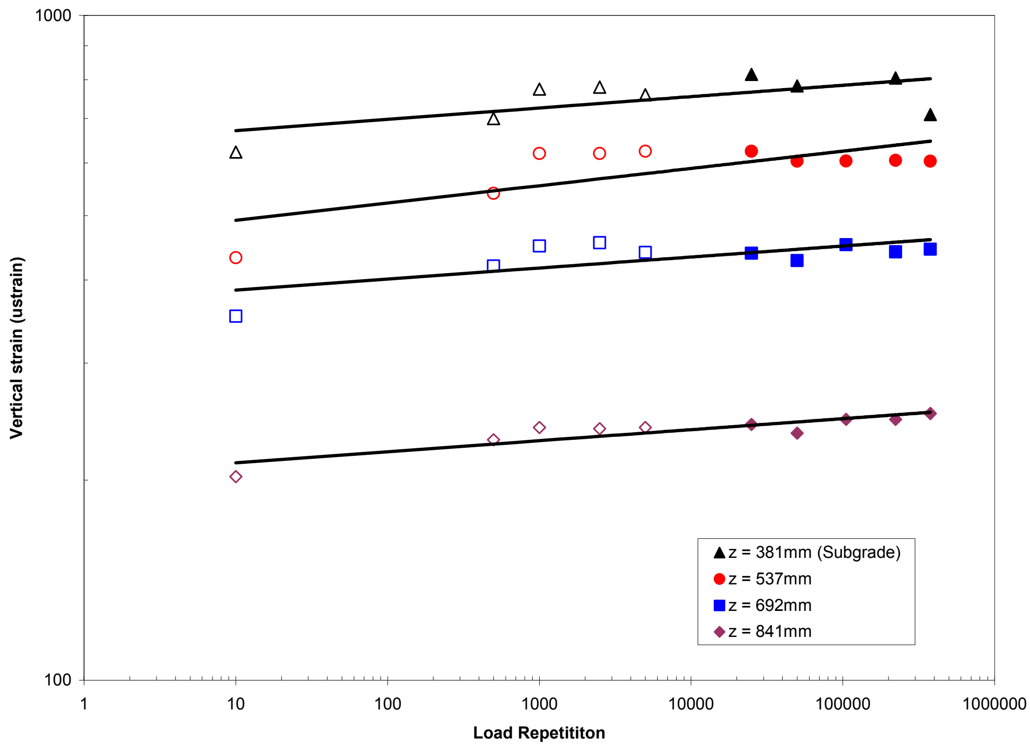

Figure 57. Change in vertical strains as a function of load repetitions (log-log scale) in the subgrade (703C3).

In the longitudinal direction, we found that the strains (displacements) were compressive as the wheel approached the gages. When the wheel was on top of the gages, the strains (displacements) were expansive. As the wheel moved away from the gages, the strains (displacements) became compressive again. The compressive strains (displacements) at the tail end usually were smaller then the approach end. The maximum strains (displacements) are presented in Appendix E, Tables E-2 to E-7. As before, the maximum strains (displacements) occurred when the wheel was in position 2.

The changes in the longitudinal strains as a function of load repetitions are presented in Figure 58. As with TS701, the longitudinal strains in Figure 58 is the absolute sums of strains A and B, (Figure E-1, Appendix E). There is an initial sharp increase in strain with load repetition, but after 50000 load repetitions, the strain gradients are generally shallow with increasing load repetitions.

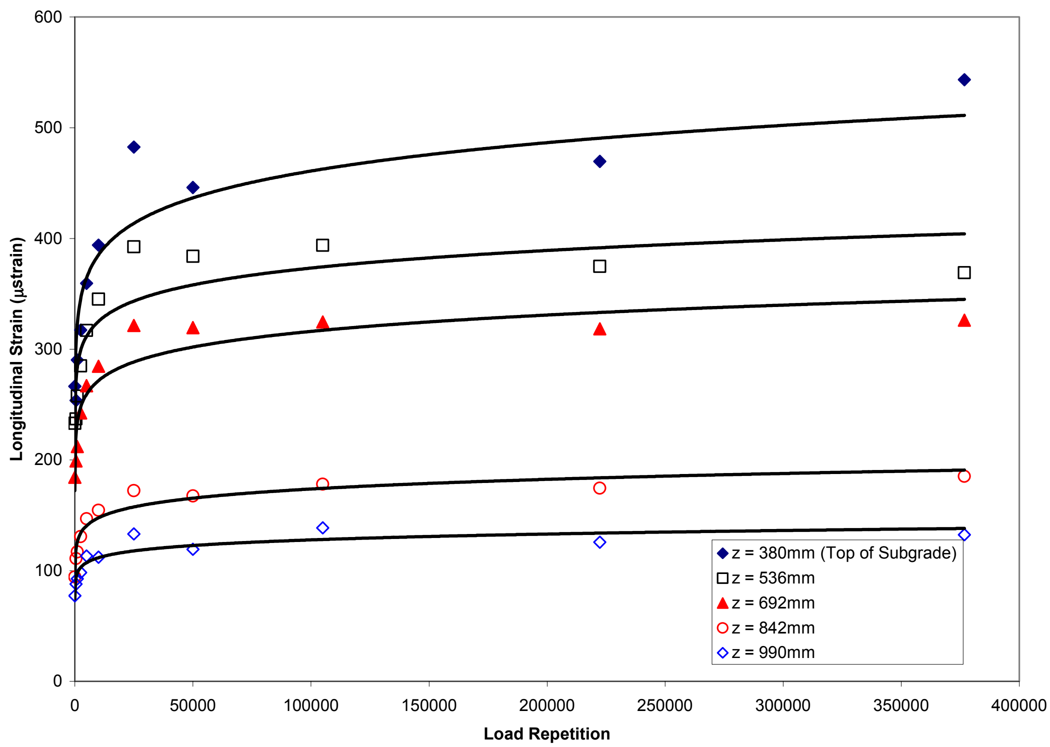

Figure 58. Change in longitudinal strain as a function of load repetitions in the subgrade (703C3) – Position 2.

The data in Figure 58 was re=plotted on a log-log scale and power curves fitted to the data, Figure 59. The coefficients for the power curves and the respective coefficients of correlations are presented in Table 8.
In the transverse direction, the strains were all expansive. Generally, the maximum strains occurred when the load was in position 3.. A typical set of transverse strain measurements in the subgrade is shown in Figures 39 and 40. The maximum transverse displacements and corresponding strains are presented in Appendix E, Tables E-8 and E-9.

Compared to the vertical and longitudinal strains, the maximum transverse strains were smaller and ranged between 130 and 200 µstrains near the top 300 mm of the subgrade. The change in the transverse strains as a function of load repetitions and depth are presented in Figure 60. Power curves were used to fit the strain versus load repetition data and the coefficients for the power curves are presented in Table 9.

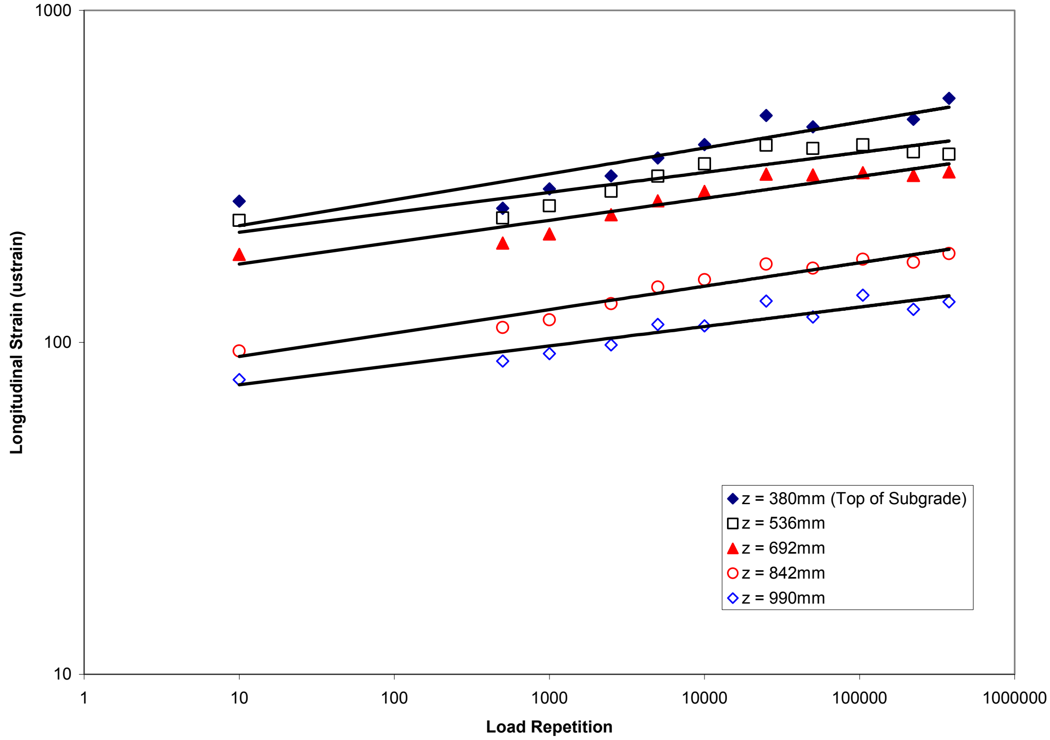

Figure 59. Change in longitudinal strains as a function of load repetitions (log-log scale) in the subgrade (703C3).

Table 8. Coefficients for power law curves for dynamic longitudinal strains.

Depth (mm)	A	n	R^2
380	188	0.0780	0.83
536	187	0.0601	0.82
682	148	0.0660	0.89
842	77	0.0706	0.94
990	65	0.0585	0.89

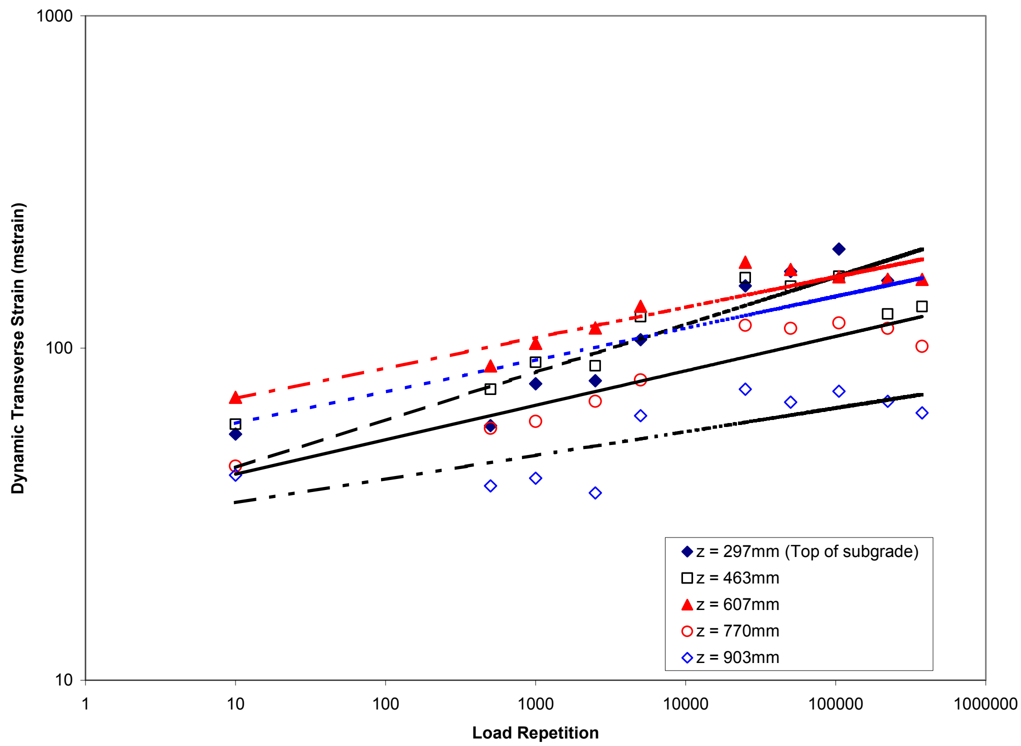

Figure 60. Change in transverse strains as a function of load repetitions (log-log scale) in the subgrade (703C3).

Table 9. Coefficients for power law curves for dynamic transverse strains.

	Depth (mm)	A	n	R^2
Subgrade	297	31.3	0.1437	0.86
	463	47.6	0.0957	0.78
	607	57.1	0.0915	0.87
	770	32.9	0.1037	0.88
	909	29.1	0.0712	0.61

From the data in Figure 60, it appears that the strain at z = 607mm is larger than that on top of the subgrade (z = 297mm). Similar results were seen in TS701.
The changes of the transverse strains with depth and load repetitions are shown in Figure 61. The maximum transverse strains occur not on top of the subgrade but at 300mm from the top of the subgrade.

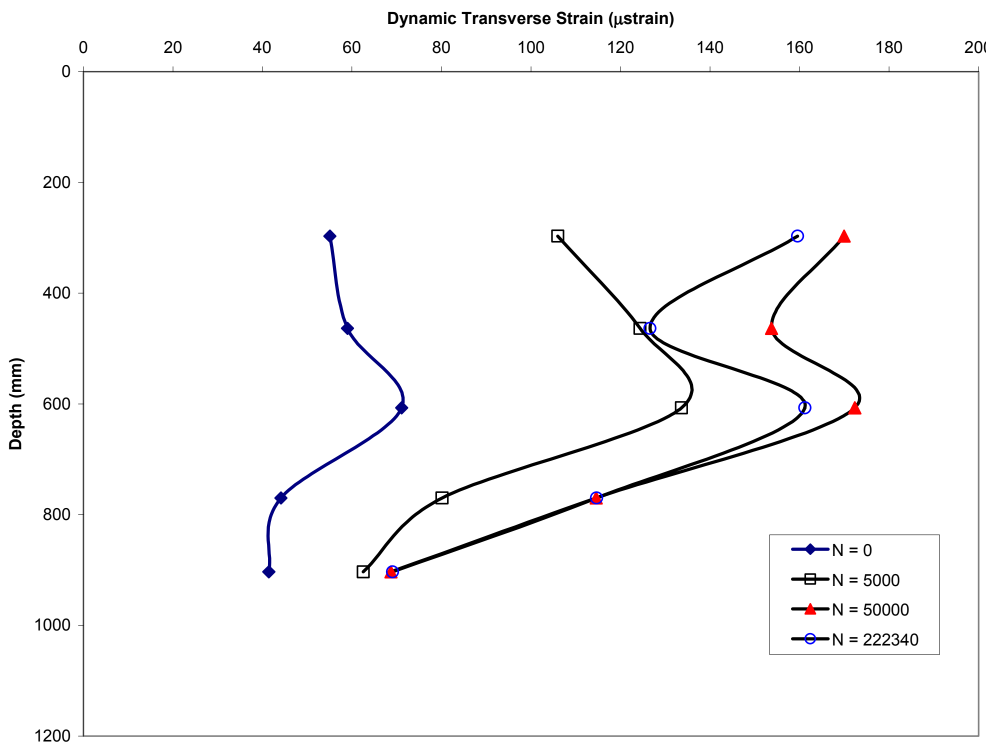

Figure 61. Change in transverse strains in the subgrade as a function of depth.

Permanent Strains

The permanent deformations and strains were obtained from static measurements of the εmu coils. The measurements are presented in Tables E-10 & 11, Appendix E. The vertical deformations at the end of the test ranged between –0.3 to- 4mm in the various layers. The total vertical deformation of the layers at the end of 222340 load repetitions was approximately –9.25 mm. This total deformation was based on the assumption that the permanent deformation in the bottom half of the base course and top of the subgrade layers were the same as that obtained at the end of 105000 load repetitions. The measurement at 222340 passes were unrealistic (-396mm & 4mm respectively) and did not fit the trend as seen at other locations and other tests.

The variation of the vertical permanent deformation with depth as a function of load repetitions is shown in Figure 62. As seen in the figure, it appears that most of the deformation occurred in asphalt layer and in the top of the base course. However, when we look at the actual deformations, the maximum deformation of the asphalt layer was approximately 1.75mm over a thickness of 76mm. In terms of strains, approximately 2% of the overall permanent strains occurred in the asphalt layer and in the top portion of the base course. The bottom half of the base course and the top of the subgrade appeared to follow the same deformation pattern, with maximum strains reaching approximately 1% each. The immediate subgrade below the top of the subgrade had permanent strains ranging between 0.8 to 1% The strains in the remaining subgrade layers were approximately 0.5% or less.

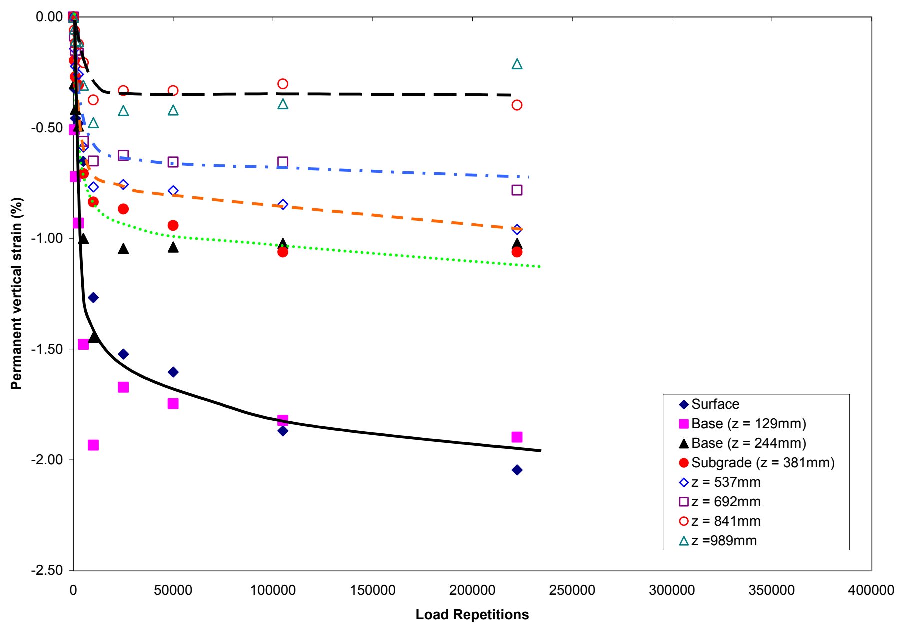

Figure 62. Change in vertical permanent strains as a function of load repetitions in the base & subgrade (703C3).

The change in the permanent deformation as a function of depth is shown in Figure 63. As can be seen in the figure, the significant deformations occurred in the base course and in the upper subgrade layers. Most of the deformations occurred earl int tests and after 50,000 passes, the change was smaller. An exponential curve best fitted the data. The data in Figure 62, with the exception of the surface and the data from z = 989mm were re-plotted on a log-log scale, Figure 64. Power curves were fitted to the data and the coefficients are presented in Table 10.

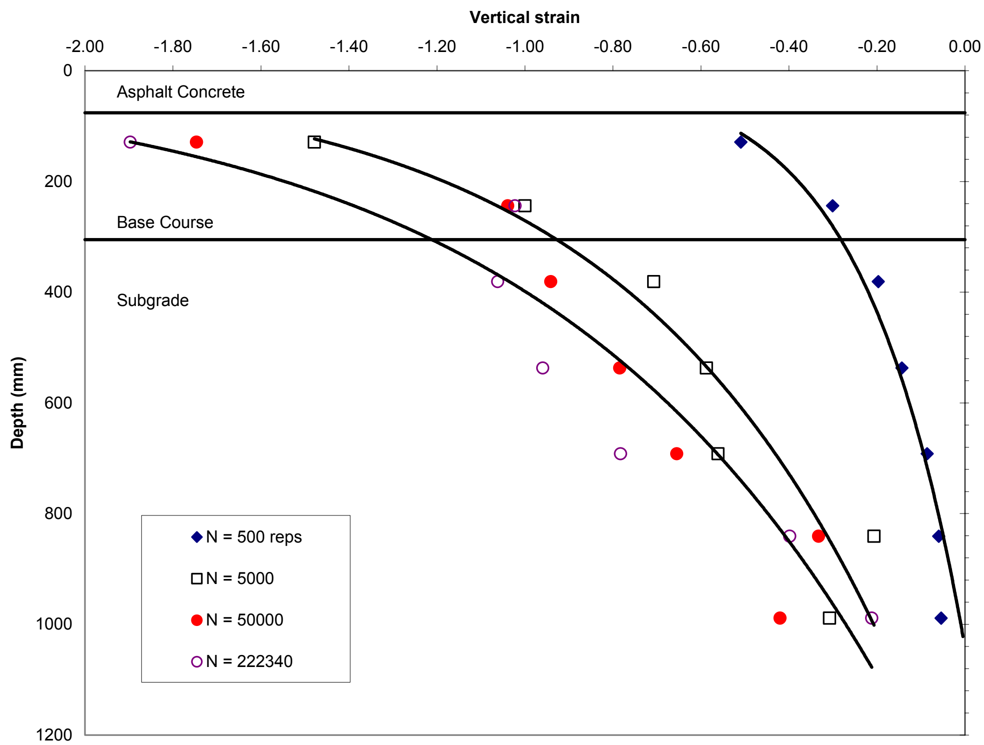

Figure 63. Permanent strain as a function of depth.

Table 10. Coefficients for power law curves for permanent vertical strains (%).

Layer	A	n	R^2
Base (z = 123mm)	0.1817	0.2056	0.86
Base (z = 244mm)	0.0856	0.2343	0.80
Subgrade (z = 377mm)	0.0294	0.3242	0.91
z = 703mm	0.0136	0.3514	0.83
z = 853mm	0.0147	0.2803	0.88

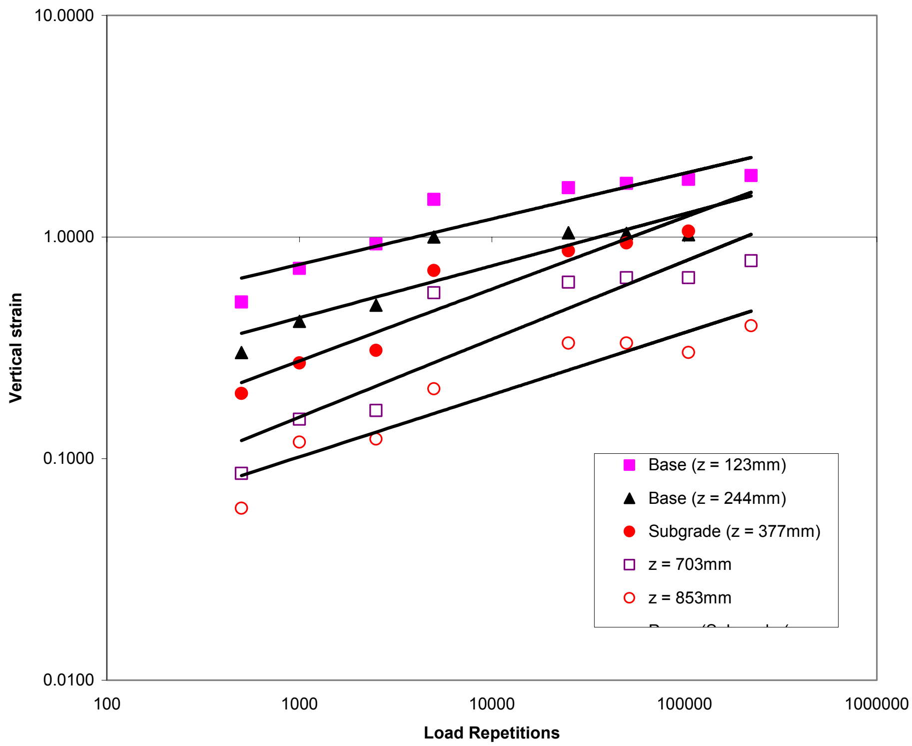

Figure 64. Change in vertical permanent strains as a function of load repetitions (log-log scale) in the base & subgrade (703C3).

In the longitudinal direction, the strains were less then 0,5%, Figure 65. The data suggested that the strains were compressive. In the transverse direction, we also found that the transverse strains were in the same magnitude as the longitudinal strain. The maximum strains ranged between – 0.2 to –0.4%.

Surface Profile Measurements

Twenty four surface profile measurements were made periodically to determine the surface deformation as a function of load repetitions. Of the 24 measurements, the first (1,2) and last two (23, 24) measurements were taken in the acceleration and deceleration areas. The measurements at these locations are not reported. The coil gages for measuring dynamic and permanent deformation are in the vicinity of locations 16 to 19, Figure 19. A typical set of surface deformation as a function load repetitions is shown at position 17 in Figure 66. A ten point running average was applied to the data shown in Figure 66. The maximum rut depth was extracted from the data after the ten point averaging was done. The maximum rut depths across the test section as a function of load repetitions is presented in Table E-13.

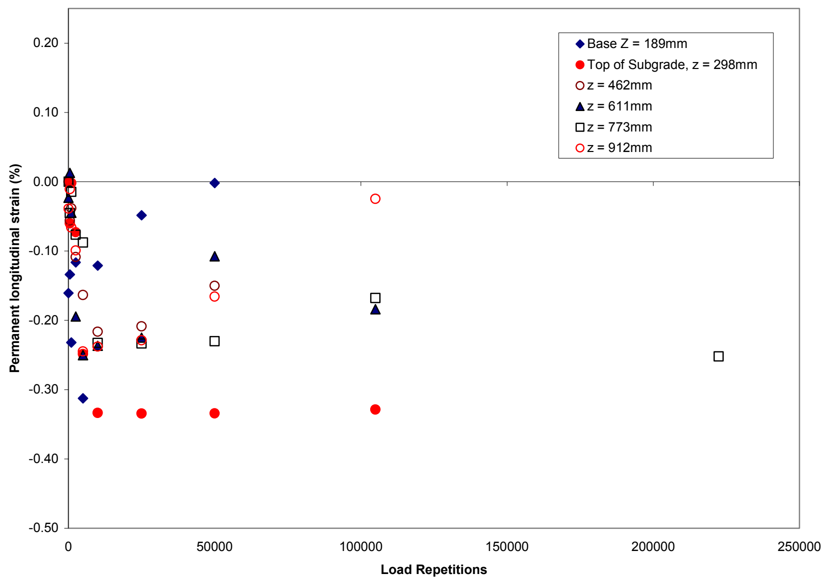

Figure 65. Change in longitudinal permanent strains as a function of load repetitions in the base & subgrade (703C3).

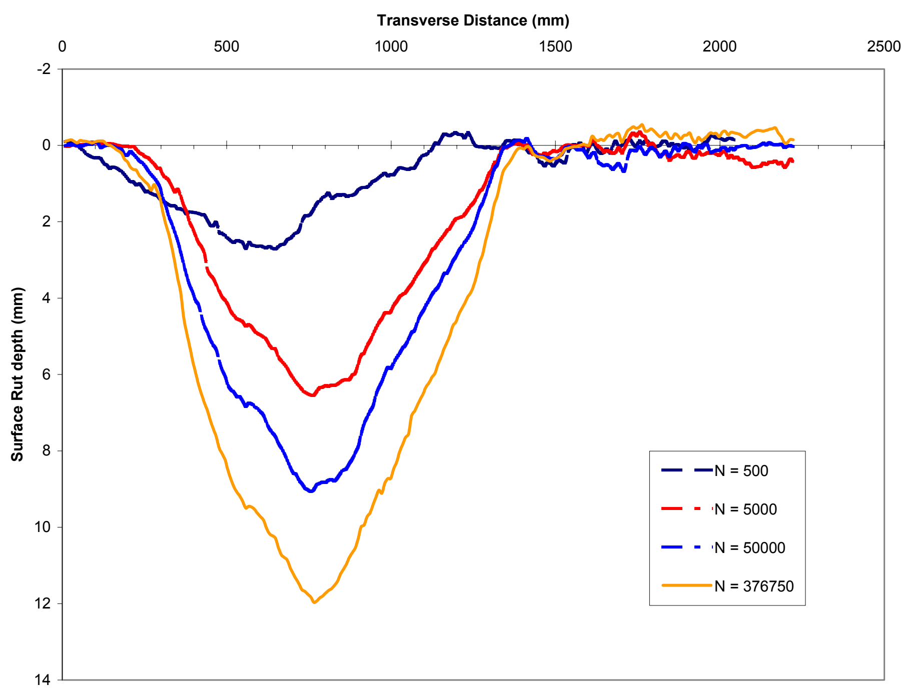

Figure 66. Typical rut depth response as a function of load passes.

The variation in rut depth in the longitudinal direction started around 19% at the beginning of the test and was in the vicinity of 10% at the end of the test. As seen in Figure 67, most of the variation at the locations 3 to 5.

A comparison of the total rut depth measured from the profilometer and strain coil gages is shown in Figure 68. The coil gages were located near position 17 for the surface rut measurements. For the comparison, the average surface rut from positions 16 to 18 were used. The maximum difference between the 2 sets of data is approximately 3mm. The results are tabulated in Table 11. Note since the coil data at top of the subgrade at 222340 passes was missing, the permanent deformation from the previous set of measurements (at 105000 passes) was used.

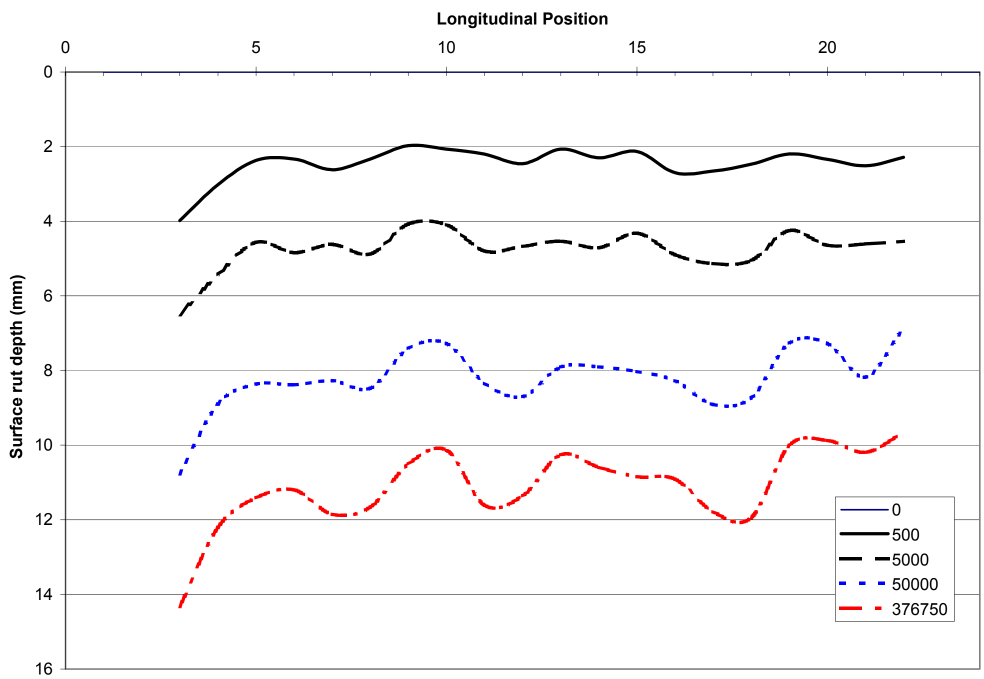

Figure 67. Longitudinal surface rutting as a function of load repetitions.

Table 11. Deformation from surface profile and subsurface coil measurements (mm)

Load Repetitions	Surface Profile	Coil gage
500	2.44	2.13
1000	3.11	2.85
2500	4.09	3.34
5000	4.81	6.53
5000	5.99	9.10
25000	7.20	8.27
50000	8.30	8.57
105000	9.43	8.95
222340	10.67	11.73
376750	11.25	

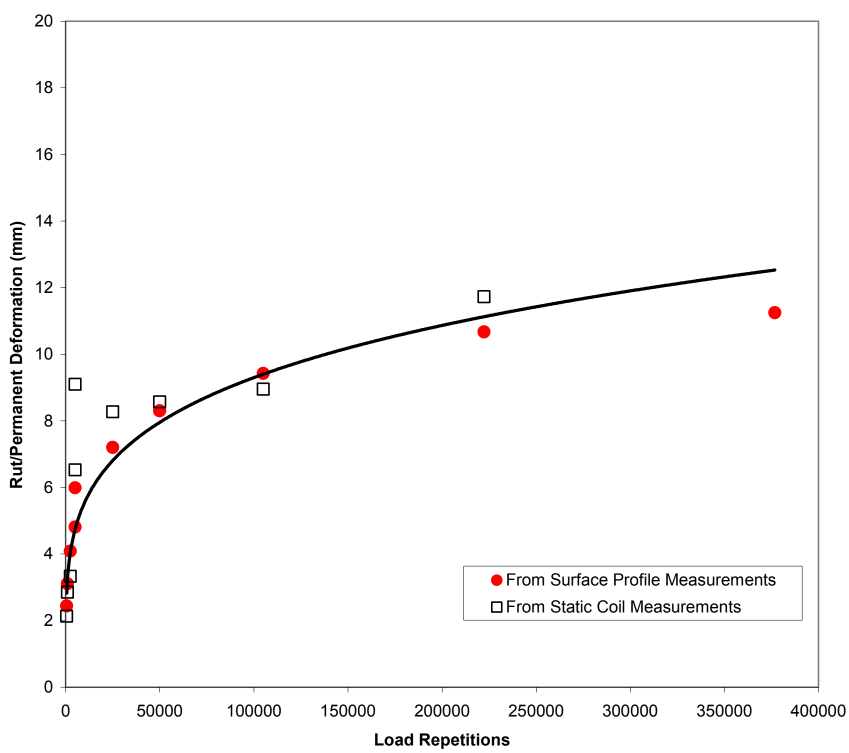

Figure 68. Comparison of total pavement deformation from surface profilometer and coil gage measurements.

703C5

This was the first window to be tested in this test section. Testing of window 703C5 began on April 17th, 1998 and ended on April 28th, 1998. Based on load measurements from the HVS and tire pressure monitoring during the tests, the mean test load was 79-kN with a COV of 1.6 %, Figure 69a. The mean tire pressure was 688-kPa with a COV of 4.2%.

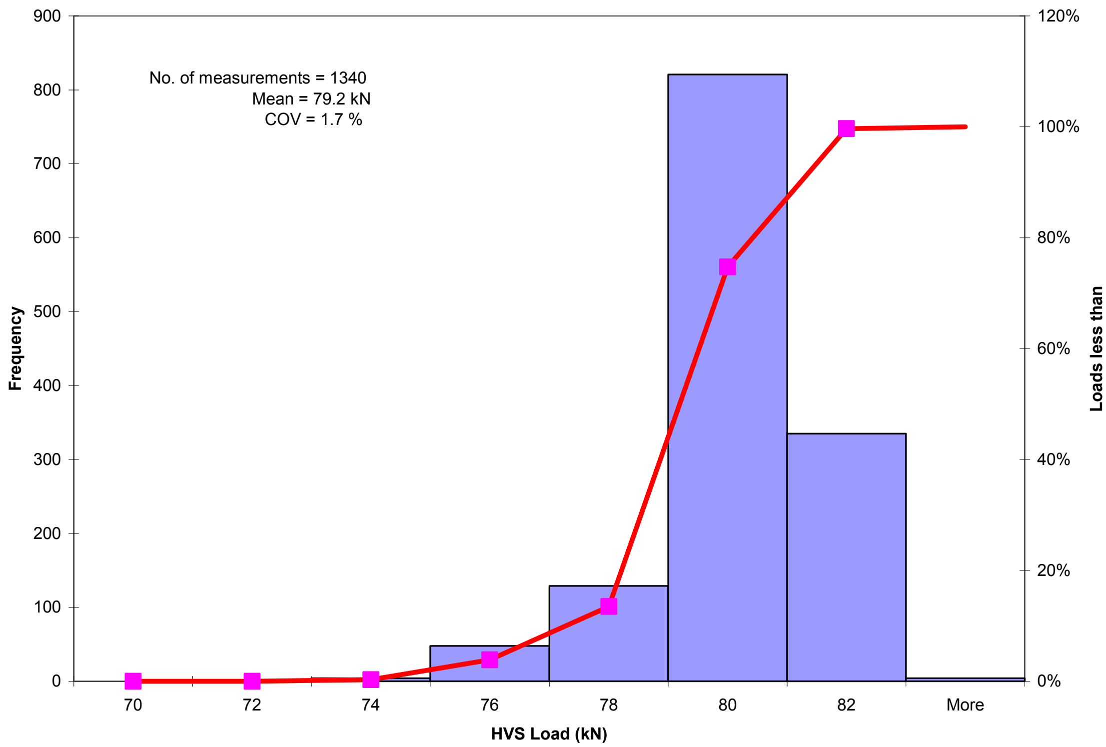

Figure 69a. Statistical presentation of test loads on 703C5.

The average sub-surface temperature in the test section was 17.1 °C with a COV of 1.2%. The average moisture content in the test section during the test was 14.1 % with a COV of 3.0%, Figure 70. The target moisture content during construction was 15 ± 2%. The average moisture measurements as a function of depth are presented in Table 12. The nearest VITEL gages to this window were located at depths of 610mm and 1090mm. Note the approximate 1.5% drop in moisture content at z = 610mm at the end of the test.

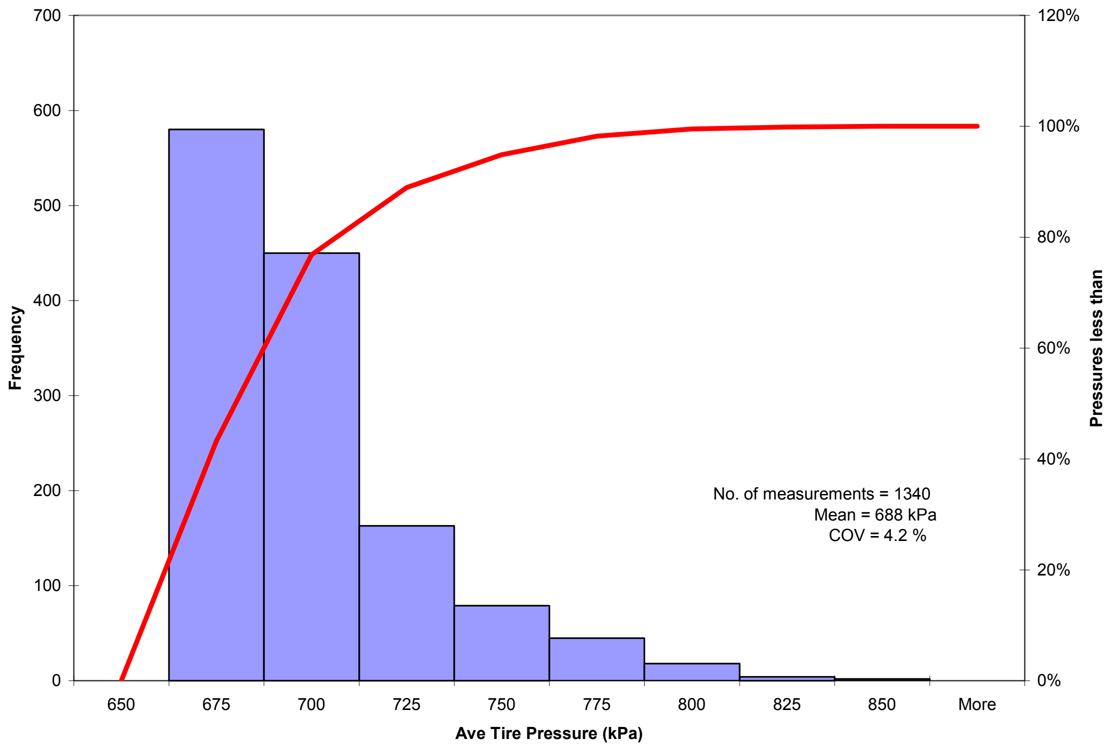

Figure 69b. Statistical presentation of test tire pressures on 703C5

Table 12. Average moisture content as a function of depth during testing of 703C5.

Depth from top of AC (mm)	Gravimetric moisture content (%)
360	13.43
610	14.27
910	14.25
1090	14.58

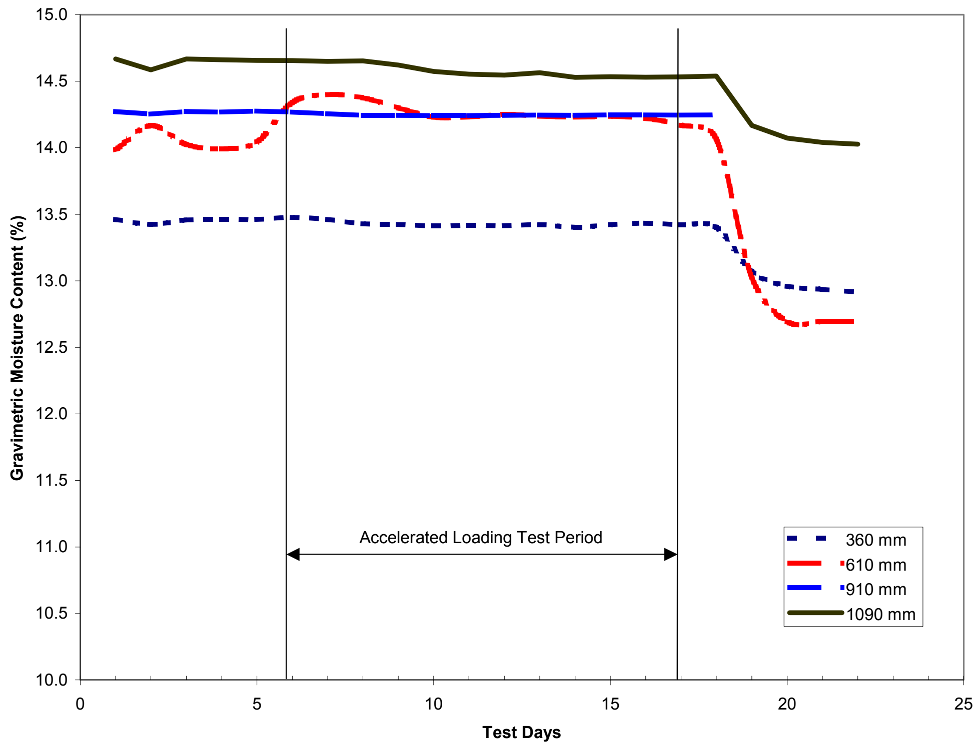

Figure 70. Distribution of moisture content in test section during testing of 703C5.

Dynamic Stress

Stress measurements were made at two locations in thetest window. One was located in the base course at a depth of 171mm, the second was located in the subgrade at a depth of 430mm from the top of the asphalt concrete layer Figures 12c & d. At these locations, three DYNATEST pressure cells were installed to measure the vertical, longitudinal and transverse dynamic stresses. Typical responses from the pressure cells are presented in Figures 71 and 72.

The vertical stress response was similar to those from 703C2 and 703C3. The longitudinal stresses were also similar in the subgrade, except that we did not see any development of extension stresses with increasing load repetitions. We did see development of extension stresses in the base course with increasing load repetitions, Figures 71b and 72b. As discussed previously, the drop in the longitudinal stresses in base course as as the wheel is over the gage may be explained to the thickness of the gage. The responses of the transverse stresses were the same as in previous windows. However, we did not see any development of extension stresses in the subgrade with increasing load repetitions. We did development of extensional transverse stresses with increasing load repetitions in 703C2.

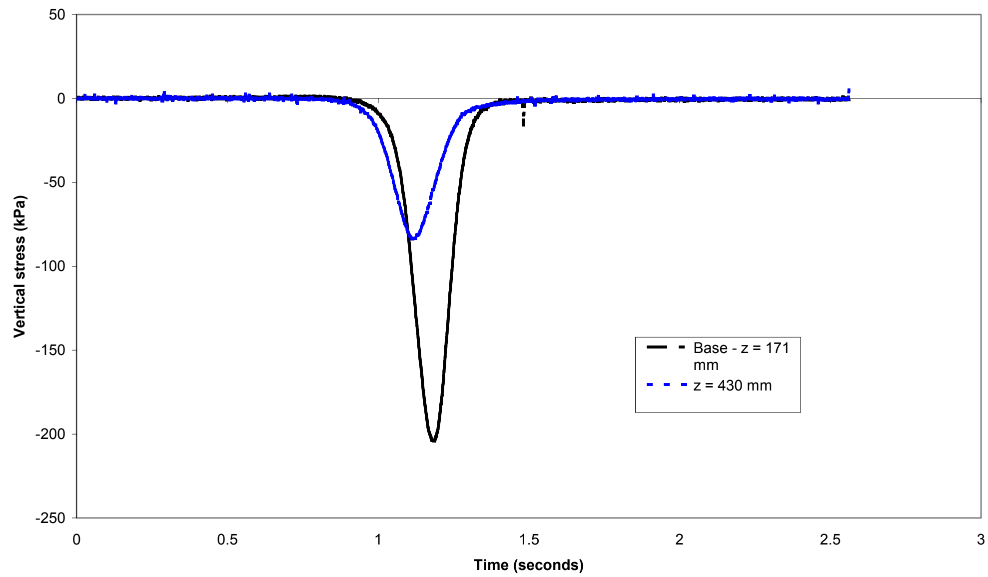

Figure 71a. Typical vertical stress response in 703C5 from wheel loading of 79-kN and 688-kPa tire pressure (N = 500 repetitions).

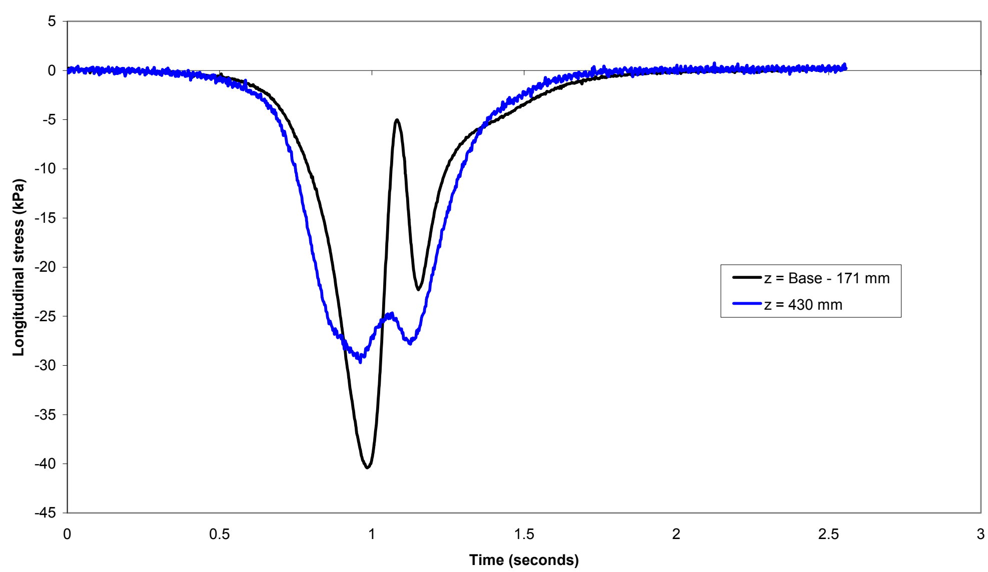

Figure 71b. Typical longitudinal stress response in 703C5 from wheel loading of 79-kN and 688-kPa tire pressure (N = 500 repetitions).

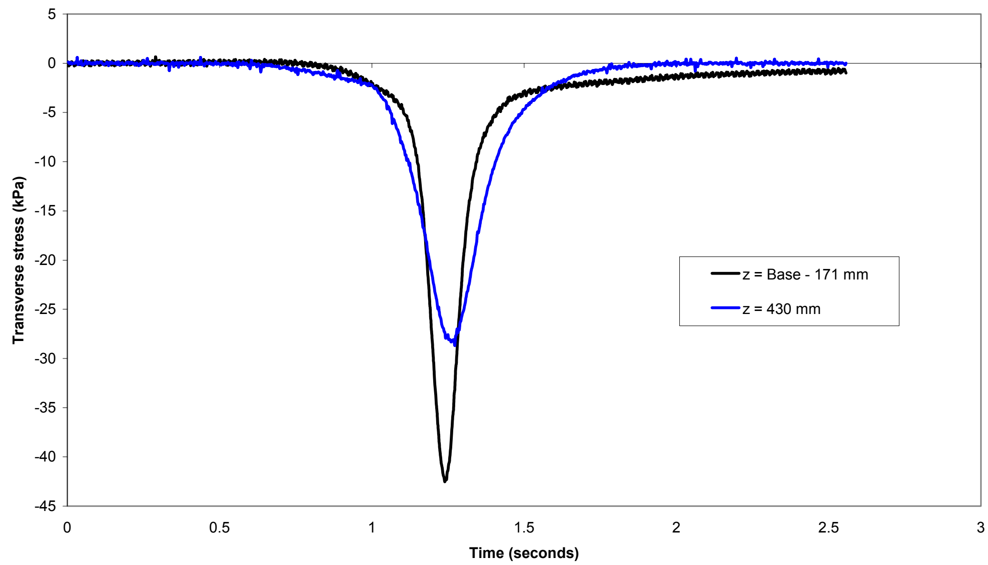

Figure 71c. Typical transverse stress response in 703C5 from wheel loading of 79-kN and 688-kPa tire pressure (N = 500 repetitions).

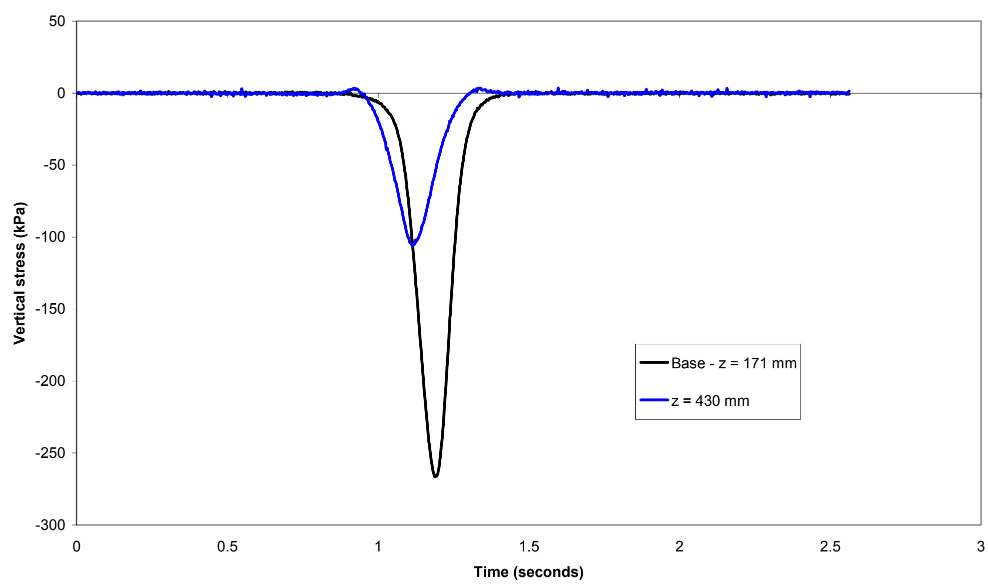

Figure 72a. Typical vertical stress response in 703C5 from wheel loading of 79-kN and 688-kPa tire pressure (N = 50000 repetitions).

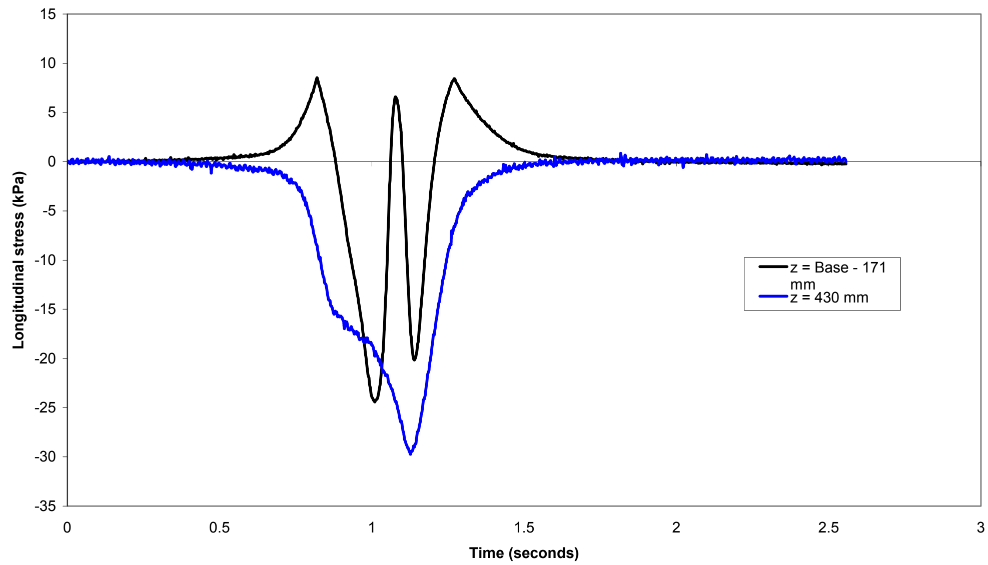

Figure 72b. Typical longitudinal stress response in 703C5 from wheel loading of 79-kN and 688-kPa tire pressure (N = 50000 repetitions).

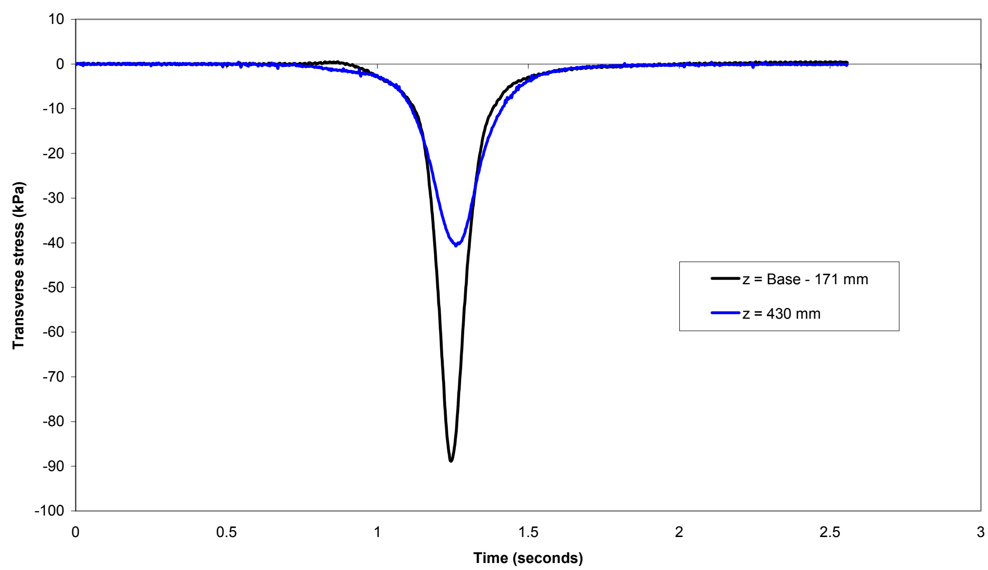

Figure 72c. Typical transverse stress response in 703C5 from wheel loading of 79-kN and 688-kPa tire pressure (N = 50000 repetitions).

Measured stresses from the test are presented in Table F-1to F-3, Appendix F. Negative values indicate compressive stress. In the vertical direction, the stresses were compressive and increased with increasing load repetitions. At the end of 5000 load repetitions, the stress in the base course increased approximately 40%. After, 5000 load repetitions, the increase was more gradual, Figure 73. In the subgrade, the response was similar. The stress increased by 37% at the end of 5000 repetitions. After that, the increase was more gradual, Figure 73.

With respect to the longitudinal stresses the peak stresses were compressive in the base and subgrade. The peak longitudinal compressive stress in the base course initially increased in compression and after 5000 passes we started to see a decrease in the stress, but still was compressive, Figure 74. In the subgrade, there is a slight reduction in the compressive stress with increased load repetitions, Figure 74.

The peak transverse stresses were also compressive and tended to increase with increasing load repetitions. As with the other stresses, there is a sharp increase in stresses till 5000 passes. After that, the stresses are still increasing, but more gradually.
The stresses are re-plotted on a log=log scale and power curves fitted to the data, Figures 76 to 78. The coefficients of the power curves are presented in Table 13. The longitudinal stresses in the base course were not re-plotted because of its large deviation from a power curve, Figure 74.

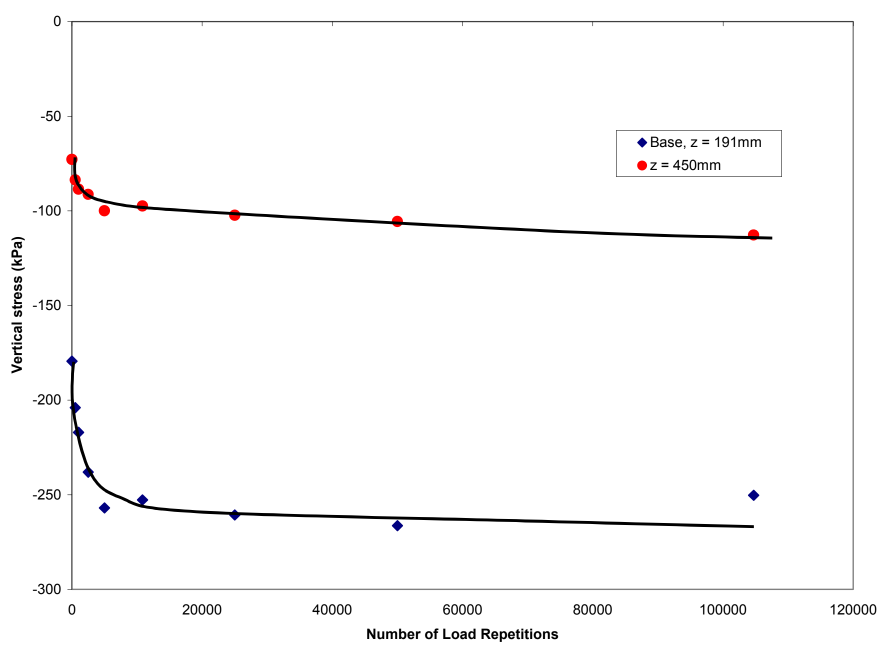

Figure 73. Vertical stresses in the base and at the top of the subgrade as a function of load repetitions (703C5).

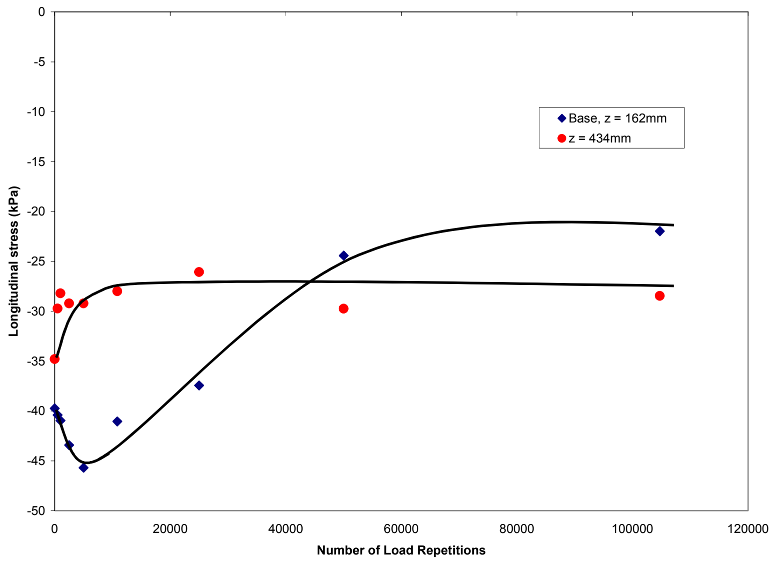

Figure 74. Longitudinal stresses in the base and at top of the subgrade as a function of load repetition (703C5).

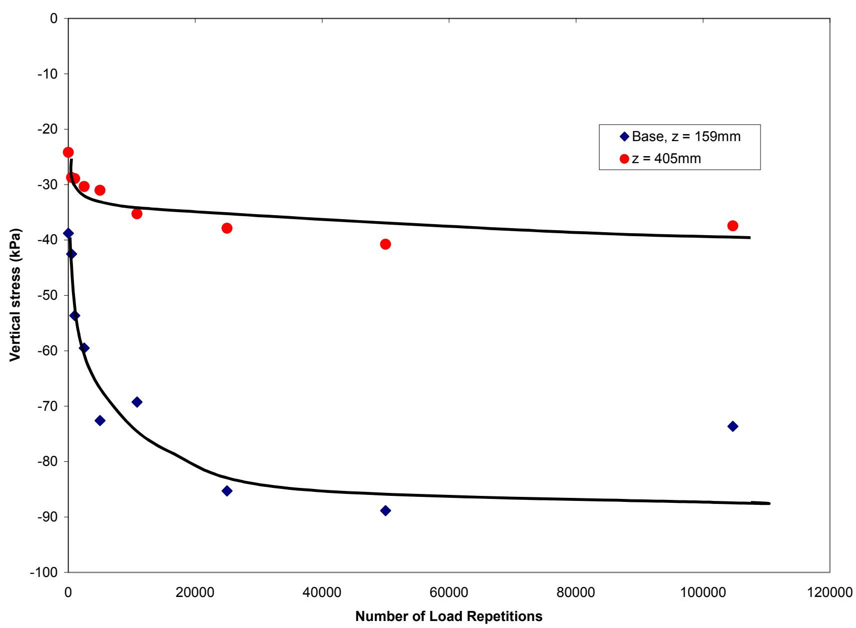

Figure 75. Transverse stresses in the base and at top of the subgrade as a function of load repetition (703C5).

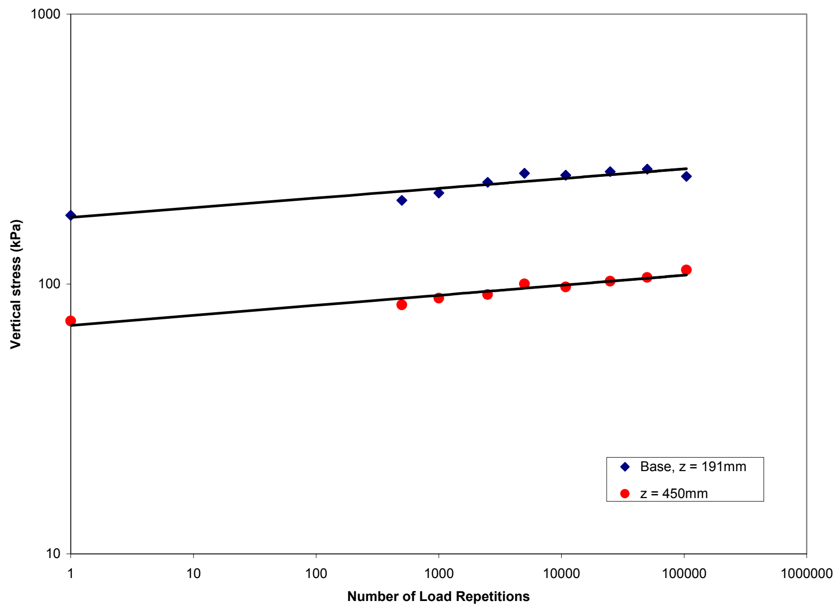

Figure 76. Vertical stresses in the base and at the top of the subgrade as a function of load repetitions (703C5) – log-log scale.

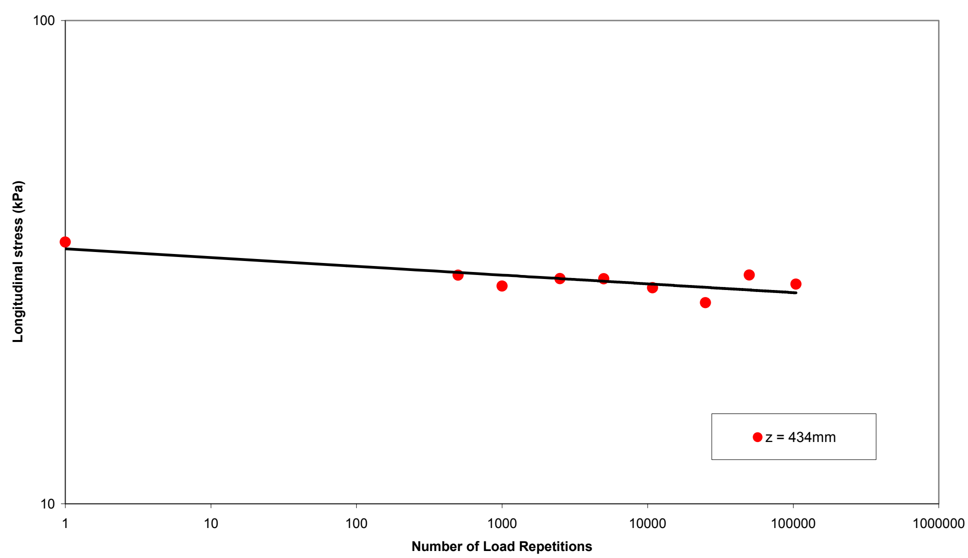

Figure 77. Longitudinal stresses in the base and at the top of the subgrade as a function of load repetitions (703C5) – log-log scale.

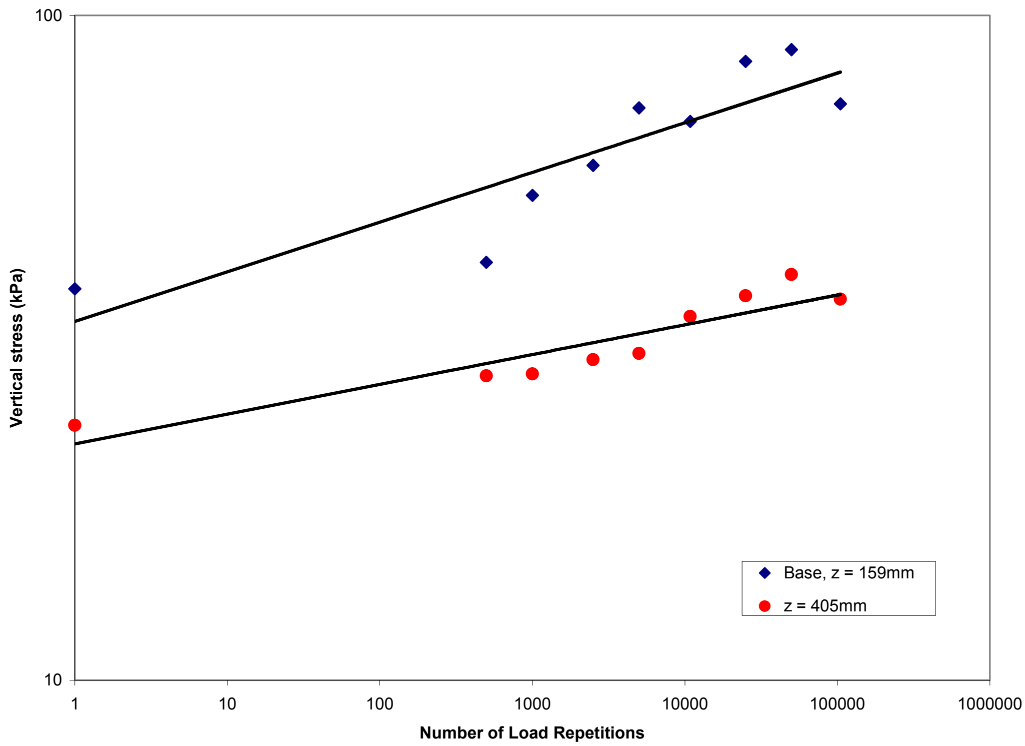

Figure 78. Transverse stresses in the base and at the top of the subgrade as a function of load repetitions (703C5) – log-log scale.

Table 13. Coefficients for power law curves for dynamic stresses in the base and subgrade.

Stress	Base			Subgrade		
	A	n	R^2	A	n	R^2
Vertical	157.1	0.0507	0.94	65.1	0.045	0.97
Longitudinal				34.6	-0.0208	0.58
Transverse	28.9	0.0948	0.84	20.4	0.0566	0.91

Dynamic Strains

As before, vertical, longitudinal and transverse dynamic strains were measured as a function of load repetitions at the 3 wheel locations. Generally, the vertical strains were compressive, while the longitudinal and transverse strains were expansive. It was also found that in general the maximum displacements (strains) occurred when the wheel was in position 2.

The maximum displacements and strains in Table F-4 to F-13 in Appendix F were obtained after the data was smoothed using a 10 points averaging scheme. As with other windows and test sections, in the longitudinal and transverse directions the displacements (strains), were measured at the actual location of the coil gages. The difference between the vertical and horizontal strain measurements is about 75mm below the horizontal strain. Three sets of measurements are reported for the longitudinal strain, initial compressive strain, maximum expansive strain and the compression strain during unloading (see Figure D-2, Appendix D).

The trend in vertical strains as a function of load repetitions is shown in Figure 79. The response of the upper 300-mm of subgrade is different from either the base or of the subgrade below. The strains at the onset of loading (initial conditions) were in the 4000 to 5000 µstrain level in the upper subgrade. These values were higher than those measured in the upper base course layer. The strains in the lower part of the base course was approximately 5 times less then in the upper base course. This difference dropped to about 3 times near the end of the test. The lower strains in the lower base course

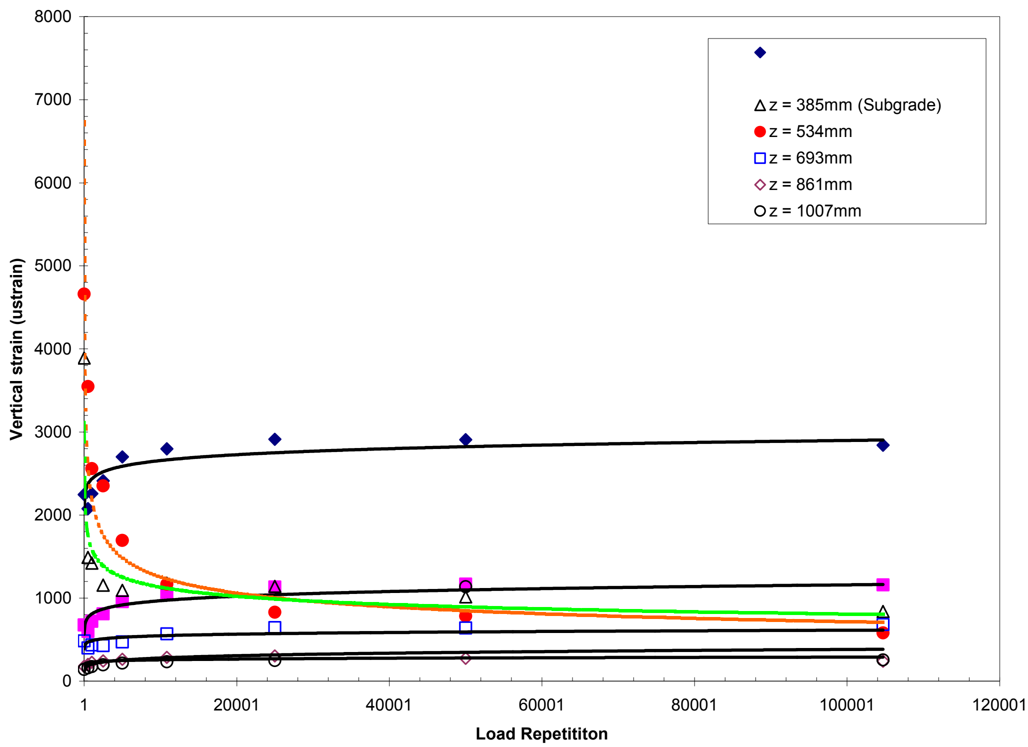

Figure 79. Change in vertical strains as a function of load repetitions in the base & subgrade (703C5).

indicates that the lower layer is moving together with the large movement of the upper subgrade layer. In the upper subgrade layer, the strains decrease with increasing load repetitions, Figure 79. The maximum vertical strains are presented in Table 14.

Using the data in table 14, the data was re-plotted on a log-log scale and power curves fitted to them, Figures 80 and 81. The coefficients for the power curves are presented in Table 15.

Table 14. Maximum vertical strains in TS703C5 (Load = 79-kN, p = 688-kPa).

Repetitions	z = 120 mm	z = 245 mm	z = 385 mm	z = 534 mm	z = 693 mm	z = 861 mm	z = 1007 mm
0	-2248	-676	-3891	-4660	-483	-178	-141
500	-2078	-599	-1490	-3547	-400	-203	-161
1000	-2257	-721	-1423	-2558	-437	-226	-174
2500	-2412	-811	-1156	-2352	-428	-244	-197
5000	-2701	-957	-1093	-1695	-473	-264	-218
10830	-2797	-1041	-1181	-1167	-571	-288	-234
25000	-2913	-1134	-1141	-831	-645	-304	-248
50000	-2908	-1168	-1015	-785	-640	-276	-1137
104720	-2840	-1159	-840	-582	-681	-242	-256

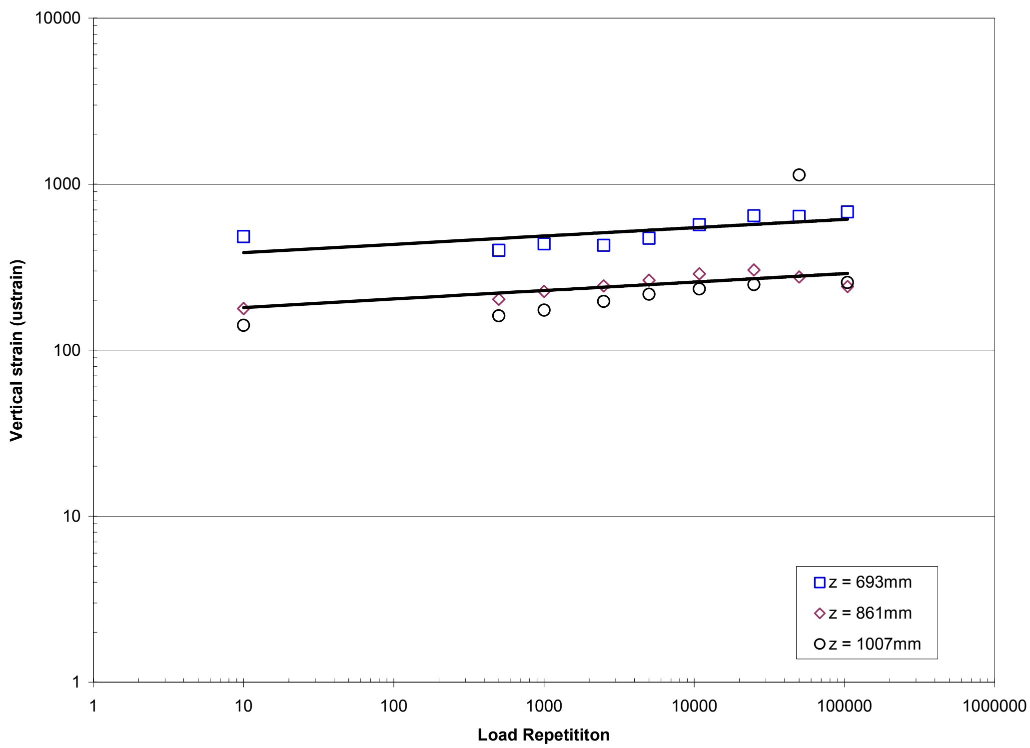

Figure 80. Change in vertical strains as a function of load repetitions (log-log scale) in the subgrade (703C5).

Table 15. Coefficients for power law curves for dynamic vertical strains

	Depth (mm)	A	n	R^2
Subgrade	383+	7173	-0.195	0.81
	693	345	0.050	0.49
	861+	161	0.050	0.70
	989	204	0.017	0.78

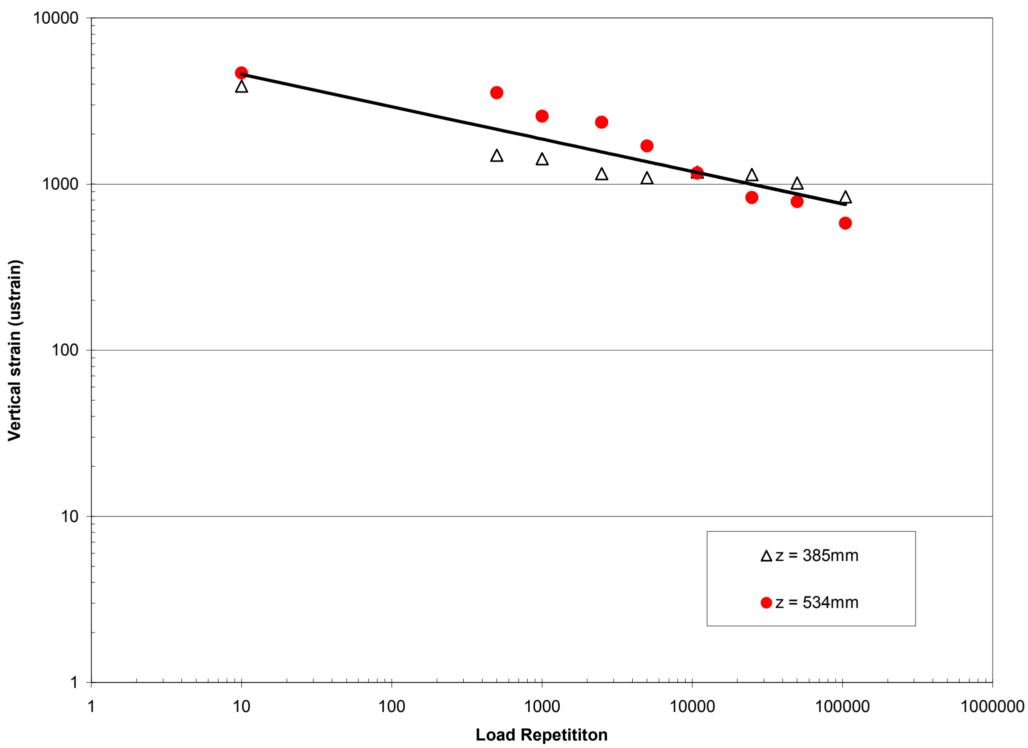

Figure 81. Change in vertical strains in the upper subgrade as a function of load repetitions (log-log scale) in the subgrade (703C5).

In the longitudinal direction, we found that the strains (displacements) were compressive as the wheel approached the gages. When the wheel was on top of the gages, the strains (displacements) were expansive. As the wheel moved away from the gages, the strains (displacements) became compressive again. The compressive strains (displacements) at the tail end usually were smaller then the approach end. The maximum strains (displacements) are presented in Appendix F, Tables F-6 to F-11. As before, the maximum strains (displacements) occurred when the wheel was in position 2.

The changes in the longitudinal strains as a function of load repetitions are presented in Figure 82. As with TS701, the longitudinal strains in Figure 82 is the absolute sums of strains A and B, (Figure E-1, Appendix E). The longitudinal strain response is very similar to the vertical strains. The strains at the top base course layer was significantly high (15000 to 30000 μstrains, see Table F-10, Appendix F). Again in the upper subgrade layers, the strains decrease with increasing load repetitions, Figure 82). In the other parts of the subgrade, the strains increase with increasing load repetitions.

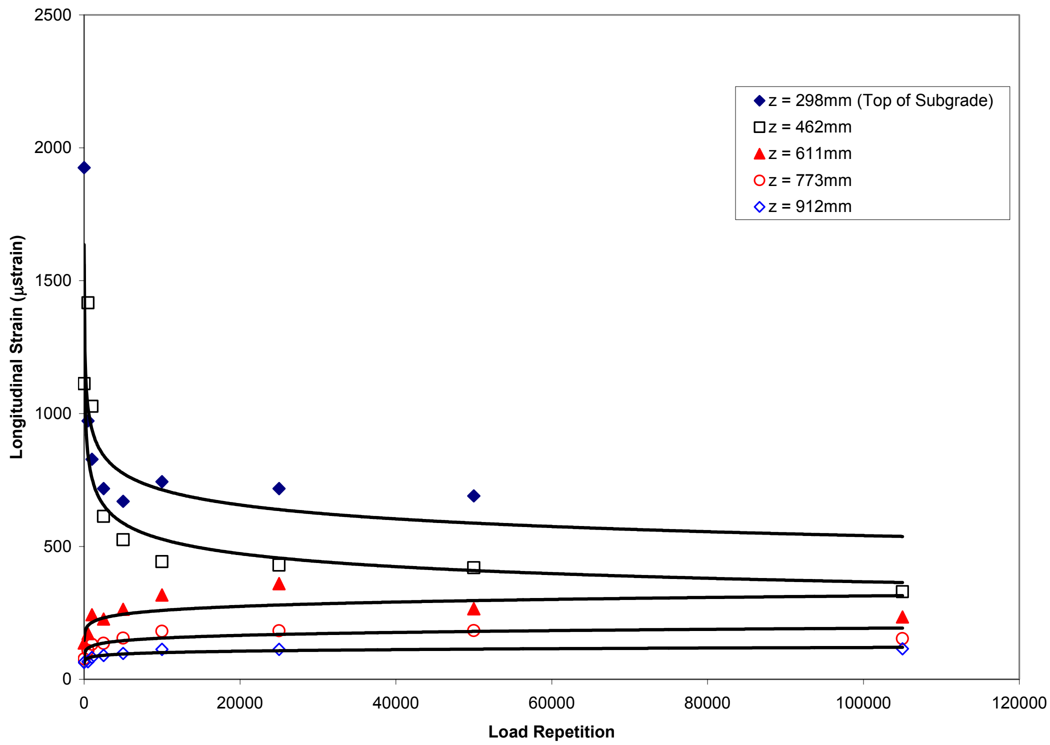

Figure 82. Change in longitudinal strain as a function of load repetitions in the subgrade (703C5) – Position 2.

The data in Figure 82 was re-plotted on a log-log scale and power curves fitted to the data, Figures 83 and 84. The coefficients for the power curves and the respective

Table 16. Coefficients for power law curves for dynamic longitudinal strains.
coefficients of correlations are presented in Table 16.

	Depth (mm)	A	n	R^2
Subgrade	298+	2281	-0.145	0.71
	611	121	0.083	0.63
	773	66	0.093	0.85
	990	50	0.077	0.84

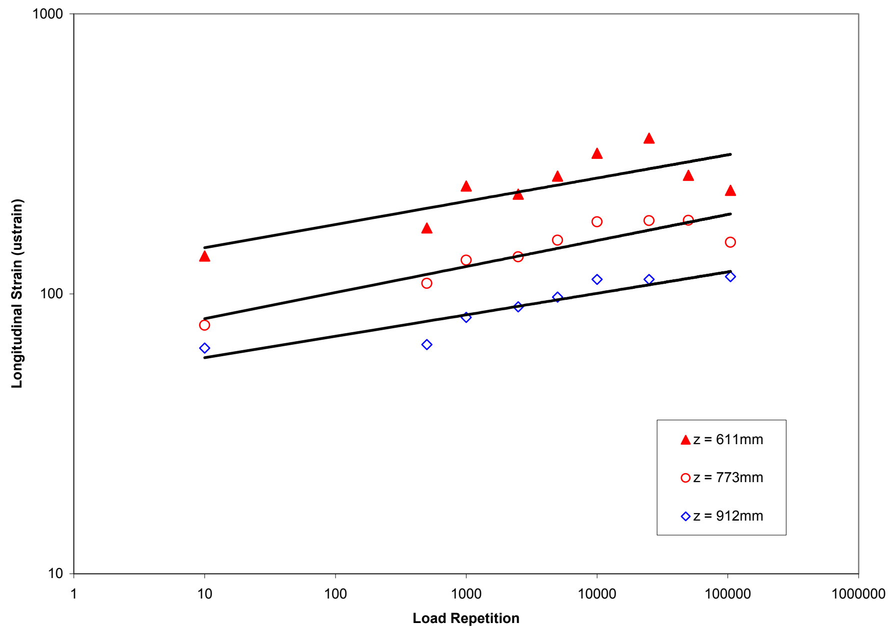

Figure 83. Change in longitudinal strains as a function of load repetitions (log-log scale) in the subgrade (703C5).

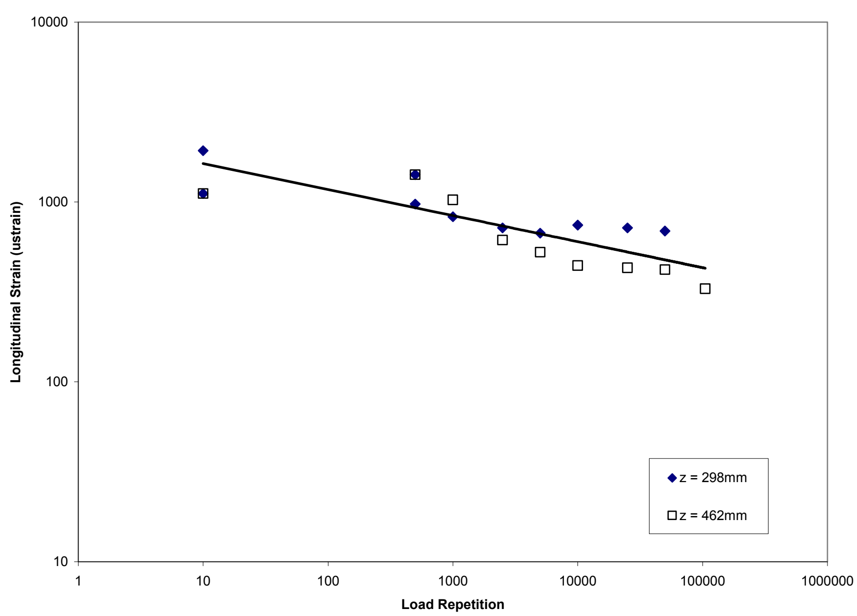

Figure 84. Change in longitudinal strains in the upper subgrade layers as a function of load repetitions (log-log scale) in the subgrade (703C5).

In the transverse direction, the strains were all expansive. Generally, the maximum strains occurred when the load was in position 3. The maximum transverse displacements and corresponding strains are presented in Appendix F, Tables F-12 and F-13. The change in the transverse strains as a function of load repetitions and depth are presented in Figure 85. Again as with the vertical and longitudinal strains, the transverse strains in the upper subgrade layers decreased with increasing load repetitions. Power curves were used to fit the strain versus load repetition data, Figures 86 and 87, and the coefficients for the power curves are presented in Table 17.

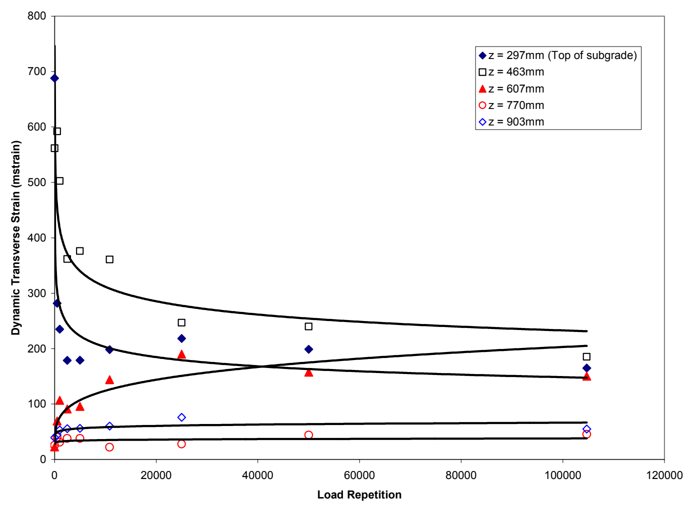

Figure 85. Change in transverse strains as a function of load repetitions in the subgrade (703C5).

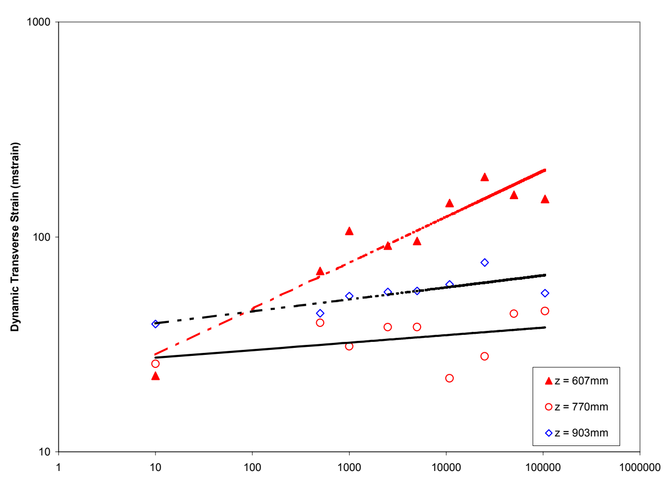

Figure 86. Change in transverse strains as a function of load repetitions in the subgrade (703C5).

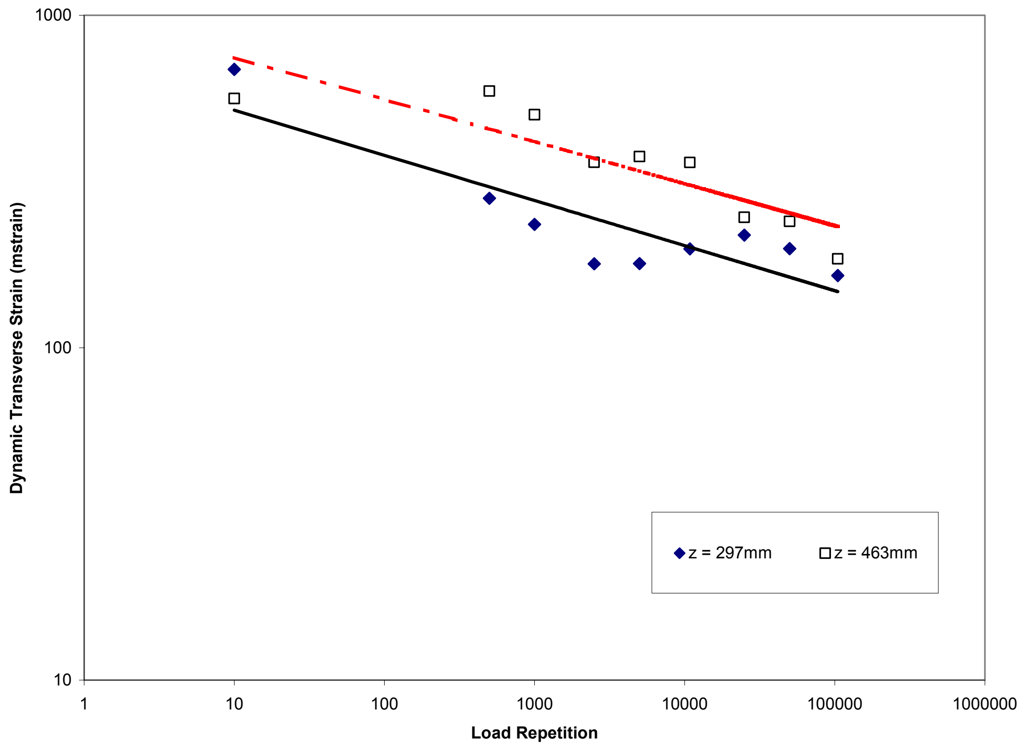

Figure 87. Change in transverse strains as a function of load repetitions in the top of the subgrade (703C5).

Table 17. Coefficients for power law curves for dynamic transverse strains.

	Depth (mm)	A	n	R^2
Subgrade	297	708.0	-0.1357	0.77
	463	998.5	-0.1265	0.78
	607	17.3	0.2138	0.89
	770	34.8	0.0558	0.64
	903	25.3	0.0349	0.151

From the data in Figure 60, it appears that the strain at z = 607mm is larger than that on top of the subgrade (z = 297mm). Similar results were seen in TS701.
The changes of the vertical, longitudinal and transverse strains with depth and load repetitions are shown in Figures 88, 89 and 90. Generally, we found that most of the vertical strains occurred at about 150-mm into the subgrade. In the longitudinal direction, the maximum strains at the top of the subgrade layers occurred at the initiation of loading. With increased load repetitions, the strains decreased and appeared to be

703

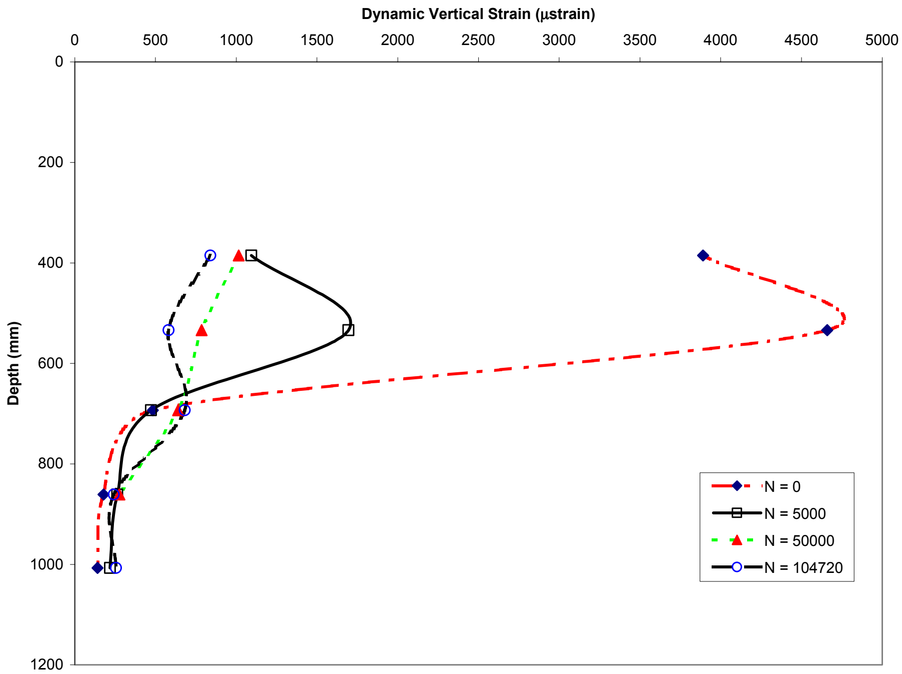

fairly constant. The maximum transverse strains occur not on top of the subgrade but at 300mm from the top of the subgrade.

th.

In the transverse direction, the data suggests initially large strains occurred in the top subgrade layers. As with the longitudinal strains, they decreased with increasing load repetitions .

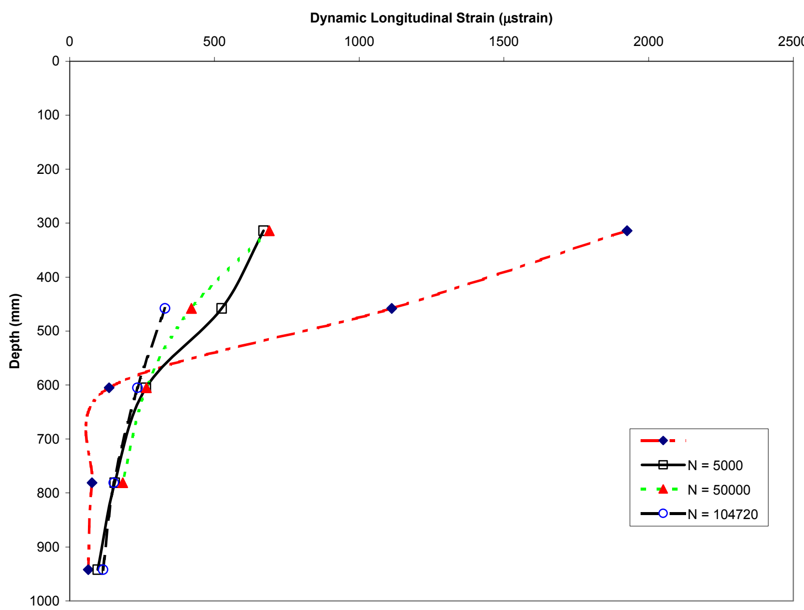

Figure 88. Change in vertical strains in the subgrade as a function of dep

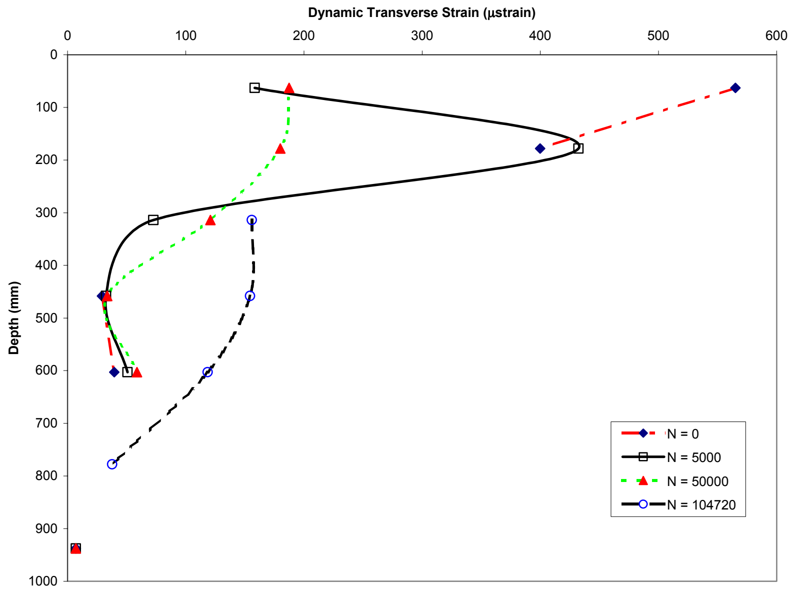

Figure 89. Change in longitudinal strains in the subgrade as a function of depth.

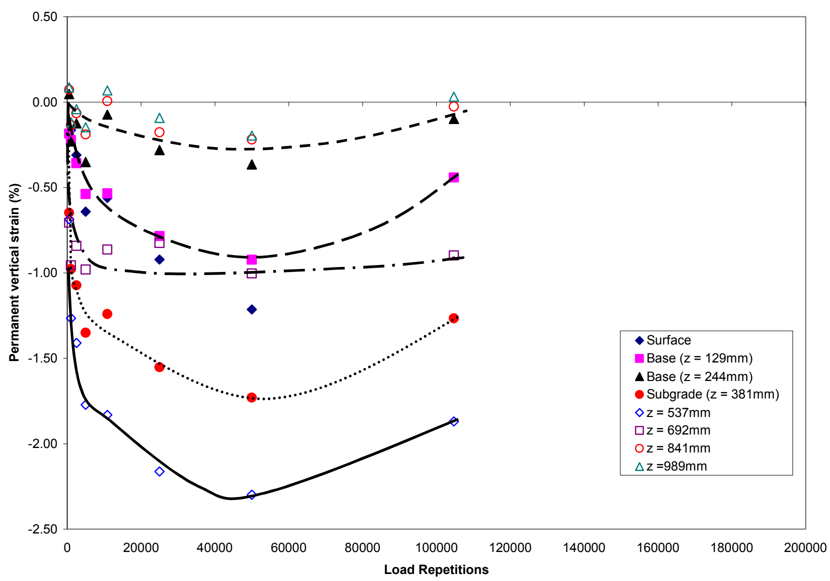

Figure 90. Change in transverse strains in the subgrade as a function of depth.

Permanent Strains

The permanent deformations and strains were obtained from static measurements of the εmu coils. The measurements are presented in Tables F-14 & F-15, Appendix F. For pass level 104720, the permanent deformations and strains were obtained from the dynamic strain measurements. Based on previous analysis with data from TS701 and with current data, we were able to use the static measurements taken during the dynamic strain measurements.

We found that the vertical deformations were significantly higher in the top 450mm of subgrade, Table F-14. We also found that the maximum deformations in all the layers occured after 50000 load repetitions, Table F-14. At the end of the test, there was a reduction in the permanent deformation, suggesting the material had failed plastically and any additional loading produced a lower rate of change. At 50000 load repetitions, the permanent deformation in the base and subgrade was approximately 1.3mm and 5.5mm respectively. The permanent deformation of the asphalt concrete surface was 1.2mm.

The variation of the vertical permanent strain with depth as a function of load repetitions is shown in Figure 91. As seen in the figure, most of the strain occurred in subgrade layer and in the top of the base course. The strain in the bottom half of the base course was about 3 times less then that in the top half of the base.

The change in the permanent vertical strains as a function of depth is shown in Figure 92. As can be seen in the figure, the significant deformations occurred in the upper subgrade layers.

Figure 91. Change in vertical permanent strains as a function of load repetitions in the base & subgrade (703C5).

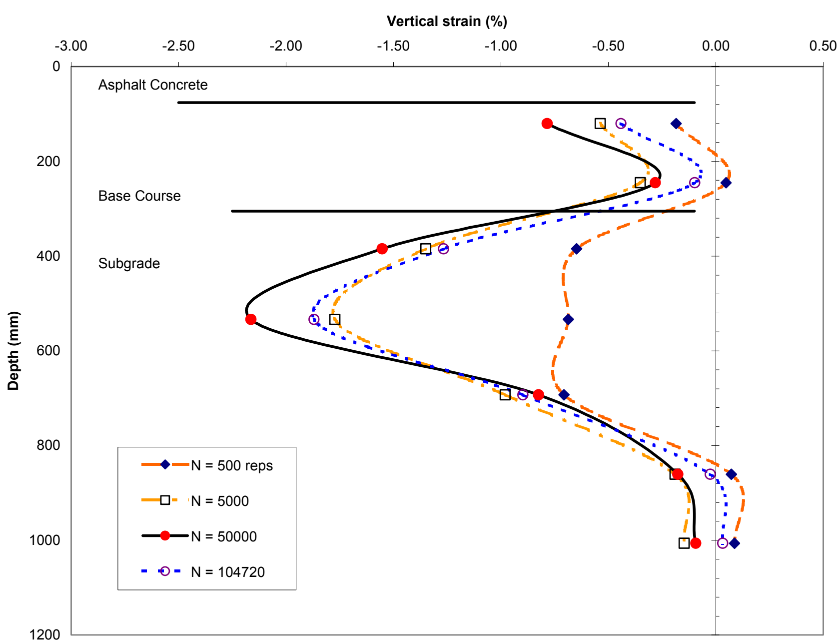

Figure 92. Permanent vertical strains as a function of depth (703C5).

The data in Figure 91, with the exception of the surface were re-plotted on a log-log scale, Figure 93. Power curves were fitted to the data and the coefficients are presented in Table 18.

Table 18. Coefficients for power law curves for permanent vertical strains (%).

Layer	A	n	R^2
Base (z = 120mm)	0.0206	0.3588	0.97
Base (z = 245mm)	0.0156	0.2778	0.33
Subgrade (z = 385mm)	0.2417	0.1855	0.89
z = 534mm	0.2187	0.2285	0.65
z = 693mm	0.6501	0.0351	0.29
z = 861mm	0.6501	0.0351	0.29
Z = 1007mm	0.0379	0.1099	0.13

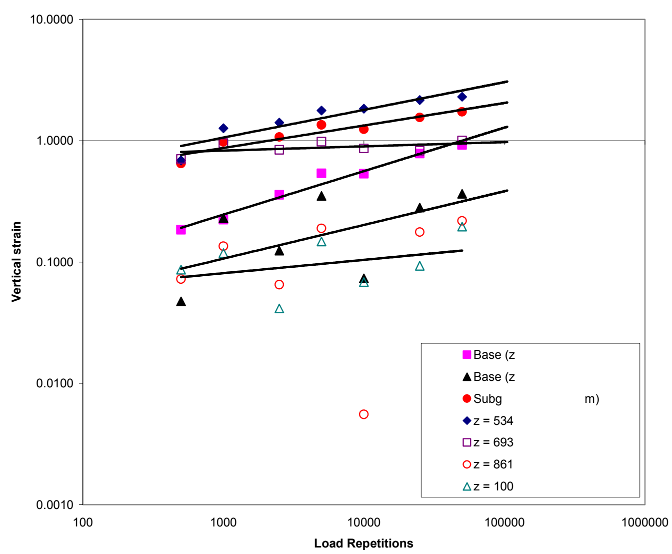

Figure 93. Change in vertical permanent strains as a function of load repetitions (log-log scale) in the base & subgrade (703C5).

With the exception of the top of the base layer (z = 63mm), Table F-14, in the longitudinal direction, the strains were less then 0.5%, Figure 94. Early in the test, the longitudinal strains were in extension. With increased load repetitions, the strains became compressive. In the subgrade, the highest longitudinal strain occurred at a depth of 150mm from the top of subgrade, Figure 95.

In the transverse direction, we also found that the transverse strains were in the same magnitude as the longitudinal strain, except that they were mostly in extension, Figure 96. The change in the permanent transverse strains in the subgrade as a function of depth is shown in Figure 97.

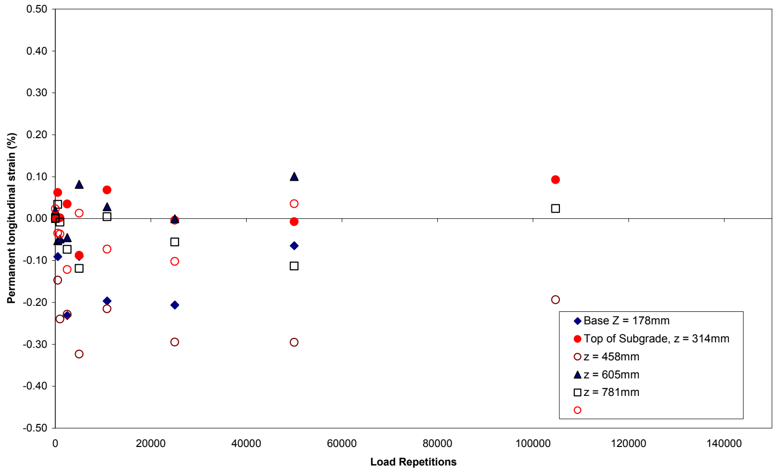

Figure 94. Change in longitudinal permanent strains as a function of load repetitions in the base & subgrade (703C5).

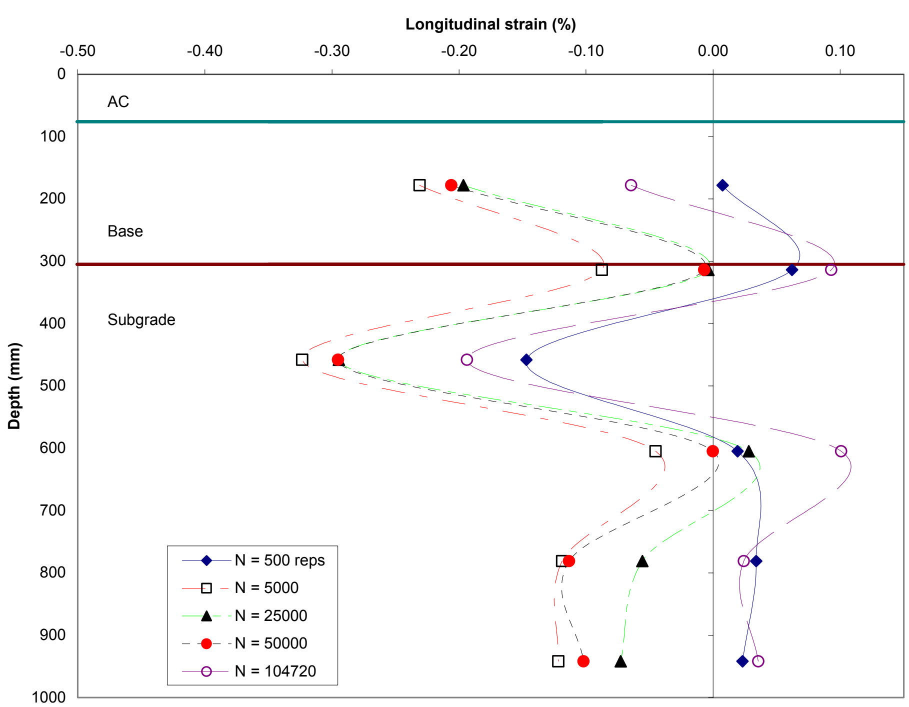

Figure 95. Permanent longitudinal strains as a function of depth, (703C5).

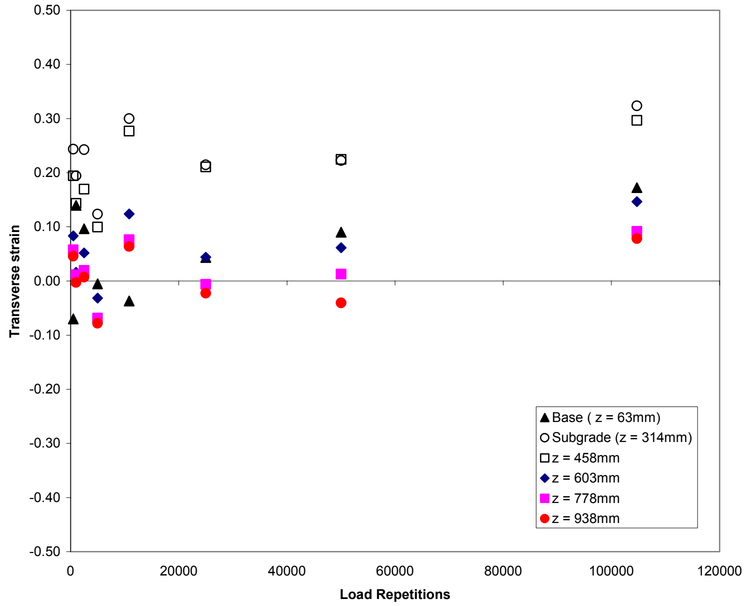

Figure 96. Change in transverse permanent strains as a function of load repetitions in the base & subgrade (703C5).

As seen in Figure 97, after 500 load repetitions, the transverse permanent strains headed towards the compression region. This was clearly seen at the lower depths. After 5000 passes, the strains started to become expansive and remained expansive to the end of the tests. The transverse strains in the bottom layer of the base were significantly higher and were outside of the calibration range and were not reported.

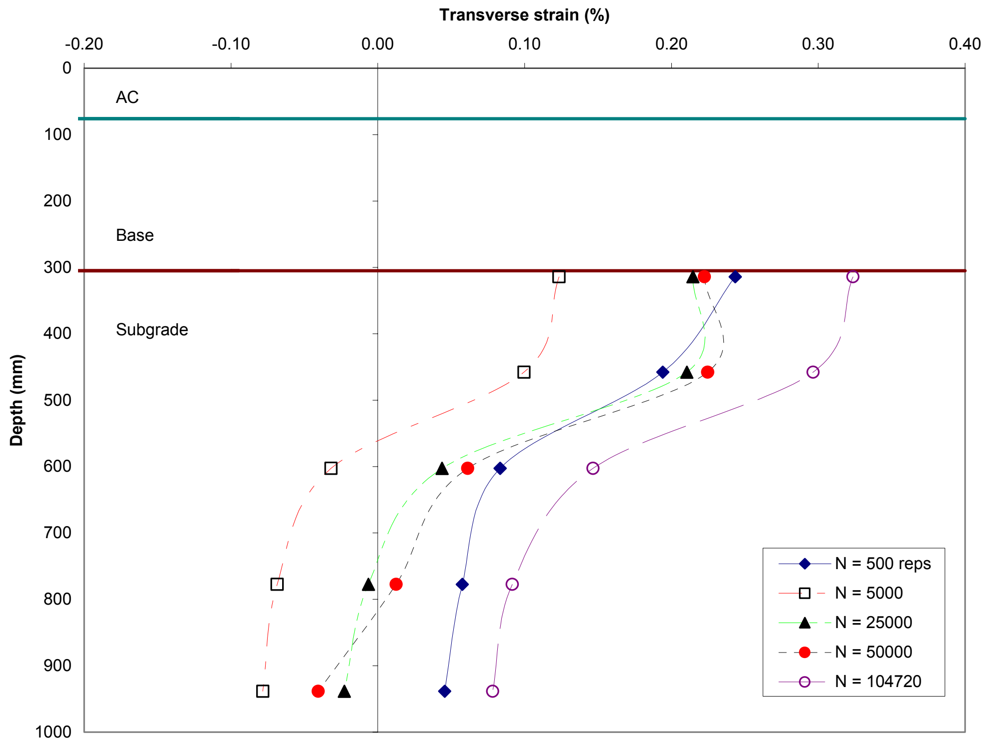

Figure 97. Permanent transverse strains as a function of depth, (703C5).

Surface Profile Measurements

As with the previous test section (TS701), twenty four surface profile measurements were made periodically to determine the surface deformation as a function of load repetitions. Of the 24 measurements, the first (1,2) and last two (23, 24) measurements were taken in the acceleration and deceleration areas. The measurements at these locations are not reported. The coil gages for measuring dynamic and permanent deformation are in the vicinity of locations 16 to 19, Figure 19. A typical set of surface deformation as a function load repetitions is shown at position 17 in Figure 98. A ten point running average was applied to the data shown in Figure 98. The maximum rut depth was extracted from the data after the ten point averaging was done. The maximum rut depths across the test section as a function of load repetitions is presented in Table F-16.

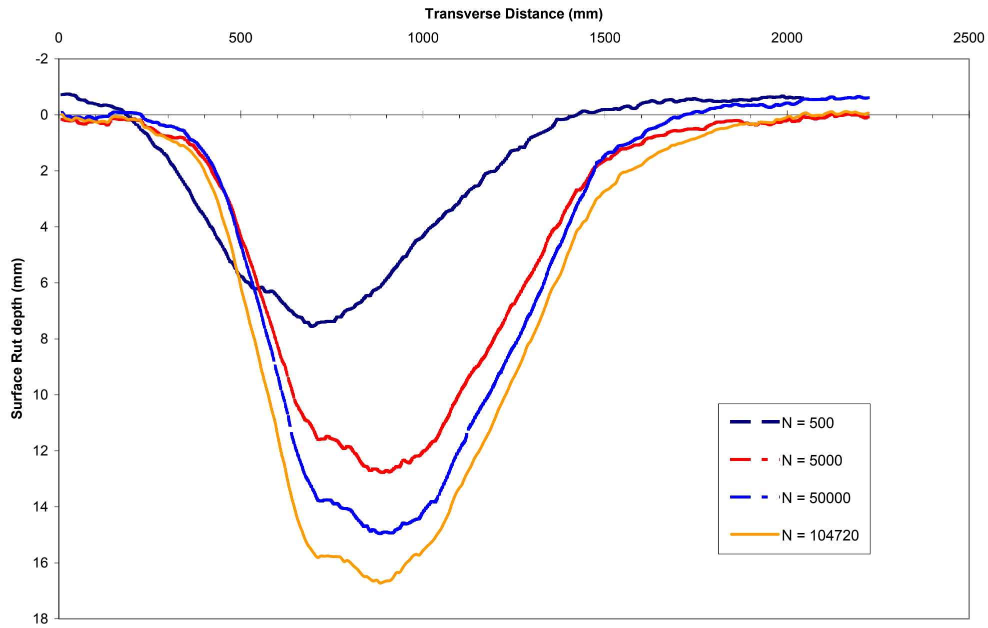

Figure 98. Typical rut depth response as a function of load passes (703C5).

The maximum variation in rut depth in the longitudinal direction is about 22% from one end to the other.

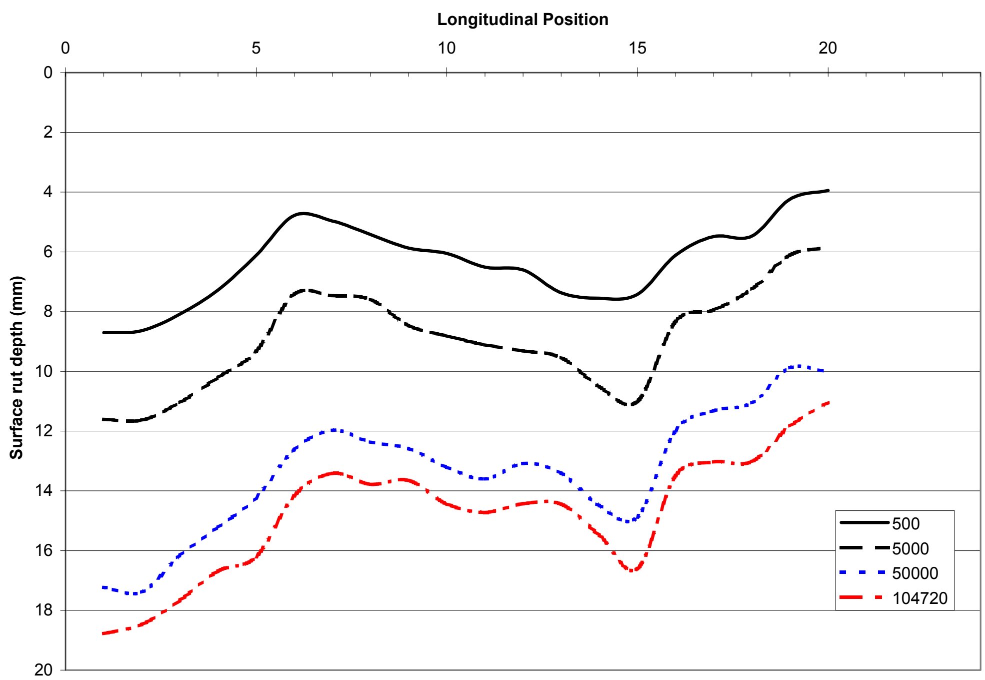

Figure 99. Longitudinal surface rutting as a function of load repetitions (703C5).

A comparison of the total rut depth measured from the profilometer and strain coil gages is shown in Figure 100. The coil gages were located near position 17 for the surface rut measurements. For the comparison, the average surface rut from positions 16 to 18 were used. At the beginning the difference between the 2 sets of data was approximately 3mm. As the test progressed, the difference dropped to about 5mm. At the end of the test, the difference increased to about 7mm. The results are tabulated in Table 19.

Table 19. Deformation from surface profile and subsurface coil measurements (mm)

Load Repetitions	Surface Profile	Coil gage
500	6.64	3.35
1000	7.40	6.07
2500	8.38	6.24
5000	9.45	8.61
5000	10.62	7.39
25000	11.93	9.69
50000	13.17	11.25
104720	14.66	6.93

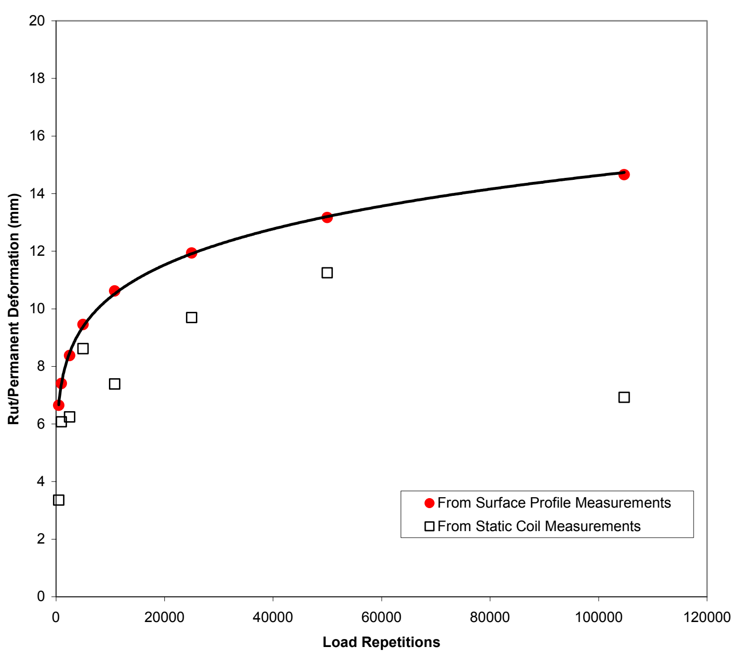

Figure 100. Comparison of total pavement deformation from surface profilometer and coil gage measurements

703C6

Testing of window 703C6 began on May 11th, 1998 and ended on October 10th, 1998. Based on load measurements from the HVS and tire pressure monitoring during the tests, the mean test load was 53-kN with a COV of 3.0 %, Figure 101a. The mean tire pressure was 709-kPa with a COV of 8.4%, Figure 101b.

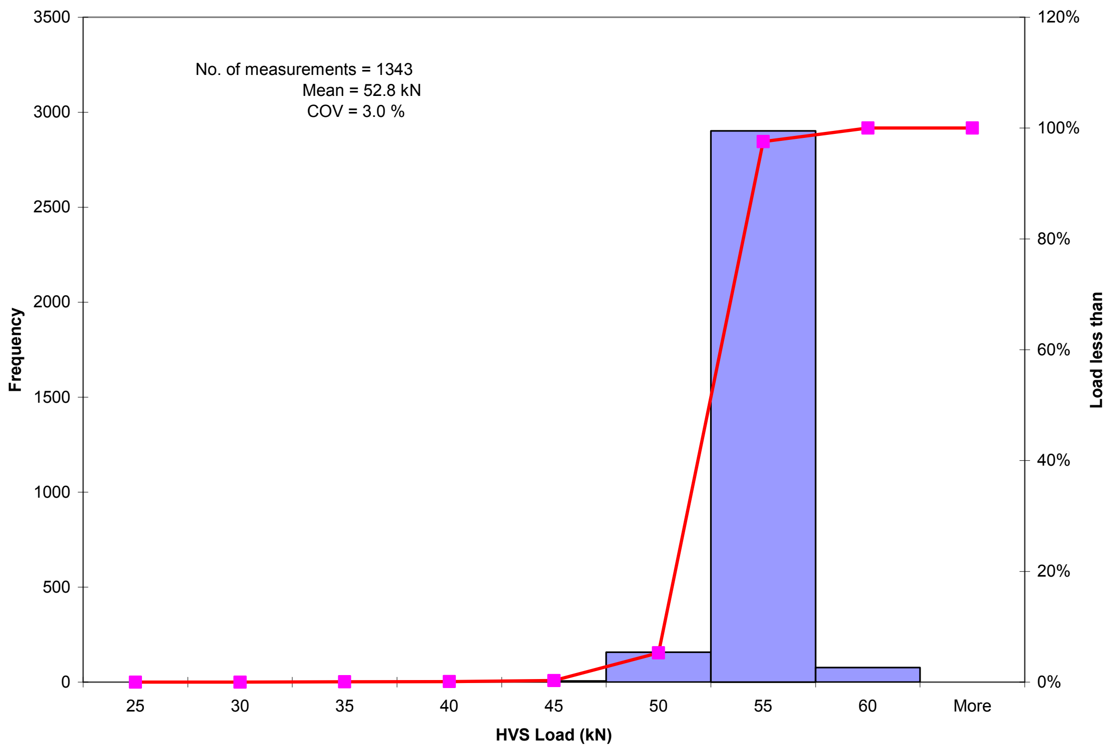

Figure 101a. Statistical presentation of test loads on 703C6.

The average sub-surface temperature in the test section was 18.6 °C with a COV of 5.8%. The average moisture content in the test section during the test was 13.1 % with a COV of 6.0%, Figure 102. The target moisture content during construction was 15 ± 2%. The average moisture measurements as a function of depth are presented in Table 20. The nearest VITEL gages to this window were located at depths of 1.09m and 1.52m.

Dynamic Stress

Stress measurements were made at the top of the subgrade, Figures 12c & d. Three DYNATEST pressure cells were also installed to measure the vertical, longitudinal and transverse dynamic stresses. These cells were installed at a depth of 160mm from the surface. Typical vertical, longitudinal and transverse stress response curves are shown in Figures 103 to 105.

Maximum stresses from the test are presented in Table G-1, Appendix G. Negative values indicate compressive stress. With respect to the vertical stress near the top of the subgrade (z = 453 mm), in general, the stresses increased with increased load repetitions,

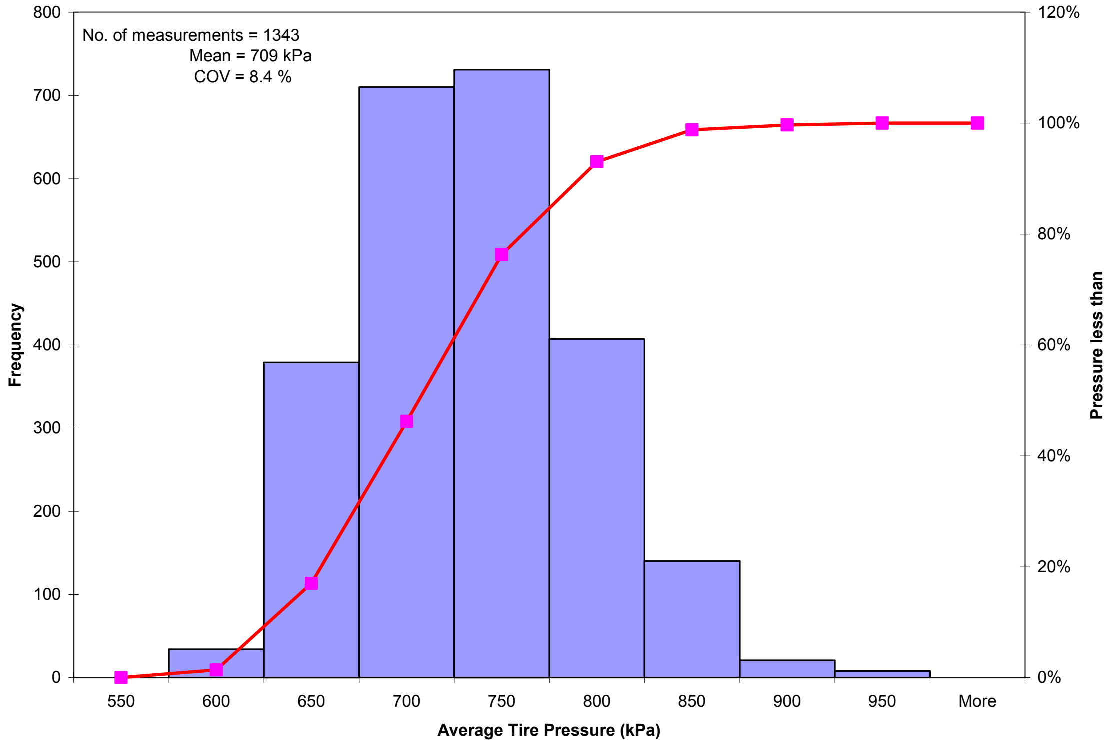

Figure 101b. Statistical presentation of test tire pressures on 703C6.

Table 20. Average moisture content as a function of depth during testing of 703C6.

Depth from top of AC (mm)	Gravimetric moisture content (%)
360	12.84
610	12.54
910	No Data
1090	14.02

Figure 102. Distribution of moisture content in test section during testing of 703C6.

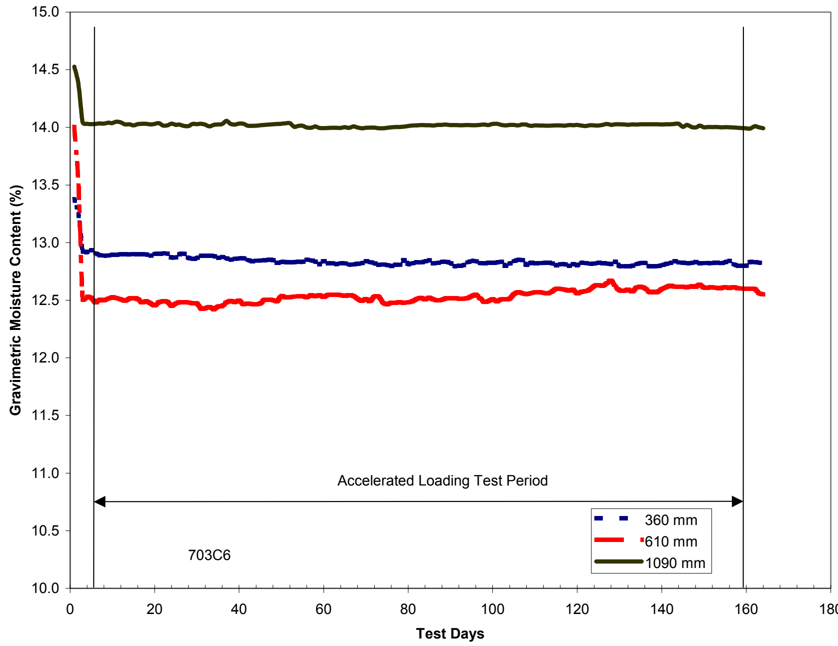

Figure 103. The vertical stress started around 50-kPa at the beginning of loading and

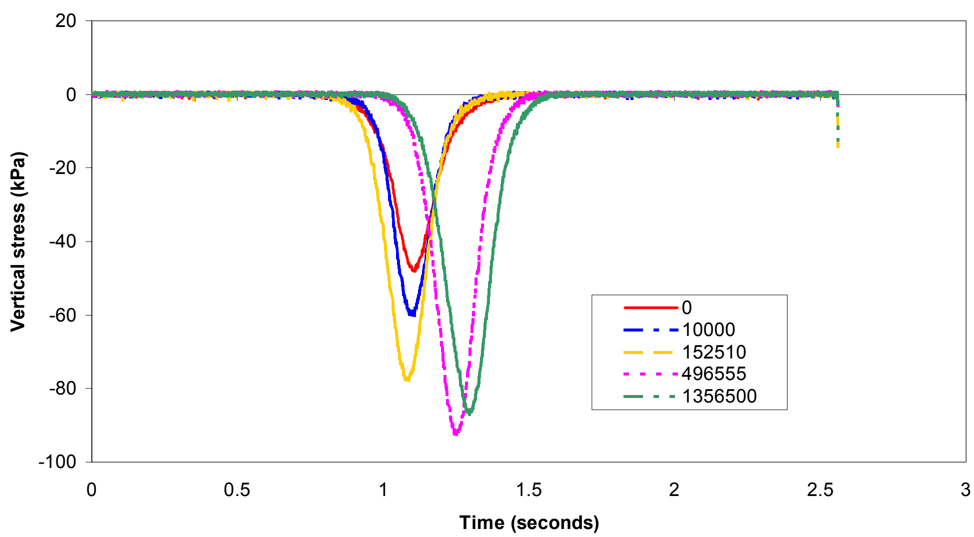

Figure 103. Dynamic vertical stress response in the top 150mm of subgrade (703C6).

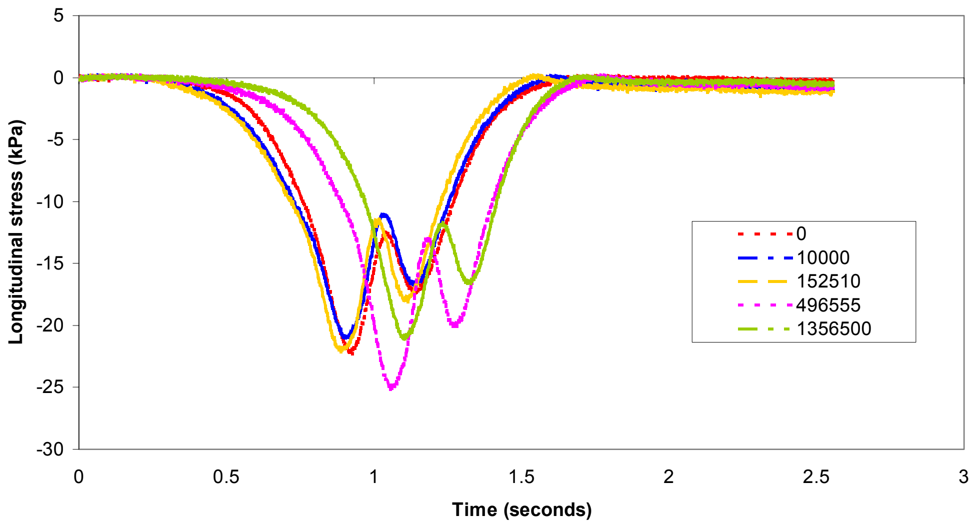

Figure 104. Dynamic longitudinal stress response in the top 150mm of subgrade (703C6).

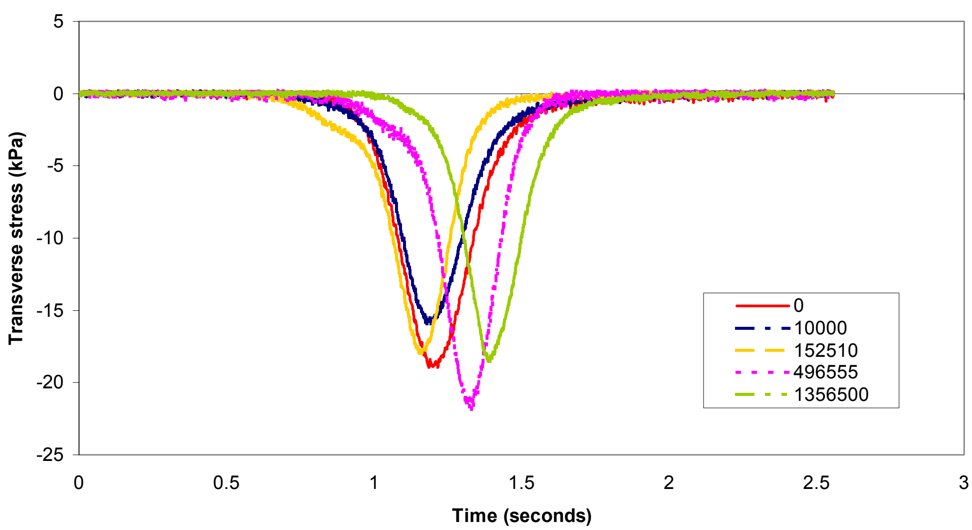

Figure 105. Dynamic transverse stress response in the top 150mm of subgrade (703C6).

ended around 90-kPa after 1356500 load repetitions. A power curve was fitted to the data and presented in Figure 106. With respect to the longitudinal stresses, the peak stress during the accelerated loading phase remained around 22-kPa with a coefficient of variation of approximately 6%. The R^2 for a power fit, Figure 106, was low suggesting further substantiating our conclusion of no significant change in the longitudinal stress with increased load repetitions. In the transverse direction, generally the stress was increasing with increasing load repetitions, Figure 105. The transverse stresses ranged between 13.5 to 20-kPa during the accelerated loading phase. A power curve was also fitted to the data and the results are presented in Figure 106 and in Table 21.

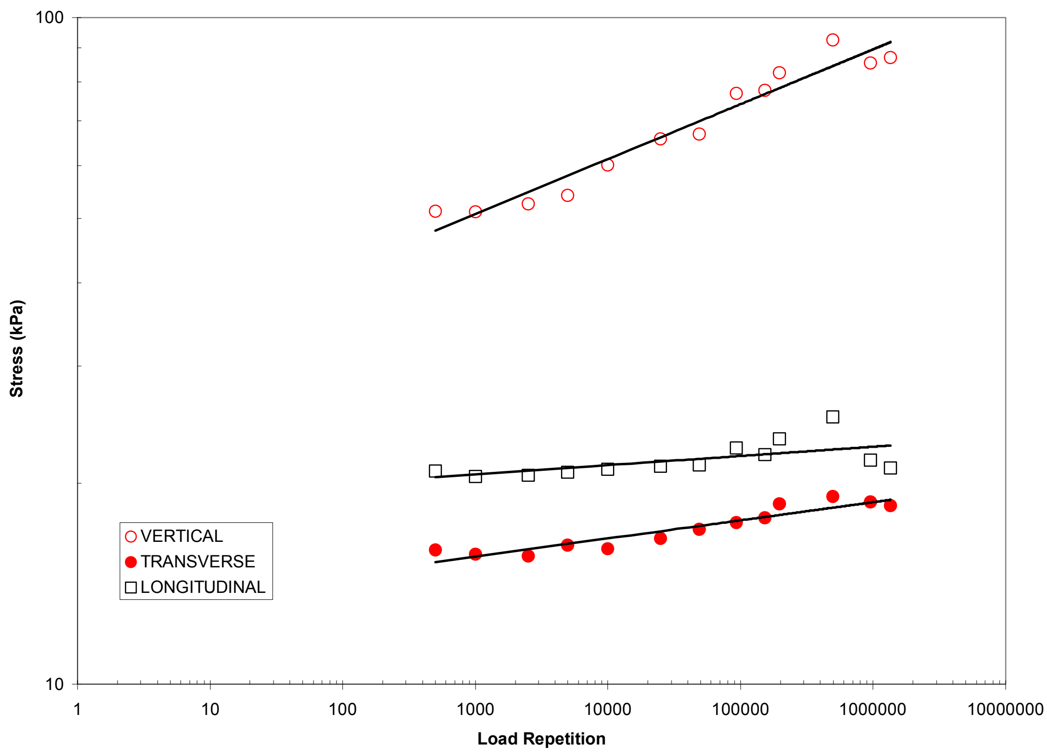

Figure 106. Development of stresses as a function of load repetitions in the top 150 mm of subgrade (703C6).

Table 21. Power curve coefficients for measured stresses in 703C6.

Stress Direction	A	n	R^2
Vertical	28.71	0.0824	0.95
Longitudinal	18.76	0.0138	0.37
Transverse	12.88	0.0272	0.88

Dynamic Strains

Vertical, longitudinal and transverse dynamic strains were measured as a function of load repetitions at the 3 wheel locations. There were two locations for strain measurements in the base. Coils were installed at the bottom of the asphalt and at the bottom of the base layer. A third coil was installed halfway in between the two other coils in the base. This coil failed and vertical strain measurements were attempted between the coil pairs located under the asphalt layer and the bottom of the base. The distance between the coil pairs was 229mm. As seen in Tables H-1, the coils worked partially through the test (up to 10000 load repetitions). The vertical strains were compressive, while the longitudinal and transverse strains were expansive. It was also found that in general the maximum displacements (strains) occurred when the wheel was in position 2.

The maximum displacements and strains presented in Tables H-1 to H-6 in Appendix H were obtained after the data was smoothed using a 10 points averaging scheme. As with other windows and test sections, in the longitudinal and transverse directions the displacements (strains), were measured at the actual location of the coil gages. The difference between the vertical and horizontal strain measurements is about 75mm below the horizontal strain locations. Three sets of measurements are reported for the longitudinal strain, initial compressive strain, maximum expansive strain and the compression strain during unloading (see Figure D-2, Appendix D).

The vertical displacements at the top of the subgrade ranged around 0.1mm. This translated to an average strain of approximately 750mm, Tables H-1 and H-2. The trend of the vertical dynamic strains as a function of load repetitions is shown in Figure 107. We found that there were small changes in the vertical dynamic strains as a function of load repetitions in the upper 457mm of subgrade. The dynamic strains at 838mm from the AC surface and lower appeared to increase with increasing load repetitions. We fitted a power curve to the strain measurements at depths of 838mm and 983mm. The coefficients for the power curves are presented in Table 22. The coefficient of correlation of the power curves for the strain measurements in the upper 457mm subgrade layer was significantly poor. Based on visual inspection, we estimated that the same power coefficients for the strains at 838mm could be used in the upper 457mm, Table 22.

Table 22. Coefficients for power law curves for dynamic vertical strains.

	Depth (mm)	A	n	R^2
Subgrade	383	540	0.0282	
	540	320	0.0282	
	702	250	0.0282	
	838	157	0.0282	0.50
	983	71	0.0621	0.96

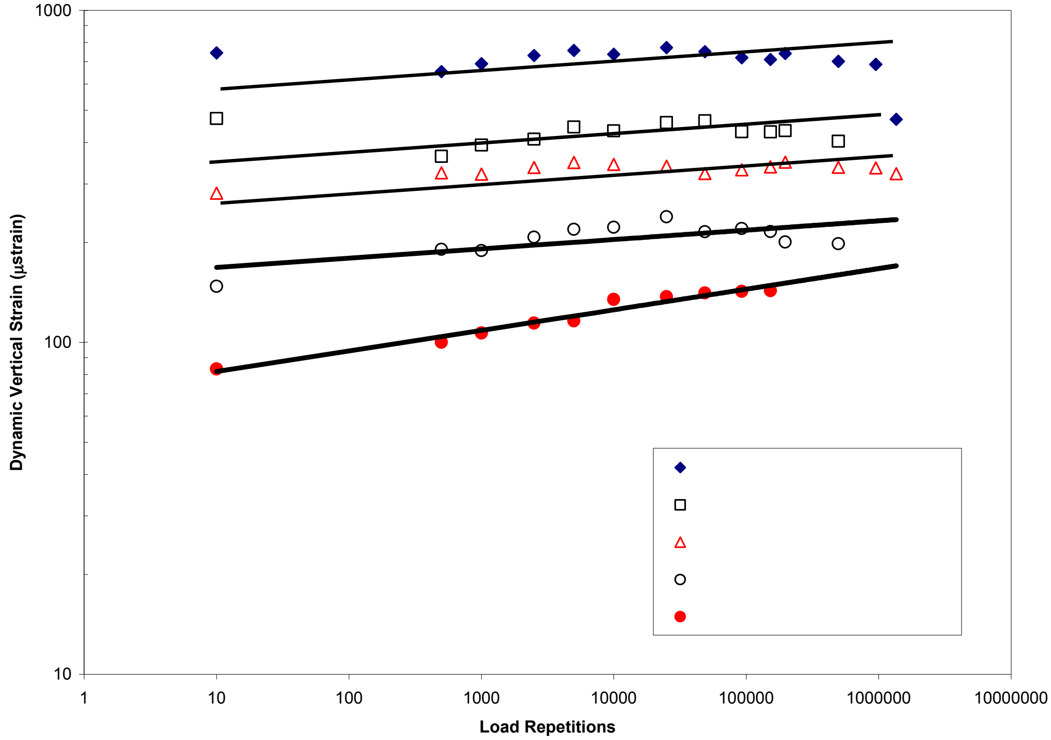

Figure 107. Change in vertical strains as a function of load repetitions in the base & subgrade (703C6).

In the longitudinal direction, we found that the strains (displacements) were compressive as the wheel approached the gages. When the wheel was on top of the gages, the strains (displacements) were expansive. As the wheel moved away from the gages, the strains (displacements) became compressive again. The compressive strains (displacements) at the tail end usually were smaller then the approach end. The maximum strains (displacements) are presented in Appendix H, Tables H-3 to H-9. As before, the maximum strains (displacements) occurred when the wheel was in position 2. As with the vertical strains, the longitudinal strain gages in the middle of the base (z = 152mm) failed. Also as seen in the tables, the longitudinal strain gages at the top of the subgrade (z = 304mm) failed after 25000 passes. In addition all the gages failed after 150000 passes.

The changes in the longitudinal strains as a function of load repetitions are presented in Figure 108. As with TS701, the longitudinal strains in Figure 108 is the absolute sums of strains A and B, (Figure E-1, Appendix E). We found that with the limited data, the response at the top of the subgrade and at z = 464mm could be combined into one. Also a similar combination can be made with the data at z = 709mm and at z = 931mm. The coefficients for the power curves and the respective coefficients of correlations are presented in Table 23.

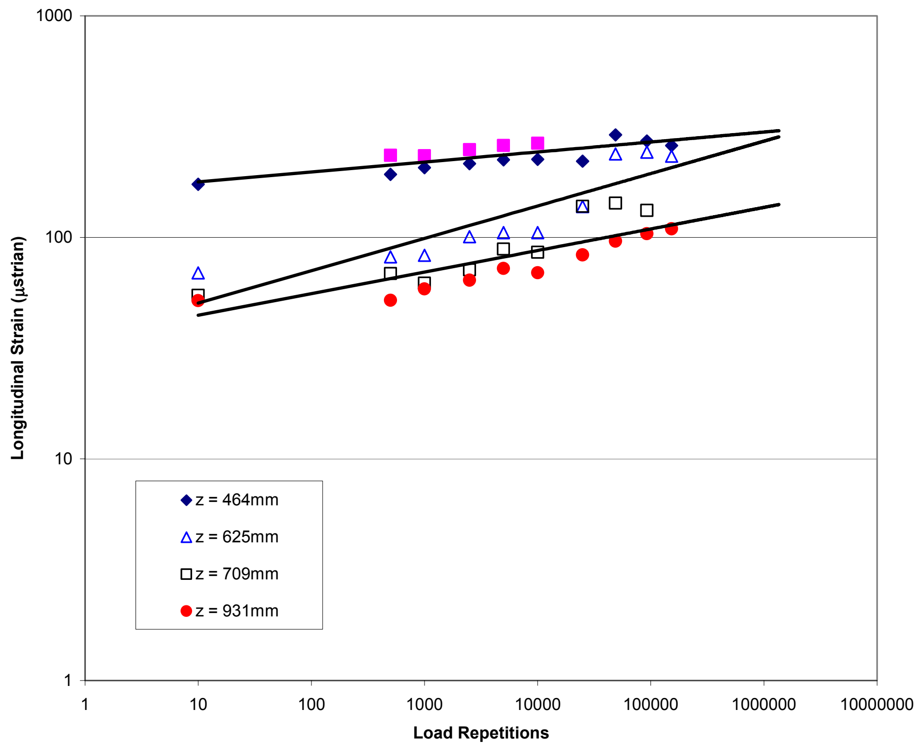

Figure 108. Change in longitudinal strains as a function of load repetitions (log-log scale) in the subgrade (703C6).

Table 23. Coefficients for power law curves for dynamic longitudinal strains.

	Depth (mm)	A	n	R^2
Subgrade	304	161	0.045	0.63
	464	161	0.045	0.63
	625	36	0.146	0.78
	709	36	0.097	0.69
	931	36	0.097	0.69

In the transverse direction, the strains were all expansive. Again we were unable to measure the transverse strains in the base course. Also, the transverse strains in the subgrade at z = 709mm and below were extremely noisy. The remaining maximum transverse displacements and strains are presented in Tables H-10 and H-11 in Appendix H. In case of the transverse displacements (strains), the maximums occurred when the load was in position 3. The changes in the transverse strains as a function of load repetitions in the subgrade are presented in Figure 109. The transverse strain at the top of the subgrade remained fairly constant throughout the test at around 200 µstrain. Power curves were used to fit the strain versus load repetition data and the coefficients for the power curves are presented in Table 24.

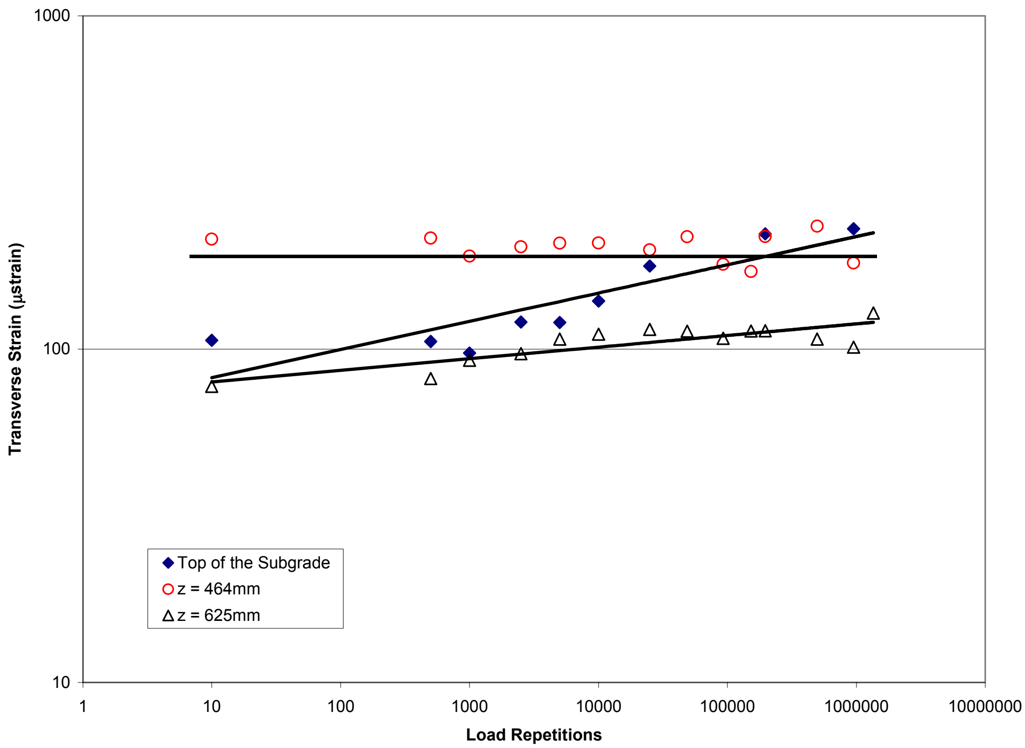

Figure 109. Change in transverse strains as a function of load repetitions in the subgrade (703C6).

Table 24. Coefficients for power law curves for dynamic transverse strains.

	Depth (mm)	A	n	R^2
	304			
	464	67	0.0848	0.77
	625	73	0.0349	0.69
Subgrade	709			
	931			

Permanent Strains

As with the dynamic strain measurements, one of the coil gages used to the measure the vertical deformation in the base course failed at the end of construction. Up to and including 10000 load repetitions, the total deformation of the base course was based on the coil measurements located at the bottom of the asphalt layer and on top of the base course. After 10,000 passes, coil gage at the bottom of the asphalt layer also failed. Attempts to measure the vertical deformation using the X-X and Y-Y gages were marginally successful. The problem with using the data from the X-X or Y-Y gages was that there was no reference (zero load application) data. The vertical subgrade permanent deformation as a function of load repetitions is presented in Figure 110 and n Table H-12 in Appendix H.

With respect to the subgrade, it was found that most of the deformation occurred in the upper subgrade layers. The second subgrade layer showed a pronounced dilation after about 500000 load repetitions. We have not seen this type of behavior in the other test windows or in TS701. For the moment, we think that this effect may be due to instrumentation error. However, future review of the data will be made based on results from other test sections. The deformation of the bottom 2 layers appear to follow a similar pattern. Based on the results and assuming that the deformation pattern at z – 464mm is the same as the top of the subgrade, the total deformation of the subgrade is approximately 9.5mm.

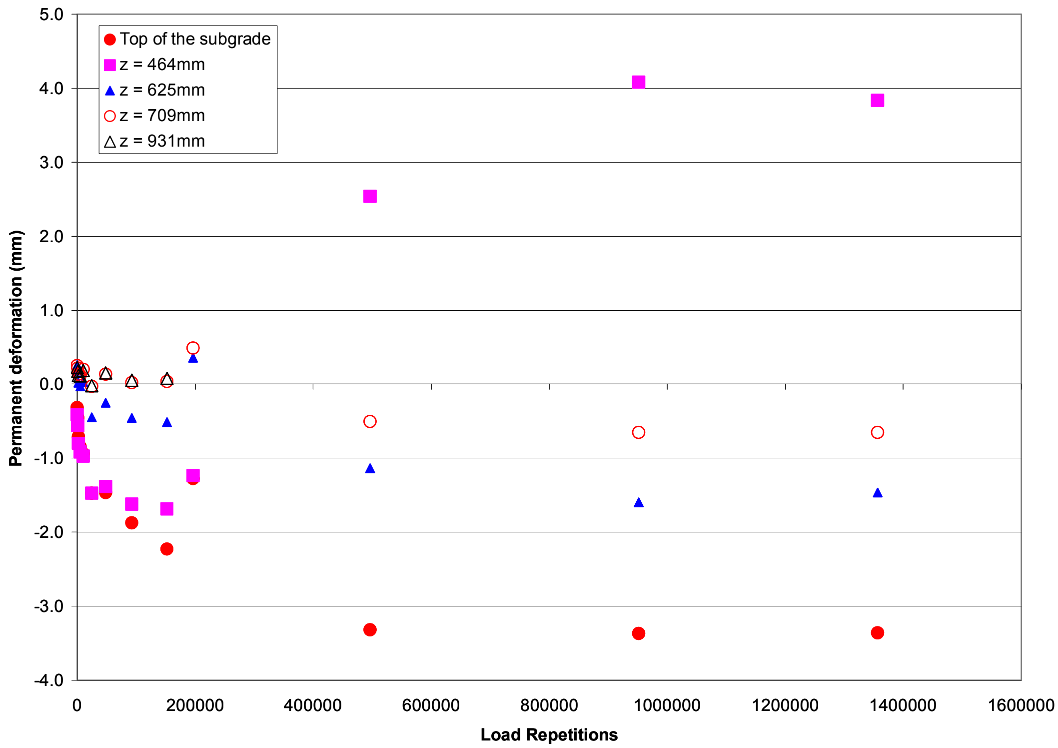

Figure 110. Development of vertical permanent deformation as a function of load repetition and depth (703C6).

The corresponding permanent vertical strains are presented in Table H-13, Appendix H. The change in the vertical strain with depth as a function of load repetitions is shown in Figure 111. Again, it shows that proportionally, the highest strains in the subgrade are in the upper 300mm of the subgrade layer. The average vertical strains for the upper subgrade layer (z = 304 and z – 464mm) and the vsertical strain at z = 625mm as a function of load repetition in log-log format are presented in Figure 112. Power curves were fitted to the data and coefficients tabulated in Table 35.

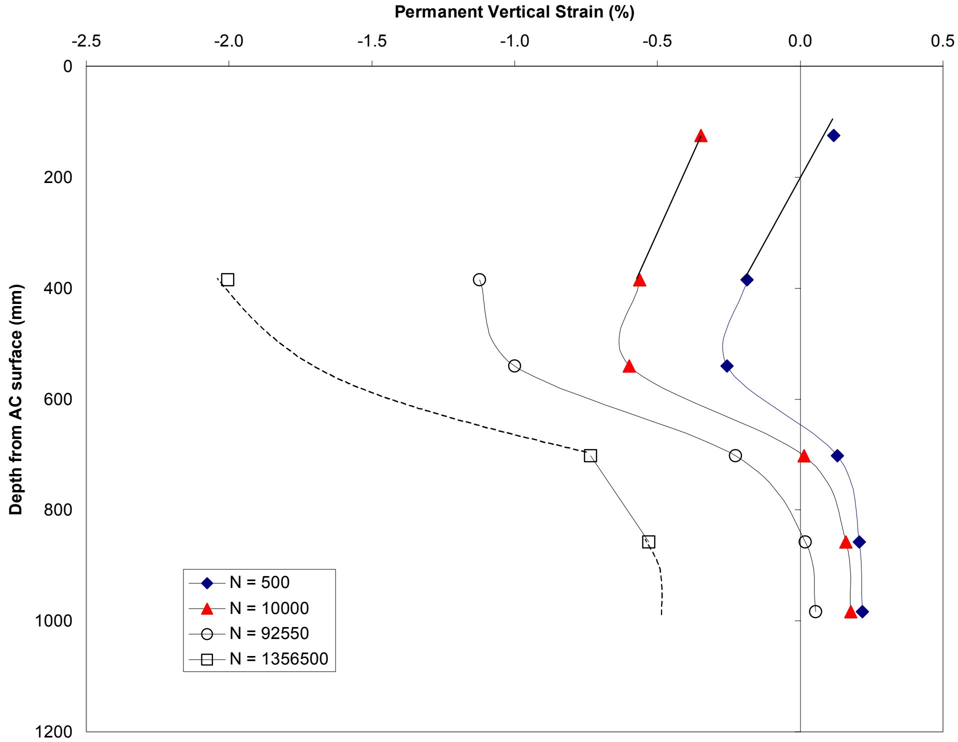

Figure 111. Permanent vertical strain as function of depth.

Table 25. Coefficients for power law curves for permanent vertical strains.

	Depth (mm)	A	n	R^2
Subgrade	304-464	0.0523	0.2609	0.93
	625	0.0002	0.6154	0.84

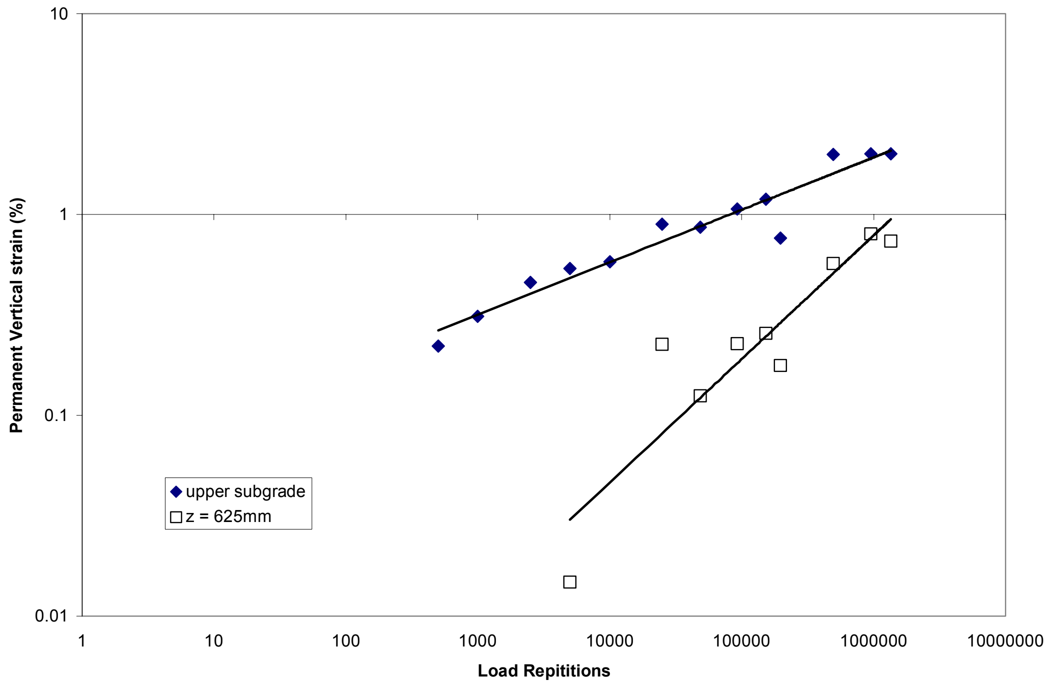

Figure 112. Permanent strain development in the subgrade as a function of load repetition.

The deformation and strains in the longitudinal direction are presented in Tables H-12 and H-13, Appendix H. The measured deformations at the top of the subgrade were extremely large (100 to 200 mm range) and are outside the calibrated range of the coils. Changes in the longitudinal deformation in the subgrade with respect to load repetition as a function of depth are shown in Figure 113. The range of the longitudinal deformation was ± 0.4mm. Initially, the longitudinal strains were extensive and with increased load repetitions, the strains became compressive, Figure 114.
The deformation and strains in the transverse direction are presented in Tables H-12 and H-13, Appendix H. The measured transverse deformations at the top of the subgrade were extremely large (100 to 200 mm range) and are outside the calibrated range of the coils. Changes in the transverse deformation in the subgrade with respect to load repetition as a function of depth are shown in Figure 115. The range of the longitudinal deformation was 0.6 to –0.4mm. Initially, the longitudinal strains were extensive and with increased load repetitions, the strains became compressive.

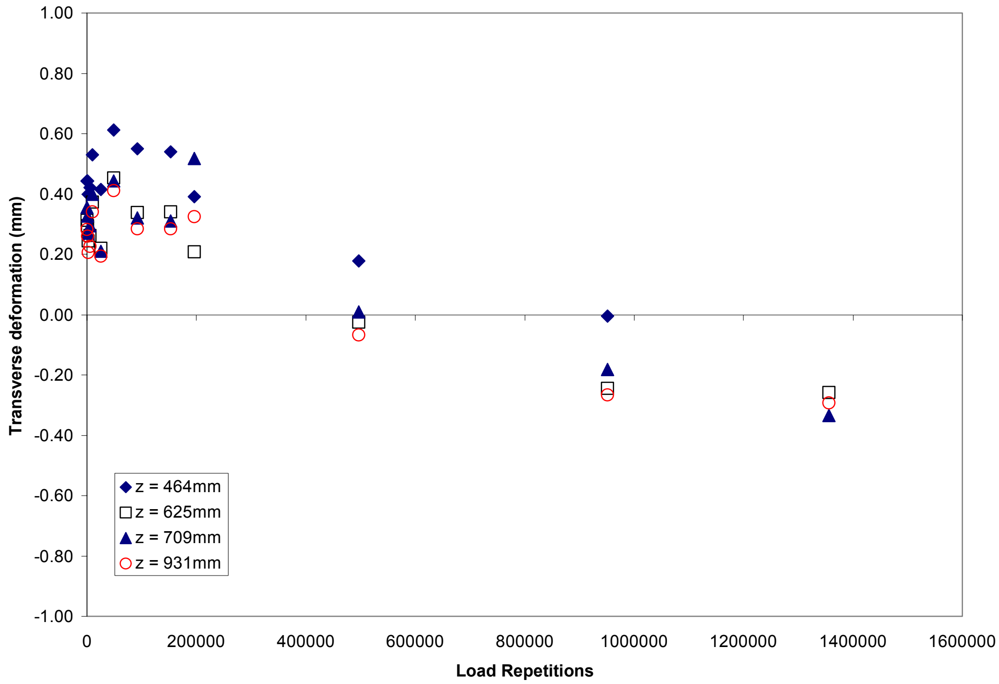

Figure 115. Devevolpment of transverse strains as a function of load repetition (703C6).

Surface Profile Measurements

Twenty-four surface profile measurements were made periodically to determine the surface deformation as a function of load repetitions. Of the 24 measurements, the first (1,2) and last two (23, 24) measurements were taken in the acceleration and deceleration areas. The measurements at these locations are not reported. The coil gages for measuring dynamic and permanent deformation are in the vicinity of locations 16 to 19, Figure 19. A typical set of surface deformation as a function load repetitions is shown at position 17 in Figure 116. A ten point running average was applied to the data shown in Figure 116. The maximum rut depth was extracted from the data after the ten point averaging was done. The maximum rut depths across the test section as a function of load repetitions is presented in Table H-14.

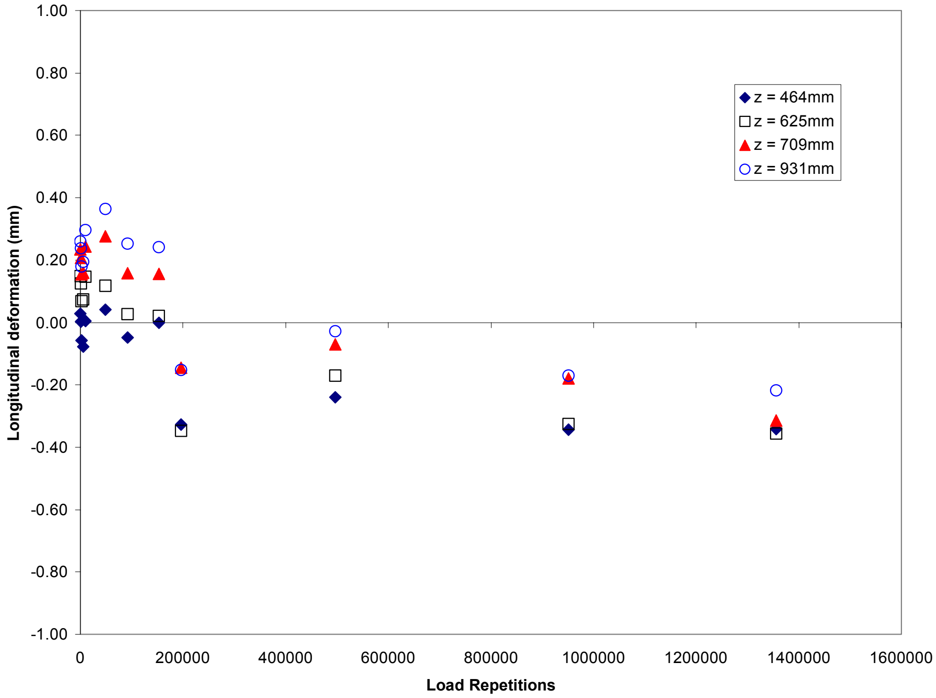

Figure 113. Development of longitudinal deformation as a function of load repetition (703C6).

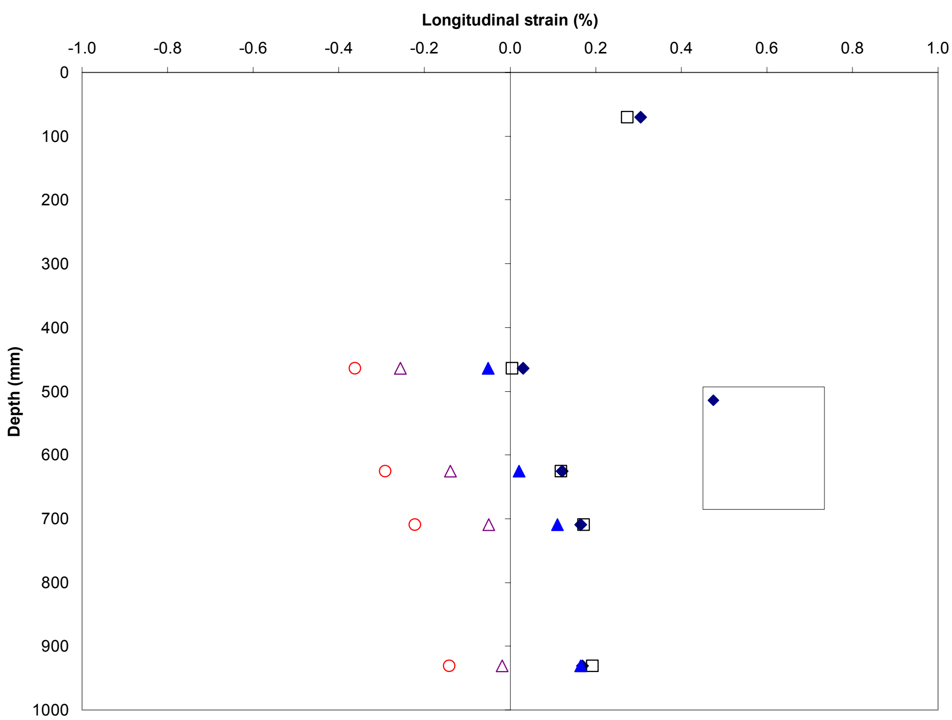

Figure 114. Variation of longitudinal strain asa function of depth.

The maximum variation in rut depth in the longitudinal direction is about 17% from one end to the other. The higher variations occurred earlier in the loading phase and reduced to about 8% after 10000 load repetitions. A typical set of longitudinal rut depth measurements as a function of load repetitions are shown in Figure 117.

A comparison of the total rut depth measured from the profilometer and strain coil gages is shown in Figure 100. The coil gages were located near position 17 for the surface rut measurements. For the comparison, the average surface rut from positions 16 to 18 were used. The difference between the coil gage and surface profile measurements were reasonably close, the difference was between 1 to 2 mm. After 10,000 load repetitions, the difference became large. This large difference is due to the loss of the surface, and base deformations in the coil measurements. The maximum difference was 4.25mm between the two sets of measurements and it occurred at about 50000 load repetitions. At the end of the test, the difference was about 3mm. The results are tabulated in Table 26.

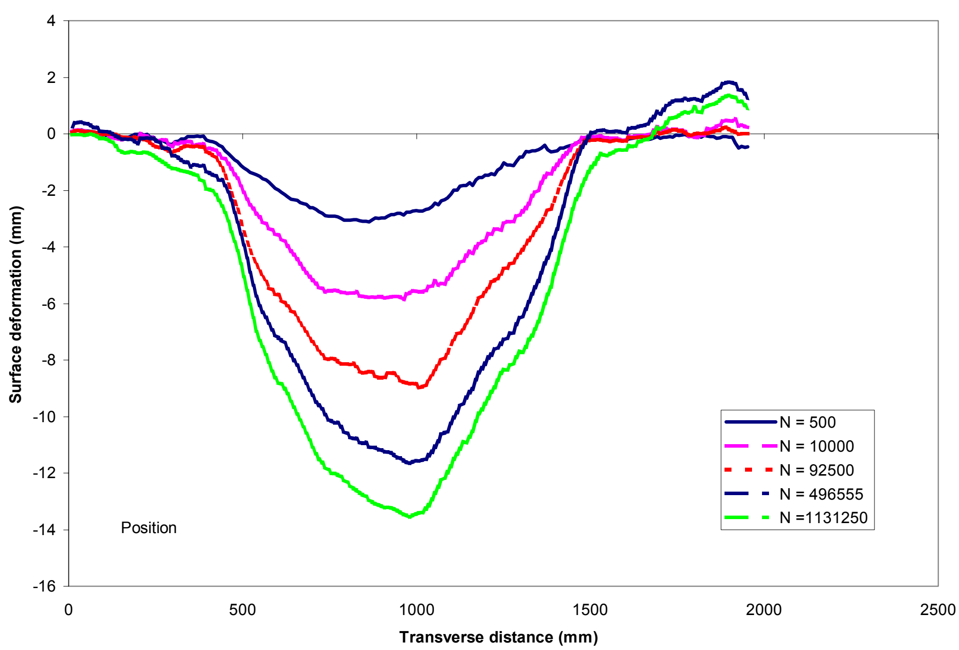

Figure 116. Typical rut depth response as a function of load passes (703C6).

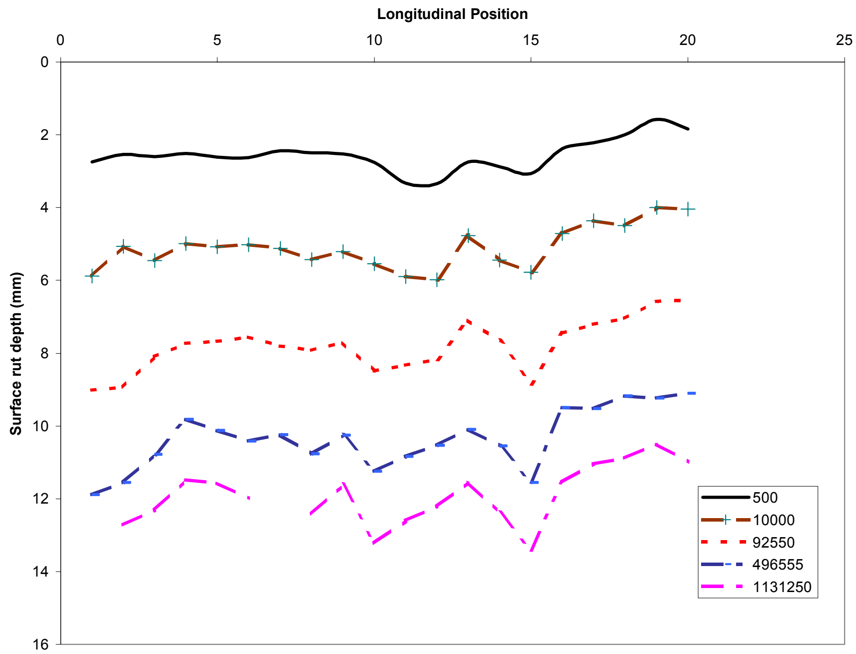

Figure 117. Longitudinal surface rutting as a function of load repetitions (703C6).

Table 26. Deformation from surface profile and subsurface coil measurements (mm)

Load Repetition	Surface Profile	Coil Gages
500	2.55	-0.47
1000	3.03	1.04
2500	3.72	2.31
5000	4.17	3.18
10000	4.95	3.27
25000	6.24	3.45
48772	7.06	2.81
92550	7.83	3.88
152510	8.32	4.32
496555	10.20	8.29
951065	11.60	8.99
1131250	12.00	
1356500		8.83

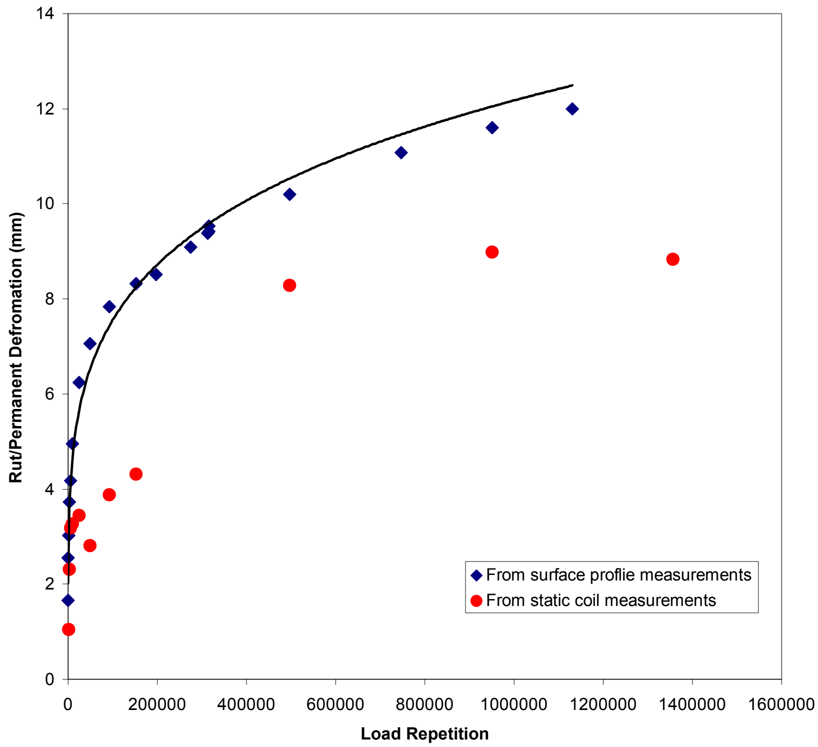

Figure 118. Comparison of total pavement deformation from surface profilometer and coil gage measurements.

APPENDIX A

Table A-1. As constructed densities of the various layers.

		Depth below AC surface (meters)					
Station	BASE	0.305	0.61	0.762	0.914	1.067	1.219
			Density (kg/m3)				
1	1856	1934	1912	1791	1801	1860	1848
2	2151	1947	1889	1864	1841	1764	1870
3	2167	1864	1835	1803	1851	1775	1917
4	2190	1950	1811	1815	1856	1804	1907
5	1982	1868	1774	1836	1841	1774	1915
6	2087	1891	1698		1868	1746	1897
7	2087	1872	1824		1854	1742	1904
8	2231	1909	1904	1766	1804	1734	1888
9	2231	1925		1840	1812	1775	1878
10	2344	1970		1795	1783	1735	1889
11	2199	1944	1832	1838	1793	1923	1896
12	1992	1925	1774	1822	1815	1782	1912
13	2247	1901		1843	1804	1737	1860
14	1878	1941		1833	1832	1748	
15	2051	1960		1865	1865	1824	
16	1990	1917		1840	1856	1791	1859
17	2210	1905	1846	1897	1857	1774	1886
18	2183	1926	1891	1807	1875	1758	1873
19	2392	1944		1872	1870	1721	1891
20	2231	1937		1815	1836	1750	1917
21	2360	1937	1896	1830	1864	1769	1928
22	2103	1865	1840	1840	1870	1758	
23	2328	1888	1729	1836	1867	1787	
24	2199	1897	1901	1851	1872	1896	1886
25	2167	1947		1867	1856	1917	
26	2055	1893	1799	1840	1859	1881	
27	2007	1918	1899	1840	1796	1750	1875
28	1990	1881	1926	1876	1876	1804	1912
29	2079	1854	1926	1820	1870	1798	1901
30	2119	1923		1852	1852	1766	2019

Table A-2. Moisture content in upper subgrade and base course.

Station	BASE	0.305	0.61	0.762	0.914	1.067	1.219
		Depth below AC surface (meters)					
		Moisture Content (%)					
1	3.4	12.3	12.5	17.4	17.0	15.0	14.7
2	3.4	11.6	14.4	14.0	16.2	17.1	13.3
3	3.8	15.3	16.0	17.4	15.0	17.1	11.5
4	4.2	11.2	15.4	16.7	14.5	17.9	12.5
5	4.2	13.2	19.7	15.3	14.7	17.6	12.4
6	4.0	12.8	22.4		14.2	18.7	13.0
7	4.0	12.4	16.2		14.4	18.8	13.0
8	3.7	11.9	14.7	19.3	16.2	18.1	13.4
9	3.5	11.2		15.9	17.3	17.2	13.5
10	3.6	10.6		16.6	16.6	18.3	13.5
11	3.7	11.4	14.7	15.8	16.8	13.3	13.5
12	2.6	10.5	17.7	15.4	15.3	17.6	13.0
13	3.6	11.6		15.4	15.8	19.3	14.0
14	4.0	10.7		15.8	15.5	18.3	
15	3.8	11.0		14.1	14.1	16.1	
16	4.0	11.9		15.3	14.3	16.0	14.5
17	3.8	9.0	15.6	13.9	14.8	17.2	14.1
18	4.4	11.9	13.9	15.2	14.2	17.7	14.3
19	3.5	10.1		15.8	14.1	18.5	14.2
20	4.3	10.2		16.6	14.9	19.0	13.2
21	3.7	10.6	14.0	15.9	13.6	17.8	12.9
22	3.8	9.5	15.7	15.8	13.8	18.1	
23	3.7	9.6	21.3	15.4	14.1	17.9	
24	2.8	11.0	12.9	14.0	13.5	13.2	14.2
25	2.9	10.7		14.6	14.4	12.0	
26	3.5	10.1	18.1	14.9	14.1	13.7	
27	3.4	11.6	14.0	15.0	14.9	18.0	14.1
28	3.3	12.9	13.3	13.9	15.3	16.0	13.4
29	3.7	11.7	13.3	16.1	14.2	17.7	13.4
30	3.5	10.1		16.2	14.3	19.5	12.1

Table A-3. Measured layer thickness in TS703

STATION	Depth below AC surface (m)				
	0.305	0.61	0.914	1.219	BASE
	Layer Thickness (mm)				
1	137.16	371.86	271.27	365.76	
2	149.35	390.14	246.89	353.57	
3	173.74	368.81	249.94	332.23	252.98
4	173.74	356.62	265.18	316.99	252.98
5	167.64	347.47	277.37	310.90	262.13
6	192.02	289.56	329.18	298.70	262.13
7	201.17	274.32	344.42	292.61	265.18
8	195.07	295.66	341.38	274.32	252.98
9	188.98	295.66	326.14	307.85	259.08
10	210.31	274.32	341.38	289.56	262.13
11	222.50	304.80	338.33	289.56	259.08
12	252.98	332.23	310.90	304.80	271.27
13	155.45	350.52	274.32	390.14	
14	161.54	347.47	286.51	362.71	
15	146.30	359.66	307.85	329.18	240.79
16	155.45	350.52	286.51	338.33	249.94
17	155.45	338.33	320.04	307.85	243.84
18	176.78	316.99	326.14	301.75	240.79
19	198.12	283.46	341.38	283.46	252.98
20	179.83	301.75	335.28	277.37	237.74
21	176.78	301.75	332.23	274.32	249.94
22	188.98	310.90	335.28	277.37	256.03
23	210.31	338.33	320.04	286.51	274.32
24	240.79	332.23	307.85	304.80	277.37

Table A-3. Measured layer thickness in TS703 (continued)

STATION	Depth below AC surface (m)				
	0.305	0.61	0.914	1.219	BASE
	Layer Thickness (mm)				
25	219.46	274.32	271.27	368.81	277.37
26	204.22	289.56	298.70	374.90	237.74
27	167.64	320.04	332.23	341.38	256.03
28	164.59	341.38	292.61	344.42	240.79
29	164.59	338.33	301.75	320.04	231.65
30	179.83	323.09	307.85	304.80	237.74
31	213.36	301.75	310.90	307.85	237.74
32	207.26	298.70	316.99	301.75	219.46
33	198.12	304.80	301.75	286.51	234.70
34	192.02	323.09	304.80	301.75	256.03
35	231.65	326.14	310.90	298.70	256.03
36	234.70	316.99	307.85	323.09	265.18
37	262.13	243.84	262.13	362.71	256.03
38	219.46	289.56	277.37	374.90	252.98
39	188.98	316.99	304.80	359.66	265.18
40	182.88	344.42	277.37	359.66	237.74
41	182.88	344.42	286.51	356.62	240.79
42	207.26	332.23	298.70	316.99	231.65
43	216.41	326.14	298.70	316.99	231.65
44	210.31	313.94	304.80	310.90	231.65
45	195.07	313.94	316.99	289.56	231.65
46	201.17	316.99	329.18	283.46	228.60
47	204.22	329.18	326.14	280.42	256.03
48	192.02	323.09	304.80	326.14	259.08

APPENDIX B

Table B-1. Location of Coil gages in test section 703.

ID	X (m)	Y (m)	Z (mm)	Window	Layer
EMU471	7.54	4.63	77.85	C1	1
EMU462	7.58	4.49	76.73	C1	1
EMU466	7.69	4.61	82.59	C1	1
EMU288	7.55	4.64	187.55	C1	2
EMU307	7.56	4.49	184.63	C1	2
EMU326	7.67	4.62	194.49	C1	2
EMU309	7.54	4.61	305.63	C1	3
EMU323	7.55	4.48	303.53	C1	3
EMU304	7.67	4.61	305.58	C1	3
EMU322	7.54	4.60	455.23	C1	4
EMU282	7.52	4.46	451.74	C1	4
EMU324	7.66	4.59	459.88	C1	4
EMU262	7.54	4.60	604.55	C1	5
EMU267	7.54	4.45	603.29	C1	5
EMU266	7.67	4.59	608.73	C1	5
EMU361	7.55	4.61	778.72	C1	6
EMU364	7.54	4.44	775.20	C1	6
EMU268	7.70	4.59	773.24	C1	6
EMU363	7.55	4.59	915.46	C1	7
EMU384	7.55	4.43	918.64	C1	7
EMU261	7.70	4.57	921.75	C1	7
EMU345	7.56	4.56	1056.28	C1	8
EMU269	7.57	4.42	1053.04	C1	8
EMU362	7.69	4.57	1053.07	C1	8
EMU465	7.54	3.39	58.12	C2	1
EMU461	7.59	3.27	58.41	C2	1
EMU464	7.68	3.43	59.22	C2	1
EMU243	7.54	3.40	188.21	C2	2
EMU281	7.58	3.29	187.79	C2	2
EMU249	7.68	3.43	182.35	C2	2
EMU301	7.55	3.40	300.31	C2	3
EMU388	7.59	3.26	298.31	C2	3
EMU248	7.72	3.44	299.07	C2	3
EMU245	7.56	3.38	454.26	C2	4
EMU342	7.58	3.27	454.59	C2	4
EMU247	7.71	3.42	455.40	C2	4

Table B-1. Location of Coil gages in test section 703 (continued).

ID	X (m)	Y (m)	Z (mm)	Window	Layer
EMU372	7.57	3.40	625.44	C2	5
EMU381	7.58	3.28	624.18	C2	5
EMU250	7.70	3.41	625.89	C2	5
EMU391	7.58	3.39	781.15	C2	6
EMU264	7.58	3.25	781.31	C2	6
EMU370	7.71	3.40	776.76	C2	6
EMU313	7.58	3.40	925.45	C2	7
EMU312	7.60	3.24	924.84	C2	7
EMU351	7.74	3.39	918.88	C2	7
EMU290	7.59	3.39	1069.39	C2	8
EMU314	7.60	3.28	1067.78	C2	8
EMU371	7.73	3.41	1060.70	C2	8
EMU460	7.65	2.25	68.23	C3	1
EMU469	7.64	2.10	72.31	C3	1
EMU463	7.81	2.24	68.84	C3	1
EMU241	7.64	2.23	189.54	C3	2
EMU331	7.64	2.10	191.78	C3	2
EMU246	7.79	2.24	189.14	C3	2
EMU283	7.65	2.25	298.39	C3	3
EMU321	7.63	2.10	297.06	C3	3
EMU346	7.78	2.25	297.79	C3	3
EMU386	7.65	2.24	462.72	C3	4
EMU390	7.63	2.08	463.42	C3	4
EMU244	7.79	2.24	461.51	C3	4
EMU270	7.64	2.23	612.07	C3	5
EMU352	7.61	2.08	607.07	C3	5
EMU254	7.78	2.25	610.64	C3	5
EMU396	7.68	2.24	771.66	C3	6
EMU311	7.65	2.09	770.16	C3	6
EMU394	7.81	2.25	772.55	C3	6
EMU278	7.67	2.24	909.41	C3	7
EMU375	7.64	2.09	903.36	C3	7
EMU310	7.81	2.24	912.09	C3	7
EMU272	7.65	2.24	1067.63	C3	8
EMU291	7.64	2.11	1068.15	C3	8
EMU251	7.80	2.23	1068.46	C3	8
EMU467	18.03	4.62	56.65	C4	1

Table B-1. Location of Coil gages in test section 703 (continued).

EMU369	18.04	4.46	57.08	C4	1
EMU470	18.17	4.63	57.96	C4	1
EMU302	18.02	4.60		C4	2
EMU451	18.04	4.44		C4	2
EMU452	18.16	4.62		C4	2
EMU287	18.01	4.57	314.52	C4	3
EMU325	18.03	4.42	314.23	C4	3
EMU289	18.15	4.61	316.50	C4	3
EMU382	18.01	4.58	469.87	C4	4
EMU383	18.03	4.43	463.67	C4	4
EMU343	18.16	4.59	467.28	C4	4
EMU318	18.01	4.57	652.04	C4	5
EMU373	18.01	4.43	648.92	C4	5
EMU252	18.17	4.59	649.22	C4	5
EMU336	18.05	4.58	789.64	C4	6
EMU334	18.04	4.41	786.20	C4	6
EMU330	18.20	4.59	791.40	C4	6
EMU256	18.04	4.57	933.69	C4	7
EMU393	18.04	4.41	937.03	C4	7
EMU271	18.19	4.59	940.53	C4	7
EMU378	18.05	4.57	1088.30	C4	8
EMU292	18.04	4.43	1092.05	C4	8
EMU357	18.19	4.59	1090.88	C4	8
EMU366	18.02	3.30	62.64	C5	1
EMU472	18.04	3.15	62.77	C5	1
EMU473	18.19	3.32	63.27	C5	1
EMU350	18.02	3.30	177.80	C5	2
EMU450	18.05	3.16	177.80	C5	2
EMU385	18.19	3.31	177.80	C5	2
EMU367	18.01	3.31	312.17	C5	3
EMU453	18.05	3.16	314.23	C5	3
EMU454	18.19	3.30	313.20	C5	3
EMU355	18.02	3.30	457.37	C5	4
EMU377	18.03	3.14	457.78	C5	4
EMU276	18.19	3.29	457.40	C5	4
EMU293	18.05	3.28	610.02	C5	5
EMU316	18.04	3.15	602.66	C5	5

Table B-1. Location of Coil gages in test section 703 (continued).

ID	X (m)	Y (m)	Z (mm)	Window	Layer
EMU274	18.19	3.29	607.77	C5	5
EMU333	18.08	3.31	776.27	C5	6
EMU358	18.09	3.16	777.54	C5	6
EMU275	18.23	3.33	783.80	C5	6
EMU295	18.09	3.31	945.00	C5	7
EMU338	18.09	3.16	938.39	C5	7
EMU395	18.22	3.32	945.41	C5	7
EMU255	18.06	3.33	1068.13	C5	8
EMU258	18.08	3.18	1065.96	C5	8
EMU317	18.20	3.34	1074.22	C5	8
EMU368	18.03	2.03	70.86	C6	1
EMU327	18.04	1.88	71.21	C6	1
EMU468	18.19	2.01	69.29	C6	1
EMU294	18.03	2.06		C6	2
EMU459	18.04	1.91		C6	2
EMU458	18.18	2.05		C6	2
EMU242	18.03	2.08	305.97	C6	3
EMU456	18.04	1.94	303.99	C6	3
EMU455	18.18	2.08	303.74	C6	3
EMU329	18.19	2.06	463.34	C6	4
EMU457	18.04	2.09	463.75	C6	4
EMU349	18.05	1.95	464.74	C6	4
EMU296	18.20	2.07	617.62	C6	5
EMU297	18.05	2.08	624.79	C6	5
EMU374	18.05	1.93	624.94	C6	5
EMU376	18.11	2.09	786.66	C6	6
EMU353	18.10	1.94	791.48	C6	6
EMU273	18.24	2.07	788.81	C6	6
EMU277	18.10	2.09	928.93	C6	7
EMU354	18.10	1.93	933.14	C6	7
EMU253	18.25	2.07	929.32	C6	7
EMU397	18.10	2.09	1037.12	C6	8
EMU298	18.11	1.93	1043.82	C6	8
EMU335	18.11	1.93	1043.81	C6	8

Table B-2. Calibration coefficients for coil gages.

	Vertical (Z)				Longitudinal (X)				Transverse (Y)			
	Coil ID				Coil ID				Coil ID			
703C1	Transmit	Receive	a	n	Transmit	Receive	a	n	Transmit	Receive	a	n
Layer 1	471	288	8.4488	-0.4195	471	466	6.8613	-0.291	471	462	6.6466	-0.2891
Layer 2	288	309	8.4373	-0.4149	288	326	6.6814	-0.279	288	307	6.9126	-0.2928
Layer 3	309	322	8.0998	-0.3796	309	304	6.6938	-0.291	309	323	6.9	-0.2837
Layer 4	322	262	8.0878	-0.3825	322	324	6.6646	-0.293	322	282	6.8787	-0.2905
Layer 5	262	361	7.9286	-0.3606	262	266	6.7268	-0.295	262	267	6.9248	-0.2914
Layer 6	361	363	8.1566	-0.3776	361	268	6.7161	-0.289	361	364	6.9107	-0.2844
Layer 7	363	345	8.0965	-0.3806	363	261	6.7059	-0.284	363	384	6.9181	-0.2955
Layer 8					345	362	6.7052	-0.289	345	269	6.9054	-0.2849
703C2			a	n			a	n			a	n
Layer 1	465	243	8.4641	-0.4193	465	464	6.6599	-0.292	465	461	6.868	-0.2912
Layer 2	243	301	8.4367	-0.4112	243	249	6.6935	-0.29	243	281	6.9127	-0.2917
Layer 3	301	245	8.0528	-0.3799	301	248	6.6775	-0.293	301	388	6.8794	-0.2827
Layer 4	245	372	8.0145	-0.38	245	247	6.649	-0.287	245	342	6.8853	-0.2877
Layer 5	372	391	8.0687	-0.3799	372	250	6.701	-0.287	372	381	6.8965	-0.2897
Layer 6	391	313	8.0511	-0.378	391	370	6.6687	-0.293	391	264	6.8865	-0.2926
Layer 7	313	290	8.0768	-0.38	313	351	6.6757	-0.286	313	312	6.8721	-0.2832
Layer 8					290	371	6.7068	-0.293	290	314	6.8919	-0.29
703C3			a	n			a	n			a	n
Layer 1	460	241	8.4606	-0.4204	460	463	6.6745	-0.293	460	469	6.8799	-0.2936
Layer 2	241	283	8.4122	-0.4189	241	246	6.7062	-0.296	241	331	6.9154	-0.2942
Layer 3	283	386	8.116	-0.3779	283	346	6.7115	-0.29	283	321	6.9235	-0.2865
Layer 4	386	270	8.1343	-0.3795	386	244	6.7161	-0.29	386	390	6.9345	-0.2946
Layer 5	270	396	8.0416	-0.3823	270	254	6.6748	-0.291	270	352	6.8929	-0.3949
Layer 6	396	278	8.0751	-0.3813	396	394	6.6761	-0.29	396	311	6.896	-0.2929
Layer 7	278	272	8.1443	-0.3775	278	310	6.6906	-0.287	278	375	6.9114	-0.2937
Layer 8					272	251	6.6869	-0.299	272	291	6.8724	-0.2842
703C4			a	n			a	n			a	n
Layer 1	467	302	8.4425	-0.42	467	470	6.6778	-0.289	467	369	6.867	-0.283
Layer 2	302	287	8.4082	-0.4112	302	452	6.75165	-0.289	302	451	6.8865	-0.291
Layer 3	287	382	8.043	-0.3819	287	289	6.6877	-0.288	287	325	7.3851	-0.2917
Layer 4	382	318	8.0586	-0.3794	382	343	7.1853	-0.288	382	383	6.9573	-0.2925
Layer 5	318	336	8.0689	-0.3825	318	252	6.6575	-0.29	318	373	6.8817	-0.2902
Layer 6	336	256	8.0976	-0.3791	336	330	6.6612	-0.29	336	334	6.8757	-0.2915
Layer 7	256	378	8.0519	-0.3813	256	271	6.6618	-0.291	256	393	6.8479	-0.2915
Layer 8					378	357	6.6564	-0.289	378	292	6.8699	-0.2884

Table B-2. Calibration coefficients for coil gages (continued).

		Vertical (Z)			Longitudinal (X)			Transverse (Y)				
	Coil ID				Coil ID				Coil ID			
703C5	Transmit	Receive	a	n	Transmit	Receive	a	n	Transmit	Receive	a	n
Layer 1	366	350	8.4359	-0.4201	366	473	6.7102	-0.29	366	472	6.8676	-0.2902
Layer 2	350	367	8.7911	-0.3829	350	385	7.3401	-0.288	350	450	7.0813	-0.2871
Layer 3	367	355	8.0498	-0.3842	367	454	6.8727	-0.29	367	453	6.6657	-0.2902
Layer 4	355	293	8.0986	-0.3800	355	276	6.6753	-0.289	355	377	6.8734	-0.2872
Layer 5	293	333	6.7387	-0.3815	293	274	6.6772	-0.289	293	316	6.8952	-0.2899
Layer 6	333	295	8.1294	-0.3815	333	275	6.7905	-0.29	333	358	6.9263	-0.2919
Layer 7	295	255	8.1084	-0.3805	295	395	6.6744	-0.291	295	338	6.8701	-0.2865
Layer 8	255				255	317	7.0875	-0.29	255	258	6.8545	-0.2924
703C6			a	n			a	n			a	n
Layer 1	368	294	8.4579	-0.4191	368	468	6.6703	-0.297	368	327	6.8936	-0.3046
Layer 2	294	242	8.0901	-0.3827	294	458	6.6963	-0.286	294	459	6.887	-0.2889
Layer 3	242	329	8.1505	-0.3824	242	455	6.686	-0.287	242	456	6.9023	-0.2901
Layer 4	329	296	8.1392	-0.38	329	349	6.8364	-0.283	329	457	6.8786	-0.2847
Layer 5	296	376	8.0547	-0.3817	296	374	6.6659	-0.293	296	297	6.8863	-0.2924
Layer 6	376	277	8.0732	-0.3807	376	273	6.6755	-0.292	376	353	6.8819	-0.2912
Layer 7	277	397	8.092	-0.3815	277	253	6.6716	-0.293	277	354	6.9042	-0.2928
Layer 8					397	335	6.6507	-0.293	397	298	6.8728	-0.2933

Table B-4. Location of stress cell and calibration coefficients.

ID	Window	Orientation	X (m)	Y (m)	Z (mm)	Full Scale Range (kPa)	Gain factors (GF) mv/V/kPa
Dynatest							
A.6.30	C1	X	6.15	4.59	432.28	200	167
A.6.24	C1	Y	5.59	4.54	457.75	200	164
B.3.8	C1	Z	5.91	4.57	479.44	800	39.4
A.6.16	C2	X	6.24	3.34	403.79	200	166
A.6.26	C2	X	5.91	3.30	141.44	200	161
A.6.29	C2	X	6.24	3.34	762.00	200	163
A.6.20	C2	Y	5.65	3.36	409.03	200	166
A.6.33	C2	Y	5.39	3.28	139.85	200	166
A.6.31	C2	Y	5.65	3.36	762.00	200	166
B.6.6	C2	Z	5.65	3.28	171.87	800	39.7
B.6.7	C2	Z	5.94	3.35	452.91	800	39.2
A.6.5	C2	Z	5.94	3.35	1066.80	200	167
B3.5	C2	Z	5.94	3.35	762.00	800	30.4
A.6.10	C3	X	6.24	2.28	425.09	200	170
A.6.11	C3	Y	5.64	2.27	423.56	200	164
B.3.4	C3	Z	5.98	2.28	434.94	800	40
A.6.1	C4	X	17.18	4.50	411.42	200	159
A.6.15	C4	Y	16.59	4.54	426.12	200	162
B.3.2	C4	Z	16.89	4.53	449.19	800	39
A.6.25	C5	X	17.05	3.31	161.89	200	167
A.6.3	C5	X	17.19	3.35	434.43	200	158
A.6.18	C5	Y	16.62	3.36	405.32	200	163
A.6.19	C5	Y	16.49	3.26	158.85	200	155
B.3.6	C5	Z	16.73	3.28	191.13	800	40.6
B.6.9	C5	Z	16.92	3.35	449.73	800	40.3
A.6.14	C6	X	16.90	2.24	423.79	200	167
B.6.8	C6	Z	16.68	2.23	457.84	800	39.5
A.6.6	C6	Y	16.42	2.21	432.00	200	161
Geokon							
GEOKY	C2	Y	4.04	3.35	97.47		
GEOKZ	C2	Z	4.72	3.29	193.63		

Table B-5. Location of VITEL Hydra Moisture Probes in test Section 703.

ID	X (m)	Y (m)	Z (mm)
V332	9.4	4.0	355.6
V123	11.9	3.7	609.6
V124	8.5	1.2	914.4
V127	12.7	3.2	1092.2
V122	16.4	1.5	1524.0
V398	4.1	5.4	1778.0

Table B-6. Location of thermocouples in test section 703.

ID	X (m)	Y (m)	Z (mm)
TC10	Air		
TC9	Tunnel		
TC8	3.6	4.0	76.2
TC7	3.6	4.0	190.5
TC6	3.6	4.0	330.2
TC4	3.6	4.0	482.6
TC5	3.6	4.0	635.0
TC3	3.6	4.0	711.2
TC2	3.6	4.0	1016.0
TC1	3.6	4.0	1320.8

APPENDIX C

703C2 STRESS

Table C-1. Measured maximum vertical stresses as a function of load applications (703C2)

703C2	BASE COURSE		
DYNATEST	z = 172 mm		
Load Repetitions	VERTICAL STRESS (kPa)		
	Position 1	Position 2	Position 3
0	-441.61	-399.02	-248.08
500	-493.35	-432.04	-292.70
1000	-422.06	-386.00	-252.32
2500	-409.55	-355.74	-246.14
5000	-443.75	-391.87	-277.42
10000	-462.68	-398.05	-292.83
25000	-449.12	-410.16	-283.76
50000	-428.97	-384.65	-267.16

	BASE COURSE		
GEOKON	z = 194 mm		
Load Repetition	VERTICAL STRESS (kPa)		
	Position 1	Position 2	Position 3
0	-333.62	-328.50	-200.25
500	-342.09	-312.00	-178.62
1000	-359.37	-326.35	-167.78
2500	-362.57	-325.74	-164.18
5000	-363.19	-339.09	-169.38
10000	-348.96	-324.99	-162.10
25000	-341.87	-321.42	-154.52
50000	-333.80	-311.26	-152.36

	TOP OF SUBGRADE		
DYNATEST	z = 453 mm		
Load Repetition	VERTICAL STRESS (kPa)		
	Position 1	Position 2	Position 3
0	-85.72	-90.89	-80.76
500	-83.22	-89.22	-84.49
1000	-88.54	-95.89	-85.97
2500	-95.09	-103.62	-94.38
5000	-100.32	-107.82	-99.14
10000	-101.80	-110.19	-103.02
25000	-100.77	-110.24	-106.00
50000	-102.93	-113.49	-110.29

Table C-1. Measured maximum vertical stress as a function of load applications (703C2) - continued

DYNATEST Load Repetitions	SUBGRADE z = 762 mm VERTICAL STRESS (kPa)		
	Position 1	Position 2	Position 3
0	-37.82	-41.80	-42.55
500	-43.79	-40.86	-44.17
1000	-38.86	-43.81	-43.97
2500	-42.05	-46.20	-48.14
5000	-48.92	-45.98	-48.34
10000	-45.24	-48.49	-45.72
25000	-43.33	-40.24	-41.52
50000	-36.81	-45.67	-39.93

DYNATEST	SUBGRADE z = 1067 mm VERTICAL STRESS (kPa)		
Load Repetitions	Position 1	Position 2	Position 3
0	-19.61	-22.31	-23.05
500	-16.52	-18.25	-20.05
1000	-16.40	-17.51	-17.67
2500	-16.44	-18.02	-17.91
5000	-16.17	-17.27	-17.03
10000	-15.14	-17.08	-16.57
25000	-12.32	-13.70	-12.96
50000	-8.06	-9.64	-8.91

Table C-2. Measured maximum longitudinal stresses as a function of load applications (703C2)

703C2	BASE COURSE		
DYNATEST	z = 141 mm		
Load Repetitions	LONGITUDINAL STRESS (kPa)		
	Position 1	Position 2	Position 3
0	-63.93	-60.48	-55.89
500	-75.61	-68.02	-56.95
1000	-66.82	-71.07	-55.84
2500	-66.65	-64.75	-50.27
5000	-65.88	-62.66	-46.62
10000	-60.95	-52.26	-42.90
25000	-56.57	-54.97	-41.31
50000	-52.08	-42.63	-29.54

	TOP OF SUBGRADE		
DYNATEST	z = 404 mm		
Load Repetition	LONGITUDINAL STRESS (kPa)		
	Position 1	Position 2	Position 3
0	-27.66	-29.27	-21.28
500	-25.26	-25.68	-18.66
1000	-26.31	-27.08	-18.40
2500	-28.29	-29.12	-20.65
5000	-27.78	-27.97	-19.83
10000	-22.31	-22.92	-14.56
25000	-14.02	-15.35	-7.86
50000	-8.64	-9.48	-2.93

	SUBGRADE		
DYNATEST	z = 762 mm		
Load Repetitions	LONGITUDINAL STRESS (kPa)		
	Position 1	Position 2	Position 3
0	-10.25	-11.74	-11.52
500	-10.81	-10.34	-11.44
1000	-9.55	-11.43	-11.11
2500	-9.68	-10.61	-11.48
5000	-10.00	-10.50	-12.31
10000	-9.96	-10.83	-11.31
25000	-13.00	-14.28	-14.65
50000	-13.47	-15.30	-14.11

Table C-3. Measured maximum transverse stress as a function of load applications (703C2).

703C2	BASE COURSE		
DYNATEST	z = 140 mm		
Load Repetitions	TRANSVERSE STRESS (kPa)		
	Position 1	Position 2	Position 3
0	-92.62	-97.04	-61.62
500	-85.77	-93.03	-53.06
1000	-81.59	-95.58	-42.86
2500	-77.49	-84.75	-31.15
5000	-85.24	-93.70	-41.95
10000	-91.33	-102.75	-41.49
25000	-73.02	-83.12	-39.38
50000	-79.46	-87.82	-37.49

	BASE COURSE		
GEOKON	z = 194 mm		
Load Repetition	TRANSVERSE STRESS (kPa)		
	Position 1	Position 2	Position 3
0	-87.99	-97.31	-83.09
500	-68.08	-88.55	-73.20
1000	-86.72	-102.95	-75.49
2500	-88.48	-113.77	-94.30
5000	-103.17	-110.16	-84.63
10000	-90.91	-119.78	-86.43
25000	-100.47	-120.95	-90.34
50000	-110.12	-135.63	-92.32

	TOP OF SUBGRADE		
DYNATEST	z = 405 mm		
Load Repetition	TRANSVERSE STRESS (kPa)		
	Position 1	Position 2	Position 3
0	-17.16	-18.82	-14.97
500	-16.77	-17.09	-12.87
1000	-16.63	-17.77	-13.56
2500	-18.88	-19.84	-15.89
5000	-23.86	-24.72	-21.99
10000	-24.05	-25.14	-22.76

25000	-16.55	-17.85	-15.84
50000	-10.99	-12.28	-10.98

Table C-3. Measured maximum transverse stress as a function of load applications (703C2) - continued

DYNATEST Load Repetitions	SUBGRADE z = 762 mm TRANSVERSE STRESS (kPa)		
	Position 1	Position 2	Position 3
0	-9.63	-8.99	-7.81
500	-8.91	-8.92	-6.85
1000	-8.73	-8.37	-6.70
2500	-8.38	-7.75	-6.83
5000	-9.57	-9.12	-6.74
10000	-9.85	-9.29	-7.30
25000	-11.47	-10.34	-6.94
50000	-10.10	-9.91	-8.41

APPENDIX D

703C2 DISPLACEMENTS & STRAINS

Table D-1. Measured maximum dynamic vertical displacements as a function of load applications (703C2).

Position 1

Repetitions	z = 76mm	z = 188mm	z = 300mm	z = 454mm	z = 625mm	z = 781mm	z= 925mm
0	-0.4173	-0.1077	-0.0826	-0.0702	-0.0417	-0.0188	-0.0142
500	-0.4047	-0.1078	-0.0989	-0.0729	-0.0512	-0.0203	-0.0153
1000	-0.4115	-0.1088	-0.0986	-0.0869	-0.0516	-0.0220	-0.0159
2500	-0.4220	-0.1114	-0.0917	-0.0853	-0.0534	-0.0230	-0.0177
5000	-0.4238	-0.1190	-0.0898	-0.0854	-0.0552	-0.0245	-0.0182
10000	-0.4446	-0.1286	-0.0894	-0.0838	-0.0570	-0.0249	-0.0192
25000	-0.4330	-0.1354	-0.0748	-0.0695	-0.0527	-0.0252	-0.0190
50000	-0.4524	-0.1325	-0.0684	-0.0629	-0.0493	-0.0239	-0.0188

Position 2

Repetitions	z = 76mm	z = 188mm	z = 300mm	z = 454mm	z = 625mm	z = 781mm	z= 925mm
0	-0.4429	-0.1713	-0.1907	-0.1643	-0.0840	-0.0310	-0.0216
500	-0.4244	-0.1738	-0.1906	-0.1722	-0.0931	-0.0346	-0.0231
1000	-0.4527	-0.1851	-0.2007	-0.1782	-0.0982	-0.0365	-0.0255
2500	-0.4498	-0.1894	-0.1857	-0.1634	-0.0985	-0.0378	-0.0261
5000	-0.4726	-0.1966	-0.1834	-0.1696	-0.1023	-0.0400	-0.0288
10000	-0.4631	-0.2146	-0.1765	-0.1660	-0.1032	-0.0411	-0.0288
25000	-0.4881	-0.2247	-0.1546	-0.1428	-0.0988	-0.0421	-0.0298
50000	-0.4796	-0.2162	-0.1439	-0.1334	-0.0932	-0.0397	-0.0293

Position 3

Repetitions	z = 76mm	z = 188mm	z = 300mm	z = 454mm	z = 625mm	z = 781mm	z= 925mm
0	-0.2611	-0.1331	-0.1026	-0.0850	-0.0505	-0.0192	-0.0140
500	-0.2532	-0.1337	-0.1226	-0.0903	-0.0743	-0.0215	-0.0159
1000	-0.2504	-0.1354	-0.1229	-0.1079	-0.0644	-0.0240	-0.0166
2500	-0.2512	-0.1383	-0.1141	-0.1058	-0.0664	-0.0250	-0.0184
5000	-0.2552	-0.1476	-0.1114	-0.1062	-0.0678	-0.0268	-0.0189
10000	-0.2473	-0.1597	-0.1104	-0.1038	-0.0708	-0.0275	-0.0205
25000	-0.2732	-0.1684	-0.0928	-0.0854	-0.0640	-0.0275	-0.0211
50000	-0.2900	-0.1651	-0.0840	-0.0773	-0.0610	-0.0263	-0.0198

Table D-2. Maximum dynamic vertical strains as a function of load applications (703C2).

Position 1

Repetitions	z = 123 mm	z = 244 mm	z = 377 mm	z = 540 mm	z = 703 mm	z = 853 mm	z = 997 mm
0	-3873	-1120	-705	-436	-282	-146	-100
500	-3787	-1130	-855	-559	-344	-164	-117
1000	-3863	-1145	-859	-553	-353	-184	-122
2500	-3976	-1171	-801	-542	-368	-190	-134
5000	-4008	-1250	-780	-546	-378	-207	-139
10000	-4223	-1355	-778	-534	-391	-209	-151
25000	-4139	-1430	-651	-442	-358	-210	-154
50000	-4330	-1408	-593	-401	-339	-202	-145

Position 2

Repetitions	z = 123 mm	z = 244 mm	z = 377 mm	z = 540 mm	z = 703 mm	z = 853 mm	z = 997 mm
0	-3283	-1440	-1320	-839	-461	-236	-157
500	-3172	-1465	-1329	-883	-512	-263	-168
1000	-3394	-1562	-1402	-914	-541	-278	-186
2500	-3389	-1601	-1300	-840	-543	-288	-190
5000	-3573	-1664	-1286	-874	-565	-305	-210
10000	-3514	-1818	-1239	-856	-570	-313	-210
25000	-3726	-1906	-1086	-736	-546	-321	-217
50000	-3673	-1837	-1014	-688	-516	-303	-214

Position 3

Repetitions	z = 123 mm	z = 244 mm	z = 377 mm	z = 540 mm	z = 703 mm	z = 853 mm	z = 997 mm
0	-1935	-1118	-709	-433	-277	-146	-102
500	-1891	-1127	-854	-559	-409	-164	-116
1000	-1878	-1143	-858	-554	-355	-183	-121
2500	-1893	-1170	-799	-544	-366	-191	-134
5000	-1929	-1249	-780	-546	-374	-204	-138
10000	-1876	-1353	-775	-534	-391	-210	-149
25000	-2086	-1429	-652	-441	-354	-210	-154
50000	-2225	-1406	-593	-400	-338	-201	-144

Table D-3. Measured maximum dynamic longitudinal displacements as a function of load applications (703C2).

Position 1

Repetitions	z = 76mm	z = 188mm	z = 300mm	z = 454mm	z = 625mm	z = 781mm	z= 925mm
0	-1.0141	0.0515	5.4873	0.0192	0.0208		0.0220
500	-1.0302	0.0501	5.1592	0.0264	0.0392		0.0211
1000	-1.0220	0.0585	6.0263	0.0257	0.0208		0.0167
2500	-1.0209		5.6014	0.0243	0.0208		0.0197
5000	-1.0428		4.5026	0.0275	0.0209		0.0176
10000	-1.0945		4.9167	0.0289	0.0228		0.0192
25000	-0.9625		4.0225	0.0250	0.0240		0.0189
50000	-1.1688		3.4811	0.0187	0.0217		0.0148

Position 2

Repetitions	z = 76mm	z = 188mm	z = 300mm	z = 454mm	z = 625mm	z = 781mm	z= 925mm
0	-0.8877	0.0618	6.8857	0.0492	0.0264		0.0135
500	-0.8648	0.0677	8.5944	0.0516	0.0334		0.0178
1000	-0.9451	0.0817	8.9619	0.0572	0.0346		0.0176
2500	-0.8265		8.4537	0.0513	0.0373		0.0197
5000	-0.9989		7.7731	0.0522	0.0397		0.0191
10000	-0.8983		10.3415	0.0519	0.0396		0.0213
25000	-1.1117		6.1255	0.0449	0.0453		0.0201
50000	-0.8731		5.7858	0.0376	0.0428		0.0179

Position 3

Repetitions	z = 76mm	z = 188mm	z = 300mm	z = 454mm	z = 625mm	z = 781mm	z= 925mm
0	-0.5930	0.0731	6.6223	0.0296	0.0153		0.0157
500	-0.5845	0.0637	6.4236	0.0369	0.0416		0.0153
1000	-0.5473	0.0763	7.4185	0.0344	0.0226		0.0115
2500	-0.5527		6.9112	0.0367	0.0286		0.0181
5000	-0.5907		5.7512	0.0392	0.0302		0.0182
10000	-0.5992		6.2266	0.0434	0.0324		0.0177
25000	-0.6668		5.0108	0.0359	0.0340		0.0187
50000	-0.8091		4.3075	0.0292	0.0310		0.0155

Table D-4. Measured maximum dynamic longitudinal strains as a function of load applications (703C2).

Position 1

Repetitions	z = 76mm	z = 188mm	z = 300mm	z = 454mm	z = 625mm	z = 781mm	z= 925mm
0	-6589	406	9961	154	86		87
500	-6673	354	9345	182	274		83
1000	-6611	407	10934	174	124		59
2500	-6607		10281	184	154		96
5000	-6743		8832	192	167		93
10000	-7067		9882	218	174		88
25000	-6206		8185	181	183		103
50000	-7522		7367	139	166		84

Position 2

Repetitions	z = 76mm	z = 188mm	z = 300mm	z = 454mm	z = 625mm	z = 781mm	z= 925mm
0	-4625	334	10109	248	140		70
500	-4505	366	12466	260	177		93
1000	-4921	441	13000	288	184		91
2500	-4304		12383	258	198		102
5000	-5197		11820	263	211		99
10000	-4670		15878	261	210		111
25000	-5758		9934	225	240		104
50000	-4523		9758	189	227		93

Position 3

Repetitions	z = 76mm	z = 188mm	z = 300mm	z = 454mm	z = 625mm	z = 781mm	z= 925mm
0	-3089	395	9607	149	81		81
500	-3043	344	9308	186	221		80
1000	-2850	412	10767	173	120		60
2500	-2878		10141	185	152		94
5000	-3072		9022	197	160		94
10000	-3112		10003	218	172		92
25000	-3455		8151	180	180		97
50000	-4198		7283	147	165		81

Table D-5. Measured maximum dynamic transverse displacements as a function of load applications (703C2).

Position 1

Repetitions	z = 76mm	z = 188mm	z = 300mm	z = 454mm	z = 625mm	z = 781mm	z= 925mm
0	0.2204	0.0624	0.0240		0.0119	0.0082	0.0068
500	0.2003	0.0604	0.0265		0.0465	0.0222	0.0069
1000	0.2031	0.0587	0.0267		0.0135	0.0153	0.0078
2500	0.2044	0.0665	0.0300		0.0143	0.0105	0.0077
5000	0.1988	0.0767	0.0299		0.0154	0.0109	0.0084
10000	0.2374	0.0743	0.0323		0.0152	0.0100	0.0082
25000		0.0788	0.0309		0.0157	0.0245	0.0084
50000		0.0833	0.0312		0.0145	0.0097	0.0076

Position 2

Repetitions	z = 76mm	z = 188mm	z = 300mm	z = 454mm	z = 625mm	z = 781mm	z= 925mm
0	0.2428	0.0463	0.0195		0.0173	0.0150	0.0098
500	0.2506	0.0470	0.0192		0.0206	0.0175	0.0112
1000	0.2647	0.0500	0.0239		0.0221	0.0176	0.0114
2500	0.2737	0.0737	0.0245		0.0231	0.0185	0.0128
5000	0.2548	0.0552	0.0269		0.0241	0.0203	0.0129
10000	0.2738	0.0584	0.0279		0.0254	0.0211	0.0132
25000		0.0710	0.0291		0.0254	0.0382	0.0131
50000		0.0722	0.0287		0.0244	0.0193	0.0130

Position 3

Repetitions	z = 76mm	z = 188mm	z = 300mm	z = 454mm	z = 625mm	z = 781mm	z= 925mm
0	0.2742	0.0759	0.0278		0.0121	0.0076	0.0062
500	0.2894	0.0740	0.0317		0.0460	0.0257	0.0067
1000	0.2949	0.0721	0.0316		0.0150	0.0155	0.0071
2500	0.3080	0.0817	0.0357		0.0165	0.0112	0.0071
5000	0.2989	0.0979	0.0357		0.0168	0.0112	0.0080
10000	0.3106	0.0915	0.0390		0.0175	0.0101	0.0075
25000		0.0970	0.0374		0.0175	0.0286	0.0080
50000		0.1022	0.0373		0.0168	0.0096	0.0074

Table D-6. Measured maximum dynamic transverse strains as a function of load applications (703C2).

Position 1

Repetitions	z = 76mm	z = 188mm	z = 300mm	z = 454mm	z = 625mm	z = 781mm	z= 925mm
0							
500							
1000							
2500							
5000							
10000							
25000							
50000							

Position 2

Repetitions	z = 76mm	z = 188mm	z = 300mm	z = 454mm	z = 625mm	z = 781mm	z= 925mm
0	1540	337	138		135	111	74
500	730	268	129		151	127	79
1000	1153	290	160		160	132	81
2500	1025	273	165		165	134	93
5000	982	244	179		176	150	97
10000	1074	302	181		185	159	96
25000		380	178		186	287	94
50000		382	182		172	144	84

Position 3

Repetitions	z = 76mm	z = 188mm	z = 300mm	z = 454mm	z = 625mm	z = 781mm	z= 925mm
0	1884	542	185		90	54	41
500	1247	386	170		40	190	43
1000	1460	313	151		107	107	52
2500	1559	394	177		118	75	52
5000	1491	562	187		118	74	52
10000	1552	477	186		125	72	53
25000		474	177		128	209	56
50000		497	153		118	64	55

Table D-7. Measured permanent displacements as a function of load applications (703C2).

Vertical Deformation (mm)

	Load Repetitions							
Depth (mm)	0	500	1000	2500	5000	10000	25000	50000
Surface	0.000	-0.573	-0.643	-1.017	-1.241	-1.514	-1.955	-2.537
76	0.000	-0.788	-1.280	-1.936	-2.326	-2.848	-3.624	-4.121
181	0.000	-0.442	-0.561	-0.778	-0.897	-1.060	-1.260	-1.534
300	0.000	-1.239	-1.494	-1.851	-1.994	-2.170	-2.436	-2.755
454	0.000	-0.822						
625	0.000	-0.277	-0.568	-0.729	-0.812	-0.864	-1.160	-1.343
781	0.000	-0.085	-0.106	-0.216	-0.222	-0.253	-0.328	-0.498
925	0.000	-0.014	-0.021	-0.107	-0.090	-0.097	-0.141	-0.289

Longitudinal Deformation (mm)

	Load Repetitions							
Depth (mm)	0	500	1000	2500	5000	10000	25000	50000
76	0.000	1.194	0.986	0.857	1.549	1.790	2.950	3.328
181	0.000	0.036	-0.147					
300	0.000							
454	0.000	0.781	0.629	0.568	0.777	0.863	0.789	0.788
625	0.000	0.301	0.204	0.223	0.323	0.516	0.157	0.386
781	0.000							
925	0.000	0.051	-0.109	-0.220	-0.070	-0.013	-0.073	-0.116

Transverse Deformation (mm)

	Load Repetitions							
Depth (mm)	0	500	1000	2500	5000	10000	25000	50000
76	0.000	0.959	0.838	0.875	1.461	1.719		
181	0.000	0.190	0.141	0.093	0.181	0.177	0.177	0.120
300	0.000	0.463	0.432	0.401	0.537	0.510	0.501	0.449
454	0.000							
625	0.000	0.233	0.075	0.066	0.158	0.163	0.113	0.144
781	0.000	0.106	0.044	-0.006	0.098	0.086	0.100	0.069
925	0.000	0.064	-0.012	-0.068	0.027	0.017	0.032	-0.021

Table D-8. Measured permanent strains as a function of load applications (703C2).

Vertical strain

	Load Repetitions							
Depth (mm)	0	500	1000	2500	5000	10000	25000	50000
Surface	0.0000	-0.0073	-0.0082	-0.0130	-0.0159	-0.0194	-0.0250	-0.0325
123	0.0000	-0.0058	-0.0095	-0.0143	-0.0172	-0.0210	-0.0268	-0.0304
244	0.0000	-0.0037	-0.0046	-0.0064	-0.0074	-0.0088	-0.0104	-0.0127
377	0.0000	-0.0086	-0.0103	-0.0128	-0.0138	-0.0150	-0.0168	-0.0190
540	0.0000	-0.0051						
703	0.0000	-0.0015	-0.0031	-0.0040	-0.0045	-0.0047	-0.0064	-0.0074
853	0.0000	-0.0006	-0.0008	-0.0016	-0.0017	-0.0019	-0.0025	-0.0038
997	0.0000	-0.0001	-0.0002	-0.0008	-0.0007	-0.0007	-0.0010	-0.0021

Longitudinal strain

	Load Repetitions							
Depth (mm)	0	500	1000	2500	5000	10000	25000	50000
76	0.0000	0.0046	0.0038	0.0033	0.0060	0.0070	0.0115	0.0129
181	0.0000	0.0001	-0.0006					
300	0.0000	-0.0450	-0.0319	-0.0432	-0.0649	-0.1439	-0.1330	-0.1975
454	0.0000	0.0031	0.0025	0.0023	0.0031	0.0034	0.0031	0.0031
625	0.0000	0.0013	0.0009	0.0010	0.0014	0.0022	0.0007	0.0016
781	0.0000							
925	0.0000	0.0002	-0.0004	-0.0009	-0.0003	-0.0001	-0.0003	-0.0005

Transverse Deformation (mm)

	Load Repetitions							
Depth (mm)	0	500	1000	2500	5000	10000	25000	50000
76	0.0000	0.0060	0.0052	0.0054	0.0091	0.0107		
181	0.0000	0.0014	0.0010	0.0007	0.0013	0.0013	0.0013	0.0009
300	0.0000	0.0030	0.0028	0.0026	0.0035	0.0033	0.0033	0.0029
454	0.0000							
625	0.0000	0.0017	0.0006	0.0005	0.0012	0.0012	0.0008	0.0011
781	0.0000	0.0008	0.0003	0.0000	0.0007	0.0006	0.0007	0.0005
925	0.0000	0.0004	-0.0001	-0.0005	0.0002	0.0001	0.0002	-0.0001

Table D-9. Maximum surface rut (mm) as a function of longitudinal location & load repetitions.

Location	Repetitions					
	500	1000	2500	10000	25000	50000
Pos. 3	4.02	4.44	5.61	8.57	10.22	12.01
Pos. 4	4.07	4.58	6.10	8.64	10.40	12.16
Pos. 5	5.60	6.38	7.87	10.80	13.41	14.90
Pos. 6	8.15	8.66	9.86	12.84	14.85	16.29
Pos. 7	9.38	10.15	11.70	14.91	16.86	18.49
Pos. 8	10.64	11.43	12.62	15.60	17.02	18.76
Pos. 9	10.98	11.26	13.25	16.21	18.10	19.51
Pos. 10	8.69	9.54	10.94	14.27	16.62	18.04
Pos. 11	9.96	11.46	13.14	16.21	18.47	20.16
Pos. 12	8.69	9.54	10.94	14.27	16.62	18.04
Pos. 13	7.18	8.76	9.22	12.38	14.84	16.44
Pos. 14	6.70	7.16	8.87	10.69	13.12	15.20
Pos. 15	5.51	6.68	7.92	10.79	13.16	14.89
Pos. 16	6.26	6.94	8.18	11.18	13.18	15.37
Pos. 17	6.57	7.59	8.64	11.82	13.65	15.26
Pos. 18	7.06	8.20	9.84	12.10	14.55	16.24
Pos. 19	6.35	7.49	9.26	11.96	14.00	15.83
Pos. 20	6.94	8.42	10.33	12.89	15.32	16.86
Pos. 21	6.88	7.41	9.60	12.00	13.80	15.45
Pos. 22	5.03	6.13	7.34	9.65	11.51	13.08

APPENDIX E

703C3 DISPLACEMENTS & STRAINS

Table E-1. Measured maximum dynamic vertical displacements (mm) as a function of load applications (703C3).

Position 1							
Repetitions	z = 68 mm	z = 190 mm	z = 298 mm	z = 463 mm	z = 612 mm	z = 772 mm	z = 909 mm
0							
500							
1000							
2500							
5000							
10000							
25000	-0.1999	-0.0858	-0.0568	-0.0484	-0.0441	-0.0194	-0.0231
50000	-0.2043	-0.1036	-0.0556	-0.0470	-0.0434	-0.0192	-0.0225
105000	-0.2027	-0.0918	-0.0386	-0.0462	-0.0442	-0.0199	-0.0223
222340	-0.2044	-0.0905	-0.0544	-0.0461	-0.0452	-0.0208	-0.0234
376750	-0.1992	-0.0886	-0.0562	-0.0469	-0.0462	-0.0205	-0.0231

Position 2							
Repetitions	z = 68 mm	z = 190 mm	z = 298 mm	z = 463 mm	z = 612 mm	z = 772 mm	z = 909 mm
0							
500							
1000							
2500							
5000							
10000							
25000	-0.5724	-0.1744	-0.1140	-0.0847	-0.0710	-0.0338	-0.0332
50000	-0.5642	-0.1839	-0.1095	-0.0818	-0.0693	-0.0328	-0.0341
105000	-0.5651	-0.1830		-0.0818	-0.0731	-0.0344	-0.0344
222340	-0.5660	-0.1775	-0.1125	-0.0819	-0.0714	-0.0344	-0.0337
376750	-0.5630	-0.1798	-0.0979	-0.0816	-0.0720	-0.0351	-0.0344

Position 3							
Repetitions	z = 68 mm	z = 190 mm	z = 298 mm	z = 463 mm	z = 612 mm	z = 772 mm	z = 909 mm
0							
500							
1000							
2500							
5000							
10000							

25000	-0.4169	-0.1736	-0.1146	-0.0846	-0.0715	-0.0369	-0.0334
50000	-0.4095	-0.1764	-0.1099	-0.0827	-0.0682	-0.0362	-0.0351
105000	-0.4190	-0.1767	-0.1128	-0.0822	-0.0722	-0.0371	-0.0348
222340	-0.4162	-0.1726	-0.1143	-0.0832	-0.0713	-0.0373	-0.0343
376750	-0.4124	-0.1712	-0.0327	-0.0842	-0.0717	-0.0384	-0.0347

Table E-2. Maximum dynamic vertical strains (µstrains) as a function of load applications (703C3).

Position 1							
Repetitions	z = 129 mm	z = 244 mm	z = 381 mm	z = 537 mm	z = 692 mm	z = 841 mm	z = 989 mm
0							
500							
1000							
2500							
5000							
10000							
25000	-2025	-754	-499	-437	-334	-167	-179
50000	-2063	-910	-488	-422	-329	-161	-171
105000	-2060	-809	-335	-419	-332	-168	-175
222340	-2059	-793	-486	-425	-340	-175	-173
376750	-2009	-786	-501	-421	-347	-177	-175

Position 2							
Repetitions	z = 129 mm	z = 244 mm	z = 381 mm	z = 537 mm	z = 692 mm	z = 841 mm	z = 989 mm
0							
500							
1000							
2500							
5000							
10000							
25000	-4631	-1230	-816	-625	-439	-243	-212
50000	-4561	-1295	-783	-604	-428	-235	-217
105000	-4578	-1291		-604	-452	-247	-219
222340	-4586	-1252	-805	-605	-441	-247	-215
376750	-4564	-1268	-709	-603	-445	-252	-219

Position 3							
Repetitions	z = 129 mm	z = 244 mm	z = 381 mm	z = 537 mm	z = 692 mm	z = 841 mm	z = 989 mm
0							
500							
1000							
2500							
5000							
10000							
25000	-3372	-1224	-820	-624	-442	-265	-213
50000	-3311	-1242	-786	-610	-421	-259	-224
105000	-3395	-1246	-809	-608	-447	-266	-222

222340	-3370	-1217	-818	-615	-441	-267	-219
376750	-3343	-1203	-236	-622	-444	-276	-221

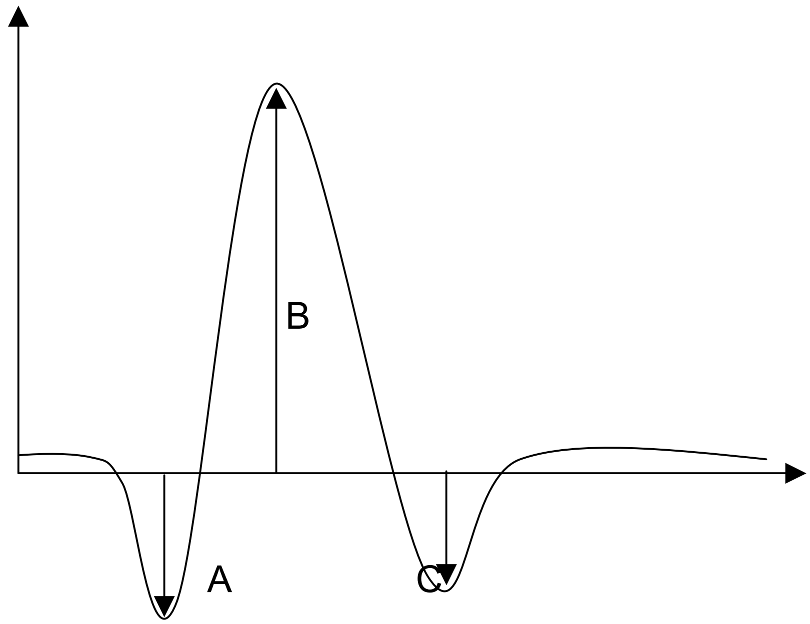

Figure E-1. Strain measurements in Tables E4 to E10.

Table E-2. Measured maximum dynamic longitudinal displacements (mm) as a function of load applications (703C3) – Position 1.

Position 1	A						
Repetitions	z = 69 mm	z = 189 mm	z = 298 mm	z = 462 mm	z = 611 mm	z = 773 mm	z = 912 mm
0		-0.0135	-0.0029	-0.0018	0.1145	0.1284	0.0012
500		-0.0276	-0.0031	-0.0018	-0.0021	-0.0030	-0.0021
1000		-0.0331	-0.0041	-0.0024	-0.0015	-0.0031	-0.0028
2500		-0.0289	-0.0031	-0.0021	-0.0019	-0.0030	-0.0019
5000		-0.0269	-0.0209	-0.0174	-0.0167	-0.0124	-0.0116

10000		-0.0264	-0.0108	-0.0112	-0.0126	-0.0120	-0.0126
25000		-0.0177	-0.0110	-0.0119	-0.0125	-0.0120	-0.0120
50000		-0.0251	-0.0106	-0.0118	-0.0135	-0.0131	-0.0124
105000		-0.0249	-0.0092	-0.0117	-0.0121	-0.0116	-0.0128
222340		-0.0275	-0.0112	-0.0112	-0.0124	-0.0116	-0.0116
376750		-0.0219	-0.0117	-0.0116	-0.0130	-0.0121	-0.0127

	B						
Repetitions	z = 69 mm	z = 189 mm	z = 298 mm	z = 462 mm	z = 611 mm	z = 773 mm	z = 912 mm
0		0.0346	0.0161	0.0172	0.2113	0.2647	0.0093
500		0.0421	0.0169	0.0189	0.0182	0.0086	0.0083
1000		0.0195	0.0210	0.0216	0.0207	0.0101	0.0100
2500		0.0192	0.0232	0.0243	0.0225	0.0109	0.0104
5000		0.0331	0.0201	0.0177	0.0176	0.0193	0.0191
10000		0.0336	0.0231	0.0205	0.0198	0.0193	0.0186
25000		0.0544	0.0273	0.0229	0.0227	0.0196	0.0188
50000		0.0344	0.0257	0.0236	0.0212	0.0193	0.0186
105000		0.0429	0.0530	0.0260	0.0221	0.0192	0.0189
222340		0.0463	0.0290	0.0259	0.0225	0.0193	0.0184
376750		0.0523	0.0276	0.0252	0.0214	0.0197	0.0185

	C						
Repetitions	z = 69 mm	z = 189 mm	z = 298 mm	z = 462 mm	z = 611 mm	z = 773 mm	z = 912 mm
0		-0.0135	-0.0029	-0.0018	0.1145	0.1284	0.0012
500		-0.0276	-0.0031	-0.0018	-0.0021	-0.0030	-0.0021
1000		-0.0331	-0.0041	-0.0024	-0.0015	-0.0031	-0.0028
2500		-0.0289	-0.0031	-0.0021	-0.0019	-0.0030	-0.0019
5000		-0.0270	-0.0106	-0.0115	-0.0121	-0.0123	-0.0109
10000		-0.0264	-0.0108	-0.0112	-0.0126	-0.0120	-0.0126
25000		-0.0177	-0.0110	-0.0119	-0.0125	-0.0120	-0.0120
50000		-0.0251	-0.0106	-0.0118	-0.0135	-0.0131	-0.0124
105000		-0.0249	-0.0092	-0.0117	-0.0121	-0.0116	-0.0128
222340		-0.0275	-0.0112	-0.0112	-0.0124	-0.0116	-0.0116
376750		-0.0219	-0.0117	-0.0116	-0.0130	-0.0121	-0.0127

Table E-3. Measured maximum dynamic longitudinal displacements (mm) as a function of load applications (703C3) – Position 2.

Position 2	A						
Repetitions	z = 69 mm	z = 189 mm	z = 298 mm	z = 462 mm	z = 611 mm	z = 773 mm	z = 912 mm
0		-0.0201	-0.0071	-0.0041	-0.0030	-0.0031	-0.0021
500		-0.0416	-0.0061	-0.0037	-0.0029	-0.0039	-0.0023

1000		-0.0223	-0.0072	-0.0042	-0.0031	-0.0041	-0.0032
2500		-0.0237	-0.0067	-0.0039	-0.0034	-0.0042	-0.0019
5000		-0.0237	-0.0067	-0.0039	-0.0034	-0.0042	-0.0019
10000		-0.0214	-0.0066	-0.0062	-0.0055	-0.0037	-0.0029
25000		-0.0163	-0.0088	-0.0075	-0.0065	-0.0039	-0.0040
50000		-0.0290	-0.0072	-0.0060	-0.0078	-0.0048	-0.0017
105000		-0.0274		-0.0078	-0.0071	-0.0038	-0.0035
222340		-0.0262	-0.0091	-0.0076	-0.0065	-0.0036	-0.0022
376750		-0.0250	-0.0051	-0.0069	-0.0066	-0.0055	-0.0028

	B						
Repetitions	z = 69 mm	z = 189 mm	z = 298 mm	z = 462 mm	z = 611 mm	z = 773 mm	z = 912 mm
0		0.0629	0.0289	0.0257	0.0223	0.0098	0.0091
500		0.0523	0.0282	0.0266	0.0245	0.0113	0.0105
1000		0.0466	0.0321	0.0287	0.0261	0.0118	0.0103
2500		0.0540	0.0362	0.0325	0.0299	0.0137	0.0124
5000		0.0555	0.0408	0.0338	0.0310	0.0142	0.0129
10000		0.0553	0.0466	0.0378	0.0335	0.0173	0.0134
25000		0.0825	0.0564	0.0426	0.0377	0.0195	0.0154
50000		0.0606	0.0530	0.0431	0.0361	0.0181	0.0157
105000		0.0638	0.0261	0.0463	0.0375	0.0204	0.0167
222340		0.0656	0.0544	0.0439	0.0373	0.0202	0.0161
376750		0.0712	0.0675	0.0439	0.0382	0.0198	0.0165

	C						
Repetitions	z = 69 mm	z = 189 mm	z = 298 mm	z = 462 mm	z = 611 mm	z = 773 mm	z = 912 mm
0		-0.0201	-0.0071	-0.0041	-0.0030	-0.0031	-0.0021
500		-0.0416	-0.0061	-0.0037	-0.0029	-0.0039	-0.0023
1000		-0.0223	-0.0072	-0.0042	-0.0031	-0.0041	-0.0032
2500		-0.0237	-0.0067	-0.0039	-0.0034	-0.0042	-0.0019
5000		-0.0310	-0.0077	-0.0066	-0.0056	-0.0057	-0.0036
10000		-0.0214	-0.0066	-0.0062	-0.0055	-0.0037	-0.0029
25000		-0.0163	-0.0088	-0.0075	-0.0065	-0.0039	-0.0040
50000		-0.0290	-0.0072	-0.0060	-0.0078	-0.0048	-0.0017
105000		-0.0274	-0.3165	-0.0078	-0.0071	-0.0038	-0.0035
222340		-0.0262	-0.0091	-0.0076	-0.0065	-0.0036	-0.0022
376750		-0.0250	-0.0051	-0.0069	-0.0066	-0.0055	-0.0028

Table E-4. Measured maximum dynamic longitudinal displacements (mm) as a function of load applications (703C3) – Position 3.

Position 1	A

Repetitions	z = 69 mm	z = 189 mm	z = 298 mm	z = 462 mm	z = 611 mm	z = 773 mm	z = 912 mm
0		-0.0230	-0.0081	-0.0043	-0.0025	-0.0038	-0.0023
500		-0.0304	-0.0055	-0.0036	-0.0025	-0.0044	-0.0024
1000		-0.0355	-0.0065	-0.0044	-0.0034	-0.0037	-0.0024
2500		-0.0183	-0.0063	-0.0044	-0.0031	-0.0030	-0.0023
5000		-0.0184	-0.0130	-0.0096	-0.0098	-0.0023	-0.0021
10000		-0.0273	-0.0090	-0.0072	-0.0054	-0.0039	-0.0036
25000		-0.0326	-0.0096	-0.0082	-0.0071	-0.0030	-0.0032
50000		-0.0297	-0.0077	-0.0076	-0.0056	-0.0040	-0.0031
105000		-0.0302	-0.0091	-0.0082	-0.0074	-0.0043	-0.0038
222340		-0.0268	-0.0096	-0.0071	-0.0061	-0.0046	-0.0030
376750		-0.0293	-0.0102	-0.0075	-0.0070	-0.0049	-0.0039

Repetitions	B						
	z = 69 mm	z = 189 mm	z = 298 mm	z = 462 mm	z = 611 mm	z = 773 mm	z = 912 mm
0		0.0639	0.0296	0.0262	0.0229	0.0103	0.0093
500		0.0590	0.0281	0.0267	0.0249	0.0113	0.0102
1000		0.0395	0.0323	0.0288	0.0264	0.0118	0.0110
2500		0.0617	0.0376	0.0323	0.0294	0.0143	0.0121
5000		0.0771	0.0444	0.0350	0.0313	0.0152	0.0128
10000		0.0641	0.0491	0.0376	0.0341	0.0174	0.0131
25000		0.0722	0.0578	0.0414	0.0369	0.0196	0.0153
50000		0.0622	0.0557	0.0416	0.0371	0.0187	0.0142
105000		0.0658	0.0603	0.0464	0.0380	0.0191	0.0149
222340		0.0728	0.0563	0.0432	0.0382	0.0188	0.0156
376750		0.0722	0.0561	0.0444	0.0375	0.0186	0.0161

Repetitions	C						
	z = 69 mm	z = 189 mm	z = 298 mm	z = 462 mm	z = 611 mm	z = 773 mm	z = 912 mm
0		-0.0230	-0.0081	-0.0043	-0.0025	-0.0038	-0.0023
500		-0.0304	-0.0055	-0.0036	-0.0025	-0.0044	-0.0024
1000		-0.0355	-0.0065	-0.0044	-0.0034	-0.0037	-0.0024
2500		-0.0183	-0.0063	-0.0044	-0.0031	-0.0030	-0.0023
5000		-0.0165	-0.0097	-0.0071	-0.0064	-0.0054	-0.0032
10000		-0.0273	-0.0090	-0.0072	-0.0054	-0.0039	-0.0036
25000		-0.0326	-0.0096	-0.0082	-0.0071	-0.0030	-0.0032
50000		-0.0297	-0.0077	-0.0076	-0.0056	-0.0040	-0.0031
105000		-0.0302	-0.0091	-0.0082	-0.0074	-0.0043	-0.0038
222340		-0.0268	-0.0096	-0.0071	-0.0061	-0.0046	-0.0030
376750		-0.0293	-0.0102	-0.0075	-0.0070	-0.0049	-0.0039

Table E-5. Measured maximum dynamic longitudinal strains (µstrains) as a function of load applications (703C3) – Position 1.

Position 1	A						
Repetitions	z = 69 mm	z = 189 mm	z = 298 mm	z = 462 mm	z = 611 mm	z = 773 mm	z = 912 mm
0		-73	-37	-25			
500		-66	-36	-27	-28	-7	-10
1000		-97	-40	-30	-29	-5	-7
2500		-94	-51	-33	-35	-9	-6
5000		-118	-61	-49	-48	-16	-11
10000		-137	-77	-53	-62	-14	-20
25000		-154	-108	-67	-65	-13	-13
50000		-177	-113	-70	-76	-16	-15
105000		-194	-123	-72	-68	-14	-19
222340		-180	-124	-71	-74	-13	-18
376750		-201	-153	-77	-80	-13	-17

	B						
Repetitions	z = 69 mm	z = 189 mm	z = 298 mm	z = 462 mm	z = 611 mm	z = 773 mm	z = 912 mm
0		259	119	134	1493	1857	64
500		316	125	148	132	63	57
1000		146	156	169	151	74	69
2500		144	172	190	164	80	72
5000		339	210	200	174	87	82
10000		351	240	226	188	103	88
25000		536	281	253	211	115	97
50000		349	268	257	202	109	88
105000		424	520	259	218	118	92
222340		458	287	252	220	119	97
376750		507	277	251	219	116	96

	C						
Repetitions	z = 69 mm	z = 189 mm	z = 298 mm	z = 462 mm	z = 611 mm	z = 773 mm	z = 912 mm
0		-101	-22	-14	774	815	8
500		-214	-23	-14	-15	-22	-14
1000		-248	-30	-19	-11	-23	-20
2500		-227	-23	-16	-14	-22	-13
5000		-173	-25	-29	-35	-29	-9
10000		-172	-30	-31	-32	-30	-24
25000		-67	-26	-35	-35	-28	-13
50000		-163	-25	-33	-45	-33	-21
105000		-147	-66	-25	-35	-26	-21
222340		-154	-21	-25	-37	-23	-17

376750		-121	-23	-31	-37	-26	-14

Table E-6. Measured maximum dynamic longitudinal strains (μstrains) as a function of load applications (703C3) – Position 2.

Position 2	A						
Repetitions	z = 69 mm	z = 189 mm	z = 298 mm	z = 462 mm	z = 611 mm	z = 773 mm	z = 912 mm
0		-166	-73	-43	-33	-8	-8
500		-121	-54	-36	-34	-9	-9
1000		-140	-59	-42	-39	-10	-9
2500		-137	-73	-48	-46	-12	-6
5000		-180	-99	-71	-60	-22	-15
10000		-187	-108	-78	-75	-19	-17
25000		-214	-130	-94	-91	-19	-21
50000		-231	-148	-93	-88	-24	-13
105000		-243		-102	-94	-20	-22
222340		-226	-175	-103	-94	-13	-16
376750		-259	-95	-112	-102	-18	-16

	B						
Repetitions	z = 69 mm	z = 189 mm	z = 298 mm	z = 462 mm	z = 611 mm	z = 773 mm	z = 912 mm
0		471	214	201	163	72	63
500		392	209	208	178	83	72
1000		349	237	225	190	87	71
2500		405	268	255	218	100	85
5000		417	302	265	226	105	89
10000		415	345	296	244	127	92
25000		619	418	334	274	143	106
50000		454	393	337	262	133	108
105000		478	244	337	273	150	115
222340		491	403	319	271	148	111
376750		533	505	319	278	145	113

	C						
Repetitions	z = 69 mm	z = 189 mm	z = 298 mm	z = 462 mm	z = 611 mm	z = 773 mm	z = 912 mm
0		-151	-53	-32	-22	-23	-14
500		-312	-45	-29	-21	-28	-16
1000		-167	-53	-33	-22	-30	-22
2500		-178	-49	-30	-25	-31	-13
5000		-233	-57	-52	-41	-42	-24
10000		-160	-49	-49	-40	-27	-20

25000		-122	-65	-59	-47	-29	-27
50000		-217	-53	-47	-57	-35	-11
105000		-205		-57	-52	-28	-24
222340		-196	-67	-55	-47	-26	-15
376750		-187	-38	-50	-48	-40	-19

Table E-7. Measured maximum dynamic longitudinal strains (μstrains) as a function of load applications (703C3) – Position 3.

Position 3	**A**						
Repetitions	z = 69 mm	z = 189 mm	z = 298 mm	z = 462 mm	z = 611 mm	z = 773 mm	z = 912 mm
0		-157	-70	-45	-35	-8	-10
500		-156	-64	-39	-37	-9	-12
1000		-154	-60	-44	-37	-11	-7
2500		-139	-64	-49	-45	-11	-10
5000		-138	-96	-75	-71	-17	-14
10000		-217	-112	-81	-66	-19	-21
25000		-370	-131	-99	-85	-20	-18
50000		-277	-140	-103	-84	-22	-20
105000		-285	-172	-101	-91	-19	-19
222340		-294	-159	-105	-89	-18	-20
376750		-275	-179	-109	-97	-20	-20

	B						
Repetitions	z = 69 mm	z = 189 mm	z = 298 mm	z = 462 mm	z = 611 mm	z = 773 mm	z = 912 mm
0		478	219	205	167	76	64
500		442	208	209	181	83	70
1000		296	239	226	192	87	76
2500		463	278	253	214	105	83
5000		579	329	274	228	111	88
10000		481	364	295	249	128	90
25000		542	428	324	269	144	105
50000		466	412	325	270	137	97
105000		493	447	337	277	140	102
222340		545	416	314	278	138	107
376750		541	418	323	272	136	111

	C						
Repetitions	z = 69 mm	z = 189 mm	z = 298 mm	z = 462 mm	z = 611 mm	z = 773 mm	z = 912 mm
0		-172	-60	-33	-18	-28	-16
500		-228	-40	-28	-18	-32	-16
1000		-266	-48	-34	-24	-27	-17
2500		-138	-46	-35	-23	-22	-16
5000		-124	-72	-55	-47	-40	-22

10000		-205	-67	-57	-39	-28	-25
25000		-244	-71	-64	-52	-22	-22
50000		-222	-57	-59	-41	-29	-21
105000		-226	-68	-59	-54	-32	-26
222340		-201	-71	-52	-44	-34	-21
376750		-219	-76	-54	-51	-36	-27

Table E-8. Measured maximum dynamic transverse displacements (mm) as a function of load applications (703C3).

Position 1							
Repetitions	z = 72 mm	z = 192 mm	z = 297 mm	z = 463 mm	z = 607 mm	z = 770 mm	z = 903 mm
0			0.0032	0.0077	0.2892	0.2763	0.0041
500			0.0048	0.0080	0.0097	0.0081	0.0030
1000			0.0047	0.0111	0.0135	0.0080	0.0043
2500			0.0068	0.0111	0.0132	0.0093	0.0038
5000			0.0094	0.0138	0.0162	0.0107	0.0056
10000							
25000			0.0136	0.0183	0.0209	0.0146	0.0072
50000			0.0160	0.0168	0.0191	0.0174	0.0050
105000			0.0456	0.0173	0.0211	0.0152	0.0070
222340			0.0165	0.0152	0.0197	0.0151	0.0076
376750			0.0164	0.0143	0.0215	0.0153	0.0063

Position 2							
Repetitions	z = 72 mm	z = 192 mm	z = 297 mm	z = 463 mm	z = 607 mm	z = 770 mm	z = 903 mm
0			0.0086	0.0099	0.0125	0.0082	0.0067
500			0.0091	0.0126	0.0155	0.0107	0.0062
1000			0.0122	0.0151	0.0182	0.0112	0.0065
2500			0.0125	0.0148	0.0202	0.0129	0.0059
5000			0.0166	0.0207	0.0234	0.0149	0.0100
10000							
25000			0.0241	0.0272	0.0318	0.0218	0.0121
50000			0.0266	0.0257	0.0303	0.0214	0.0110
105000			0.0303	0.0275	0.0288	0.0222	0.0119
222340			0.0250	0.0212	0.0284	0.0214	0.0111
376750				0.0223	0.0283	0.0189	0.0103

Position 3							
Repetitions	z = 72 mm	z = 192 mm	z = 297 mm	z = 463 mm	z = 607 mm	z = 770 mm	z = 903 mm

0			0.0080	0.0100	0.0131	0.0078	0.0057
500			0.0102	0.0121	0.0143	0.0090	0.0066
1000			0.0111	0.0151	0.0169	0.0075	0.0063
2500			0.0139	0.0162	0.0196	0.0110	0.0079
5000			0.0143	0.0203	0.0199	0.0152	0.0118
10000							
25000			0.0230	0.0272	0.0279	0.0174	0.0107
50000			0.0264	0.0262	0.0298	0.0150	0.0124
105000				0.0251	0.0296	0.0211	0.0114
222340			0.0241	0.0241	0.0282	0.0202	0.0114
376750			0.0244	0.0221	0.0315	0.0173	0.0123

Table E-9. Measured maximum dynamic transverse strains (µstrains) as a function of load applications (703C3).

Position 1							
Repetitions	z = 72 mm	z = 192 mm	z = 297 mm	z = 463 mm	z = 607 mm	z = 770 mm	z = 903 mm
0			20	46			25
500			31	48	55	44	19
1000			30	66	77	43	27
2500			44	67	75	50	24
5000			60	83	92	58	35
10000							
25000			87	110	119	79	45
50000			102	100	108	93	31
105000			293	104	120	82	44
222340			105	91	112	81	48
376750			104	86	122	82	39

Position 2							
Repetitions	z = 72 mm	z = 192 mm	z = 297 mm	z = 463 mm	z = 607 mm	z = 770 mm	z = 903 mm
10			55	59	71	44	41
500			58	75	88	57	38
1000			78	91	103	60	41
2500			80	89	115	69	37
5000			106	124	134	80	63
10000							
25000			154	163	181	117	75
50000			170	154	172	115	69
105000			199	165	164	119	74
222340			160	127	161	115	69
376750				133	161	101	64

Position 3							
Repetitions	z = 72 mm	z = 192 mm	z = 297 mm	z = 463 mm	z = 607 mm	z = 770 mm	z = 903 mm
0			51	60	74	42	36
500			65	72	81	48	41
1000			71	90	96	40	39
2500			89	97	111	59	49
5000			92	122	115	82	74
10000							
25000			147	163	159	94	67
50000			169	157	169	80	77
105000				150	169	113	71
222340			153	144	160	109	71
376750			157	132	179	93	76

Table E-10. Measured permanent displacements (mm) as a function of load applications (703C3).

Vertical	Load Repetitions									
Depth (mm)	0	500	1000	2500	5000	10000	25000	50000	105000	222340	37675
76	0.0000	-0.2766	-0.3919	-0.4117	-0.5580	-1.0846	-1.3037	-1.3724	-1.6004	-1.7511	-1.433
129	0.0000	-0.6401	-0.9061	-1.1693	-1.8574	-2.4283	-2.0995	-2.1934	-2.2883	-2.3824	-2.182
244	0.0000	-0.4303	-0.5953	-0.7046	-1.4308	-2.0716	-1.4964	-1.4866	-1.4631		
381	0.0000	-0.2777	-0.3811	-0.4348	-0.9978	-1.1784	-1.2232	-1.3273	-1.4976	-3.9670	-2.453
537	0.0000	-0.1956	-0.3049	-0.3539	-0.8020	-1.0483	-1.0330	-1.0711	-1.1552	-1.3102	-1.073
692	0.0000	-0.1394	-0.2451	-0.2683	-0.9128	-1.0577	-1.0179	-1.0654	-1.0656	-1.2727	-0.898
841	0.0000	-0.0836	-0.1661	-0.1714	-0.2890	-0.5240	-0.4647	-0.4652	-0.4221	-0.5570	-0.199
989	0.0000	-0.0857	-0.1682	-0.1769	-0.4848	-0.7505	-0.6653	-0.6613	-0.6170	-0.3333	-0.371

Longitudinal	Load Repetitions									
Depth (mm)	0	500	1000	2500	5000	10000	25000	50000	105000	222340	37675
69	0.0000	-0.7704		-0.5326							
189	0.0000	-0.2149	-0.1789	-0.3101	-0.1555	-0.4179	-0.1617	-0.0649	-0.0024	0.0805	0.213
298	0.0000	-0.0814	-0.0026	-0.0986	-0.3363	-0.4513	-0.4525	-0.4524	-0.4449	-2.5931	-1.021
462	0.0000	-0.0716	-0.0488	-0.1392	-0.2091	-0.2769	-0.2670	-0.1924			
611	0.0000	-0.0316	0.0177	-0.0615	-0.2674	-0.3441	-0.3257	-0.3091	-0.1479	-0.2529	0.073
773	0.0000	-0.0617	-0.0200	-0.1045	-0.1196	-0.3175	-0.3187	-0.3139	-0.2289	-0.3440	-0.024
912	0.0000	-0.0567	-0.0155	-0.0960	-0.1442	-0.3563	-0.3464	-0.3331	-0.2413	-0.0358	-0.010

Transverse	Load Repetitions									
Depth (mm)	0	500	1000	2500	5000	10000	25000	50000	105000	222340	37675
69	0.0000										
189	0.0000										

298	0.0000	0.0231	0.1246	0.0397	0.0224	-0.1021	-0.2293	-0.0438	0.0107		-0.543
462	0.0000	0.0071	0.0820	-0.0224	-0.1535	-0.3934	-0.3356	-0.2791	-0.2073	-0.2172	0.112
611	0.0000	-0.0403	0.0577	-0.0805	-0.2522	-0.4288	-0.3996	-0.3651	-0.1702	-0.2814	0.279
773	0.0000	-0.0583	0.0027	-0.0937	-0.0712	-0.3718	-0.3687	-0.3558	-0.2055	-0.3136	0.132
912	0.0000	-0.0526	-0.0089	-0.0955	-0.0028	-0.2659	-0.2568	-0.2345	-0.1080	0.1805	0.192

Table E-11. Measured permanent strains (%) as a function of load applications (703C3).

Vertical	Load Repetitions										
Depth (mm)	0	500	1000	2500	5000	10000	25000	50000	105000	222340	376750
76	0.00	-0.32	-0.46	-0.48	-0.65	-1.27	-1.52	-1.60	-1.87	-2.05	-1.67
129	0.00	-0.51	-0.72	-0.93	-1.48	-1.93	-1.67	-1.75	-1.82	-1.90	-1.74
244	0.00	-0.30	-0.42	-0.49	-1.00	-1.45	-1.05	-1.04	-1.02		-0.62
381	0.00	-0.20	-0.27	-0.31	-0.71	-0.84	-0.87	-0.94	-1.06	-2.81	-1.74
537	0.00	-0.14	-0.22	-0.26	-0.59	-0.77	-0.76	-0.78	-0.85	-0.96	-0.79
692	0.00	-0.09	-0.15	-0.17	-0.56	-0.65	-0.63	-0.66	-0.66	-0.78	-0.55
841	0.00	-0.06	-0.12	-0.12	-0.21	-0.37	-0.33	-0.33	-0.30	-0.40	-0.14
989	0.00	-0.05	-0.11	-0.11	-0.31	-0.48	-0.42	-0.42	-0.39	-0.21	-0.24

Longitudinal	Load Repetitions										
Depth (mm)	0	500	1000	2500	5000	10000	25000	50000	105000	222340	376750
69	0.00	-0.10	-0.49	-0.07	4.52	1.18	1.09				
189	0.00	-0.16	-0.13	-0.23	-0.12	-0.31	-0.12	-0.05	0.00	0.06	0.16
298	0.00	-0.06	0.00	-0.07	-0.25	-0.33	-0.33	-0.33	-0.33	-1.92	-0.75
462	0.00	-0.06	-0.04	-0.11	-0.16	-0.22	-0.21	-0.15			
611	0.00	-0.02	0.01	-0.04	-0.19	-0.25	-0.24	-0.22	-0.11	-0.18	0.05
773	0.00	-0.05	-0.01	-0.08	-0.09	-0.23	-0.23	-0.23	-0.17	-0.25	-0.02
912	0.00	-0.04	-0.01	-0.07	-0.10	-0.24	-0.24	-0.23	-0.17	-0.02	-0.01

Transverse	Load Repetitions										
Depth (mm)	0	500	1000	2500	5000	10000	25000	50000	105000	222340	376750
69	0.00										
189	0.00										
298	0.00	0.01	0.08	0.03	0.01	-0.07	-0.15	-0.03	0.01		-0.35
462	0.00	0.00	0.05	-0.01	-0.09	-0.24	-0.20	-0.17	-0.12	-0.13	0.07
611	0.00	-0.02	0.03	-0.05	-0.14	-0.24	-0.23	-0.21	-0.10	-0.16	0.16
773	0.00	-0.03	0.00	-0.05	-0.04	-0.20	-0.20	-0.19	-0.11	-0.17	0.07
912	0.00	-0.03	-0.01	-0.06	0.00	-0.17	-0.16	-0.15	-0.07	0.11	0.12

Table E-12. Maximum surface rut (mm) as a function of longitudinal location & load repetitions.

Position	Load Repetitions										
	0	500	1000	2500	5000	5000	25000	50000	105000	211000	376750
3	0.00	3.99	4.60	5.68	6.50	7.93	9.06	10.77	11.69	13.52	14.33
4	0.00	3.02	3.68	4.74	5.43	6.62	7.71	8.90	10.55	11.37	12.21
5	0.00	2.37	3.08	3.85	4.56	5.81	6.54	8.37	9.56	10.56	11.41
6	0.00	2.33	2.60	3.95	4.84	5.50	7.04	8.39	9.15	10.50	11.20
7	0.00	2.62	2.89	3.55	4.62	5.91	7.44	8.27	9.63	11.01	11.85
8	0.00	2.33	2.31	3.64	4.88	5.71	6.85	8.48	9.05	10.69	11.66
9	0.00	1.97	2.30	3.24	4.08	5.05	5.78	7.41	8.70	9.67	10.51
10	0.00	2.07	2.26	3.07	4.09	5.11	5.96	7.28	8.41	9.55	10.13
11	0.00	2.20	2.72	3.75	4.80	5.82	6.81	8.34	9.81	10.57	11.61
12	0.00	2.46	3.03	3.96	4.67	6.39	7.00	8.70	9.48	11.29	11.36
13	0.00	2.06	2.52	3.35	4.54	5.09	6.41	7.91	9.38	10.97	10.26
14	0.00	2.30	2.70	3.78	4.71	5.57	6.82	7.90	9.06	10.49	10.59
15	0.00	2.13	3.17	3.73	4.32	5.58	6.69	8.03	9.00	10.18	10.84
16	0.00	2.70	3.61	3.94	4.89	5.75	7.09	8.27	9.76	10.62	10.91
17	0.00	2.66	3.51	4.27	5.13	6.42	7.46	8.91	10.03	11.13	11.78
18	0.00	2.47	2.97	4.49	5.05	6.11	7.81	8.73	9.80	11.17	11.95
19	0.00	2.20	2.84	3.50	4.25	5.44	6.34	7.27	8.45	9.71	10.01
20	0.00	2.34	2.90	3.43	4.64	5.25	5.92	7.28	8.51	9.52	9.87
21	0.00	2.52	2.82	3.62	4.61	5.43	6.60	8.18	9.13	9.74	10.20
22	0.00	2.29	2.58	3.04	4.54	5.42	6.66	6.87	7.53	9.19	9.66

APPENDIX F

703C5 STRESS

Table F-1. Measured maximum vertical stresses as a function of load applications (703C5)

703C5	BASE COURSE		
DYNATEST	z = 191 mm		
Load Repetitions	VERTICAL STRESS (kPa)		
	Position 1	Position 2	Position 3
0	-183.82	-179.44	-161.76
500	-212.12	-203.99	-186.36
1000	-230.03	-217.12	-192.89
2500	-254.18	-238.05	-207.03
5000	-268.28	-256.99	-227.08
10000	-263.69	-252.80	-207.68
25000	-273.82	-260.71	-219.36
50000	-273.77	-266.39	-230.04
104720	-255.84	-250.27	-210.78

	TOP OF SUBGRADE		
DYNATEST	z = 450 mm		
Load Repetition	VERTICAL STRESS (kPa)		
	Position 1	Position 2	Position 3
0	-50.60	-72.89	-73.65
500	-56.71	-83.67	-79.88
1000	-62.04	-88.54	-87.96
2500	-61.48	-91.33	-88.83
5000	-68.17	-100.00	-96.25
10000	-64.87	-97.41	-93.16
25000	-69.69	-102.33	-95.37
50000	-68.78	-105.68	-96.82
104720	-76.47	-112.74	-102.44

Table F-2. Measured maximum longitudinal stresses as a function of load applications (703C5)

703C5	BASE COURSE		
DYNATEST	z = 162 mm		
Load Repetitions	LONGITUDINAL STRESS (kPa)		
	Position 1	Position 2	Position 3
0	-33.18	-39.73	-40.42
500	-36.78	-40.41	-36.93
1000	-38.83	-40.96	-38.93
2500	-41.90	-43.42	-40.99
5000	-42.30	-45.70	-44.59
10000	-39.93	-41.04	-40.61
25000	-35.21	-37.45	-39.24
50000	-22.57	-24.42	-26.64
104720	-18.22	-21.98	-24.59

	TOP OF SUBGRADE		
DYNATEST	z = 434 mm		
Load Repetition	LONGITUDINAL STRESS (kPa)		
	Position 1	Position 2	Position 3
0	-28.59	-34.80	-32.95
500	-23.51	-29.73	-26.87
1000	-20.77	-28.21	-27.16
2500	-19.68	-29.22	-27.23
5000	-19.66	-29.22	-27.41
10000	-17.58	-28.00	-25.84
25000	-16.38	-26.07	-23.37
50000	-19.73	-29.74	-27.58
104720	-18.54	-28.47	-26.68

Table F-3. Measured maximum transverse stress as a function of load applications (703C5).

703C5	BASE COURSE		
DYNATEST	z = 159 mm		
Load Repetitions	TRANSVERSE STRESS (kPa)		
	Position 1	Position 2	Position 3
0	-25.87	-38.78	-29.94
500	-30.18	-42.53	-33.39
1000	-35.39	-53.63	-34.41
2500	-41.80	-59.50	-37.81
5000	-43.36	-72.61	-42.55
10000	-45.70	-69.27	-47.00
25000	-55.14	-85.31	-49.27
50000	-55.54	-88.86	-55.69
104720	-48.38	-73.63	-44.58

	TOP OF SUBGRADE		
DYNATEST	z = 405 mm		
Load Repetition	TRANSVERSE STRESS (kPa)		
	Position 1	Position 2	Position 3
0	-30.91	-24.18	-14.73
500	-27.78	-28.70	-21.80
1000	-27.35	-28.91	-24.30
2500	-27.61	-30.35	-25.19
5000	-27.91	-31.01	-25.37
10000	-32.04	-35.27	-28.15
25000	-35.94	-37.88	-27.61
50000	-38.28	-40.76	-28.68
104720	-34.83	-37.44	-27.10

Table F-4. Measured maximum dynamic vertical displacements (mm) as a function of load applications (703C5).

Position 1							
Repetitions	z = 63 mm	z = 178 mm	z = 312 mm	z = 457 mm	z = 610 mm	z = 776 mm	z = 945 mm
0	-0.3406	-0.0587	-0.4210	-0.6955	-0.0649	-0.0212	-0.0153
500	-0.2722	-0.0558	-0.1353	-0.4502	-0.0491	-0.0239	-0.0162
1000	-0.2866	-0.0676	-0.1163	-0.3178	-0.0569	-0.0238	-0.0181
2500	-0.3144	-0.0757	-0.0964	-0.2930	-0.0564	-0.0265	-0.0194
5000	-0.3368	-0.0883	-0.0862	-0.2075	-0.0589	-0.0285	-0.0211
10830	-0.3531	-0.0942	-0.0942	-0.1408	-0.0723	-0.0301	-0.0222
25000	-0.3572	-0.1030	-0.0894	-0.1022	-0.0802	-0.0326	-0.0241
50000	-0.3444	-0.1061	-0.0788	-0.0955	-0.0836	-0.0289	-0.0228
104720	-0.3641	-0.1065	-0.0810	-0.0511	-0.0813	-0.0269	-0.0248

Position 2							
Repetitions	z = 63 mm	z = 178 mm	z = 312 mm	z = 457 mm	z = 610 mm	z = 776 mm	z = 945 mm
0	-0.3164	-0.0817	-0.4842	-0.7514	-0.0869	-0.0263	-0.0169
500	-0.2915	-0.0724	-0.1835	-0.5663	-0.0712	-0.0300	-0.0193
1000	-0.3159	-0.0871	-0.1748	-0.4064	-0.0777	-0.0335	-0.0209
2500	-0.3378	-0.0979	-0.1417	-0.3725	-0.0762	-0.0361	-0.0236
5000	-0.3776	-0.1154	-0.1337	-0.2678	-0.0841	-0.0390	-0.0261
10830	-0.3914	-0.1256	-0.1444	-0.1841	-0.1016	-0.0427	-0.0280
25000	-0.4062	-0.1366	-0.1392	-0.1307	-0.1149	-0.0449	-0.0297
50000	-0.4047	-0.1407	-0.1236	-0.1233	-0.1138	-0.0410	-0.1346
104720	-0.3974	-0.1399	-0.1028	-0.0917	-0.1211	-0.0358	-0.0307

Position 3							
Repetitions	z = 63 mm	z = 178 mm	z = 312 mm	z = 457 mm	z = 610 mm	z = 776 mm	z = 945 mm
0	-0.3941	-0.0710	-0.5259	-0.8745	-0.0797	-0.0239	-0.0166
500	-0.3774	-0.0684	-0.1680	-0.5629	-0.0609	-0.0262	-0.0173
1000	-0.4044	-0.0804	-0.1450	-0.3962	-0.0704	-0.0284	-0.0192
2500	-0.4201	-0.0942	-0.1195	-0.3646	-0.0718	-0.0314	-0.0213
5000	-0.4688	-0.1088	-0.1068	-0.2569	-0.0726	-0.0338	-0.0239
10830	-0.4735	-0.1165	-0.1161	-0.1758	-0.0894	-0.0358	-0.0258
25000	-0.4874	-0.1261	-0.1112	-0.1261	-0.1003	-0.0392	-0.0277

50000	-0.4924	-0.1326	-0.0974	-0.1171	-0.1029	-0.0349	-0.0260
104720	-0.4837	-0.1316	-0.0816	-0.0903	-0.1072	-0.0307	-0.0269

Table F-5. Maximum dynamic vertical strains (μstrains) as a function of load applications (703C5).

Position 1							
Repetitions	z = 120 mm	z = 245 mm	z = 385 mm	z = 534 mm	z = 693 mm	z = 861 mm	z = 1007 mm
0	-3049	-589	-4236	-5432	-443	-161	-138
500	-2435	-565	-1362	-3518	-343	-180	-144
1000	-2561	-669	-1182	-2491	-397	-190	-163
2500	-2818	-779	-976	-2302	-399	-213	-179
5000	-3012	-905	-873	-1632	-410	-227	-200
10830	-3167	-966	-951	-1109	-507	-242	-215
25000	-3204	-1047	-913	-799	-560	-264	-232
50000	-3073	-1104	-801	-747	-583	-236	-220
104720	-3221	-1061	-792	-392	-565	-213	-225

Position 2							
Repetitions	z = 120 mm	z = 245 mm	z = 385 mm	z = 534 mm	z = 693 mm	z = 861 mm	z = 1007 mm
0	-2248	-676	-3891	-4660	-483	-178	-141
500	-2078	-599	-1490	-3547	-400	-203	-161
1000	-2257	-721	-1423	-2558	-437	-226	-174
2500	-2412	-811	-1156	-2352	-428	-244	-197
5000	-2701	-957	-1093	-1695	-473	-264	-218
10830	-2797	-1041	-1181	-1167	-571	-288	-234
25000	-2913	-1134	-1141	-831	-645	-304	-248
50000	-2908	-1168	-1015	-785	-640	-276	-1137
104720	-2840	-1159	-840	-582	-681	-242	-256

Position 3							
Repetitions	z = 120 mm	z = 245 mm	z = 385 mm	z = 534 mm	z = 693 mm	z = 861 mm	z = 1007 mm
0	-2800	-588	-4240	-5438	-445	-162	-138
500	-2690	-565	-1363	-3523	-341	-177	-144
1000	-2883	-666	-1180	-2495	-395	-192	-160
2500	-3001	-780	-975	-2302	-403	-212	-177
5000	-3352	-902	-873	-1626	-408	-228	-199
10830	-3387	-965	-949	-1114	-502	-242	-215
25000	-3495	-1046	-912	-802	-563	-265	-232
50000	-3537	-1101	-800	-745	-579	-236	-217
104720	-3460	-1090	-667	-572	-602	-207	-225

Table F-6. Measured maximum dynamic longitudinal displacements (mm) as a function of load applications (703C5) – Position 1.

A							
Repetitions	z = 63 mm	z = 178 mm	z = 314 mm	z = 458 mm	z = 605 mm	z = 781 mm	z = 942 mm
0	-6.7649	-0.0278	-0.0639	-0.1346	-0.0200	-0.0181	-0.0161
500	-2.0060	-0.0224	-0.0338	-0.0549	-0.0183	-0.0179	-0.0158
1000	-1.9205	-0.0226	-0.0294	-0.0362	-0.0199	-0.0165	-0.0156
2500	-1.3793	-0.0234	-0.0294	-0.0297	-0.0178	-0.0199	-0.0160
5000	-0.5568	-0.0241	-0.0279	-0.0291	-0.0189	-0.0192	-0.0165
10830	-0.2197	-0.0232	-0.0258	-0.0240	-0.0211	-0.0183	-0.0157
25000	-0.3071	-0.0248	-0.0252	-0.0232	-0.0217	-0.0174	-0.0155
50000	-0.5507	-0.0231	-0.0236	-0.0223	-0.0232	-0.0183	-0.0146
104720	-2.0463	-0.0263	-0.0242	-0.0273	-0.0235	-0.0175	-0.0158

B							
Repetitions	z = 63 mm	z = 178 mm	z = 314 mm	z = 458 mm	z = 605 mm	z = 781 mm	z = 942 mm
0	-2.2446	-0.0152	-0.0776	-0.1244	-0.0126	-0.0069	-0.0044
500	-1.2617	-0.0122	-0.0391	-0.0654	-0.0094	-0.0065	-0.0032
1000	-1.3066	-0.0125	-0.0321	-0.0425	-0.0094	-0.0090	-0.0047
2500	-0.2892	-0.0095	-0.0315	-0.0320	-0.0083	-0.0073	-0.0043
5000	-0.2674	-0.0166	-0.0301	-0.0318	-0.0095	-0.0085	-0.0042
10830	-0.2336	-0.0152	-0.0276	-0.0243	-0.0097	-0.0064	-0.0036
25000	-0.0599	-0.0161	-0.0217	-0.0214	-0.0105	-0.0061	-0.0041
50000	-0.1566	-0.0154	-0.0193	-0.0209	-0.0143	-0.0056	-0.1250
104720	-1.2886	-0.0159	-0.0153	-0.0210	-0.0144	-0.0077	-0.0053

C							
Repetitions	z = 63 mm	z = 178 mm	z = 314 mm	z = 458 mm	z = 605 mm	z = 781 mm	z = 942 mm
0	-2.8093	-0.0164	-0.0722	-0.1625	-0.0117	-0.0049	-0.0022
500	-1.6571	-0.0106	-0.0315	-0.0560	-0.0078	-0.0030	-0.0035
1000	-1.5017	-0.0121	-0.0259	-0.0331	-0.0078	-0.0049	-0.0029
2500	-0.8601	-0.0129	-0.0255	-0.0235	-0.0065	-0.0069	-0.0031
5000	-0.8743	-0.0152	-0.0235	-0.0229	-0.0080	-0.0064	-0.0039
10830	-0.5356	-0.0166	-0.0210	-0.0175	-0.0092	-0.0056	-0.0040
25000	-0.2837	-0.0149	-0.0173	-0.0137	-0.0094	-0.0054	-0.0032

50000	-0.6794	-0.0150	-0.0160	-0.0136	-0.0123	-0.0070	-0.0020
104720	-2.2561	-0.0170	-0.0106	-0.0134	-0.0115	-0.0102	-0.0055

Table F-7. Measured maximum dynamic longitudinal displacements (mm) as a function of load applications (703C5) – Position 2.

A							
Repetitions	z = 63 mm	z = 178 mm	z = 314 mm	z = 458 mm	z = 605 mm	z = 781 mm	z = 942 mm
0	-2.2446	-0.0152	-0.0776	-0.1244	-0.0126	-0.0069	-0.0044
500	-1.2617	-0.0122	-0.0391	-0.0654	-0.0094	-0.0065	-0.0032
1000	-1.3066	-0.0125	-0.0321	-0.0425	-0.0094	-0.0090	-0.0047
2500	-0.2892	-0.0095	-0.0315	-0.0320	-0.0083	-0.0073	-0.0043
5000	-0.2674	-0.0166	-0.0301	-0.0318	-0.0095	-0.0085	-0.0042
10830	-0.2336	-0.0152	-0.0276	-0.0243	-0.0097	-0.0064	-0.0036
25000	-0.0599	-0.0161	-0.0217	-0.0214	-0.0105	-0.0061	-0.0041
50000	-0.1566	-0.0154	-0.0193	-0.0209	-0.0143	-0.0056	-0.1250
104720	-1.2886	-0.0159	-0.0153	-0.0210	-0.0144	-0.0077	-0.0053

B							
Repetitions	z = 63 mm	z = 178 mm	z = 314 mm	z = 458 mm	z = 605 mm	z = 781 mm	z = 942 mm
0	7.1148	0.0644	0.2495	0.0575	0.0083	0.0071	0.0051
500	19.5862	0.0405	0.1202	0.1627	0.0169	0.0132	0.0065
1000	12.9818	0.0368	0.1020	0.1282	0.0276	0.0149	0.0075
2500	10.3376	0.0492	0.0897	0.0752	0.0267	0.0172	0.0090
5000	7.7879	0.0469	0.0844	0.0634	0.0307	0.0197	0.0101
10830	8.9727	0.0468	0.0936	0.0571	0.0391	0.0263	0.0130
25000	8.8764	0.0507	0.0942	0.0554	0.0450	0.0269	0.0125
50000	8.1392	0.0576	0.0911	0.0540	0.0337	0.0279	-0.0109
104720	15.8024	0.0560	0.0746	0.0406	0.0254	0.0239	0.0116

C							
Repetitions	z = 63 mm	z = 178 mm	z = 314 mm	z = 458 mm	z = 605 mm	z = 781 mm	z = 942 mm

0	-2.2446	-0.0014	-0.0271	-0.1079	-0.0126	-0.0069	-0.0044
500	-1.2617	-0.0061	-0.0199	-0.0474	-0.0094	-0.0065	-0.0032
1000	-1.3066	-0.0042	-0.0172	-0.0240	-0.0094	-0.0090	-0.0047
2500	-0.2892	-0.0028	-0.0135	-0.0157	-0.0080	-0.0073	-0.0043
5000	-0.2259	-0.0159	-0.0120	-0.0144	-0.0095	-0.0085	-0.0042
10830	-0.2336	-0.0104	-0.0134	-0.0085	-0.0094	-0.0064	-0.0036
25000	0.2695	-0.0076	-0.0091	-0.0083	-0.0099	-0.0061	-0.0041
50000	0.2013	-0.0051	-0.0081	-0.0082	-0.0067	-0.0052	-0.0945
104720	-1.2886	-0.0101	-0.0064	-0.0081	-0.0104	-0.0038	-0.0053

Table F-8. Measured maximum dynamic longitudinal displacements (mm) as a function of load applications (703C5) – Position 3.

A							
Repetitions	z = 63 mm	z = 178 mm	z = 314 mm	z = 458 mm	z = 605 mm	z = 781 mm	z = 942 mm
0	-2.8093	-0.0164	-0.0722	-0.1625	-0.0117	-0.0049	-0.0022
500	-1.6571	-0.0106	-0.0315	-0.0560	-0.0078	-0.0030	-0.0035
1000	-1.5017	-0.0121	-0.0259	-0.0331	-0.0078	-0.0049	-0.0029
2500	-0.8601	-0.0129	-0.0255	-0.0235	-0.0065	-0.0069	-0.0031
5000	-0.8743	-0.0152	-0.0235	-0.0229	-0.0080	-0.0064	-0.0039
10830	-0.5356	-0.0166	-0.0210	-0.0175	-0.0092	-0.0056	-0.0040
25000	-0.2837	-0.0149	-0.0173	-0.0137	-0.0094	-0.0054	-0.0032
50000	-0.6794	-0.0150	-0.0160	-0.0136	-0.0123	-0.0070	-0.0020
104720	-2.2561	-0.0170	-0.0106	-0.0134	-0.0115	-0.0102	-0.0055

B							
Repetitions	z = 63 mm	z = 178 mm	z = 314 mm	z = 458 mm	z = 605 mm	z = 781 mm	z = 942 mm
0	12.5630	0.0741	0.2766	0.0349	0.0037	0.0081	0.0048
500	22.1725	0.0406	0.1082	0.1507	0.0143	0.0129	0.0067
1000	14.0536	0.0483	0.0882	0.1134	0.0242	0.0156	0.0082
2500	11.4604	0.0377	0.0770	0.0647	0.0244	0.0172	0.0098
5000	8.2293	0.0451	0.0708	0.0560	0.0248	0.0183	0.0098
10830	8.6588	0.0421	0.0799	0.0468	0.0318	0.0236	0.0117
25000	8.5540	0.0424	0.0803	0.0462	0.0376	0.0240	0.0121
50000	7.3524	0.0531	0.0759	0.0451	0.0293	0.0270	0.0147
104720	15.4784	0.0561	0.0630	0.0351	0.0202	0.0203	0.0103

C							
Repetitions	z = 63 mm	z = 178 mm	z = 314 mm	z = 458 mm	z = 605 mm	z = 781 mm	z = 942 mm
0	-2.8093	-0.0007	-0.0310	-0.1625	-0.0117	-0.0047	-0.0022
500	-1.6571	-0.0044	-0.0194	-0.0560	-0.0078	-0.0030	-0.0035
1000	-1.5017	-0.0098	-0.0182	-0.0331	-0.0078	-0.0049	-0.0029
2500	-0.8601	-0.0075	-0.0134	-0.0197	-0.0065	-0.0065	-0.0027
5000	-0.8743	-0.0108	-0.0124	-0.0168	-0.0080	-0.0064	-0.0039
10830	-0.0818	-0.0113	-0.0107	-0.0131	-0.0092	-0.0044	-0.0040
25000	-0.2837	-0.0095	-0.0088	-0.0117	-0.0094	-0.0052	-0.0032
50000	-0.6794	-0.0052	-0.0079	-0.0113	-0.0058	-0.0032	-0.0020
104720	-2.2561	-0.0095	-0.0062	-0.0105	-0.0093	-0.0050	-0.0055

Table F-9. Measured maximum dynamic longitudinal strains (µstrains) as a function of load applications (703C5) – Position 1.

Position 1	A						
Repetitions	z = 63 mm	z = 178 mm	z = 314 mm	z = 458 mm	z = 605 mm	z = 781 mm	z = 942 mm
0	-12743	-99	-503	-1091	-81	-25	-23
500	-3908	-64	-219	-378	-53	-23	-25
1000	-3816	-70	-179	-222	-55	-28	-23
2500	-2903	-78	-177	-158	-46	-40	-26
5000	-1209	-92	-164	-155	-55	-38	-32
10830	-489	-101	-147	-118	-61	-33	-26
25000	-709	-95	-123	-94	-67	-29	-24
50000	-1359	-95	-116	-97	-82	-39	-20
104720	-4479	-101	-107	-150	-82	-34	-41

	B						
Repetitions	z = 63 mm	z = 178 mm	z = 314 mm	z = 458 mm	z = 605 mm	z = 781 mm	z = 942 mm
0	1535	441	1923	237	24	44	29
500	23154	240	750	1014	91	72	41
1000	15700	257	614	765	158	87	56
2500	9524	243	535	435	155	94	63
5000	8684	272	491	378	161	105	64
10830	9844	251	555	315	207	131	76
25000	10724	256	559	311	244	135	80
50000	7747	326	531	307	190	150	92
104720	30673	383	449	238	133	123	63

	C						
Repetitions	z = 63 mm	z = 178 mm	z = 314 mm	z = 458 mm	z = 605 mm	z = 781 mm	z = 942 mm
0	-12743	-6	-213	-1091	-81	-25	-23
500	-4381	-33	-135	-378	-53	-17	-25
1000	-3816	-77	-128	-222	-55	-28	-23
2500	-3061	-44	-95	-134	-46	-39	-26
5000	-1511	-67	-86	-114	-55	-38	-32
10830	-1584	-133	-75	-90	-61	-26	-26
25000	-766	-66	-64	-78	-67	-29	-24
50000	-1593	-351	-55	-76	-41	-23	-22
104720	-4931	-127	-20	-19	-58	-24	-41

Table F-10. Measured maximum dynamic longitudinal strains (μstrains) as a function of load applications (703C3) – Position 2.

Position 1	A						
Repetitions	z = 63 mm	z = 178 mm	z = 314 mm	z = 458 mm	z = 605 mm	z = 781 mm	z = 942 mm
0	-1626	-91	-540	-837	-70	-24	-19
500	-1281	-73	-272	-441	-52	-27	-17
1000	-1053	-75	-223	-287	-48	-22	-21
2500	-672	-57	-219	-216	-54	-30	-19
5000	-520	-99	-209	-215	-58	-37	-19
10830	-630	-91	-192	-164	-63	-30	-17
25000	-570	-96	-151	-145	-69	-26	-19
50000	-434	-92	-134	-141	-94	-31	-858
104720	-1648	-95	-106	-142	-94	-42	-19

	B						
Repetitions	z = 63 mm	z = 178 mm	z = 314 mm	z = 458 mm	z = 605 mm	z = 781 mm	z = 942 mm
0	11079	384	1737	387	54	39	34
500	30602	242	835	1098	110	73	44
1000	20785	777	709	865	181	82	51
2500	17538	294	623	508	175	95	61
5000	13629	280	587	428	201	109	69
10830	15792	279	650	386	256	145	88
25000	16706	303	655	374	295	149	85
50000	16271	344	634	365	221	154	1411
104720	27774	334	518	274	166	132	79

	C						
Repetitions	z = 63 mm	z = 178 mm	z = 314 mm	z = 458 mm	z = 605 mm	z = 781 mm	z = 942 mm
0	-3495	-8	-189	-726	-82	-38	-30
500	-2125	-36	-138	-320	-61	-36	-22
1000	-2296	-25	-119	-162	-62	-50	-32
2500	-1361		-94	-106	-52	-40	-29
5000	-1239	-121	-83	-97	-62	-47	-29
10830	-943	-184	-93	-57	-61	-36	-24
25000	-677	-68	-63	-56	-65	-34	-28

50000	-395	-88	-56	-55	-44	-29	-649
104720	-3716	-345	-44	-55	-68	-21	-36

Table F-11. Measured maximum dynamic longitudinal strains (μstrains) as a function of load applications (703C5) – Position 3.

Position 1	A						
Repetitions	z = 63 mm	z = 178 mm	z = 314 mm	z = 458 mm	z = 605 mm	z = 781 mm	z = 942 mm
0	-1571	-98	-503	-961	-40	-27	-14
500	-955	-63	-219	-305	-40	-18	-18
1000	-1245	-72	-180	-188	-47	-27	-14
2500	-1124	-77	-177	-159	-39	-38	-21
5000	-560	-91	-163	-154	-42	-32	-18
10830	-939	-99	-146	-118	-58	-31	-13
25000	-486	-89	-121	-93	-61	-30	-13
50000	-375	-90	-112	-92	-81	-39	-11
104720	-866	-101	-74	-91	-75	-56	-14

	B						
Repetitions	z = 63 mm	z = 178 mm	z = 314 mm	z = 458 mm	z = 605 mm	z = 781 mm	z = 942 mm
0	19928	442	1924	235	24	45	32
500	34672	242	752	1016	94	71	45
1000	22420	288	613	766	159	86	56
2500	19413	256	535	437	160	95	67
5000	14342	269	492	378	162	101	67
10830	15181	251	555	316	208	130	79
25000	16067	253	559	312	246	133	82
50000	14680	318	528	305	192	149	100
104720	27117	335	438	237	132	112	70

	C						
Repetitions	z = 63 mm	z = 178 mm	z = 314 mm	z = 458 mm	z = 605 mm	z = 781 mm	z = 942 mm
0	-4456	-4	-216	-1095	-76	-26	-15
500	-3015	-26	-135	-378	-51	-16	-24
1000	-2628	-267	-127	-223	-51	-27	-20

2500	-2404	-44	-93	-133	-43	-36	-18
5000	-2069	-64	-86	-114	-52	-35	-27
10830	-1225	-147	-74	-88	-60	-24	-27
25000	-1172	-90	-61	-79	-61	-29	-21
50000	-1860	-288	-55	-76	-38	-18	-26
104720	-4574	-56	-43	-71	-61	-27	-37

Table F-12. Measured maximum dynamic transverse displacements (mm) as a function of load applications (703C5).

Position 1							
Repetitons	z = 63 mm	z = 178 mm	z = 314 mm	z = 458 mm	z = 603 mm	z = 778 mm	z = 938 mm
0	0.2286	0.0266	0.0701	0.0489	0.0032	0.0060	0.0074
500	0.2709	0.0282	0.0331	0.0699	0.0075	0.0060	0.0075
1000	0.2590	5.4038	0.0285	0.0579	0.0099	0.0054	0.0073
2500	0.2523	52.2132	0.0241	0.0584	0.0079	0.0083	0.0079
5000	0.2451	3.6384	0.0203	0.0533	0.0105	0.0074	0.0085
10830	0.2721	2.7552	0.0254	0.0412	0.0156	0.0083	0.0090
25000	0.2432	2.9611	0.0259	0.0246	0.0200	0.0057	0.0096
50000	0.2372	4.0833	0.0248	0.0233	0.0162	0.0067	0.0097
104720	0.2361	6.9083	0.0193	0.0215	0.0164	0.0074	0.0070

Position 2							
Repetitons	z = 63 mm	z = 178 mm	z = 314 mm	z = 458 mm	z = 603 mm	z = 778 mm	z = 938 mm
0	0.3030	0.0305	0.1045	0.0833	0.0034	0.0057	0.0067
500	0.3156	0.0316	0.0429	0.0881	0.0103	0.0066	0.0075
1000	0.3064	119.5981	0.0358	0.0748	0.0159	0.0057	0.0090
2500	0.3085	24.4986	0.0272	0.0538	0.0136	0.0063	0.0094
5000	0.3067	5.2847	0.0273	0.0559	0.0143	0.0063	0.0095
10830	0.2976	4.1504	0.0302	0.0537	0.0214	0.0045	0.0102
25000	0.3145	4.9458	0.0332	0.0367	0.0283	0.0046	0.0129
50000	0.2891	5.9789	0.0303	0.0357	0.0234	0.0076	-0.0121
104720	0.3153	10.3602	0.0259	0.0276	0.0224	0.0086	0.0098

Position 3							
Repetitons	z = 63 mm	z = 178 mm	z = 314 mm	z = 458 mm	z = 603 mm	z = 778 mm	z = 938 mm
0	0.3224	0.0304	0.0858	0.0593	0.0028	0.0056	0.0069
500	0.3052	0.0314	0.0401	0.0855	0.0064	0.0055	0.0066
1000	0.3054	8.0363	0.0339	0.0701	0.0094	0.0046	0.0064
2500	0.3047	21.9640	0.0287	0.0713	0.0064	0.0063	0.0081
5000	0.3155	4.5147	0.0241	0.0643	0.0108	0.0056	0.0090
10830	0.3088	3.4452	0.0298	0.0492	0.0168	0.0070	0.0091
25000	0.3038	3.7155	0.0311	0.0286	0.0234	0.0050	0.0090
50000	0.3161	5.0956	0.0286	0.0268	0.0180	0.0068	0.0108
104720	0.3216	8.9637	0.0238	0.0230	0.0177	0.0073	0.0000

Table F-13. Measured maximum dynamic transverse strains (µstrains) as a function of load applications (703C5).

Position 1							
Repetitions	z = 63 mm	z = 178 mm	z = 314 mm	z = 458 mm	z = 603 mm	z = 778 mm	z = 938 mm
0	1786	204	565	399	6	27	39
500	2108	217	260	574	43	23	35
1000	2014	45226	224	472	66	17	38
2500	1959	145502	186	478	43	41	47
5000	1901	10420	158	431	73	33	50
10830	2113	7953	195	330	114	29	48
25000	1887	8776	203	192	158	18	53
50000	1829	12436	188	179	119	33	59
104720	1830	19954	143	164	118	31	35

Position 2							
Repetitions	z = 63 mm	z = 178 mm	z = 314 mm	z = 458 mm	z = 603 mm	z = 778 mm	z = 938 mm
10	1896	198	688	562	23	26	39
500	1973	172	282	592	69	40	44
1000	1916	258417	235	503	107	31	53
2500	1924	66279	179	362	91	38	55
5000	1917	12112	179	376	96	38	56
10830	1856	9594	198	361	144	22	60
25000	1963	11732	218	247	190	28	76
50000	1805	14562	199	240	157	44	
104720	1967	23948	165	185	150	45	55

Position 3							
Repetitions	z = 63 mm	z = 178 mm	z = 314 mm	z = 458 mm	z = 603 mm	z = 778 mm	z = 938 mm

0	2015	202	565	400	6	29	40
500	1908	211	263	575	43	24	37
1000	1906	53898	223	471	63	17	38
2500	1900	30443	188	479	43	37	48
5000	1972	10349	158	432	73	33	51
10830	1927	7963	195	330	113	30	53
25000	1896	8814	204	192	157	17	52
50000	1973	12419	187	180	121	34	59
104720	2007	20718	156	155	119	38	

Table F14. Measured permanent displacements (mm) as a function of load applications (703C5).

Vertical									
Depth (mm)	0	500	1000	2500	5000	10830	25000	50000	104720
Surface	0.0000	-0.1860	-0.1771	-0.3357	-0.6940	-0.6070	-0.9967	-1.3136	
63	0.0000	-0.2594	-0.3134	-0.5017	-0.7557	-0.7509	-1.1019	-1.2967	-0.6204
178	0.0000	0.0572	-0.2785	-0.1503	-0.4241	-0.0886	-0.3396	-0.4404	-0.1182
312	0.0000	-0.8030	-1.2114	-1.3291	-1.6726	-1.5373	-1.9233	-2.1435	-1.5692
457	0.0000	-1.1039	-2.0335	-2.2675	-2.8491	-2.9449	-3.4772	-3.6956	-3.0054
610	0.0000	-1.2685	-1.7152	-1.5118	-1.7600	-1.5497	-1.4809	-1.8010	-1.6124
776	0.0000	0.1070	-0.1998	-0.0963	-0.2805	0.0082	-0.2613	-0.3236	-0.0387
945	0.0000	0.1038	-0.1421	-0.0497	-0.1767	0.0821	-0.1117	-0.2349	0.0381

Longitudinal									
Depth (mm)	0	500	1000	2500	5000	10830	25000	50000	104720
63	0.0000								
178	0.0000	0.0126	-0.1518	-0.0879	-0.3872	-0.1511	-0.3295	-0.3454	-0.1083
314	0.0000	0.0892	0.0028	0.0501	-0.1259	0.0980	-0.0054	-0.0102	0.1337
458	0.0000	-0.2181	-0.3556	-0.3388	-0.4799	-0.3192	-0.4371	-0.4381	-0.2874
605	0.0000	0.0294	-0.0805	-0.0742	-0.0690	0.1248	0.0429	-0.0003	0.1537
781	0.0000	0.0614	-0.0150	-0.1333	-0.2151	0.0081	-0.1008	-0.2051	0.0436
942	0.0000	0.0341	-0.0514	-0.0541	-0.1795	0.0192	-0.1073	-0.1504	0.0523

Transverse									
Depth (mm)	0	500	1000	2500	5000	10830	25000	50000	104720
63	0.0000	-0.1122	0.2234	0.1544	-0.0085	-0.0592	0.0692	0.1440	0.2759
178	0.0000								
314	0.0000	0.3700	0.2952	0.3685	0.1876	0.4556	0.3263	0.3382	0.4920

458	0.0000	0.2882	0.2126	0.2520	0.1478	0.4111	0.3126	0.3336	0.4402
603	0.0000	0.1238	0.0238	0.0768	-0.0474	0.1842	0.0651	0.0912	0.2179
778	0.0000	0.0958	0.0196	0.0323	-0.1140	0.1270	-0.0105	0.0209	0.1524
938	0.0000	0.0772	-0.0048	0.0120	-0.1326	0.1076	-0.0385	-0.0687	0.1324

Table F-15. Measured permanent strains (%) as a function of load applications (703C5).

Vertical									
Depth (mm)	0	500	1000	2500	5000	10830	25000	50000	104720
Surface	0.00	-0.17	-0.16	-0.31	-0.64	-0.56	-0.92	-1.21	
63	0.00	-0.18	-0.22	-0.36	-0.54	-0.53	-0.78	-0.92	-0.44
178	0.00	0.05	-0.23	-0.12	-0.35	-0.07	-0.28	-0.36	-0.10
312	0.00	-0.65	-0.98	-1.07	-1.35	-1.24	-1.55	-1.73	-1.27
457	0.00	-0.69	-1.26	-1.41	-1.77	-1.83	-2.16	-2.30	-1.87
610	0.00	-0.71	-0.96	-0.84	-0.98	-0.86	-0.82	-1.00	-0.90
776	0.00	0.07	-0.13	-0.07	-0.19	0.01	-0.18	-0.22	-0.03
945	0.00	0.09	-0.12	-0.04	-0.15	0.07	-0.09	-0.20	0.03

Longitudinal									
Depth (mm)	0	500	1000	2500	5000	10830	25000	50000	104720
63	0.00								
178	0.00	0.01	-0.09	-0.05	-0.23	-0.09	-0.20	-0.21	-0.06
314	0.00	0.06	0.00	0.03	-0.09	0.07	0.00	-0.01	0.09
458	0.00	-0.15	-0.24	-0.23	-0.32	-0.22	-0.29	-0.30	-0.19
605	0.00	0.02	-0.05	-0.05	-0.05	0.08	0.03	0.00	0.10
781	0.00	0.03	-0.01	-0.07	-0.12	0.00	-0.06	-0.11	0.02
942	0.00	0.02	-0.03	-0.04	-0.12	0.01	-0.07	-0.10	0.04

Transverse									
Depth (mm)	0	500	1000	2500	5000	10830	25000	50000	104720
63	0.00	-0.07	0.14	0.10	-0.01	-0.04	0.04	0.09	0.17
178	0.00								
314	0.00	0.24	0.19	0.24	0.12	0.30	0.21	0.22	0.32
458	0.00	0.19	0.14	0.17	0.10	0.28	0.21	0.22	0.30
603	0.00	0.08	0.02	0.05	-0.03	0.12	0.04	0.06	0.15
778	0.00	0.06	0.01	0.02	-0.07	0.08	-0.01	0.01	0.09
938	0.00	0.05	0.00	0.01	-0.08	0.06	-0.02	-0.04	0.08

Table E-12. Maximum surface rut (mm) as a function of longitudinal location & load repetitions.

Position	Load Repetitions										
	0	500	1000	2500	5000	5000	25000	50000	105000	211000	376750
3	0.00	3.99	4.60	5.68	6.50	7.93	9.06	10.77	11.69	13.52	14.33
4	0.00	3.02	3.68	4.74	5.43	6.62	7.71	8.90	10.55	11.37	12.21
5	0.00	2.37	3.08	3.85	4.56	5.81	6.54	8.37	9.56	10.56	11.41
6	0.00	2.33	2.60	3.95	4.84	5.50	7.04	8.39	9.15	10.50	11.20
7	0.00	2.62	2.89	3.55	4.62	5.91	7.44	8.27	9.63	11.01	11.85
8	0.00	2.33	2.31	3.64	4.88	5.71	6.85	8.48	9.05	10.69	11.66
9	0.00	1.97	2.30	3.24	4.08	5.05	5.78	7.41	8.70	9.67	10.51
10	0.00	2.07	2.26	3.07	4.09	5.11	5.96	7.28	8.41	9.55	10.13
11	0.00	2.20	2.72	3.75	4.80	5.82	6.81	8.34	9.81	10.57	11.61
12	0.00	2.46	3.03	3.96	4.67	6.39	7.00	8.70	9.48	11.29	11.36
13	0.00	2.06	2.52	3.35	4.54	5.09	6.41	7.91	9.38	10.97	10.26
14	0.00	2.30	2.70	3.78	4.71	5.57	6.82	7.90	9.06	10.49	10.59
15	0.00	2.13	3.17	3.73	4.32	5.58	6.69	8.03	9.00	10.18	10.84
16	0.00	2.70	3.61	3.94	4.89	5.75	7.09	8.27	9.76	10.62	10.91
17	0.00	2.66	3.51	4.27	5.13	6.42	7.46	8.91	10.03	11.13	11.78
18	0.00	2.47	2.97	4.49	5.05	6.11	7.81	8.73	9.80	11.17	11.95
19	0.00	2.20	2.84	3.50	4.25	5.44	6.34	7.27	8.45	9.71	10.01
20	0.00	2.34	2.90	3.43	4.64	5.25	5.92	7.28	8.51	9.52	9.87
21	0.00	2.52	2.82	3.62	4.61	5.43	6.60	8.18	9.13	9.74	10.20
22	0.00	2.29	2.58	3.04	4.54	5.42	6.66	6.87	7.53	9.19	9.66

APPENDIX G

703C6 STRESS

Table G-1. Measured maximum stresses as a function of load applications (703C6)

703C6	TOP OF SUBGRADE		
DYNATEST	z = 458 mm		
Load Repetitions	VERTICAL STRESS (kPa)		
	Position 1	Position 2	Position 3
0	-22.66	-46.87	-47.85
500	-22.30	-47.93	-50.41
1000	-22.54	-49.04	-53.37
2500	-24.17	-52.70	-55.94
5000	-26.36	-54.53	-60.24
10000	-57.12	-54.69	-24.80
25000	-25.04	-56.82	-60.64
48772	-19.15	-29.90	-50.82
92550	-21.38	-55.93	-52.91
152510	-19.45	-53.17	-52.07
196700	-78.95	-79.66	-45.56
496555	-48.72	-90.16	-84.08
951065	-48.11	-85.84	-94.40
1356500	-55.32	-87.49	-66.77

	TOP OF SUBGRADE		
DYNATEST	z = 424 mm		
Load Repetition	LONGITUDINAL STRESS (kPa)		
	Position 1	Position 2	Position 3
0	-17.16	-22.37	-21.21
500	-15.46	-20.97	-20.71
1000	-15.34	-20.55	-20.68
2500	-13.65	-18.39	-18.99
5000	-12.39	-16.51	-17.23
10000	-1.24	-1.24	-1.09
25000	-1.30	-1.47	-1.27
48772	-1.43	-1.44	-1.48
92550	-1.49	-1.55	-1.38
152510	-1.45	-1.69	-1.53
196700	-13.51	-14.17	-10.24
496555	-12.18	-17.50	-15.95
951065	-12.01	-17.35	-17.12
1356500	-16.38	-20.49	-17.47

Table G-1. Measured maximum stresses as a function of load applications (703C6) – cont.

DYNATEST Load Repetition	TOP OF SUBGRADE z = 432 mm TRANSVERSE STRESS (kPa)		
	Position 1	Position 2	Position 3
0	-19.11	-16.69	-15.15
500	-16.01	-13.80	-14.26
1000	-15.80	-13.60	-14.09
2500	-15.68	-13.68	-14.12
5000	-16.15	-12.79	-13.44
10000	-10.70	-9.63	-12.96
25000	-5.90	-3.46	-4.38
48772	-1.29	-0.79	-0.45
92550	-0.27	-0.32	-0.50
152510	-0.39	-0.38	-0.38
196700	-10.82	-8.94	-9.88
496555	-9.06	-9.63	-11.50
951065	-6.14	-6.66	-6.37
1356500	-3.04	-1.80	-2.60

APPENDIX H

DYNAMIC STRAINS

Table H-1. Measured maximum dynamic vertical displacements (mm) as a function of load applications (703C6).

Position 1						
Repetitions	z= 120mm	z = 385mm	z = 540mm	z = 702mm	z = 858mm	z = 983mm
0	-0.7462	-0.1198	-0.0913	-0.0468	-0.0146	-0.0079
500	-0.7863	-0.0924	-0.0640	-0.0484	-0.0170	-0.0095
1000	-0.7267	-0.0947	-0.0640	-0.0504	-0.0172	-0.0096
2500	-0.7390	-0.1005	-0.0693	-0.0535	-0.0188	-0.0101
5000	-0.8178	-0.1006	-0.0727	-0.0568	-0.0193	-0.0103
10000	-1.2105	-0.0994	-0.0704	-0.0545	-0.0199	-0.0104
25000		-0.1039	-0.0784	-0.0465	-0.0205	-0.0109
48772		-0.0938	-0.0750	-0.0498	-0.0191	-0.0115
92550		-0.0983	-0.0735	-0.0483	-0.0196	-0.0112
152510		-0.0979	-0.0703	-0.0477	-0.0187	-0.0123
196700		-0.0991	-0.0733	-0.0530	-0.0183	
496555			-0.0665	-0.0516	-0.0203	
951065		-0.0844		-0.0496		
1356500		-0.0812	-0.0667	-0.0525		

Position 2						
Repetitions	z= 120mm	z = 385mm	z = 540mm	z = 702mm	z = 858mm	z = 983mm
0	-0.6438	-0.1238	-0.0767	-0.0568	-0.0181	-0.0085
500	-0.6527	-0.1084	-0.0587	-0.0654	-0.0234	-0.0103
1000	-0.6682	-0.1143	-0.0634	-0.0648	-0.0232	-0.0109
2500	-0.6602	-0.1210	-0.0660	-0.0679	-0.0254	-0.0117
5000	-0.7707	-0.1252	-0.0717	-0.0702	-0.0269	-0.0119
10000	-0.7306	-0.1219	-0.0699	-0.0694	-0.0273	-0.0133
25000		-0.1282	-0.0737	-0.0675	-0.0294	-0.0141
48772		-0.1246	-0.0747	-0.0643	-0.0265	-0.0144
92550		-0.1193	-0.0692	-0.0659	-0.0271	-0.0146
152510		-0.1175	-0.0690	-0.0672	-0.0265	-0.0147
196700		-0.1235	-0.0700	-0.0700	-0.0248	
496555			-0.0665	-0.0668	-0.0243	
951065		-0.1129		-0.0665		

1356500		-0.0771	-0.0606	-0.0638		

Table H-1. Maximum dynamic vertical displacements (mm) as a function of load applications (703C6) – cont.

Position 3						
Repetitions	z= 120mm	z = 385mm	z = 540mm	z = 702mm	z = 858mm	z = 983mm
0	-0.9930	-0.0666	-0.0217	-0.0461	-0.0198	-0.0079
500	-0.9873	-0.0843	-0.0232	-0.0533	-0.0240	-0.0106
1000	-1.0327	-0.0841	-0.0265	-0.0549	-0.0245	-0.0109
2500	-1.0196	-0.0913	-0.0289	-0.0572	-0.0262	-0.0119
5000	-1.0201	-0.0950	-0.0323	-0.0578	-0.0275	-0.0122
10000	-1.9189	-0.0918	-0.0316	-0.0569	-0.0285	-0.0126
25000		-0.1000	-0.0373	-0.0506	-0.0294	-0.0137
48772		-0.0896	-0.0346	-0.0551	-0.0262	-0.0129
92550		-0.0860	-0.0318	-0.0537	-0.0273	-0.0134
152510		-0.0882	-0.0316	-0.0531	-0.0202	-0.0138
196700		-0.0905	-0.0328	-0.0552	-0.0253	
496555			-0.0360	-0.0526	-0.0248	
951065		-0.0847		-0.0577		
1356500		-0.0806	-0.0219	-0.0400	-0.0227	

Table H-2. Maximum dynamic vertical strains (µstrains) as a function of load applications (703C6).

Position 1						
Repetitions	z= 120mm	z = 385mm	z = 540mm	z = 702mm	z = 858mm	z = 983mm
0	-3352	-893	-698	-274	-117	-67
500	-3536	-690	-486	-300	-141	-88
1000	-3282	-709	-486	-308	-154	-96
2500	-3339	-751	-534	-327	-157	-95
5000	-3697	-755	-554	-348	-168	-103
10000	-5464	-744	-541	-333	-178	-105
25000		-781	-602	-287	-185	-117
48772		-703	-576	-306	-168	-115
92550		-739	-573	-300	-176	-121
152510		-740	-546	-295	-167	-129
196700		-740	-554	-316	-148	
496555			-506	-310	-166	
951065		-640		-311		
1356500		-595	-482	-315		

Position 2						
Repetitions	z= 120mm	z = 385mm	z = 540mm	z = 702mm	z = 858mm	z = 983mm
0	-2314	-745	-473	-281	-148	-83
500	-2348	-654	-363	-324	-191	-100
1000	-2418	-691	-393	-321	-189	-107
2500	-2382	-731	-409	-337	-207	-114
5000	-2784	-757	-445	-348	-219	-116
10000	-2648	-738	-434	-344	-222	-135
25000		-773	-459	-339	-239	-137
48772		-751	-465	-323	-215	-141
92550		-721	-431	-331	-220	-143
152510		-711	-430	-338	-216	-143
196700		-742	-434	-349	-201	
496555		-702	-404	-337	-198	
951065		-688		-335		
1356500		-469	-367	-322	-156	

Table H-2. Maximum dynamic vertical strains (µstrains) as a function of load applications (703C6) – cont.

Position 3						
Repetitions	z= 120mm	z = 385mm	z = 540mm	z = 702mm	z = 858mm	z = 983mm
0	-3568	-400	-134	-228	-161	-77
500	-3552	-509	-144	-264	-195	-103
1000	-3723	-508	-164	-272	-200	-107
2500	-3683	-552	-180	-284	-214	-116
5000	-3684	-575	-200	-287	-225	-119
10000	-6945	-555	-196	-282	-232	-123
25000		-603	-232	-254	-239	-134
48772		-540	-215	-277	-213	-126
92550		-520	-198	-270	-222	-131
152510		-534	-197	-267	-164	-135
196700		-544	-203	-275	-205	
496555		-511	-218	-265	-202	
951065		-516		-291		
1356500		-491	-133	-202	-186	

Table H-3. Measured maximum dynamic longitudinal displacements (mm) as a function of load applications (703C6) – Position 1.

A							
Repetitions	z = 70mm	z = 152mm	z = 304mm	z = 464mm	z = 625mm	z = 709mm	z = 931mm
0			-0.0266	-0.0203	-0.0130	-0.0136	-0.0125
500			-0.0236	-0.0175	-0.0130	-0.0144	-0.0131
1000			-0.0243	-0.0174	-0.0125	-0.0132	-0.0129
2500			-0.0256	-0.0201	-0.0126	-0.0128	-0.0115
5000			-0.0268	-0.0173	-0.0136	-0.0137	-0.0125
10000			-0.0233	-0.0171	-0.0126	-0.0144	-0.0134
25000				-0.0230	-0.0204	-0.0150	-0.0135
48772				-0.0238	-0.0214	-0.0137	-0.0147
92550				-0.0231	-0.0188	-0.0125	-0.0133
152510				-0.0232	-0.0174		-0.0135
196700							
496555							
951065							
1356500							

B							
Repetitions	z = 70mm	z = 152mm	z = 304mm	z = 464mm	z = 625mm	z = 709mm	z = 931mm
0			0.0196	0.0185	0.0207	0.0200	0.0208
500			0.0181	0.0172	0.0199	0.0195	0.0191
1000			0.0170	0.0153	0.0200	0.0193	0.0204
2500			0.0174	0.0187	0.0197	0.0201	0.0199
5000			0.0189	0.0198	0.0180	0.0179	0.0204
10000			0.0216	0.0202	0.0208	0.0196	0.0180
25000				0.0221	0.0195	0.0191	0.0187
48772				0.0212	0.0214	0.0192	0.0196
92550				0.0214	0.0182	0.0191	0.0191
152510				0.0195	0.0189		0.0184
196700							
496555							
951065							
1356500							

Table H-3. Measured maximum dynamic longitudinal displacements (mm) as a function of load applications (703C6) – Position 1 - cont.

C							
Repetitions	z = 70mm	z = 152mm	z = 304mm	z = 464mm	z = 625mm	z = 709mm	z = 931mm
0			-0.0139	-0.0121	-0.0123	-0.0124	-0.0120
500			-0.0117	-0.0117	-0.0127	-0.0128	-0.0128
1000			-0.0125	-0.0131	-0.0125	-0.0119	-0.0119
2500			-0.0126	-0.0119	-0.0126	-0.0115	-0.0115
5000			-0.0136	-0.0111	-0.0136	-0.0126	-0.0125
10000			-0.0120	-0.0128	-0.0126	-0.0126	-0.0134
25000				-0.0139	-0.0128	-0.0150	-0.0135
48772				-0.0126	-0.0110	-0.0137	-0.0135
92550				-0.0134	-0.0124	-0.0125	-0.0122
152510				-0.0128	-0.0129		-0.0107
196700							
496555							
951065							
1356500							

Table H-5. Measured maximum dynamic longitudinal displacements (mm) as a function of load applications (703C6) – Position 2.

A							
Repetitions	z = 70mm	z = 152mm	z = 304mm	z = 464mm	z = 625mm	z = 709mm	z = 931mm
0	-0.0474		-0.0174	-0.0089	-0.0048	-0.0023	-0.0029
500	-0.0405		-0.0166	-0.0091	-0.0065	-0.0029	-0.0036
1000	-0.0371		-0.0157	-0.0077	-0.0057	-0.0031	-0.0022
2500	-0.0332		-0.0156	-0.0091	-0.0047	-0.0040	-0.0033
5000	-0.0842		-0.0160	-0.0094	-0.0059	-0.0034	-0.0030
10000	-0.0779		-0.0120	-0.0080	-0.0073	-0.0026	-0.0021
25000			-5.9967	-0.0143	-0.0101	-0.0078	-0.0038
48772			-8.2729	-0.0127	-0.0094	-0.0053	-0.0033
92550			-1.3127	-0.0134	-0.0098	-0.0059	-0.0030
152510			-1.6974	-0.0111	-0.0098		-0.0032
196700							
496555							

951065							
1356500							

Table H-5. Measured maximum dynamic longitudinal displacements (mm) as a function of load applications (703C6) – Position 2 - cont.

B							
Repetitions	z = 70mm	z = 152mm	z = 304mm	z = 464mm	z = 625mm	z = 709mm	z = 931mm
0	0.2162		0.0247	0.0202	0.0094	0.0062	0.0049
500	0.2129		0.0202	0.0231	0.0112	0.0073	0.0058
1000	0.2049		0.0210	0.0269	0.0106	0.0064	0.0072
2500	0.2084		0.0234	0.0269	0.0129	0.0079	0.0071
5000	0.1617		0.0248	0.0281	0.0139	0.0098	0.0092
10000	0.0918		0.0298	0.0300	0.0141	0.0100	0.0088
25000				0.0331	0.0311	0.0160	0.0092
48772				0.0340	0.0304	0.0181	0.0107
92550				0.0303	0.0308	0.0179	0.0123
152510				0.0305	0.0292		0.0130
196700							
496555							
951065							
1356500							

C							
Repetitions	z = 70mm	z = 152mm	z = 304mm	z = 464mm	z = 625mm	z = 709mm	z = 931mm
0	-0.0246		-0.0072	-0.0070	-0.0048	-0.0023	-0.0029
500	-0.0130		-0.0055	-0.0043	-0.0065	-0.0029	-0.0036
1000	-0.0078		-0.0053	-0.0046	-0.0050	-0.0031	-0.0022
2500	-0.0080		-0.0051	-0.0056	-0.0047	-0.0040	-0.0033
5000	-0.0315		-0.0063	-0.0052	-0.0059	-0.0034	-0.0030
10000	-0.0292		-0.0069	-0.0080	-0.0073	-0.0026	-0.0021
25000				-0.0088	-0.0046	-0.0078	-0.0038
48772				-0.0082	-0.0042	-0.0053	-0.0033
92550				-0.0088	-0.0050	-0.0059	-0.0025
152510				-0.0067	-0.0050		-0.0032

196700							
496555							
951065							
1356500							

Table H-6. Measured maximum dynamic longitudinal displacements (mm) as a function of load applications (703C6) – Position 3.

A							
Repetitions	z = 70mm	z = 152mm	z = 304mm	z = 464mm	z = 625mm	z = 709mm	z = 931mm
0			-0.0105	-0.0063	-0.0044	-0.0032	-0.0024
500			-0.0132	-0.0066	-0.0063	-0.0024	-0.0024
1000			-0.0126	-0.0068	-0.0056	-0.0027	-0.0028
2500			-0.0118	-0.0090	-0.0063	-0.0037	-0.0036
5000			-0.0132	-0.0070	-0.0062	-0.0040	-0.0035
10000			-0.0096	-0.0074	-0.0073	-0.0025	-0.0032
25000				-0.0100	-0.0110	-0.0070	-0.0044
48772				-0.0085	-0.0081	-0.0051	-0.0035
92550				-0.0092	-0.0063	-0.0080	-0.0036
152510				-0.0102	-0.0088		-0.0028
196700							
496555							
951065							
1356500							

B							
Repetitions	z = 70mm	z = 152mm	z = 304mm	z = 464mm	z = 625mm	z = 709mm	z = 931mm
0			0.0156	0.0170	0.0093	0.0057	0.0053
500			0.0152	0.0221	0.0100	0.0069	0.0072
1000			0.0156	0.0229	0.0114	0.0072	0.0054
2500			0.0182	0.0266	0.0127	0.0080	0.0058
5000			0.0199	0.0264	0.0126	0.0087	0.0075
10000			0.0255	0.0256	0.0144	0.0091	0.0093
25000				0.0284	0.0260	0.0161	0.0097
48772				0.0258	0.0269	0.0153	0.0102
92550				0.0243	0.0241	0.0160	0.0102

152510				0.0238	0.0252		0.0121
196700							
496555							
951065							
1356500							

Table H-6. Measured maximum dynamic longitudinal displacements (mm) as a function of load applications (703C6) – Position 3 - cont.

C							
Repetitions	z = 70mm	z = 152mm	z = 304mm	z = 464mm	z = 625mm	z = 709mm	z = 931mm
0			-0.0060	-0.0048	-0.0044	-0.0032	-0.0024
500			-0.0048	-0.0048	-0.0063	-0.0024	-0.0024
1000			-0.0057	-0.0045	-0.0056	-0.0027	-0.0028
2500			-0.0028	-0.0044	-0.0063	-0.0037	-0.0036
5000			-0.0052	-0.0044	-0.0062	-0.0040	-0.0035
10000			-0.0056	-0.0074	-0.0073	-0.0023	-0.0032
25000				-0.0058	-0.0047	-0.0070	-0.0044
48772				-0.0069	-0.0055	-0.0051	-0.0035
92550				-0.0076	-0.0046	-0.0080	-0.0036
152510				-0.0075	-0.0044		-0.0028
196700							
496555							
951065							
1356500							

Table H-7. Measured maximum dynamic longitudinal strains (μstrains) as a function of load applications (703C6) – Position 1.

A							
Repetitions	z = 70mm	z = 152mm	z = 304mm	z = 464mm	z = 625mm	z = 709mm	z = 931mm
0			-100	-48	-19	-28	-13
500			-78	-52	-24	-21	-18
1000			-84	-56	-29	-19	-23
2500			-91	-60	-24	-16	-20
5000			-101	-50	-35	-22	-26
10000			-74	-47	-31	-19	-30
25000				-64	-38	-36	-35
48772				-76	-68	-42	-25
92550				-85	-56	-46	-22
152510				-87	-54		-22
196700							
496555							
951065							
1356500							

B							
Repetitions	z = 70mm	z = 152mm	z = 304mm	z = 464mm	z = 625mm	z = 709mm	z = 931mm
0			165	96	50	34	38
500			127	119	63	43	46
1000			135	120	61	43	41
2500			132	144	69	50	50
5000			154	150	71	45	52
10000			178	155	86	64	38
25000				191	101	85	67
48772				166	161	101	57
92550				172	157	108	75
152510				172	152		70
196700							
496555							
951065							
1356500							

Table H-7. Measured maximum dynamic longitudinal strains (µstrains) as a function of load applications (703C6) – Position 1 - cont.

C							
Repetitions	z = 70mm	z = 152mm	z = 304mm	z = 464mm	z = 625mm	z = 709mm	z = 931mm
0			-56	-30	-19	-19	-13
500			-26	-26	-24	-21	-18
1000			-19	-35	-29	-20	-23
2500			-35	-32	-24	-12	-20
5000			-38	-14	-35	-21	-26
10000			-28	-36	-31	-19	-30
25000				-51	-52	-36	-35
48772				-40	-28	-42	-25
92550				-40	-21	-46	-17
152510				-40	-22		-18
196700							
496555							
951065							
1356500							

Table H-8. Measured maximum dynamic longitudinal strains (µstrains) as a function of load applications (703C6) – Position 2.

A							
Repetitions	z = 70mm	z = 152mm	z = 304mm	z = 464mm	z = 625mm	z = 709mm	z = 931mm
0	-111		-111	-53	-11	-12	-19
500	-126		-106	-54	-12	-19	-13
1000	-117		-100	-46	-17	-18	-9
2500	-119		-99	-54	-21	-18	-16
5000	-230		-102	-56	-19	-22	-10
10000	-347		-77	-46	-18	-17	-9
25000				-41	-26	-35	-14
48772				-79	-56	-28	-23
92550				-83	-59	-19	-20

152510				-69	-59		-21
196700							
496555							
951065							
1356500							

Table H-8. Measured maximum dynamic longitudinal strains (μstrains) as a function of load applications (703C6) – Position 2 - cont.

B							
Repetitions	z = 70mm	z = 152mm	z = 304mm	z = 464mm	z = 625mm	z = 709mm	z = 931mm
0	1428		158	121	58	43	33
500	1405		129	138	69	50	39
1000	1358		134	161	66	44	49
2500	1377		149	161	80	54	48
5000	1069		158	168	86	67	63
10000	2058		190	180	87	68	60
25000				180	112	103	69
48772				212	182	114	73
92550				189	184	113	84
152510				190	174		89
196700							
496555							
951065							
1356500							

C							
Repetitions	z = 70mm	z = 152mm	z = 304mm	z = 464mm	z = 625mm	z = 709mm	z = 931mm
0	-313		-46	-42	-30	-16	-20
500	-267		-35	-26	-40	-20	-25
1000	-246		-34	-28	-35	-21	-15
2500	-219		-32	-33	-29	-27	-22
5000			-40	-31	-36	-23	-20
10000	-516		-44	-48	-45	-18	-14
25000				-31	-11	-36	-32
48772				-51	-25	-34	-23

92550				-55	-30	-38	-17
152510				-44	-30		-22
196700							
496555							
951065							
1356500							

Table H-9. Measured maximum dynamic longitudinal strains (μstrains) as a function of load applications (703C5) – Position 3.

A							
Repetitions	z = 70mm	z = 152mm	z = 304mm	z = 464mm	z = 625mm	z = 709mm	z = 931mm
0			-67	-38	-12	-13	-8
500			-84	-39	-14	-13	-9
1000			-80	-41	-10	-17	-16
2500			-75	-54	-13	-17	-17
5000			-84	-42	-14	-15	-12
10000			-61	-36	-21	-17	-11
25000				-67	-50	-23	-23
48772				-53	-48	-12	-19
92550				-57	-37	-16	-23
152510				-64	-53		-19
196700							
496555							
951065							
1356500							

B							
Repetitions	z = 70mm	z = 152mm	z = 304mm	z = 464mm	z = 625mm	z = 709mm	z = 931mm
0			99	101	57	39	36
500			97	132	62	47	49
1000			99	137	70	49	37
2500			116	159	78	55	40
5000			127	158	78	59	51

10000			163	153	89	62	63
25000				124	88	60	78
48772				161	161	97	70
92550				152	144	102	70
152510				148	151		83
196700							
496555							
951065							
1356500							

Table H-9. Measured maximum dynamic longitudinal strains (µstrains) as a function of load applications (703C6) – Position 3 - cont.

C							
Repetitions	z = 70mm	z = 152mm	z = 304mm	z = 464mm	z = 625mm	z = 709mm	z = 931mm
0			-38	-28	-27	-22	-16
500			-31	-29	-39	-17	-17
1000			-36	-27	-34	-19	-19
2500			-18	-27	-39	-25	-25
5000			-33	-26	-38	-27	-24
10000			-36	-44	-45	-19	-22
25000				-18	-7	-26	-30
48772				-43	-33	-32	-24
92550				-47	-28	-51	-25
152510				-47	-27		-19
196700							
496555							
951065							
1356500							

Table H-10. Measured maximum dynamic transverse displacements (mm) as a function of load applications (703C6).

Position 1							
Repetitions	z = 70mm	z = 152mm	z = 304mm	z = 464mm	z = 625mm	z = 709mm	z = 931mm
0			0.0076	0.0164	0.0126		
500			0.0081	0.0197	0.0135		
1000			0.0084	0.0192	0.0138		
2500			0.0088	0.0206	0.0140		
5000			0.0105	0.0221	0.0150		
10000			0.0118	0.0215	0.0147		
25000			39.1414	0.0227	0.0143		
48772				0.0221	0.0137		
92550				0.0225	0.0141		
152510				0.0212	0.0146		
196700			0.0199	0.0225	0.0140		
496555				0.0241	0.0147		
951065			0.0116	0.0147	0.0111		
1356500					0.0126		

Position 2							
Repetitions	z =	z =	z =	z = 464mm	z =	z = 709mm	z = 931mm

	70mm	152mm	304mm		625mm		
0			0.0174	0.0281	0.0127		
500			0.0182	0.0293	0.0135		
1000			0.0184	0.0277	0.0149		
2500			0.0196	0.0291	0.0151		
5000			0.0213	0.0303	0.0166		
10000			0.0239	0.0301	0.0180		
25000			56.8658	0.0311	0.0174		
48772				0.0311	0.0193		
92550				0.0291	0.0177		
152510				0.0274	0.0191		
196700			0.0296	0.0273	0.0163		
496555				0.0292	0.0154		
951065			0.0306	0.0227	0.0145		
1356500					0.0184		

Table H-10. Measured maximum dynamic transverse displacements (mm) as a function of load applications (703C6) - cont.

Position 3							
Repetitions	z = 70mm	z = 152mm	z = 304mm	z = 464mm	z = 625mm	z = 709mm	z = 931mm
0			0.0187	0.0134	0.0050		
500			0.0244	0.0226	0.0074		
1000			0.0229	0.0221	0.0078		
2500			0.0256	0.0236	0.0093		
5000			0.0294	0.0252	0.0096		
10000			0.0307	0.0231	0.0105		
25000			58.4382	0.0246	0.0136		
48772				0.0243	0.0140		
92550				0.0220	0.0129		
152510				0.0214	0.0122		
196700			0.0353	0.0199	0.0111		
496555			0.0366	0.0211	0.0119		
951065			0.0341	0.0163	0.0127		
1356500					0.0117		

Table H-11. Measured maximum dynamic transverse strains (μstrains) as a function of load applications (703C6).

Position 1							
Repetitions	z = 70mm	z = 152mm	z = 304mm	z = 464mm	z = 625mm	z = 709mm	z = 931mm
0			44	142	90		
500			54	169	94		
1000			53	161	99		
2500			59	173	98		
5000			67	182	110		
10000			76	178	103		
25000			136	169	96		
48772				186	100		
92550				169	95		
152510				158	86		
196700			164	197	100		
496555				214	106		
951065			85	121	78		
1356500					97		

Position 2							
Repetitions	z = 70mm	z = 152mm	z = 304mm	z = 464mm	z = 625mm	z = 709mm	z = 931mm
0			106	214	77		
500			105	215	82		
1000			97	190	93		
2500			121	203	97		
5000			120	208	107		
10000			139	208	111		
25000			178	199	115		
48772				218	113		
92550				180	108		
152510				171	113		
196700			222	218	114		
496555				234	107		
951065			230	181	101		
1356500					129		

Table H-11. Measured maximum dynamic transverse strains (μstrains) as a function of load applications (703C6) - cont.

Position 3							
Repetitions	z = 70mm	z = 152mm	z = 304mm	z = 464mm	z = 625mm	z = 709mm	z = 931mm
0			123	98	26		
500			138	156	40		
1000			125	152	54		
2500			141	162	54		
5000			154	172	55		
10000				162	60		
25000			199	142	80		
48772				172	79		
92550				139	76		
152510				130	74		
196700			264	159	77		
496555			275	169	83		
951065			256	131	89		
1356500					81		

Table H12. Measured permanent deformations (mm) as a function of load applications (703C6).

Vertical														
Depth (mm)	0	500	1000	2500	5000	10000	25000	48772	92550	152510	196700	496555	951065	1356500
Surface	0.0000	0.1406	-0.1322	-0.3103	-0.5640	-0.7929								
124	0.0000	0.3253	-0.4743	-0.7646	-1.0433	-0.9669								
242														
385	0.0000	-0.3124	-0.4573	-0.7064	-0.8531	-0.9423	-1.4718	-1.4635	-1.8792	-2.2279	-1.2765	-3.3229	-3.3652	-3.3566
540	0.0000	-0.4152	-0.5622	-0.8041	-0.9164	-0.9693	-1.4771	-1.3808	-1.6210	-1.6893	-1.2346	2.5376	4.0791	3.8330
702	0.0000	0.2591	0.1860	0.0196	-0.0294	0.0264	-0.4499	-0.2486	-0.4542	-0.5109	0.3532	-1.1371	-1.5979	-1.4666
858	0.0000	0.2537	0.2197	0.1331	0.1188	0.1980	-0.0298	0.1339	0.0217	0.0344	0.4849	-0.5059	-0.6568	-0.6533
983	0.0000	0.2232	0.1773	0.1224	0.1072	0.1802	-0.0170	0.1534	0.0542	0.0767				

Longitudinal														
Depth (mm)	0	500	1000	2500	5000	10000	25000	48772	92550	152510	196700	496555	951065	1356500
70														
152														
304	0.0000	0.0284	0.0019	-0.0578	-0.0770	0.0049		0.0414	-0.0479	-0.0011	-0.3276	-0.2404	-0.3434	-0.3410
464	0.0000	0.1492	0.1253	0.0689	0.0742	0.1460		0.1175	0.0263	0.0206	-0.3473	-0.1704	-0.3252	-0.3570
625	0.0000	0.2335	0.2074	0.1548	0.1600	0.2439		0.2768	0.1576	0.1561	-0.1444	-0.0695	-0.1802	-0.3151
709	0.0000	0.2592	0.2385	0.1792	0.1941	0.2955		0.3630	0.2524	0.2415	-0.1527	-0.0287	-0.1696	-0.2181
931	0.0000	0.0691	0.0319	0.0279	0.0339	0.0619								

Table H12. Measured permanent deformations (mm) as a function of load applications (703C6) - cont.

Transverse														
Depth (mm)	0	500	1000	2500	5000	10000	25000	48772	92550	152510	196700	496555	951065	1356500
70	0.0000	0.6974	0.4587	0.4758	3.9596									
152														
304	0.0000	0.4450	0.4365	0.3835	0.3993	0.4806								
464	0.0000	0.4423	0.4425	0.3999	0.4215	0.5289	0.4160	0.6130	0.5494	0.5403	0.3904	0.1779	-0.0050	
625	0.0000	0.3121	0.2942	0.2440	0.2622	0.3737	0.2201	0.4523	0.3378	0.3411	0.2071	-0.0252	-0.2443	-0.2587
709	0.0000	0.3546	0.3266	0.2709	0.2951	0.3989	0.2098	0.4435	0.3212	0.3109	0.5168	0.0082	-0.1828	-0.3346
931	0.0000	0.2829	0.2610	0.2052	0.2258	0.3413	0.1939	0.4101	0.2842	0.2849	0.3249	-0.0676	-0.2664	-0.2933

Table H13. Measured permanent strain (%) as a function of load applications (703C6).

Vertical														
Depth (mm)	0	500	1000	2500	5000	10000	25000	48772	92550	152510	196700	496555	951065	1356500
Surface	0.000	0.142	0.134	0.314	0.571	0.803								
124	0.000	0.117	-0.171	-0.275	-0.376	-0.348								
242														
385	0.000	-0.187	-0.273	-0.422	-0.510	-0.563	-0.879	-0.874	-1.123	-1.331	-0.763	-1.985	-2.010	-2.005
540	0.000	-0.256	-0.347	-0.496	-0.565	-0.598	-0.911	-0.852	-1.000	-1.042	-0.762	1.565	2.516	2.365
702	0.000	0.130	0.093	0.010	-0.015	0.013	-0.225	-0.125	-0.228	-0.256	0.177	-0.570	-0.801	-0.735
858	0.000	0.206	0.179	0.108	0.097	0.161	-0.024	0.109	0.018	0.028	0.394	-0.411	-0.534	-0.531
983	0.000	0.218	0.173	0.120	0.105	0.176	-0.017	0.150	0.053	0.075				

Longitudinal														
Depth (mm)	0	500	1000	2500	5000	10000	25000	48772	92550	152510	196700	496555	951065	1356500
70														
152														
304	0.000	0.030	0.002	-0.062	-0.082	0.005		0.044	-0.051	-0.001	-0.349	-0.256	-0.365	-0.363
464	0.000	0.122	0.103	0.056	0.061	0.119		0.096	0.022	0.017	-0.284	-0.139	-0.266	-0.292
625	0.000	0.165	0.147	0.109	0.113	0.172		0.196	0.111	0.110	-0.102	-0.049	-0.127	-0.223
709	0.000	0.169	0.156	0.117	0.127	0.193		0.237	0.165	0.157	-0.100	-0.019	-0.111	-0.142
931	0.000	0.305	0.141	0.123	0.150	0.274								

Table H13. Measured permanent strain (%) as a function of load applications (703C6) - cont.

Transverse														
Depth (mm)	0	500	1000	2500	5000	10000	25000	48772	92550	152510	196700	496555	951065	1356500
70	0.000	0.492	0.324	0.336	2.794									
152														
304	0.000	0.335	0.328	0.289	0.300	0.362								
464	0.000	0.354	0.355	0.320	0.338	0.424	0.333	0.491	0.440	0.433	0.313	0.143	-0.004	
625	0.000	0.218	0.205	0.170	0.183	0.261	0.154	0.316	0.236	0.238	0.145	-0.018	-0.171	-0.181
709	0.000	0.193	0.178	0.148	0.161	0.217	0.114	0.242	0.175	0.170	0.282	0.004	-0.100	-0.182
931	0.000	0.181	0.167	0.131	0.144	0.218	0.124	0.262	0.181	0.182	0.207	-0.043	-0.170	-0.187

Table H-14. Maximum surface rut (mm) as a function of longitudinal location & load repetitions (703C6).

Position	0	170	500	1000	2500	5000	10000	48772	92550	152510	196700	316069	496555	951065	1131250
Pos3	0.00	1.91	2.74	3.45	4.07	4.94	5.88	8.27	9.01	9.51	9.90	11.47	11.89	12.71	0.00
Pos4	0.00	1.89	2.54	2.92	3.69	4.34	5.06	7.38	8.92	9.26	9.90	10.49	11.55	12.28	12.72
Pos5	0.00	1.71	2.60	3.20	3.90	4.37	5.46	7.42	8.09	8.65	9.35	9.92	10.78	11.97	12.31
Pos6	0.00	1.47	2.51	2.76	3.63	4.32	4.99	6.99	7.73	8.00	8.64	9.42	9.81	11.39	11.47
Pos7	0.00	1.86	2.61	3.14	3.84	4.46	5.07	7.15	7.67	8.58	8.61	9.46	10.12	11.38	11.56
Pos8	0.00	1.90	2.63	3.01	3.78	4.19	5.01	7.00	7.55	8.40	8.72	9.61	10.41	11.46	12.00
Pos9	0.00	1.54	2.44	3.03	3.61	4.17	5.12	6.96	7.81	8.47	8.65	9.51	10.24	11.54	0.00
Pos10	0.00	1.91	2.50	3.29	3.57	4.45	5.43	7.45	7.92	8.91	9.10	10.02	10.76	12.09	12.41
Pos11	0.00	1.60	2.52	3.02	3.84	4.18	5.20	6.84	7.70	8.55	8.62	9.60	10.25	11.53	11.62
Pos12	0.00	2.02	2.75	3.74	4.12	4.76	5.55	7.81	8.48	9.03	9.77	10.83	11.24	12.65	13.22
Pos13	0.00	2.14	3.32	3.35	4.09	5.07	5.89	8.12	8.32	9.16	9.35	10.05	10.84	12.32	12.60
Pos14	0.00	2.20	3.35	3.65	3.99	5.27	5.98	7.87	8.17	9.42	9.45	9.86	10.53	11.88	12.21
Pos15	0.00	1.50	2.74	2.98	3.63	4.12	4.77	6.70	7.09	7.80	8.49	9.82	10.09	11.36	11.53
Pos16	0.00	1.86	2.88	3.27	4.02	4.43	5.44	7.26	7.65	8.66	8.84	9.69	10.55	12.11	12.38
Pos17	0.00	2.01	3.07	3.55	4.40	4.92	5.78	7.90	8.83	9.43	9.70	10.73	11.55	12.99	13.42
Pos18	0.00	1.53	2.37	2.89	3.60	3.90	4.71	6.83	7.46	7.76	8.21	9.01	9.50	10.94	11.54
Pos19	0.00	1.42	2.22	2.66	3.17	3.71	4.37	6.44	7.21	7.76	7.62	8.87	9.53	10.87	11.04
Pos20	0.00	1.07	2.00	2.15	2.91	3.41	4.49	6.37	7.04	7.76	7.77	8.88	9.18	10.50	10.88
Pos21	0.00	0.85	1.57	1.94	2.66	3.23	3.99	6.06	6.58	7.46	7.45	8.44	9.23	10.53	10.50
Pos22	0.00	0.97	1.84	2.08	2.72	3.11	4.05	6.22	6.53	7.52	7.62	9.02	9.11	10.94	10.98